

LIBRARY Michigan State University

This is to certify that the

dissertation entitled

INTEGRAL EQUATION DESCRIPTION OF INTEGRATED DIELECTRIC WAVEGUIDES

presented by

Jonathan Scott Bagby

has been accepted towards fulfillment of the requirements for

<u>Doctoral</u> degree in <u>Electrical</u>

Engineering

Date 8/24/84

MSU is an Affirmative Action Equal Opportunity Institution

0-12771

Dennis P. Nyquist



RETURNING MATERIALS:
Place in book drop to remove this checkout from your record. FINES will be charged if book is returned after the date stamped below.

INTEGRAL EQUATION DESCRIPTION OF INTEGRATED DIELECTRIC WAVEGUIDES

Ву

Jonathan Scott Bagby

A DISSERTATION

Submitted to
Michigan State University
in partial fulfillment of the requirements
for the degree of

DOCTOR OF PHILOSOPHY

Department or Electrical Engineering and Systems Science

ABSTRACT

INTEGRAL EQUATION DESCRIPTION OF INTEGRATED DIELECTRIC WAVEGUIDES

Βv

Jonathan Scott Bagby

An equivalent polarization integral equation is advanced for use in the analysis of integrated dielectric waveguiding systems. This inhomogeneous Fredholm equation of the second kind in the unknown total waveguide core electric field provides a conceptually exact formulation of the guidance properties of a wide class of practical integrated dielectric waveguides.

The integral equation is applied to a generalized axially uniform integrated dielectric waveguiding system. This axial uniformity renders the axial integral convolutional in nature, prompting the use of a spatial Fourier transform. This results in an inhomogeneous Fredholm equation for the unknown transformed total core field.

Subsequent inversion of the transformed field with the aid of the residue theorem allows identification of two components of the total core field: the surface waves of the guide and the radiation spectrum. These are found in terms of the sources exciting the waveguide, leading to conventional results for excitation of surface waves and a new formulation of the excitation of the radiation spectrum. The behavior of the kernel of the transformed integral

equation in the complex plane leads to general criterion for prediction of the important phenomena of guided mode leakage. The problem of line source excitation of the asymmetric slab is addressed, as well as the determination of the eigenvalues of the uniform rectangular strip waveguide.

The integral equation is also applied to the interesting problem of plane truncated integrated dielectric waveguides. A modified Weiner-Hopr technique is used to generate iterative formulae for predicting the radiation and reflection of surface waves incident on the truncation from within the waveguide, as well as the excitation or surface waves due to sources outside of the truncated waveguide.

Rapid convergence or the iterative technique is demonstrated through application to the truncated asymmetric slab waveguide.

Application of moment method and Neumann series techniques to the integral equation is discussed. Utilization of the integral equation for the analysis of microwave integrated circuits is identified as an important avenue of further study.

···to

Dennis Nyquist rriend and mentor

and

Sara Bagby friend and partner

ACKNOWLEDGEMENT

A list of the people who helped me achieve this point in my life would be much too lengthly for inclusion here, but a few of these individuals deserve special thanks:

Sara Bagby, ror unending support and encouragement;

Dennis Nyquist, who first inspired me as an undergraduate;

John Kreer and George VanDusen, two administrators who always gave me the benefit of a doubt;

Walt and Carol Bagby and Dan and Sally Meeuwsen, ror always being there when needed;

Byron Drachman, Kun-Mu Chen, and Jes Asmussen, who supplied thoughtful teaching and guidance;

Enid Maitland, Pauline VanDyke, and Ginny Mrazek, who were always willing to help;

Pam Graves, for tireless effort in preparing this manuscript.

TABLE OF CONTENTS

				Page		
LIST	T OF TABLES					
LIST	ST OF FIGURES					
Chap	ter					
1.	Introduction					
2.	Equivalent Polarization Integral Equation					
		2.1.1 2.1.2 2.1.3	al Equation Equivalent Polarization Scattered Field Total Field Alternative Integral Equation	18 19 21 24 25		
	2.2	2.2.1	Green's Function Hertzian Potential Green's Dyad Electric Green's Dyad	25 26 33		
3.	Longitudinally Invariant Waveguides					
	3.1	3.1.1 3.1.2 3.1.3	ormed Integral Equation Longitudinal Invariance Axial Fourier Transform Transformed Integral Equation Alternative Transformed Integral Equation	36 38 39 40		
	3.2	3.2.1	ormed Green's Dyad Transformed Hertzian Potential Green's Dyad Transformed Electric Green's Dyad	41 41 44		
	3.3	3.3.1 3.3.2 3.3.3 3.3.4 3.3.5	tion of Integrated Waveguides Residue Theorem Complete Modal Spectrum Poles of e and Surface Waves Branches of e and the Radiation Spectrum Leakage from Integrated Waveguides TE Excitation of the Asymmetric Slab	45 47 49 53 57		

	3.4	3.4.1 3.4.2 3.4.3 3.4.4	rigular Strip Waveguide Field Representation Principle Terms Rerlected Terms Computational Considerations Numerical Results	83 85 89 92 98 101			
4.	Plane Truncated Waveguides						
	4.1	Prelim	Preliminaries				
		4.1.1 Modal Expansion		117 117			
			Partial Fields	118			
	4.2	Surrace Wave Rerlection and Radiation					
	•		Modal Expansion of $ec{\mathbf{E}}^{\mathrm{L}}$	121			
			Integral Operator	122			
			Iterative Equation	127			
		4.2.4	Radiated Field	129			
	4.3	Excitation of Truncated Waveguides		129			
	•		Modal Expansion or Ĕ ^L	131			
			Integral Operator	131			
		4:3:3	Iterative Equation	132			
		4.3.4	Radiation-Excitation Reciprocity	134			
	4.4	Truncated Asymmetric Slab					
	•	4.4.1 Surrace Wave Rerlection		137			
			Surrace Wave Radiation	145			
			Line Source Excitation	147			
		4.4.4	Numerical Results	150			
5.	5. Conclusion						
ADDE	ND TV	A 11	haina Debambial Openata Duad	158			
APPE	APPENDIX A: Hertzian Potential Green's Dyad						
APPE	APPENDIX B: Transformed Field in the Asymmetric Slab						
APPENDIX C: Principle and Rerlected Terms for Rectangular Strip							
APPENDIX D: Branch Integrals in Low Loss Limit							
			-	188			
LIST	OF R	EFERENC	ES	191			

LIST OF TABLES

Table

- 3.1 Normalized eigenvalues of the isolated uniform rectangular strip waveguide for several normalized guide widths compared to the results of Marcatili's approximate technique. Here n = 1.5, $n_c = 1.0$, d/a = 1.0.
- 3.2 Normalized eigenvalues of the uniform rectangular dielectric rib waveguide for several normalized guide sizes compared to the results of the EDC method. Here d=t=a, $n=n_f=1.5$, $n_g=1.1$, $n_{c}=1.0$.

LIST OF FIGURES

Figure

- 1.1 A general dielectric waveguide integrated over a tri-layered background structure.
- 1.2 A general axially uniform dielectric waveguide integrated over a tri-layered background structure.
- 1.3 An integrated rectangular strip waveguide with transversely graded core.
- 1.4 An integrated rectangular dielectric channel waveguide with transversely graded core.
- 1.5 A plane truncated integrated rectangular dielectric strip waveguide with transversely graded core.
- 2.1 Generalized dielectric system described by the equivalent polarization integral equation.
- 2.2 Field equivalent system to that in Figure 2.1 with induced equivalent polarization sources replacing dielectric obstacle.
- 2.3 Integrated tri-layered dielectric background structure described by Hertzian potential Green's dyad.
- 3.1 A general axially uniform dielectric waveguide integrated over a tri-layered background structure.
- 3.2 General integration contour in complex ζ plane enclosing poles and branch points or a complex runction.
- 3.3 Deformed Fourier inversion contour in complex ζ plane enclosing poles and branch points of transformed total electric field.
- 3.4 Deformed spectral integration contour in the complex plane for components of transformed Hertzian potential Green's dyad.
- 3.5 Complex ξ plane construction derining $arg\{\xi_p\}$.
- 3.6 Construction derining leakage angle for leaking waves of an integrated waveguide.
- 3.7 The asymmetric slab waveguide excited by a line polarization source. The structure is uniform in the x direction.

Figure

- 3.8 Deformed Fourier inversion contour in complex ζ plane for total core field in the asymmetric slab.
- 3.9 Detail or branch cuts in complex ζ plane for transformed rield in the asymmetric slab in the low loss limit.
- 3.10 Complex ζ plane construction derining branch choice for reduced transverse wavenumber parameters, γ_{δ}
- 3.11 The uniform dielectric rectangular strip integrated over a trilayered background structure.
- 3.12 Diagram illustrating Marcatili's approximation or eigenvalues of the isolated uniform rectangular strip waveguide.
- 3.13 Normalized transverse wavenumbers or the isolated uniform rectangular strip waveguide versus normalized waveguide height.
- 3.14 Normalized propagation constant of the isolated uniform rectangular strip waveguide versus normalized waveguide size compared Goell's circular harmonic analysis results.
- 3.15 Normalized distribution or dominant field component in isolated uniform rectangular strip waveguide versus normalized x coordinate for several normalized waveguide heights.
- 3.16 Normalized distribution or dominant electric rield component in isolated uniform rectangular strip waveguide versus normalized y coordinate for several normalized waveguide heights.
- 3.17 Diagram illustrating the application of the effective dielectric constant (EDC) method to a uniform rectangular dielectric rib waveguide.
- 3.18 Normalized propagation constant for uniform rectangular dielectric rib waveguide versus normalized waveguide height compared to results of EDC method.
- 4.1 A generalized plane truncated axially uniform integrated dielectric waveguide.
- 4.2 Surface wave reflection and radiation in a plane truncated dielectric waveguide when a single surface wave is incident on the truncation.
- 4.3 Excitation or surface waves in a plane truncated dielectric waveguide by a source outside or the truncation.
- 4.4 The plane truncated asymmetric slab waveguide with a surface wave incident on the truncation.
- 4.5 Integration contour in the complex ζ plane for the factor h $\stackrel{+}{\text{-}}$.

Figure

- 4.6 Uniform line polarization excitation of the truncated asymmetric slab waveguide.
- 4.7 Normalized reflected mode amplitudes in truncated symmetric slab versus normalized slab thickness compared to the results of Gelin, et. al.
- 4.8 Relative radiated power from truncated symmetric slab waveguide versus normalized slab thickness.
- 4.9 Normalized radiation and excitation patterns for the truncated symmetric slab waveguide versus aspect angle in degrees compared to the results of Angulo, et. al.
- A.1 Hertzian potential boundary conditions at a dielectric interface.
- A.2 Principle and scattered Hertzian potential components for a source in the cover medium.
- A.3 Principle and scattered Hertzian potential components ror a source in the film layer.

1. INTRODUCTION

The determination of the electromagnetic wave guiding characteristics of open boundary dielectric structures has become a problem of increasing importance in the past several years. This increased interest has been sparked by the use of open boundary dielectric waveguides in the areas of integrated optics and millimeter wave integrated circuits [1.1, 1.2]. Dielectric waveguides are already in widespread use in the telecommunications industry, where light waves guided along optical fibers are replacing the more costly and bulky wire cables in key trunk lines. Integrated optical circuits are typically used to generate and detect these optical fiber light waves, and are envisaged for applications such as monolithic signal repeaters and signal processing networks.

Open boundary dielectric waveguides can be defined for our purposes as any dielectric structure capable of guiding electromagnetic waves along and in close proximity to a waveguiding axis. Such dielectric waveguiding structures typically consist of an axially extended dielectric core region surrounded by a more or less complicated dielectric background region, as shown in Figure 1.1. If the refractive index of the dielectric core region exceeds that of the surrounding dielectric background region then the structure is capable of guiding transversely conrined electromagnetic waves. This guidance is accomplished essentially by the phenomenon or total internal

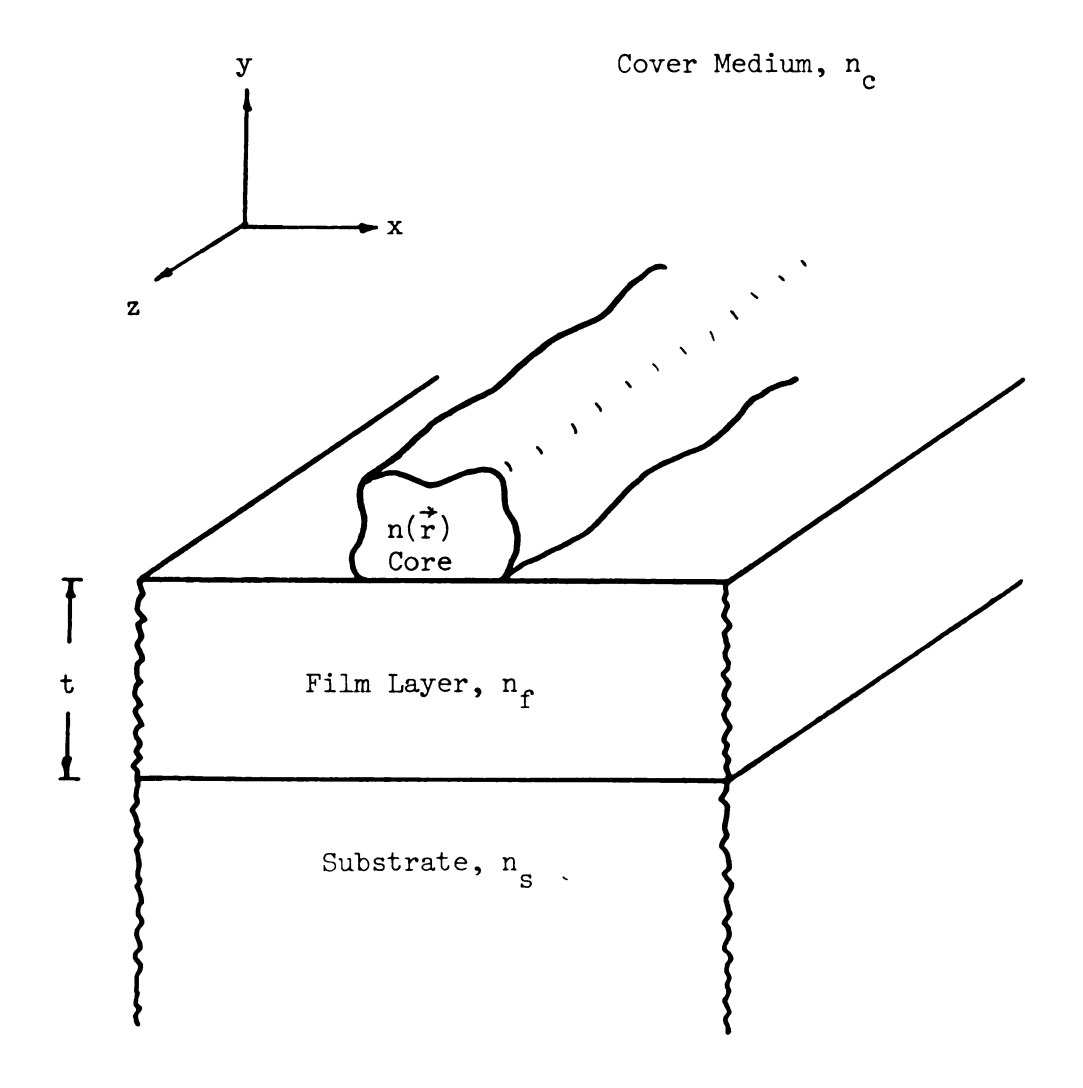


Figure 1.1: A general dielectric waveguide integrated over a trilayered background structure.

reflection at the interface between the dielectric core and the surrounding background region. For this reason dielectric waveguides are often termed surface waveguides.

Open boundary dielectric waveguides support a rich variety of waveguiding phenomena. They are capable of guiding a finite number of distinct surface wave modes as well as a contribution to the total guided field known as the radiation field. The guided surface waves are characterized by a finite number of discrete allowable propagation eigenvalues, whereas the radiation field posesses a continuum of propagation eigenvalues which does not overlap those of the guided surface waves. The total radiation field is a spectral superposition along this allowed range of eigenvalues. The guided surface waves are typically divided into transverse electric and transverse magnetic modes (denoted TE and TM modes, respectively) as well as hybrid modes.

The practical application of open boundary dielectric waveguides in integrated optics and millimeter wave integrated circuits depends critically on the propagation characteristics of these waveguides. There has been enduring interest in the determination of the propagation characteristics of practical dielectric waveguiding structures, beginning in the early part of this century [1.3] and intensifying to this date [1.4 - 1.6].

Exact solutions for the electromagnetic fields in open boundary dielectric waveguides exist for few structures, such as the asymmetric slab waveguide [1.7] and uniformly clad uniform dielectric fibers of circular and eliptic cross sectional shape [1.8]. The boundary conditions obtaining at the dielectric interface between the core and surround regions of other dielectric waveguiding structures are

inseperable. This complication renders conventional differential formulations [1.7 - 1.9] or the waveguide fields insolvable.

Differential formulations have provided approximate solutions in some cases of interest. Among these is the interesting and practical problem of surface wave propagation along the dielectric waveguide configuration known as the uniform rectangular strip waveguide and the uniform rectangular channel waveguide. These dielectric waveguide configurations are depicted in Figures 1.3 and 1.4. The technique used in the classic study by Marcatili [1.10] has been shown to yield good results with minimal effort in the case of electrically large uniform rectangular strip and channel waveguides. A potentially exact solution for surface waves supported by the uniform rectangular strip has been obtained by the circular harmonic analysis of Goell [1.11]. Practical time and storage considerations, however, render the numerical results of this means of analysis necessarily approximate. A similar difficulty obtains for the potentially exact mode matching technique utilized by Peng and Oliner, et. al., in [1.4] and [1.5]. The radiation field of the uniform rectangular strip is also addressed in this important work, but the continuous spectrum of radiation eigenvalues is quantized by the introduction of distant conducting boundaries. This renders the analysis necessarily approximate in nature.

A shortcoming common to all of the above mentioned analyses is their inability to incorporate refractive index variation in the dielectric waveguide core region, commonly known as core grading, and their inapplicability to dielectric waveguiding structures with more general core cross sectional shapes. These considerations are of

practical importance since current fabrication technology renders the construction of the uniform rectangular strip waveguide difficult at best. It is also found experimentally that the propagation characteristics of circular dielectric fibers improve when the core is transversely graded.

In this dissertation we utilize an integral equation formulation to analyze a broad class of open boundary dielectric waveguides. This equivalent polarization integral equation is related to the polarization integral equation utilized by Katsenelenbaum [1.12]. It was developed by Johnson and Nyquist in [1.13]. The equivalent polarization integral equation provides a conceptually exact formulation of the total electric field in a generalized integrated dielectric waveguiding system such as that depicted in Figure 1.1.

This integral formulation of the problem results in several advantages over conventional differential formulations. First, the above mentioned complicated boundary conditions are incorporated in a general and natural manner into the dyadic Green's function which forms the kernel of the integral equation. Thus physical phenomena which may be obscured in the formulations using differential equations plus boundary conditions specialized to a specific waveguiding system (or even destroyed by the approximations used to simplify the mathematics; see [1.4] and [1.5]) can be analyzed in a general manner. Secondly, the equivalent polarization integral equation is valid for arbitrarily graded dielectric waveguide cores or arbitrarily variable cross sectional shape. Thirdly, the integral equation is an inhomogeneous Fredholm equation of the second kind. A large array of mathematical techniques have been developed for and are immediately

applicable to such integral equations, such as the technique of Neumann series. Lastly, the domain of the integral in the equivalent polarization integral equation is the waveguide core, rather than all of space, as in other integral formulations that have been advanced. Thus numerical techniques such as the method of moments are more easily utilized.

The remainder of this dissertation is organized into four chapters. In chapter two we sketch the development of the equivalent polarization integral equation. This development in part one of chapter two is based on field equivalence principles and the identification or equivalent polarization sources in the region of the dielectric waveguide core. The result of this analysis is an inhomogeneous Fredholm integral equation or the second kind for the unknown total electric field in the dielectric waveguide core. In part two of chapter two we detail and discuss the dyadic Green's function which forms the kernel of the equivalent polarization integral equation. The components of the Green's dyad are given as two dimensional spatial frequency integrals of the infamous Sommerfeld type. The rather arduous derivation of this dyadic Green's function is relegated to Appendix A.

In chapter three we use the equivalent polarization integral equation to analyze several problems involving longitudinally invariant integrated dielectric waveguides. Such axially uniform dielectric waveguides are an important special case of the more general waveguiding systems of the type shown in Figure 1.1 since many practical integrated optical systems include dielectric waveguides which can be approximated as axially uniform. A typical

longitudinally invariant integrated dielectric waveguide is depicted in Figure 1.2. The uniformity along the waveguiding axis displayed by such systems allows us to bring the powerful tool of Fourier transform theory to bear on the problems considered in the remainder of chapter three.

This axial uniformity manifests itself in the equivalent polarization integral equation by making the integration in the axial variable convolutional in nature. This prompts a Fourier transform of the entire equation on the axial variable, with a resulting reduction in dimension of the domain of integration.

In the first part of chapter three we obtain the Fourier transformed equivalent polarization integral equation. It is an inhomogeneous Fredholm integral equation for the unknown Fourier transformed total electric field in the waveguiding system. The kernel of this integral equation is the axial Fourier transform of the dyadic Green's function of the previous chapter. It is detailed and discussed in the second part of chapter three. The remainder of chapter three is devoted to applications of the axially transformed equivalent polarization integral equation.

In the third part of chapter three we develop a general excitation theory for axially uniform integrated dielectric waveguides. This theory is based on formal Fourier inversion of the unknown axially transformed total electric field in the waveguiding system. The transformed field has in general both pole and branch point singularities in the complex axial transform variable plane.

Deformation of the Fourier inversion contour in the complex transform variable plane and subsequent application of the residue theorem of

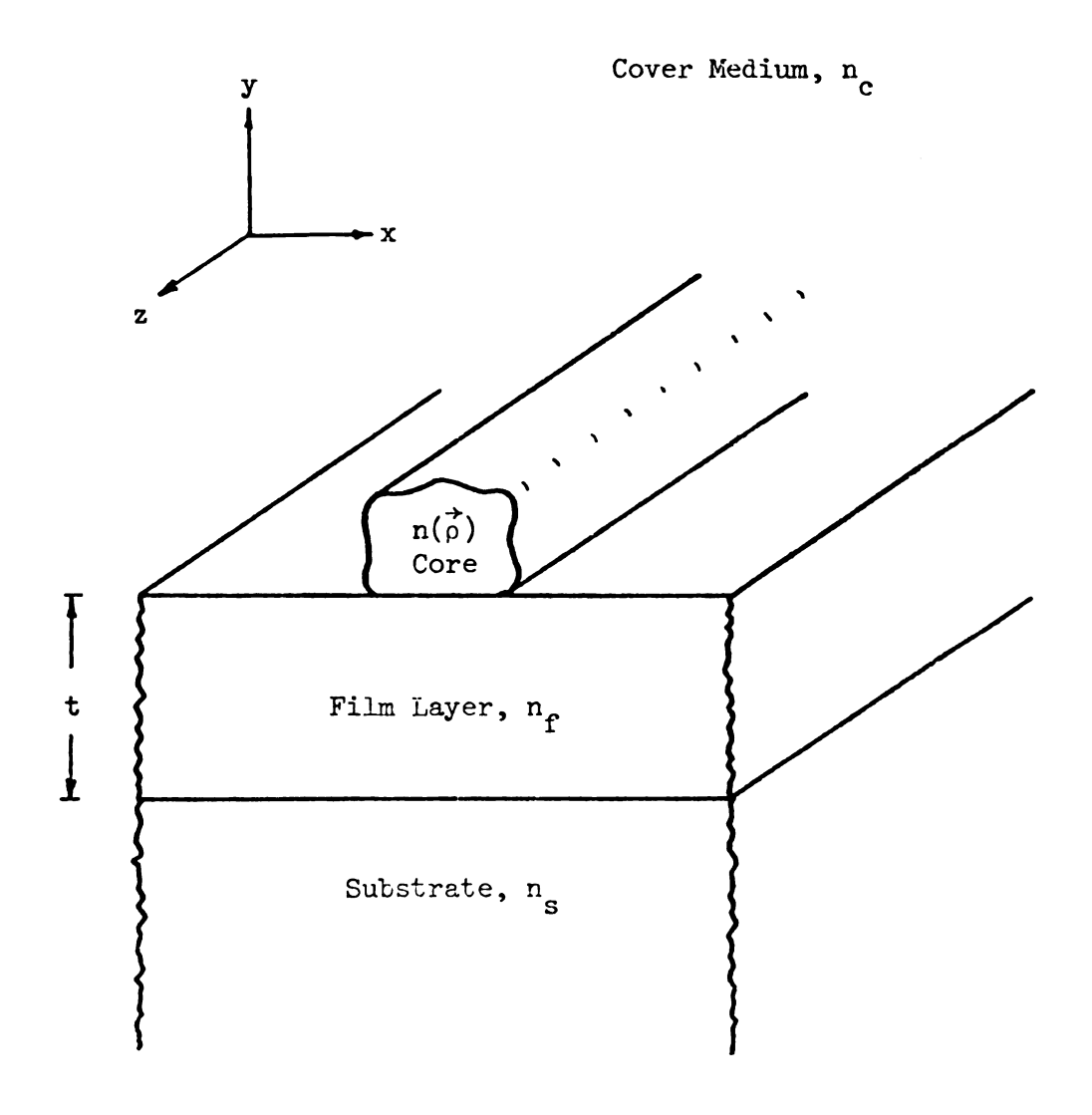


Figure 1.2: A general axially uniform dielectric waveguide integrated over a tri-layered background structure.

complex variables allows us to write the total field as a sum of two distinct terms. The first term is a sum of the residues of the transformed field at the poles enclosed in the deformed inversion contour, and the second term consists of integrals around any branch cuts associated with enclosed branch points. This decomposition allows us to characterize the complete modal spectrum of any axially uniform integrated dielectric waveguide: surface waves at the guiding system are associated with the residues of the enclosed poles, and the radiation field of the waveguide is associated with the branch integrals. This analysis also provides us with the excitation amplitudes of the various surface wave modes and radiation field spectral components in terms of the incident excitatory electric field or current. Another feature of this analysis is its ability to describe the important physical phenomena of guided mode leakage and resonance. We close this part of the chapter by applying this excitation theory to the problem of excitation of transverse electric modes in the asymmetric slab waveguide. The resulting modal and spectral component amplitudes are shown to be identical with those predicted by conventional excitation theory.

Our last application of the Fourier transformed integral equation is found in part four of chapter three. We apply the axially transformed equivalent polarization integral equation to the problem of finding the surface waves supported by the rectangular strip waveguide. This integrated dielectric waveguiding system is depicted in Figure 1.3. It is a configuration of considerable interest to workers in integrated optics (see for example, [1.4, 1.5, 1.10, 1.11]). We begin by postulating a sinusoidal representation with

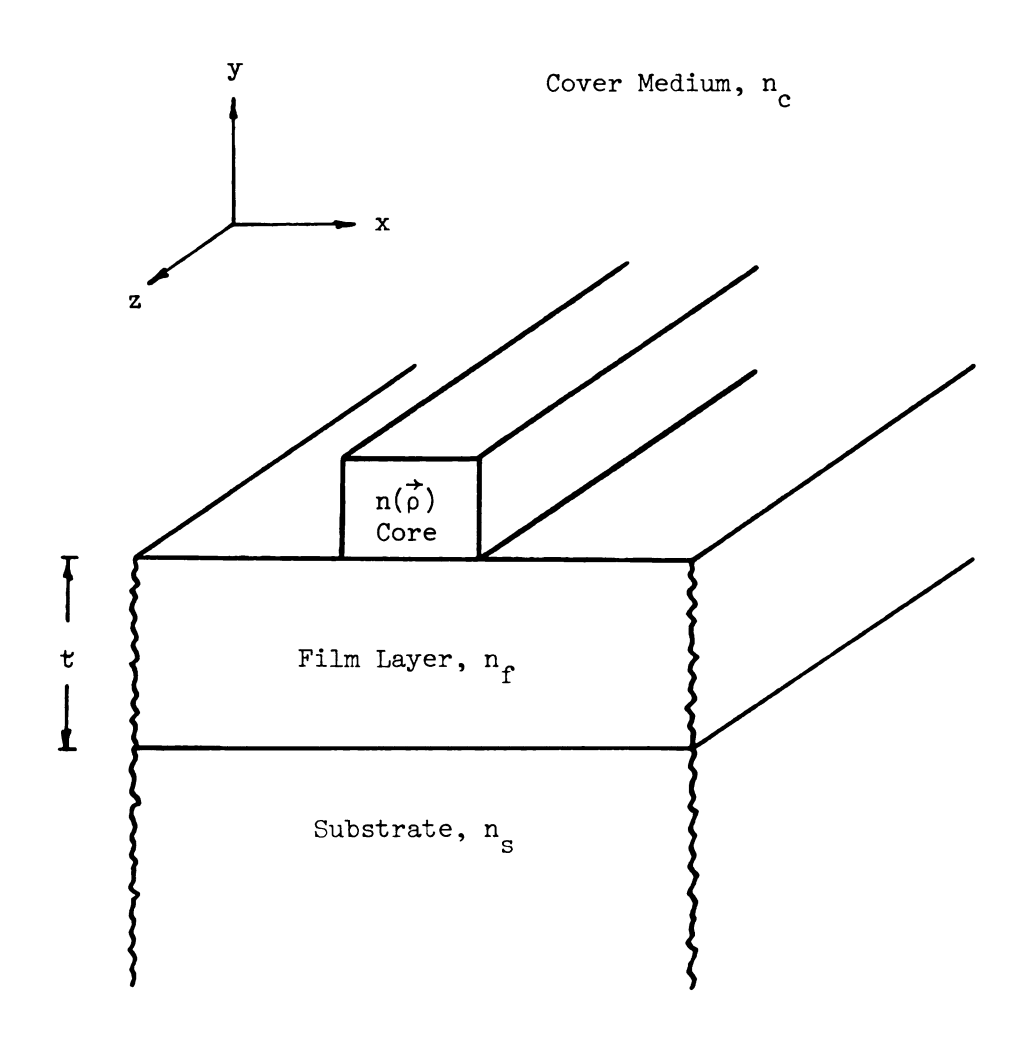


Figure 1.3: An integrated rectangular strip waveguide with transversely graded core.

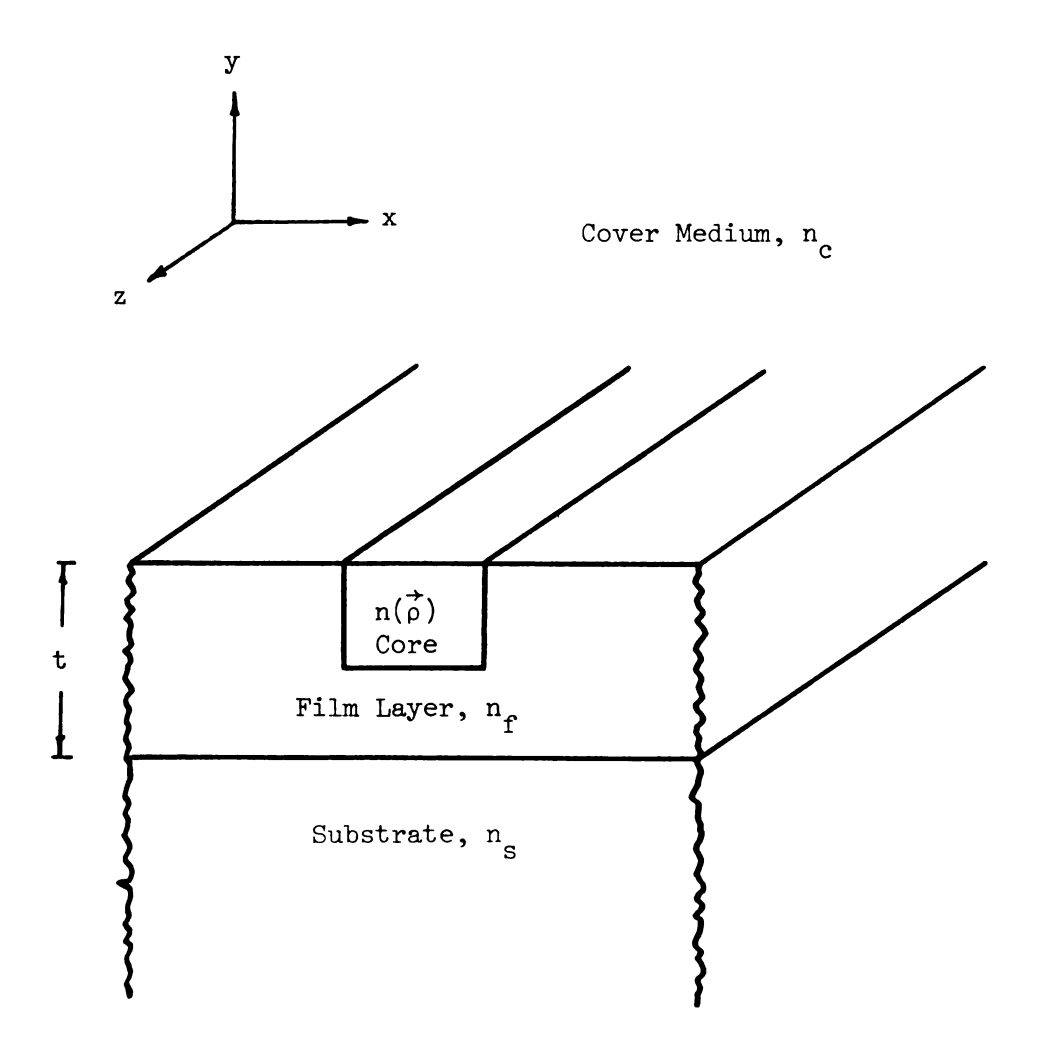


Figure 1.4: An integrated rectangular dielectric channel waveguide with transversely graded core.

unknown amplitudes and transverse spatial frequencies for the unknown axially transformed longitudinal components of the total electric and magnetic fields in the waveguide core. The axially transformed version of Maxwell's equations enable us to find all other transformed field components in terms or these two generating functions.

Substitution of the resultant expression for the total axially transformed electric field into the transformed integral equation and point-matching the equation at four locations inside of the waveguide core allows us to solve for the unknown amplitude and transverse spatial frequency constants as well as the axial propagation constant in our expressions for the total transformed electric field in the waveguide core. We thus obtain an approximate closed form expression for the fields of various guided surface wave modes of the integrated rectangular strip waveguide. Numerical results of this analysis are presented and compared with the results of other techniques.

In chapter four we apply the equivalent polarization integral equation to the problem of coupling energy into and out of plane truncated waveguides. Truncated integrated waveguide structures such as that depicted in Figure 1.5 are of considerable interest to workers in the area of integrated optics, where they are widely used as integrated laser cavities. This type of structure is also used to model junctions between separate integrated optical components.

We restrict ourselves to consideration of truncated integrated waveguides that have generally transversely graded cores of arbitrary but constant transverse cross sectional shape. The only allowed variation of the refractive index of the waveguide core in the longitudinal direction is of the form $u(z_0-z)$, where the waveguiding

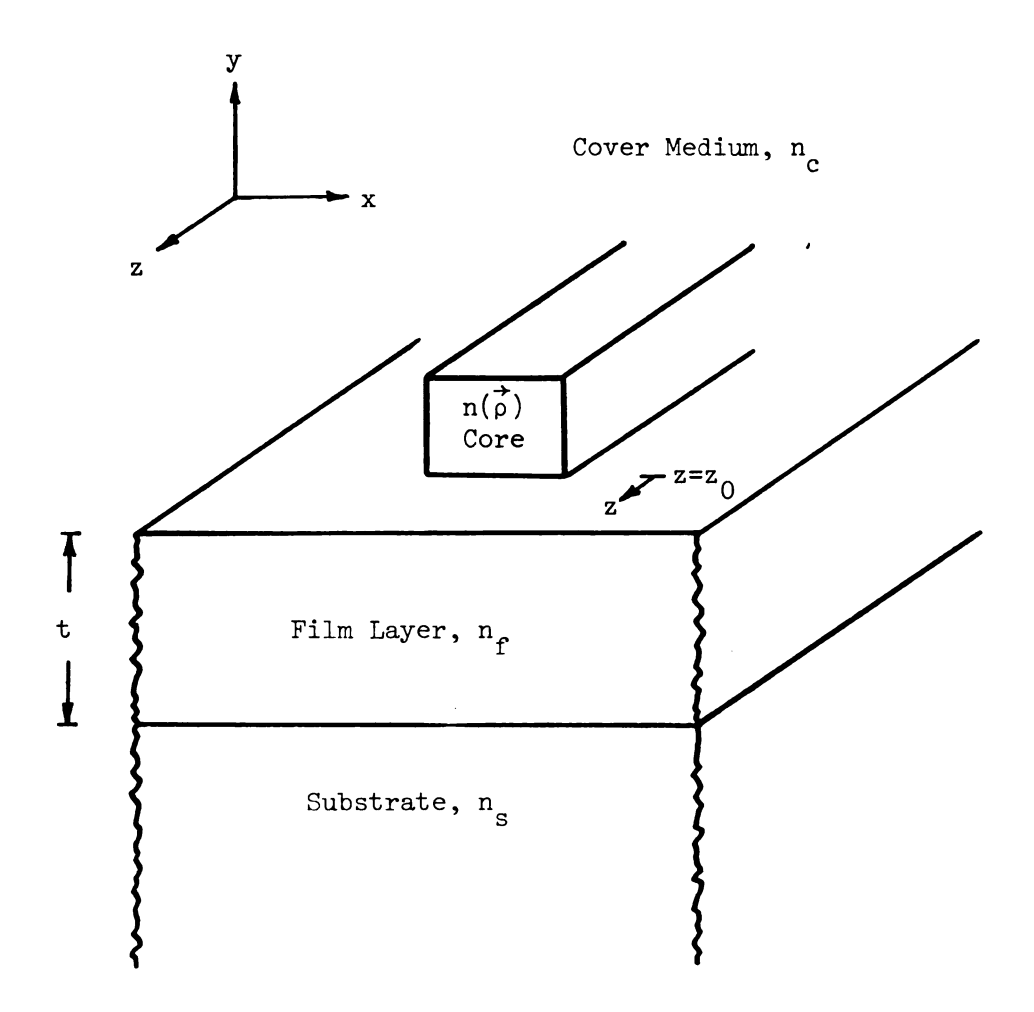


Figure 1.5: A plane truncated integrated rectangular dielectric strip waveguide with transversely graded core.

axis is taken as the z axis. This factor describes a waveguide core that is truncated at the plane $z=z_0$ and vanishes for all z greater than z_0 .

In the first part of chapter four we review some results from chapter three on the complete modal spectrum of a waveguide and develop notation to be utilized in the remainder of the chapter. We also introduce the concept of partial fields in a truncated waveguide. The two partial fields, \overrightarrow{E}^L and \overrightarrow{E}^R , are the total electric field in the system for points z behind and in front of the plane of truncation at $z = z_0$, respectively, and are zero elsewhere. The total electric field in the waveguiding system can be expressed in terms of these partial fields as $\overrightarrow{E} = \overrightarrow{E}^L + \overrightarrow{E}^R$. The partial fields play a central role in the analysis that follows.

In the second part of chapter four we analyze the problem of the reflection and radiation of a single surface wave mode of arbitrary amplitude that is incident on the truncation from within the waveguide. The partial field within the waveguide, \vec{E}^L , is written as a modal sum with unknown amplitude coefficients, and is substituted into the equivalent polarization integral equation. A linear integral operator, \mathscr{L}_m , is applied to the resultant expressions. This leads to an iterative equation which can be used to find the unknown reflected surface wave amplitudes in the modal expansion of \vec{E}^L . Once these reflected wave amplitudes are determined, the expressions also allow for evaluation of the electric field radiated out of the truncated waveguide, which is the partial field, \vec{E}^R .

In the third part of the chapter we examine the converse problem, that of excitation of surface waves in the truncated waveguide. There we assume that an impressed electric field is incident on the truncation from outside of the waveguide. A technique similar to that described above is applied to the equivalent polarization integral equation, resulting in an iterative formula for the unknown amplitudes of the surface wave modes excited in the waveguide.

We conclude the chapter in part four by applying the techniques developed in chapter four to the problem of coupling energy into and out of a truncated asymmetric slab waveguide. Numerical results are presented and discussed.

We conclude in chapter rive with some discussion and comments on the results of our applications of the equivalent polarization integral equation. Several promising areas for further study are identified.

2. EQUIVALENT POLARIZATION INTEGRAL EQUATION

In this chapter we develop an equivalent polarization electric field integral equation (EFIE) for the unknown total electric field in a generalized integrated dielectric waveguiding system. This integral equation provides the mathematical formulation or all of the topics addressed in this dissertation.

The physical system that the equivalent polarization integral equation is applicable to is a generalization of the types of integrated dielectric waveguides shown in Figures 1.1 through 1.5, and includes all of these waveguides as special cases. This generalized structure is depicted in Figure 2.1. The structure consists of an inhomogeneous dielectric obstacle, intended to represent a generalized integrated waveguide core, embedded in the ith layer of a background region which is composed of an arbitrary number N of stacked, homogeneous dielectric slabs. This background structure models a generalized version of the typical substrate, film, and cover regions of integrated dielectric waveguides.

The primary difficulty in obtaining the total electric field in a situation such as that depicted in Figure 2.1 consists of finding that part of the field scattered by the inhomogeneous dielectric obstacle (the waveguide core). We will instead solve the much simpler problem of finding the total electric field produced by a system of impressed electric currents radiating in the layered background region in the

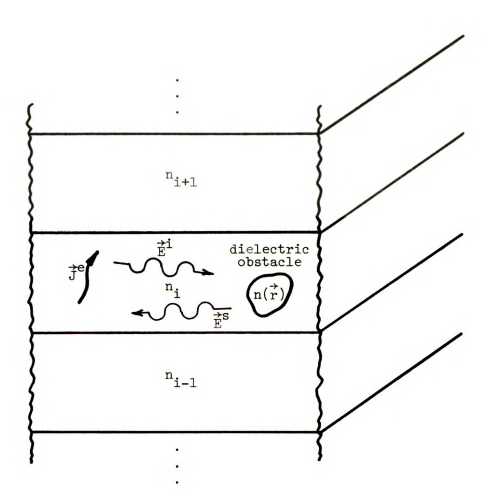


Figure 2.1: Generalized dielectric system described by the equivalent polarization integral equation.

absence of the inhomogeneous dielectric obstacle. The errects of the presence of the dielectric obstacle will be accounted for by the use of field equivalence principles. This technique involves replacing the inhomogeneous dielectric obstacle by a system of equivalent induced electric polarization sources in the volume previously occupied by the dielectric obstacle. The total electric field in the system is then given by the sum of the electric field produced by the impressed electric currents radiating in the background structure in the absence of the dielectric core plus the electric field produced by the equivalent induced electric polarization sources radiating in the same background region.

In this first part of the chapter we detail the mathematical development described above of the equivalent polarization integral equation. The second part or this chapter is devoted to presenting the dyadic Green's function which forms the kernel of the equivalent polarization integral equation. Details of the development of the Green's dyad are relegated to Appendix A.

2.1 Integral Equation

The equivalent polarization electric field integral equation is developed to describe the unknown total electric field in the system depicted in Figure 2.1. The system consists of an inhomogeneous dielectric obstacle embedded in the ith layer of a background region composed of an arbitrary number N of stacked infinite, homogeneous dielectric slabs. The inhomogeneous dielectric obstacle is described by a generally complex, spatially varying refractive index, $n(\vec{r})$. The

background slabs have uniform thicknesses t_j and constant complex refractive indices n_j , with $j=1,\dots,N$.

A system of impressed electric currents, $\vec{J}^e(\vec{r})$, in the ith layer provides an impressed electric field, denoted $\vec{E}^i(\vec{r})$. This impressed field is defined as the electric field which would be maintained in the system by the impressed electric currents \vec{J}^e radiating in the absence of the inhomogeneous dielectric obstacle, and thus includes the effects of field reflection from boundaries between adjacent uniform dielectric background layers. The impressed electric field is augmented by the scattered electric field, $\vec{E}^s(\vec{r})$. This scattered electric field is produced in the ith layer by the interaction of the impressed electric field with the inhomogeneous dielectric obstacle. The total electric field in the ith layer of the generalized waveguide system is then given by the sum of the incident and the scattered fields. We denote the total electric field in the ith layer as $\vec{E}(\vec{r})$, so that we have $\vec{E} = \vec{E}^1 + \vec{E}^s$.

2.1.1 Ampere's Law and Equivalent Polarization

The development of the equivalent polarization integral equation begins with Ampere's Law in the ith layer of the generalized waveguiding system of Figure 2.1:

$$\nabla \times \mathbf{H} = \mathbf{J}^{\mathbf{e}} + \mathbf{j} \omega \varepsilon_{0} \mathbf{n}^{2} \dot{\mathbf{E}}$$
 (1)

where a complex harmonic time dependence of $\exp(j\omega t)$ is assumed and suppressed. This convention is followed throughout the remainder of this work. We now define a refractive index contrast factor, $\delta n^2(r)$,

in the ith layer:

$$\delta n^{2}(\vec{r}) = n^{2}(\vec{r}) - n_{i}^{2} \tag{2}$$

The refractive index contrast is seen to be non-zero only in the region occupied by the inhomogeneous dielectric obstacle. Ampere's law can be written in terms of this contrast factor:

$$\nabla \times \vec{H} = \vec{J}^e + j\omega \varepsilon_0 \delta n^2 (\vec{r}) \vec{E} + j\omega \varepsilon_0 n_j \vec{E}$$
(3)

Consider the two displacement current terms on the right hand side of equation (3). We will associate the first displacement current term with the impressed current by writing it in terms of an equivalent polarization current, $\vec{P}_{eq}(\vec{r})$:

$$j\omega\varepsilon_0\delta n^{2\vec{E}} = j\omega \vec{P}_{eq} \tag{4}$$

Note that the second displacement current term in equation (3) is that which would be produced in the ith layer by the total electric field in the absence of the inhomogeneous dielectric obstacle. Then, with the impressed current written instead as an impressed polarization, \vec{J}^e = $j\omega \vec{P}^e$, we use equation (4) in equation (3) to obtain

$$\nabla \mathbf{x} \mathbf{H} = \mathbf{j} \omega [\vec{P}^e + \vec{P}_{eq}] + \mathbf{j} \omega \varepsilon_0 n_i \vec{E}$$
 (5)

Equation (5) is interpreted as stating that the total electric field in the ith layer, $\vec{E}(\vec{r})$, is supported by two electric polarization sources: an impressed polarization current, \vec{P}^e , which produces the impressed field, \vec{E}^i , and an equivalent induced electric polarization current, \vec{P}_{eq} , which exists in the region of the dielectric obstacle and produces the scattered electric field, \vec{E}^s . Then the total

electric field is given as the sum of the impressed and scattered fields, $\vec{E} = \vec{E}^1 + \vec{E}^S$.

What we have accomplished by using the definition (4) is to replace the original problem of finding the unknown total electric field in the system shown in Figure 2.1 with the equivalent problem or finding the unknown total electric field produced by the electric polarization sources \overrightarrow{P}^e and \overrightarrow{P}_{eq} radiating in the ith layer of the background structure in the absence of the inhomogeneous dielectric obstacle. This equivalent problem, which is depicted in Figure 2.2, is more readily solved than the original problem of Figure 2.1. The solution of this equivalent problem is the subject of the next section.

2.1.2 The Scattered Field

We now turn to the task of finding the scattered electric field, \vec{E}^s . As mentioned above, this is the field produced by the equivalent induced electric polarization sources occupying the volume of the inhomogeneous dielectric obstacle, \vec{P}_{eq} , radiating in the i^{th} background layer in the absence of the inhomogeneous dielectric obstacle. We will accomplish our task by first finding the scattered electric Hertzian potential, $\vec{\pi}^e(\vec{r})$, produced by the equivalent induced polarization, and then using the standard relationship between electric Hertzian potential and the associated electric field to find $\vec{E}^s(\vec{r})$.

The electric Hertzian potential satisfies an inhomogeneous vector Helmholtz equation [2.1],

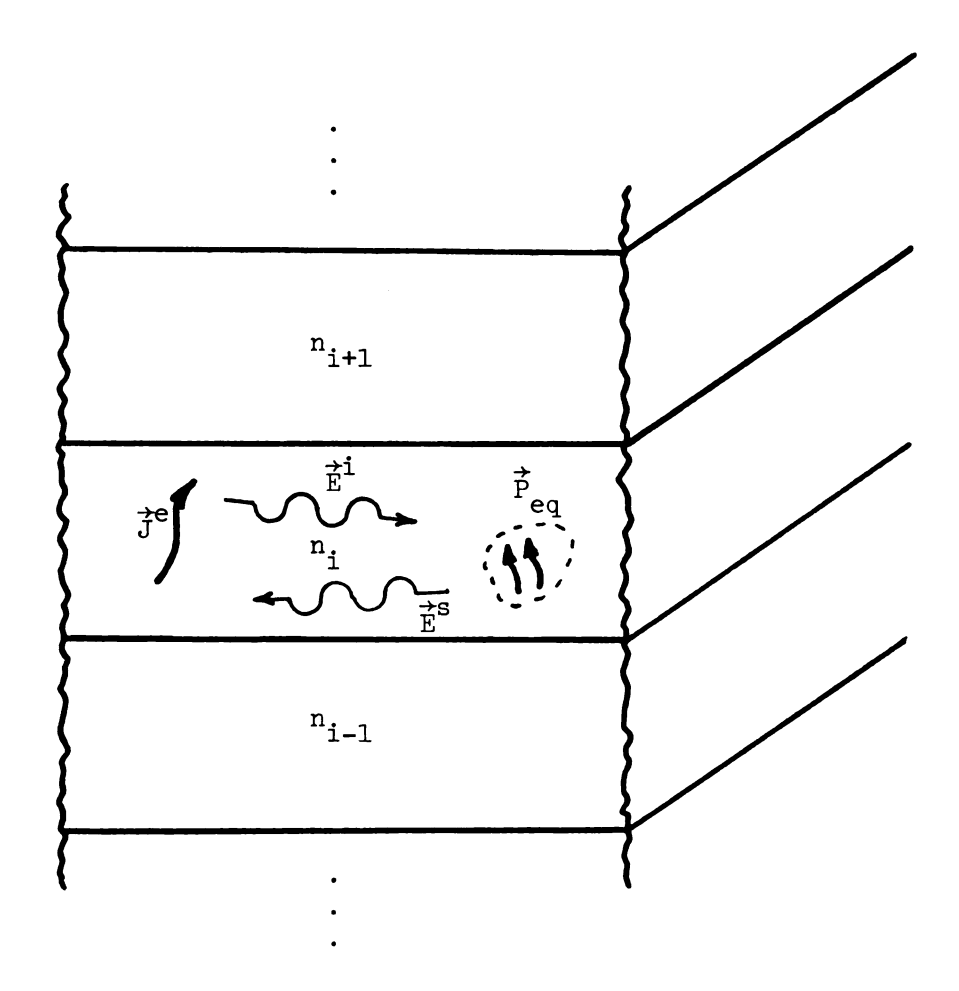


Figure 2.2: Field equivalent system to that in Figure 2.1 with induced equivalent polarization sources replacing the dielectric obstacle.

$$(\nabla^2 + k^2)_{\pi}^{\uparrow} = -\vec{P}/\epsilon \tag{6}$$

Since the scattered Hertzian potential is supported by the equivalent induced polarization \vec{P}_{eq} in the ith background layer, we have

$$(\nabla^2 + k_i^2)_{\pi}^{\dagger s} = - \vec{P}_{eq}/\epsilon_i \tag{7}$$

This forced vector Helmholtz equation has the well known (see [2.2]) formal solution

$$\vec{\pi}^{S} = \int_{V} \vec{G}(\vec{r}|\vec{r}') \cdot \frac{\vec{P}_{eq}(\vec{r}')}{\varepsilon_{i}} dV'$$
 (8)

in terms of the dyadic Green's function, G(r|r), appropriate to the layered background structure of Figure 2.2. This Hertzian potential Green's dyad is detailed in part two of this chapter and derived in Appendix A.

The scattered electric field is obtained from the scattered electric Hertzian potential in the usual manner [2.3]:

$$\vec{E}^{S} = (k_{i}^{2} + \nabla \nabla \cdot) \vec{\pi}^{S}$$
 (9)

Combining equations (8) and (9) results in an integral expression for the scattered electric field:

$$\vec{E}^{S}(\vec{r}) = (k_{i}^{2} + \nabla \nabla \cdot) \int_{V} \vec{G}(\vec{r}|\vec{r}') \cdot \frac{\vec{P}_{eq}(\vec{r}')}{\varepsilon_{i}} dV'$$
(10)

We now eliminate the equivalent induced polarization from equation (10) by substituting its definition from equation (4). We thus obtain

$$\vec{E}^{S}(\vec{r}) = (k_{i}^{2} + \nabla \nabla \cdot) \int_{V} \frac{\delta n^{2}(\vec{r}')}{n_{c}^{2}} \vec{G}(\vec{r}|\vec{r}') \cdot \vec{E}(\vec{r}') dV'$$
 (11)

We write the scattered electric field as $\vec{E}^S = \vec{E} - \vec{E}^i$ in equation (11) to obtain the equivalent polarization integral equation:

$$\vec{E}(\vec{r}) - (k_1^2 + \nabla \nabla \cdot) \int_{V} \frac{\delta n^2(\vec{r}')}{n_c^2} \vec{G}(\vec{r}|\vec{r}') \cdot \vec{E}(\vec{r}') dV' = \vec{E}^{\dot{i}}(\vec{r})$$
 (12)

This is an inhomogeneous integral equation satisfied by the unknown total electric field in the generalized dielectric waveguide system of Figure 2.1, with a forcing function $\vec{E}^i(r)$. This integral equation has several advantages over alternative integral and differential formulations of the problem. Since it is a Fredholm equation of the second kind (the unknown total field appears both inside and outside of the integral) it is in suitable form for application of iterative solution techniques, such as the Neumann series solution (see [2.4]). It is also particularly well suited for application of moment-method techniques, since the domain of integration extends only over the volume occupied by the dielectric obstacle, rather than over all of space.

2.1.4 Alternative Integral Equation

The equivalent polarization integral equation (12) can be cast into an alternative form by formally interchanging the order of integration and application of the differential operator $(k_1^2 + \nabla \nabla \cdot)$. This differential operator acts on unprimed coordinates which only occur in the dyadic Green's function. We can write the result as

$$\vec{E}(\vec{r}) - \int_{V} \frac{\delta n^{2}(\vec{r}')}{n_{i}^{2}} \vec{G}_{e}(\vec{r}|\vec{r}') \cdot \vec{E}(\vec{r}') dV' = \vec{E}^{1}(\vec{r})$$
(13)

where we have derined the electric Green's dyad:

$$\overrightarrow{G}_{\Theta}(\overrightarrow{r}|\overrightarrow{r'}) = P.V.(\overrightarrow{k_i} + \nabla \nabla \cdot) \overrightarrow{G}(\overrightarrow{r}|\overrightarrow{r'}) + \overrightarrow{L}\delta(\overrightarrow{r} - \overrightarrow{r'})$$
(14)

The notation P.V. means that the integration in (13) is understood to be in the Cauchy principle value sense [2.4], and the term $\stackrel{\leftrightarrow}{L}$ is a depolarization dyad introduced to cancel any artificially introduced polarization sources due to exclusion of principle volume region. These considerations are necessary since differentiation of the integrable Hertzian potential Green's dyad can lead to non-integrable singularities in the electric Green's dyad (see [2.5]). These points are discussed in further detail in part two of this chapter.

2.2 Dyadic Green's Function

In this section we present the dyadic Hertzian potential Green's function which forms the kernel of the equivalent polarization

integral equation (12). The details of the derivation of this Green's dvad are included in Appendix A.

The dyadic Green's function presented here is valid for a special case of the general situation depicted in Figure 2.2; this special case is shown in Figure 2.3. The Green's function describes the electric Hertzian potential produced in the upper layer of a three layered dielectric background region by an electric polarization source in the upper layer. This Green's function is appropriate to the ridge-type integrated dielectric waveguides or Figures 1.1, 1.2, 1.3 and 1.5, where the three layered background represents the substrate, film, and cover regions of these configurations. Note that this Green's dyad is not valid for the channel-type dielectric waveguide or Figure 1.4, since there the source and field points are in the middle layer of the background region (the film layer). The Hertzian potential Green's dyad appropriate to the channel waveguide is also derived in Appendix A, but will not be used in this dissertation.

2.2.1 Hertzian Potential Green's Dyad

The physical relationship between an electric polarization source and the electric Hertzian potential produced in waveguiding system of Figure 2.3 is as rollows: an infinitesimal polarization source $\vec{P}(\vec{r'})dV'$ at source point location $\vec{r'}$ produces at field point location $\vec{r'}$ the infinitesimal electric Hertzian potential $d^{\frac{1}{n'}}(r)$ given by (see [2.2])

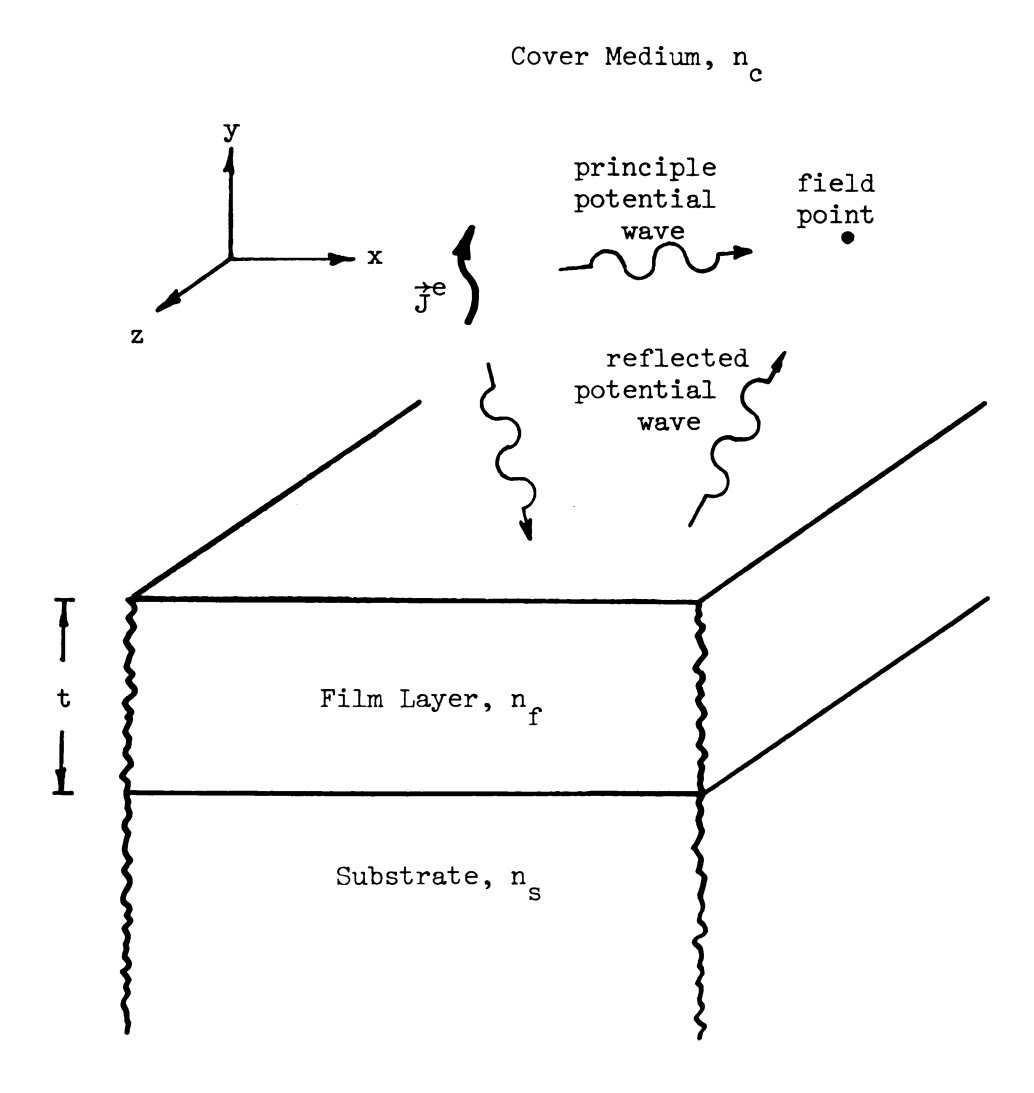


Figure 2.3: Integrated tri-layered background structure described by Hertzian potential Green's dyad.

$$d\vec{\pi}(\vec{r}) = \vec{G}(\vec{r}|\vec{r}') \cdot \frac{\vec{P}(\vec{r}')}{\varepsilon} dV'$$
 (15)

We will henceforth dispense with the index notation of part one of this chapter in describing the background regions, and instead use the subscripts s, f, and c to indicate the substrate, film, and cover regions of an integrated dielectric waveguide of the type in Figure 1.1.

It is clear from the geometry shown in Figure 2.3 that the total electric Hertzian potential in the cover region should be composed of two distinct parts, a principle part and a reflected part. The principle part is defined to be that part of the total Hertzian potential which is radiated directly through the uniform cover medium from source point to field point without undergoing reflection by the interfaces between adjacent dielectric background layers. The reflected part of the Hertzian potential is defined to be the remainder of Hertzian potential that does interact with the other background media before arriving at the field point. By considering equation (15) we see that this seperation or the total Hertzian potential into two distinct parts should manifest itself in a decomposition or the Hertzian potential Green's dyad into two parts, which we call the principle and reflected parts of the Green's dyad. This fact is mathematically demonstrated in the derivation in Appendix Α.

By the above considerations, the principle part of the Hertzian potential Green's dyad is seen to be the Green's dyad for the electric Hertzian potential produced by an electric polarization source radiating in an unbounded cover medium. This follows since such a

physical situation would result Hertzian potential radiated directly from source point to field point without undergoing reflection between media interfaces, which was our definition of the principle part of the Hertzian potential. This observation allows us to completely characterize the principle part of the Green's dyad, since the solution to an inhomogeneous vector Helmholtz equation such as equation (7) in an unbounded region is well known (see [2.6]). First, it is known that the vector direction of the solution depends solely on the direction of the source term. Hence the principle Green's dyad should be proportional to the unit dyad, $\overrightarrow{1}$. Secondly, the scalar amplitude of the Green's dyad in this situation has the well known form of the three dimensional Green's function for the scalar

There are no such simple arguements which allow us to deduce the form of the reflected part of the Green's dyad. This is due in main part to the complicated boundary conditions obtaining for electric Hertzian potential at material interfaces, which include coupling between spatial components of the Hertzian potential at the interface.

With this introduction, we now present the dyadic Hertzian potential Green's function for the physical situation depicted in Figure 2.3. As mentioned above, the Green's dyad decomposes into a principle and a reflected part:

$$\vec{G}(\vec{r}|\vec{r}') = \vec{G}^{p}(\vec{r}|\vec{r}') + \vec{G}^{r}(\vec{r}|\vec{r}')$$
 (16)

where the principle part is proportional to the unit dyad, $\overrightarrow{1}$:

$$\stackrel{\leftrightarrow}{G}^{p}(\stackrel{\rightarrow}{r}|\stackrel{\rightarrow}{r}) = \stackrel{\leftrightarrow}{I}G^{p}(\stackrel{\rightarrow}{r}|\stackrel{\rightarrow}{r})$$
(17)

and the scalar amplitude of the principle part is the above mentioned three dimensional Green's function for an unbounded medium of refractive index \mathbf{n}_{o} :

$$G^{p}(\overrightarrow{r}|\overrightarrow{r}') = \frac{e^{-jk_{c}|r-r'|}}{4\pi|r-r'|}$$
(18)

and $k_c = n_c k_0$, with k_0 the free-space wavenumber, $k_0 = \omega / c$.

The reflected part of the Hertzian potential Green's dyad has a more complicated dyadic form with non-zero off-diagonal terms. The off-diagonal terms are due to the coupling of Hertzian potential spatial components at the media interfaces. The reflected Green's dyad is given by

$$\stackrel{\leftrightarrow}{G}^{r} \stackrel{\rightarrow}{(r|r')} = \hat{x}G_{t}^{r} \hat{x} + \hat{y}(\frac{\partial}{\partial x} G_{c}^{r} \hat{x} + G_{n}^{r} \hat{y} + \frac{\partial}{\partial z} G_{c}^{r} \hat{z}) + \hat{z}G_{t}^{r} \hat{z}$$
 (19)

The different components in the reflected Green's dyad are derived in Appendix A as two dimensional spatial inverse Fourier transforms.

These integral representations of the Sommerfeld type are shown there to be

$$\begin{cases}
\vec{G}_{t}^{r}(\vec{r}|\vec{r}') \\
\vec{G}_{n}^{r}(\vec{r}|\vec{r}')
\end{cases} = \int_{-\infty}^{\infty} \begin{cases}
R_{t}(\xi) \\
R_{n}(\xi)
\end{cases} \frac{e^{j\vec{\xi}\cdot(\vec{r}-\vec{r}')}e^{-p_{c}(y+y')}}{2(2\pi)^{2}p_{c}} d^{2}\xi$$
(20)

Here $\vec{\xi}$ is a two dimensional spatial frequency variable given by

$$\vec{\xi} = \xi_{\mathbf{X}} \hat{\mathbf{x}} + \xi_{\mathbf{Z}} \hat{\mathbf{z}}$$

$$\xi^{2} = \xi_{\mathbf{X}}^{2} + \xi_{\mathbf{Z}}^{2}$$

$$d^{2}\xi = d\xi_{\mathbf{X}} d\xi_{\mathbf{Z}}$$
(21)

and $\textbf{p}_{\textbf{C}}(\xi)$ is one among the transverse wavenumber parameters defined for each dielectric layer as

$$p_{\ell}(\xi) = \sqrt{\xi^2 - k_{\ell}^2}$$

$$\ell = s, r, c$$

$$k_{\ell} = n_{\ell}k_{0}$$
(22)

where subscripts c, f, and s indicate the cover, film, and substrate regions of the background media in Figure 2.3, as mentioned above. The reflection coerricients $R_t(\xi)$ and $R_n(\xi)$ for potential components tangential and normal to the media interfaces, as well as the coupling coerricient, $C(\xi)$, all depend on the constituitive parameters and transverse wavenumbers of the various dielectric background layers in a complicated manner. They are detailed in Appendix A.

The notation t, n, and c used in equation (19) indicates the physical properties of the various Hertzian potential reflected Green's dyad components. By considering equation (15) we see that the reflected components of Hertzian potential tangential to the background layer interfaces are maintained by tangential polarization components through the terms involving the tangential reflected Green's function $G_{\mathbf{t}}^{\mathbf{r}}$. Similarly, the reflected component of Hertzian potential normal to the background interfaces is maintained by normal polarization sources through the normal reflected Green's function $G_{\mathbf{n}}^{\mathbf{r}}$ and also to tangential polarization components through terms involving derivatives of the coupling reflected Green's function $G_{\mathbf{c}}^{\mathbf{r}}$. The components of the reflected Green's dyad involving $G_{\mathbf{c}}^{\mathbf{r}}$ are due to the above mentioned complicated boundary conditions for Hertzian potential that couple tangential and normal polarization components at material interfaces.

The total Hertzian potential dyadic Green's function shares an important property with all such Green's functions in electromagnetics. This property is the reciprocity of the Green's dyad ([2.7]), and is a consequence of the Lorentz reciprocity lemma. Symbolically, the reciprocity of the Green's dyad can be stated

$$\overrightarrow{A}(\overrightarrow{r}) \cdot \overrightarrow{G}(\overrightarrow{r}|\overrightarrow{r'}) \cdot \overrightarrow{B}(\overrightarrow{r}) = \overrightarrow{B}(\overrightarrow{r'}) \cdot \overrightarrow{G}(\overrightarrow{r'}|\overrightarrow{r}) \cdot \overrightarrow{A}(\overrightarrow{r})$$
(23)

where it is understood that the indicated equality holds when the expression is integrated over both primed and unprimed coordinates. Here, $\overrightarrow{A(r)}$ and $\overrightarrow{B(r)}$ are two arbitrary electromagnetic vector source functions. This reciprocity property will be used several times in the remainder of this dissertation.

We mention for future reference at this point that the reflection and coupling coefficients detailed in Appendix A have pole singularities when ξ becomes complex and also appropriate branches of the now multi-valued transverse wavenumber parameters must be chosen. This fact will allow us later to cast the integrals in equation (20) in a more tractable form by exploiting the residue theorem of complex variables.

It is shown in Appendix A that the principle Hertzian potential Green's function of equation (18) can also be represented in a form first advanced by Banos [2.8] as a two dimension spatial inverse Fourier transform. The result is the Sommerfeld-type integral representation

$$G^{p}(\vec{r}|\vec{r}') = \int_{-\infty}^{\infty} \frac{e^{j\vec{\xi} \cdot (\vec{r} - \vec{r}')} e^{-p_{c}|y-y'|}}{2(2\pi)^{2}p_{c}} d^{2}\xi$$
 (24)

with the parameters of the integral defined as above.

The physical relationship between an electric polarization source and the electric field it produces in the waveguiding system of Figure 2.3 is as follows: An infinitesimal polarization source $\vec{P}(\vec{r'})dV'$ at source point location $\vec{r'}$ produces at the field point \vec{r} the infinitesimal electric field $d\vec{E}(\vec{r})$ given by

$$d\vec{E}(\vec{r}) = \vec{G}_{e}(\vec{r}|\vec{r}') \cdot \frac{\vec{P}(\vec{r}')}{\varepsilon_{c}} dV'$$
 (25)

The Hertzian potential Green's dyad incorporates a source point singularity through the factor $|\overrightarrow{r}-\overrightarrow{r'}|$ in the principle Green's function of equation (18). It is in this form an integrable singularity (see [2.5], [2.9]). However, once we differentiate the Hertzian potential Green's dyad as in equation (14) to form the electric field Green's dyad the singularity may no longer be integrable. In that case the integration in equation (13) must be performed in the principle value sense and a three dimensional depolarizing dyad \overrightarrow{L} must be introduced to cancel any artificially introduced polarization sources due to exclusion of the principle volume region V_{δ} . If S_{δ} is the closed surface surrounding the principle volume region, the \overrightarrow{L} is given by ([2.10], [2.11])

$$\stackrel{\leftrightarrow}{L} = - \lim_{S_{\delta} \to 0} \oint_{S_{\delta}} \frac{\hat{n}'(\vec{r} - \vec{r}')}{4\pi |\vec{r} - \vec{r}'| 3} dS' \tag{26}$$

with $\hat{\bf n}'$ the outward normal to the surface $S_{\hat{\delta}}$. This factor is calculated for several common principle volume regions by Yaghjian in [2.10].

3. LONGITUDINALLY INVARIANT WAVEGUIDES

In this chapter we specialize the equivalent polarization integral equation of the previous chapter to the case of axially uniform waveguides. Several typical axially uniform integrated dielectric waveguide configurations are shown in Figures 1.2, 1.3 and 1.4. The uniformity along the waveguiding axis displayed by these systems allows us to bring the powerful tool of Fourier transform theory to bear on the problems considered in this chapter.

This axial uniformity manifests itself in the integral equation (2.12) by making the integration in the variable z' convolutional in nature. This prompts a Fourier transform of the entire equation on the axial variable, with a resulting reduction in dimension of the domain of integration.

In the first part of this chapter we obtain the Fourier transformed equivalent polarization integral equation. It is an inhomogeneous Fredholm integral equation for the unknown Fourier transformed total electric field in the waveguiding system. The kernel of this integral equation is the axial Fourier transform of the dyadic Green's function of the previous chapter. It is detailed in the second part of this chapter. The remainder of this chapter is devoted to applications of the axially transformed integral equation.

In the third part of this chapter we develop a general excitation theory for axially uniform integrated dielectric waveguides. This

theory is based on formal Fourier inversion of the unknown axially transformed total field in the waveguiding system. The transformed field has in general both pole and branch point singularities in the complex axial transform variable plane. Deformation of the Fourier inversion contour in the complex transform variable plane and subsequent application of the residue theorem of complex variables allows us to write the total field as a sum of two distinct terms. The first term is a sum of the residues of the transformed field at the poles enclosed in the deformed inversion contour, and the second term consists of integrals around any branch cuts associated with enclosed branch points. This decomposition allows us to characterize the complete modal spectrum of any axially uniform integrated dielectric waveguide: surface waves of the guiding system are associated with the residues at the enclosed poles, and the radiation field of the waveguide is associated with the branch integrals. This analysis also provides us with the excitation amplitudes of the various surface wave modes and radiation field spectral components in terms of the incident excitatory electric field or current. Another reature of this analysis is its ability to describe the important physical phenomena of guided mode leakage and resonance. We close this part of the chapter by applying this excitation theory to the problem of excitation of transverse electric modes in the asymmetric slab waveguide. The resulting modal and spectral component amplitudes are shown to be identical with those predicted by conventional excitation theory.

Our last application of the Fourier transformed integral equation is found in part four of this chapter. We apply the axially

transformed equivalent polarization integral equation to the problem of finding the surface waves supported by the rectangular strip waveguide. This integrated dielectric waveguiding system is depicted in Figure 1.3. It is a configuration of considerable interest to workers in integrated optics. We begin by postulating a sinusoidal representation with unknown amplitudes and transverse spatial frequencies for the unknown axially transformed longitudinal components of the total electric and magnetic fields in the waveguide core. The axially transformed version of Maxwell's equations enable us to find all other transformed field components in terms of these two generating functions. Substitution of the resultant expression for the total axially transformed electric field into the transformed integral equation and point-matching the equation at rour locations inside of the waveguide core allows us to solve for the unknown amplitude and transverse spatial frequency constants as well as the axial propagation constant in our expressions for the total transformed electric rield in the waveguide core. We thus obtain an approximate closed form expression for the fields of various guided surface wave modes of the integrated rectangular strip waveguide.

3.1 Transformed Integral Equation

In this section we will specialize the general equivalent polarization integral equation of chapter two to the case of a longitudinally invariant waveguiding system. A generalized longitudinally invariant integrated dielectric waveguide is depicted in Figure 3.1. The axial uniformity of the waveguide will allow us to

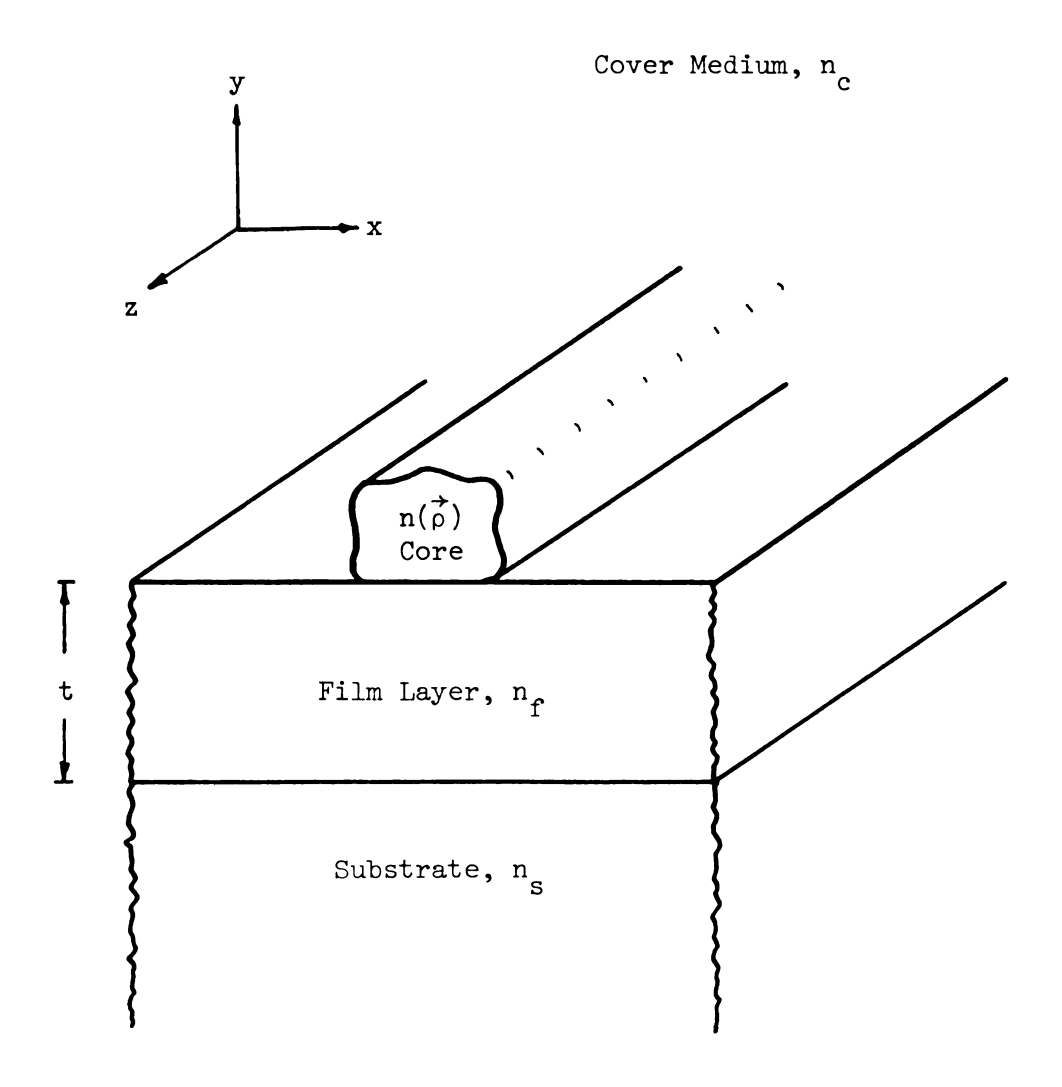


Figure 3.1: A general axially uniform dielectric waveguide integrated over a tri-layered background structure.

Fourier transform the entire integral equation on the axial variable. The result is an axially transformed inhomogeneous integral equation for the unknown transformed total electric field in the waveguiding system.

3.1.1 Longitudinal Invariance

In the case of a waveguide core of arbitrary but constant transverse cross section and arbitrary transverse grading, the refractive index contrast factor of equation (2.2) depends only on transverse position variables $\vec{\rho} = x\hat{x} + y\hat{y}$. Thus we will write the refractive index contrast as $\delta n^2(\vec{\rho})$. It is also clear from the infinite symmetry of the uniform dielectric background layers in Figure 3.1 that the (z|z') dependence in the Green's dyad $\vec{G}(\vec{r}|\vec{r}')$ for this structure is of the form (z-z') (see equations (2.20) and (2.23)). Thus we can write the equivalent polarization integral equation (2.21) in this case as

$$\vec{E}(\vec{\rho},z) - (k_c^2 + \nabla \nabla \cdot) \int_{CS} \int_{-\infty}^{\infty} \frac{\delta n^2(p')}{n_c^2} \vec{G}(\vec{\rho}|\vec{\rho}';z-z') \cdot \vec{E}(\vec{\rho},z') dS' dz'$$

$$= \vec{E}^1(\vec{\rho},z)$$
(1)

where CS denotes the constant transverse cross-section of the waveguide core in Figure 3.1. Note that the axial integral in equation (1) is convolutional in nature. This prompts the use of a spatial Fourier transform on the axial variable, z, so that the convolution property of Fourier transform theory can be exploited.

Given a vector field $\vec{f}(\vec{\rho},z)$, we define the axial Fourier transform, $f(\vec{\rho},\zeta)$, as satisfying the relations [3.1]

$$\vec{\mathbf{r}}(\vec{\rho},\zeta) = \int_{-\infty}^{\infty} \vec{\mathbf{f}}(\vec{\rho},z) e^{-\mathbf{j}\zeta z} dz$$

$$\vec{\mathbf{F}}(\vec{\rho},z) = \frac{1}{2\pi} \int_{-\infty}^{\infty} \vec{\mathbf{r}}(\vec{\rho},\zeta) e^{\mathbf{j}\zeta z} d\zeta$$
(2)

This relation will be written as

$$\vec{\mathbf{f}}(\vec{\rho},\zeta) = \mathcal{F}\{\vec{\mathbf{f}}(\vec{\rho},z)\}\$$

$$\vec{\mathbf{f}}(\vec{\rho},z) = \mathcal{F}^{-1}\{\vec{\mathbf{f}}(\vec{\rho},\zeta)\}\$$
(3)

or, more simply, $\vec{f}(\vec{\rho},z) \leftrightarrow \vec{f}(\vec{\rho},\zeta)$, to denote that $\vec{f}(\vec{\rho},z)$ and $\vec{f}(\vec{\rho},\zeta)$ are an axial Fourier transform pair satisfying equations (2).

3.1.3 Transformed Integral Equation

In Fourier transforming the integral equation (1) for axially uniform waveguides we need two results of standard Fourier theory: the differentiation theorem and the convolution theorem. The former allows us to transform the differential operators in equation (1). Symbolically, it states $\frac{\partial}{\partial z} \leftrightarrow j_{\zeta}$ [3.2]. Thus we can transform the del-operator as $\nabla \leftrightarrow \widetilde{\nabla}$, with

$$\widetilde{\nabla} = \nabla_{+} + j\zeta \hat{z} \tag{4}$$

and $\nabla_t = \hat{x} \frac{\partial}{\partial x} + \hat{y} \frac{\partial}{\partial y}$ as usual. The convolution theorem can be written as $\vec{F} * \vec{G} \leftrightarrow \vec{r} \cdot \vec{g}$, where the operation * denotes convolution of the dot

product of two vectors [3.3]. We use these results in Fourier transforming equation (1). The result is

$$\vec{e}(\vec{\rho},\zeta) - (k_c^2 + \widetilde{V}\widetilde{V}) \int_{CS} \frac{\delta n^2(\vec{\rho}')}{n_c^2} \vec{g}_{\zeta}(\vec{\rho}|\vec{\rho}') \cdot \vec{e}(\vec{\rho},\zeta) dS'$$

$$= \vec{e}^1(\vec{\rho},\zeta)$$
(5)

This is an inhomogeneous integral equation satisfied by the total uniform axially transformed electric field in the waveguide core. The kernel of the integral equation is the Fourier transform of the dyadic Green's function of the previous chapter. It is detailed in part two of this chapter.

3.1.4 Alternative Transformed Integral Equation

An alternative Fourier transformed equivalent polarization integral equation can be obtained by Fourier transforming the alternative integral equation (2.13) of chapter two. We first use the results of section 3.1.1 to specialize equation (2.13) to the case of an axially uniform waveguiding system:

$$\vec{E}(\vec{\rho},z) - \int_{-\infty}^{\infty} \int_{CS} \frac{\delta n^{2}(\vec{\rho}')}{n_{c}^{2}} \vec{G}_{e}(\vec{\rho}|\vec{\rho}'; z-z') \cdot \vec{E}(\vec{\rho},z') dS'dz'$$

$$= \vec{E}^{i}(\vec{\rho},z)$$
(6)

We now Fourier transform equation (6) on the axial variable and make use of the convolution theorem to obtain the alternative transformed integral equation:

$$\vec{e}(\vec{\rho},\zeta) - \int_{CS} \frac{\delta n^2(\vec{\rho}')}{n_0^2} \vec{g}_{e_{\zeta}}(\vec{\rho}|\vec{\rho}') \cdot \vec{e}(\vec{\rho}',\zeta) dS' = \vec{e}^{\dot{i}}(\vec{\rho},\zeta)$$
 (7)

The kernel of this integral equation is the Fourier transform of the electric dyadic Green's function of equation (2.14). Care must again be exercised to perform the integration in equation (7) in the Cauchy principle value sense. The transformed electric Green's dyad is detailed in part two of this chapter.

3.2 Transformed Green's Dyad

In this section we present the Fourier transformed dyadic Green's functions which form the kernels of the axially transformed equivalent polarization integral equations of the previous section. The details of the derivations of the original Green's dyads are given in Appendix A. It is an easy matter to Fourier transform the Green's dyads, since they are derived in Appendix A as two dimensional inverse spatial Fourier transforms. Thus, transforming the Green's dyads can be accomplished by simply removing the Fourier inversion integral corresponding to the axial transform variable.

3.2.1 Hertzian Potential Green's Dyad

The transformed Hertzian potential dyadic Green's function is defined as

$$\mathscr{F}\{\overrightarrow{G}(\overrightarrow{r}|\overrightarrow{r'})\} = \overrightarrow{g}_{\zeta}(\overrightarrow{\rho}|\overrightarrow{\rho'})e^{-j\zeta z'}$$
(8)

where $\overrightarrow{G}(\overrightarrow{r}|\overrightarrow{r'})$ is as given in section 2.2.1. The transformed Green's dyad has the rollowing physical interpretation: an infinitesimal

axially transformed polarization source $p(\rho',\zeta)$ dS' at location ρ' produces at location an infinitesimal transformed electric Hertzian potential, $d_{\pi}^{\dagger e}(\rho,\zeta)$, given by

$$d\vec{\pi}(\vec{\rho},\zeta) = \vec{g}_{\zeta}(\vec{\rho}|\vec{\rho}) \cdot \frac{\vec{p}(\vec{\rho},\zeta)}{n_{c}} dS'$$
(9)

We know by equation (2.16) and the linearity of the Fourier transform that the axially transformed Green's dyad decomposes into two parts, the principle and reflected parts. It thus has the form

$$\overrightarrow{g}_{\zeta}(\overrightarrow{\rho}|\overrightarrow{\rho}') = \overrightarrow{g}^{p}(\overrightarrow{\rho}|\overrightarrow{\rho}') + \overrightarrow{g}_{\zeta}(\overrightarrow{\rho}|\overrightarrow{\rho}')$$
(10)

The principle part is the Fourier transform of the principle Green's function of equation (2.18). This transform is the well known [3.4] two dimensional Green's function:

$$\overrightarrow{g}_{\zeta}^{p}(\overrightarrow{\rho}|\overrightarrow{\rho'}) = \overrightarrow{I}\mathscr{F}\{G^{P}(\overrightarrow{r}|\overrightarrow{r'})\} = \overrightarrow{I}\frac{1}{2\pi}K_{0}(\gamma_{c}|\overrightarrow{\rho-\rho'}|)$$
(11)

where \mathbf{K}_0 is the modified Bessel function of the second kind of order zero, and

$$\gamma_{c} = \sqrt{\zeta^2 - k_{c}^2} \tag{12}$$

The reflected part of the transformed Hertzian potential Green's dyad has the more complicated dyadic form

$$\frac{\partial^{r}}{g_{\zeta}^{r}}(\hat{\rho}|\hat{\rho}') = \hat{x}g_{\zeta t}^{r}\hat{x} + \hat{y}(\frac{\partial}{\partial x}g_{\zeta c}^{r}\hat{x} + g_{\zeta n}^{r}\hat{y} + j\zeta g_{\zeta c}^{r}\hat{z})
+ \hat{z}g_{\zeta t}^{r}\hat{z}$$
(13)

where we have transformed equation (2.19) with the help of the Fourier differentiation theorem. The components of the reflected Green's dyad

are the Fourier transforms of the components of equation (2.20). As mentioned above, these transforms are easy to find since the components of the reflected Hertzian potential Green's dyad in equation (2.20) are written as two dimensional inverse spatial Fourier transforms. Thus we can forward transform equation (2.20) on the axial variable by omitting the inversion operation corresponding to the axial transform variable. This variable is $\xi_{\rm Z}$ in equation (2.20). In this chapter we are denoting the axial transform variable as ζ , so we also make the substitution $\xi_{\rm Z} + \zeta$ and $\xi_{\rm X} + \xi$ in equation (2.20) and omit the $\xi_{\rm Z}$ integral to obtain

$$\begin{cases}
g_{\zeta t}^{r}(\overrightarrow{\rho}|\overrightarrow{\rho}^{\prime}) \\
g_{\zeta n}^{r}(\overrightarrow{\rho}|\overrightarrow{\rho}^{\prime}) \\
g_{\zeta c}^{r}(\overrightarrow{\rho}|\overrightarrow{\rho}^{\prime})
\end{cases} = \int_{-\infty}^{\infty} \begin{cases}
R_{t}(\xi) \\
R_{n}(\xi) \\
C(\xi)
\end{cases} = \frac{e^{j\pi(x-x^{\prime})}e^{-p_{c}(y+y^{\prime})}}{4\pi p_{c}} d\xi$$
(14)

where ξ is the remaining spatial frequency variable and a factor of 2π was canceled by the same factor occurring in equation (2) defining the inverse Fourier transform. We must also be careful to redefine the transverse wavenumber parameters of equation (2.22). They now become

$$p_{\ell} = \sqrt{\xi^2 + \zeta^2 - k_{\ell}^2}$$

$$k_{\ell} = n_{\ell} k_{0}$$

$$\ell = c, r, s$$
(15)

where the subscripts c, f, and s again indicate the cover, film, and substrate regions in the system depicted in Figure 3.1. The reflection and coupling coefficients R_t , R_n , and C are identical with those listed in Appendix A with the transverse wavenumbers given by the new expressions in equation (15). They again depend in a

rather complicated manner on the constituitive parameters of the background media.

We can write the transformed principle Green's function as a one dimensional spectral superposition integral by starting with the expression of equation (2.23) and following the same steps as outlined above for the reflected Green's dyad. The result is

$$g_{\zeta}^{p}(\overrightarrow{\rho}|\overrightarrow{\rho'}) = \int_{-\infty}^{\infty} \frac{e^{j \xi(x-x')}e^{-p_{c}|y-y'|}}{4\pi p_{c}} d\xi$$
 (16)

where the parameters in the integral are as given above.

This transformed Green's dyad satisfies a reciprocity property similar to that discussed in chapter two. In this case the reciprocity property is

$$\overrightarrow{a}(\overrightarrow{\rho},\zeta) \cdot \overrightarrow{g}_{\zeta}(\overrightarrow{\rho}|\overrightarrow{\rho'}) \cdot \overrightarrow{b}(\overrightarrow{\rho'},\zeta) \cdot \overrightarrow{g}_{\zeta}(\overrightarrow{\rho'}|\overrightarrow{\rho}) \cdot \overrightarrow{a}(\overrightarrow{\rho},\zeta)$$
(17)

where it is understood that the above expression is integrated over both primed and unprimed spatial coordinates.

3.2.2. Electric Green's Dyad

The kernel of the axially transformed alternative integral equation includes the transformed electric Green's dyad, $\stackrel{\leftrightarrow}{g}_{e_{\zeta}}$. This dyad has the following physical significance: an infinitesimal axially uniform transformed polarization source $\stackrel{\leftrightarrow}{p}(\stackrel{\rightarrow}{\rho},\zeta)$ dS' at source location $\stackrel{\rightarrow}{\rho}$ ' produces at field point ρ and infinitesimal transformed electric field $\stackrel{\rightarrow}{de}(\stackrel{\rightarrow}{\rho},\zeta)$ satisfying

$$\overrightarrow{de}(\overrightarrow{\rho},\zeta) = \overrightarrow{g}_{e_{\zeta}}(\overrightarrow{\rho},\overrightarrow{\rho'}) \cdot \frac{\overrightarrow{p}(\overrightarrow{\rho'},\zeta)}{\varepsilon} dS'$$
(18)

This Green's dyad is obtained by Fourier transforming the electric Green's dyad of equation (2.14) on the axial variable with the aid of the Fourier differentiation theorem. The result is

$$\frac{d}{d\theta} = \sqrt{(|\vec{\rho}| |\vec{\rho}|)} = P.V.(k_c^2 + |\vec{\nabla}\vec{\nabla}|) + |\vec{Q}| + |\vec{Q$$

where we must again take care to evaluate the possibly improper integral occurring in the integral equation in the Cauchy principle value sense. The two dimensional depolarizing dyad, \hat{k} , is included in order to cancel any artificially introduced polarization due to the axially uniform excluded source region. If C_{δ} is the closed contour surrounding the principle volume surface S_{δ} , then the appropriate depolarizing dyad can be found as in Yaghjian [3.5]:

$$\stackrel{\leftrightarrow}{\mathcal{L}} = - \lim_{C_{\mathcal{L}} \to 0} \oint \frac{\hat{\mathbf{n}}'(\vec{\rho} - \vec{\rho}')}{2\pi |\vec{\rho} - \vec{\rho}'|^2} d\ell' \tag{20}$$

with $\hat{\mathbf{n}}$ ' the outward normal to the contour \mathbf{C}_{δ} .

3.3 Excitation of Integrated Waveguides

In this part we address the problem of excitation of axially uniform integrated dielectric waveguides. This theory is based on the formal Fourier inversion of the unknown transformed total electric rield in the waveguide core, where the transformed total rield satisfies the transformed equivalent polarization integral equation (5). The Fourier inversion process is carried out with the aid of the residue theorem of complex variables.

We modify the real line Fourier inversion integration path in the transform variable plane to enclose the upper half complex plane and then analyze the behavior of the transformed total field inside of this closed contour. This analysis leads in a natural manner to a division of the complete modal spectrum of any such axially uniform dielectric waveguide into two distinct parts: the surface wave modes of the waveguide and the radiation field.

The surface wave modes are associated with the residues of the integrand of the Fourier inversion integral at simple poles inside of the deformed inversion contour. It is shown that the residues also yield the amplitudes of the various surface wave modes in terms of the incident field or current exciting the waveguide. Similarly, the radiation field of an axially uniform dielectric waveguide is associated with the integration around branch cuts in the complex transform variable plane which the deformed Fourier inversion contour must detour around. Such branch cuts are made necessary by the presence of multi-valued transverse wavenumber parameters with branch points in the upper half complex plane which occur in the dyadic Green's function of the transformed integral equation. The branch integrals are viewed as a continuous superposition of radiation field spectral components, and give the spectral amplitudes of the radiation field in terms of the incident field or current which excites the integrated waveguide.

Another result of the complex transform variable analysis is a mathematical description of the physical process of mode leakage in an integrated dielectric waveguide. We are able to predict which surface waves in a guiding system are likely to leak based on the location of

pole singularities of the transformed reflected Green's dyad in the complex plane.

We close this section with an example of this excitation theory applied to a simple guiding structure. We examine the problem of line source excitation of TE surface waves and the TE radiation field in an asymmetric slab waveguide. The results are shown to be identical with those obtained by conventional waveguide excitation theory.

3.3.1 Residue Theorem

Here we sketch the development of residue theorem of complex variables, which forms the basis of our excitation theory. Consider the closed path integral $\phi r(\zeta)$ d ζ around a contour in the complex ζ plane such as that shown in Figure 3.2. The residue theorem states that under certain conditions

$$\oint \mathbf{r}(\zeta) d\zeta = 2\pi \mathbf{j} \sum_{n} \underset{\zeta_{n}}{\text{Res}} \{ \mathbf{r}(\zeta) \}$$
 (21)

where Res denotes the residue of the integrand at a pole enclosed by the closed integration contour. The conditions under which this formula is valid are that the function $r(\zeta)$ must be analytic at all points inside of the contour except for pole singularities at the ζ_n , and must be analytic everywhere on the contour [3.6]. If the integrand contains multi-valued parameters we must be sure to choose suitable branches of these parameters in the complex plane, and to not violate the choice anywhere inside of the integration contour. One way to accomplish this is to choose a branch cut extending from the branch point of a multi-valued parameter out to complex infinity

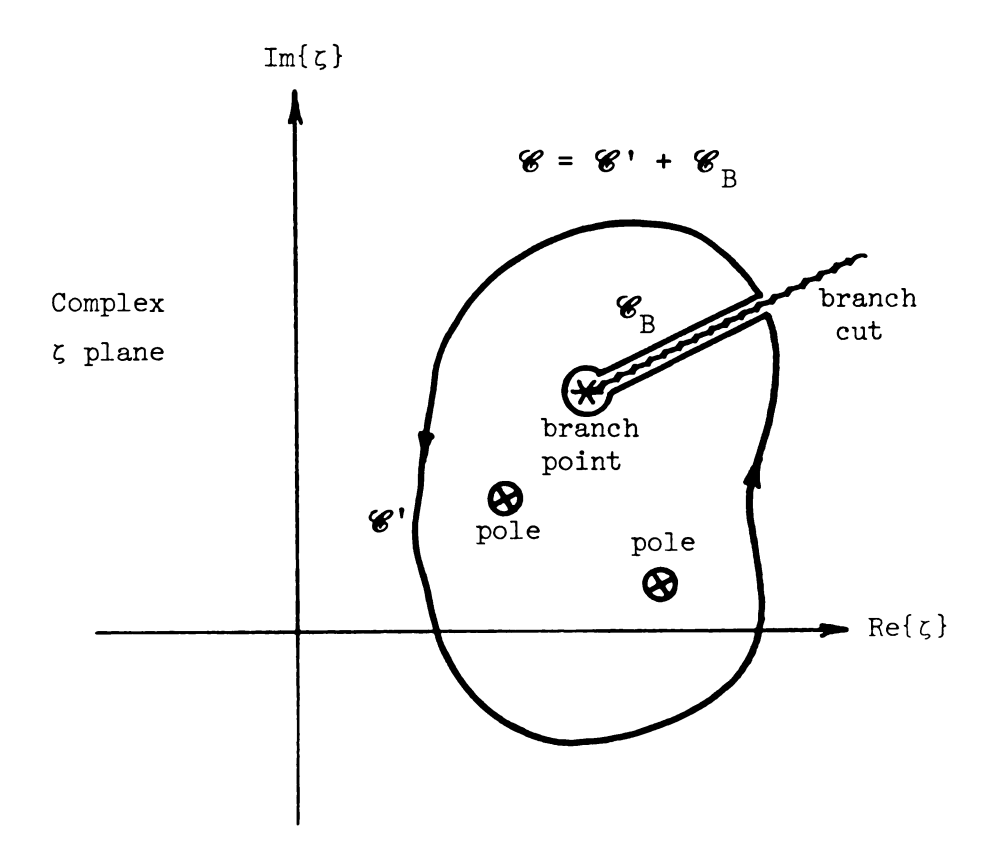


Figure 3.2: General integration contour in the complex ζ plane enclosing poles and branch points of a complex function.

[3.7], and then demand that the contour not cross over this branch cut, but rather detour around it. This situation is depicted in Figure 3.2.

If we write the closed contour \mathscr{C} as the sum of the contour \mathscr{C}' plus the branch contour \mathscr{C}_B as shown in Figure 3.2, we can write equation (21) in an alternative form:

$$\int_{\mathscr{C}'} r(\zeta) d\zeta = 2\pi j \sum_{n} \underset{\zeta}{\text{Res}} \{ r(\zeta) \} - \int_{\mathscr{C}_{B}} r(\zeta) d\zeta$$
 (22)

Equation (22) gives an alternative method for computing an integral such as that on the left hand side. We can instead calculate and sum the indicated residues at poles inside of the contour and then add on the contribution from integration around any branch cuts. This technique will be used to evaluate several key integrals in the remainder of this dissertation.

3.3.2 Complete Modal Spectrum

The unknown total electric field in the core of an axially uniform integrated waveguide is given by inverse Fourier transforming the axially transformed total field, where the transformed field satisfies the transformed integral equation (5). Mathematically,

$$\vec{E}(\vec{\rho},z) = \frac{1}{2\pi} \int_{-\infty}^{\infty} \vec{e}(\vec{\rho},\zeta) e^{j\zeta z} d\zeta$$
 (23)

We will perform this Fourier inversion with the aid of the residue theorem as outlined above. We need to modify the real line integral in equation (23) to form a closed path in the complex plane. We modify the integration path as follows: truncate the real line integration so that it extends from $\zeta = -L$ to $\zeta = L$, and then add a semi-circular path, \mathscr{C}_L , or radius L and centered at $\zeta = 0$ extending into the upper half complex plane. This semi-circular path joins the ends of the real line path to form a contour enclosing a semi-circular sector of the upper half plane, as shown in Figure 3.3. We will conceptually allow L to tend to infinity, so that the real line integration path \mathscr{C}_R approaches the integration path of the Fourier inversion integral of equation (23).

The integrand or equation (23) can in general have pole singularities located inside of this closed contour and multi-valued parameters with branch points enclosed in the contour. As mentioned in the last part, we will choose branch cuts emanating from the branch points of any multi-valued parameters in the integrand, and then insist that our closed contour detours around these branch cuts. This is the reason for the branch integral path, \mathscr{C}_{R} , shown in Figure 3.3.

Since the complete closed contour now consists of the three parts, \mathscr{C}_R + \mathscr{C}_B + \mathscr{C}_∞ , the residue theorem states that

$$\int_{\mathcal{C}_{R}} \dot{e}(\dot{\rho},\zeta) e^{j\zeta z} d\zeta = \int_{\infty}^{\infty} \dot{e}(\dot{\rho},\zeta) e^{j\zeta z} d\zeta$$

$$= 2\pi j \sum_{n} \operatorname{Res}\{\dot{e}(\dot{\rho},\zeta) e^{j\zeta z}\} - \int_{\mathcal{C}_{\infty}} \dot{e}(\dot{\rho},\zeta) e^{j\zeta z} d\zeta$$

$$- \int_{\mathcal{C}_{R}} \dot{e}(\dot{\rho},\zeta) e^{j\zeta z} d\zeta$$
(24)

where we have allowed L to tend to infinity. Under certain conditions the integral along \mathscr{C}_{∞} vanishes. In this case we can combine equations (23) and (24) to obtain the result

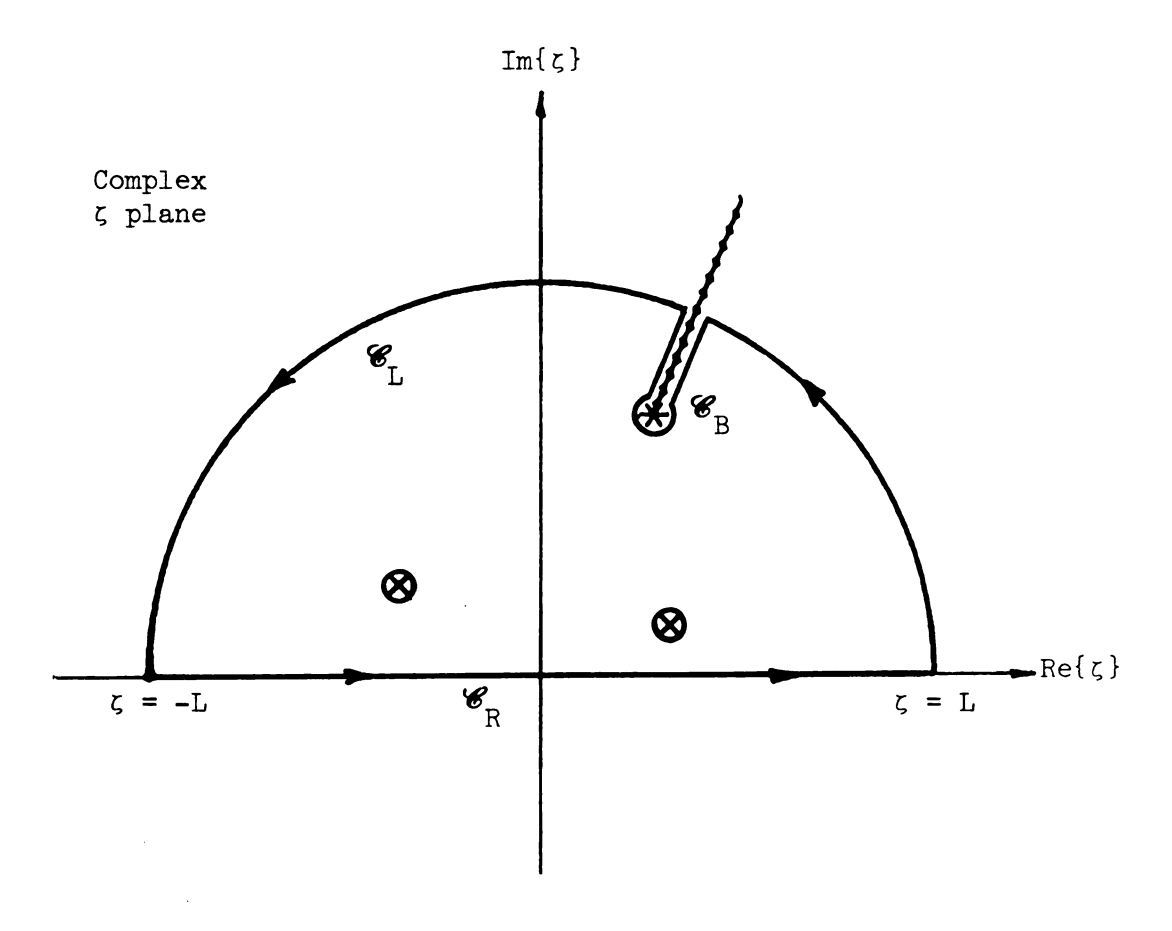


Figure 3.3: Deformed Fourier inversion contour in complex ζ plane enclosing poles and branch points of transformed total electric field.

$$\vec{E}(\vec{\rho},z) = \frac{1}{2\pi} \left\{ 2\pi j \sum_{n} \text{Res}\{\vec{e}(\vec{\rho},\zeta)e^{j\zeta z}\} - \int_{\mathcal{C}_{R}} \vec{e}(\vec{\rho},\zeta)e^{j\zeta z} d\zeta \right\}$$
(25)

The condition under which the integral along \mathscr{C}_{∞} vanishes is that the integrand vanishes as $|\rho| \to \infty$ on this path. The presence of the term $\exp(j\zeta z)$ ensures the vanishing or the integrand as long as z is greater than zero. The case of z less than zero can be accomposed by having the inversion contour close in the lower half complex ζ plane, rather than in the upper half ζ plane, as presented here.

Equation (25) gives a natural decomposition of the total electric field in any axially invariant integrated dielectric waveguide. One part of the total field is associated with the residue terms, and the other with the branch integrals. We characterize the total field in the waveguide with the aid of equation (25).

The residue terms in equation (25) are the sum of surface wave modes of the waveguide, complete with excitation amplitudes depending in an explicit manner on the incident excitatory field or current. It will be shown in the next section that these surface wave terms satisfy the homogeneous form of the integral equation (5), as we would expect by the conventional definition of surface waves.

The branch integral terms in equation (25) are a continuous superposition or radiation rield spectral components of the waveguide. Again, these terms include the spectral excitation amplitudes depending on the incident excitatory rield or current. They are the subject or section 3.3.4.

What we have accomplished here is a complete characterization of the total modal spectrum of a fairly general class of integrated dielectric waveguiding systems. We deal with this modal

characterization in more detail in the remainder of this part of the chapter.

3.3.3 Poles of e and Surface Waves

We will now show that the residue terms in equation (25) are indeed surface waves of the integrated dielectric waveguide. Surface waves of the system are defined in the usual manner as those guided fields that can be supported in the absence of excitation. Thus, we must show that the residue terms of equation (25) satisfy the homogeneous form of the transformed integral equation (5).

Suppose that the closed inversion contour of Figure 3.3 encloses a simple pole of the transformed total field $e(\rho, \zeta)$ at $\zeta = \zeta_m$. Then near this pole the transformed total field has the approximate form

$$\vec{e}(\vec{\rho}, \zeta) \cong a_m e_m(\vec{\rho}) (\zeta - \zeta_m)^{-1}$$
(26)

Substitution or equation (26) into the integral equation (5) results in

$$a_{m}(\zeta - \zeta_{m})^{-1} [\overrightarrow{e}_{m}(\overrightarrow{\rho}) - \int_{CS} \frac{\delta n^{2}(\overrightarrow{\rho'})}{n_{c}^{2}} \overrightarrow{g}_{e\zeta}(\overrightarrow{\rho}|\overrightarrow{\rho'}) \cdot \overrightarrow{e}_{m}(\overrightarrow{\rho'}) dS']$$

$$= \overrightarrow{e}^{1}(\overrightarrow{\rho}, \zeta)$$
(27)

when ζ is near $\zeta_{m^{\bullet}}$. Taking the limit as ζ + ζ_{m} gives

$$a_{m} \lim_{\zeta \to \zeta_{m}} \left\{ (\zeta - \zeta_{m})^{-1} [\overrightarrow{e}_{m}(\overrightarrow{\rho}) - \int_{CS} \frac{\delta n^{2}(\overrightarrow{\rho'})}{n_{c}^{2}} \overrightarrow{g}_{e_{\zeta}}(\overrightarrow{\rho}|\overrightarrow{\rho'}) \cdot \overrightarrow{e}_{m}(\overrightarrow{\rho'}) dS'] \right\}$$

$$= \overrightarrow{e}^{i}(\overrightarrow{\rho}, \zeta_{m})$$
(28)

Now \dot{e}^i is arbitrary, and thus is not in general singular at $\zeta = \zeta_m$. Since the term $(\zeta - \zeta_m)^{-1}$ on the left hand side of equation (25) is singular, we conclude that the total left hand side is indeterminate. This implies that $\dot{e}_m(\dot{\rho})$ satisfies the equation

$$\vec{e}_{m}(\vec{\rho}) - \int_{CS} \frac{\delta n^{2}(\vec{\rho}')}{n_{c}^{2}} \stackrel{\leftrightarrow}{g}_{e\zeta_{m}} (\vec{\rho}|\vec{\rho}') \cdot \vec{e}_{m}(\vec{\rho}') dS' = 0$$
 (29)

from which we see that \overrightarrow{e}_m is a surface wave of the waveguide with propagation constant ζ_{m^*} . Thus we have shown that the residue terms of equation (25) represent a sum of surface waves of the integrated dielectric waveguide.

We now prove that e has the form in equation (26) when ζ_m is an eigenvalue of the surface wave mode equation (26). This demonstration also allows evaluation of the modal excitation amplitude coefficient, a_m .

First operate on the transformed integral equation (5) with the linear integral operator \mathcal{L}_{m} , defined as

$$\mathscr{L}_{m}\{\cdot\} = \int_{CS} \frac{\delta n^{2}(\overrightarrow{\rho}')}{n_{c}^{2}} \stackrel{\rightarrow}{e}_{m}(\overrightarrow{\rho}) \cdot \{\cdot\} dS$$
 (30)

This results in the expression

$$\int_{CS} \frac{\delta n^{2}(\vec{\rho}')}{n_{c}^{2}} \dot{e}_{m}(\vec{\rho}) \cdot \dot{e}(\vec{\rho},\zeta) dS$$

$$- \int_{CS} \frac{\delta n^{2}(\rho)}{n_{c}^{2}} \dot{e}_{m}(\vec{\rho}) \cdot \int_{CS} \frac{\delta n^{2}(\vec{\rho}')}{n_{c}^{2}} \dot{g}_{e_{\zeta}}(\vec{\rho}|\vec{\rho}') \cdot \dot{e}(\vec{\rho},\zeta) dS' dS$$

$$= \int_{CS} \frac{\delta n^{2}(\vec{\rho})}{n_{c}^{2}} \dot{e}_{m}(\vec{\rho}) \cdot \dot{e}^{i}(\vec{\rho},\zeta) dS$$
(31)

Now use the reciprocity property from section 3.2.1 ror the transformed Green's dyad in equation (31) to get

$$\int_{CS} \frac{\delta n^{2}(\vec{\rho})}{n_{c}^{2}} \stackrel{d}{\stackrel{d}{=}}_{m}(\vec{\rho}) \stackrel{d}{\cdot} \stackrel{d}{\stackrel{d}{=}}_{(\vec{\rho},\zeta)} dS - \int_{CS} \frac{\delta n^{2}(\vec{\rho}')}{n_{c}^{2}} e(\vec{\rho}',\zeta) \int_{CS} \frac{\delta n^{2}(\vec{\rho})}{n_{c}^{2}} \stackrel{\leftrightarrow}{g}_{e\zeta}(\vec{\rho},\vec{\rho}) \stackrel{d}{\cdot} e_{m}(\vec{\rho}) dS dS' = \int_{CS} \frac{\delta n^{2}(\vec{\rho})}{n_{c}^{2}} \stackrel{d}{\stackrel{d}{=}}_{m}(\vec{\rho}) \stackrel{d}{\cdot} \stackrel{d}{\stackrel{d}{=}}_{(\vec{\rho},\zeta)} dS$$

$$(32)$$

When ζ is near ζ_m we can approximate the transformed Green's dyad by the first two terms of its Taylor series expansion about ζ_m :

$$\vec{g}_{e_{\zeta}}(\vec{\rho}|\vec{\rho}') \simeq \vec{g}_{e_{\zeta_{m}}}(\vec{\rho}'|\vec{\rho}) + \frac{\partial}{\partial \zeta} \vec{g}_{e_{\zeta}}(\vec{\rho}'|\vec{\rho})|_{\zeta_{m}}(\zeta - \zeta_{m})$$
(33)

Substitute equation (33) into the operated upon integral equation (32). After using the surface wave integral equation (29) and taking the limit as $\zeta \to \zeta_m$ we get

$$\lim_{\zeta \to \zeta_{\mathbf{m}}} (\zeta - \zeta_{\mathbf{m}}) \int_{CS} \frac{\delta n^{2}(\vec{\rho})}{n_{\mathbf{c}}^{2}} \stackrel{\overrightarrow{e}}{=} (\vec{\rho}, \zeta) \cdot \int_{CS} \frac{\delta n^{2}(\vec{\rho}')}{n_{\mathbf{c}}^{2}} \frac{\partial}{\partial \zeta} \stackrel{\overrightarrow{g}}{=} (\vec{\rho} | \vec{\rho}')|_{\zeta_{\mathbf{m}}} \stackrel{\overrightarrow{e}}{=} (\vec{\rho}') dS'$$

$$= - \int_{CS} \frac{\delta n^{2}(\vec{\rho})}{n_{\mathbf{c}}^{2}} \stackrel{\overrightarrow{e}}{=} (\vec{\rho}) \cdot \stackrel{\overrightarrow{e}}{=} (\vec{\rho}, \zeta_{\mathbf{m}}) dS$$
(34)

Since $\overrightarrow{e^i}$ is arbitrary the right hand side of equation (34) is non-zero in general. Thus we conclude that $\lim_{t \to \infty} (\zeta - \zeta_m)^{-1} \overrightarrow{e_m}(\overrightarrow{\rho}, \zeta) = 0$, or

$$\stackrel{\rightarrow}{e}(\stackrel{\rightarrow}{\rho},\varsigma) = a_{m}\stackrel{\rightarrow}{e}_{m}(\stackrel{\rightarrow}{\rho})(\varsigma - \varsigma_{m})^{-1}$$
(36)

when ζ is near ζ_m . Now substitute equation (36) into equation (35). We can solve the result for a_m :

$$a_{m} = \frac{-1}{c_{m}} \int_{CS} \frac{\delta n^{2}(\stackrel{\rightarrow}{\rho})}{n_{c}^{2}} \stackrel{\rightarrow}{e_{m}}(\stackrel{\rightarrow}{\rho}) \stackrel{\rightarrow}{e^{i}}(\stackrel{\rightarrow}{\rho}, \zeta_{m}) dS$$

$$c_{m} = \int_{CS} \int_{CS} \frac{\delta n^{2}(\stackrel{\rightarrow}{\rho})}{n_{c}^{2}} \stackrel{\rightarrow}{e_{m}}(\stackrel{\rightarrow}{\rho}) \stackrel{\rightarrow}{e^{i}}(\stackrel{\rightarrow}{\rho}) \stackrel{\rightarrow}{e^{i}}(\stackrel{\rightarrow}{\rho}) \stackrel{\rightarrow}{e^{i}}(\stackrel{\rightarrow}{\rho}) \stackrel{\rightarrow}{e^{i}}(\stackrel{\rightarrow}{\rho}) dS \stackrel{\rightarrow}{dS}$$

$$(37)$$

where $\mathbf{c}_{\mathbf{m}}$ is a modal normalization constant.

We have found an expression for the excitation amplitude of the mth surface wave mode in the waveguide in terms of an overlap integral of the impressed electric field with the mth surface wave mode. This result is of the same form as the results of conventional excitation theory ([1.6], [3.8]).

We can derive an alternative form for the excitation amplitude of equation (30) in terms of the impressed current maintaining the impressed excitatory field. This is done by using the transformed electric Green's dyad of section 3.2.2 to write the impressed transformed electric rield in terms of the impressed transformed polarization:

$$\vec{e}^{i}(\vec{\rho}, \zeta_{m}) = \int_{CS} \vec{g}_{e_{\zeta_{m}}}(\vec{\rho}|\vec{\rho}') \cdot \frac{p^{e}(\vec{\rho}', \zeta_{m})}{\varepsilon_{c}} ds'$$
(38)

Substitution of this equation into equation (37) gives

$$a_{m} = -\frac{1}{c_{m}} \int_{CS} \frac{\overrightarrow{p^{e}}(\overrightarrow{\rho}, \zeta_{m})}{\varepsilon_{c}} \cdot \overrightarrow{e_{m}}(\overrightarrow{\rho}) dS$$
 (39)

where we have used the surface wave integral equation (29) and the reciprocal property of the electric Green's dyad. Now substitute the definition of the transformed polarization into equation (39). This gives

$$a_{m} = \frac{-1}{c_{m}} \int_{CS} \int_{-\infty}^{\infty} \frac{P^{e}(\vec{\rho},z)}{\varepsilon_{c}} \cdot \vec{e}_{m}(\vec{\rho}) e^{-j\zeta_{m}z} dzdS$$
 (40)

Now $\vec{J}^e = j_\omega \vec{P}^e$ and $\vec{e}_m e^{-j\zeta_m z} = \vec{E}_m$, so we have the result

$$a_{m} = \frac{-1}{\mathbf{j}_{\omega \varepsilon_{\mathbf{C}}} \mathbf{c}_{m}} \int_{\mathbf{V}} \mathbf{j}^{\mathbf{e}}(\mathbf{r}) \cdot \mathbf{E}_{m}^{+}(\mathbf{r}) dV$$
 (41)

which is in the form of the result of conventional excitation theory ([1.6], [3.8]) for impressed currents exciting a waveguide.

3.3.4 Branches or e and the Radiation Spectrum

We have made the identification in section 3.3.2 of the total radiation field, \vec{E}_{RAD} , or an integrated dielectric waveguide with the branch integrals in equation (25). That is

$$\vec{E}_{RAD}(\vec{r}) = \frac{-1}{2^{\pi}} \int_{B} \vec{e}(\vec{\rho}, \zeta) e^{j\zeta z} d\zeta$$
 (42)

where we recall that $\vec{e}(\vec{\rho},\zeta)$ in this equation is the solution to the inhomogeneous transformed integral equation (5) for values of ζ along branch cuts in the upper half complex ζ plane. We now turn to the problem of finding how this radiated field depends on the impressed sources, \vec{J}^e . We will make use of the technique of Neumann series [3.9] to accomplish this.

We begin by substituting equation (38) for the impressed transformed electric field in terms of impressed polarization sources into the transformed integral equation (5). This gives

$$\vec{e}(\vec{\rho},\zeta) = \int_{CS_{\infty}} \vec{g}_{e_{\zeta}}(\vec{\rho}|\vec{\rho}') \cdot \left[\frac{\delta n^{2}(\vec{\rho}')}{n_{c}^{2}} \vec{e}(\vec{\rho}',\zeta) - \frac{1}{\varepsilon_{c}} \vec{p}^{e}(\vec{\rho}',\zeta) \right] ds'$$

where CS_{∞} denotes the infinite cross section $|\overset{\rightarrow}{\rho}|<\infty$. Define the iterated Green's functions

$$\mathbf{g}_{\zeta_{0}}(\overrightarrow{\rho}|\overrightarrow{\rho'}) = \mathbf{g}_{e_{\zeta}}(\overrightarrow{\rho}|\overrightarrow{\rho'})$$

$$\mathbf{g}_{\zeta_{1}+1}(\overrightarrow{\rho}|\overrightarrow{\rho'}) = \int_{CS_{\infty}} \mathbf{g}_{\zeta_{1}}(\overrightarrow{\rho}|\overrightarrow{\rho''}) \cdot \frac{\delta n^{2}(\rho'')}{n_{c}^{2}} \mathbf{g}_{e_{\zeta}}(\overrightarrow{\rho''}|\overrightarrow{\rho'}) dS''$$
(44)

Then repeated substitution of equation (43) into itself gives the result

$$\vec{e}(\vec{\rho},\zeta) = -\int_{CS_{\infty}} \vec{g}(\vec{\rho}|\vec{\rho}') \cdot \frac{\vec{p}^{e}(\vec{\rho}',\zeta)}{\varepsilon_{c}} ds'$$
(45)

where

$$\mathscr{G}_{\zeta}(\overset{\rightarrow}{\rho}|\overset{\rightarrow}{\rho'}) = \overset{\infty}{\Sigma} \mathscr{G}_{\zeta}(\overset{\rightarrow}{\rho}|\overset{\rightarrow}{\rho'})$$

$$(46)$$

This is a formal result which assumes that the series or equation (46) converges. The physical significance of this resolvent Green's dyad is as follows: an infinitesimal transformed polarization source $\vec{p}^e(\vec{\rho}^i,\zeta)dS^i$ at location $\vec{\rho}$ produces at an infinitesimal transformed electric field $\vec{de}(\vec{\rho},\zeta)$ in the waveguide core given by

$$\vec{de}(\vec{\rho},\zeta) = - \frac{\vec{\varphi}}{\zeta}(\vec{\rho}|\vec{\rho}') \cdot \frac{\vec{p}^{e}(\vec{\rho}',\zeta)}{\varepsilon} dS'$$
 (47)

Now substitute into equation (45) the definition of \vec{p}^e in terms of \vec{j}^e to obtain

$$\vec{e}(\vec{\rho}, \zeta) = \frac{-1}{j\omega\epsilon_0} \int_{CS_{\infty}} \vec{g}_{\zeta}(\vec{\rho}|\vec{\rho}') \cdot \vec{J}^e(\vec{\rho}', \zeta) dS'$$
(48)

Now use equation (48) in equation (42). This gives

$$\vec{E}_{RAD}(\vec{r}) = \frac{1}{2\pi j\omega\varepsilon_{c}} \int_{\mathcal{C}_{B}} e^{j\zeta z} \int_{CS_{\infty}} (\vec{\rho}|\vec{\rho}') \cdot \vec{J}^{e}(\vec{\rho}',\zeta) dS'd \qquad (49)$$

Equation (49) tells us explicitly that the radiation field depends on the transformed impressed current at complex spatial frequencies on the branch cut, \mathscr{C}_B . Equation (49) also confirms the opinion that the radiation field of an axially uniform integrated dielectric waveguide must in general be written as a two dimensional spectral superposition of radiation field spectral components. This is evident since $\overrightarrow{\mathcal{E}}_{\mathcal{C}}$, and hence $\overrightarrow{\mathcal{C}}_{\mathcal{C}}$, involves the one dimensional superposition on the spatial frequency variable ξ , as seen in equation (13) and (15), and the integration along \mathscr{C}_B in equation (49) is a spectral superposition in ζ along the branch cuts in the upper half complex plane.

3.3.5 Leakage of Surface Waves

We now turn to an examination of phenominon of surface wave leakage from integrated dielectric waveguides. Note that the trilayered background structure of the general waveguiding system of Figure 3.1 is a dielectric waveguide in its own right. If $\rm n_{f}>\rm n_{s}, n_{c}$ then the background structure forms an asymmetric slab waveguide. The physical explanation of the phenomenon of surface wave leakage is the coupling of guided modes of the core to guided modes of the asymmetric

slab background structure. Under certain conditions, such coupling can occur, resulting in energy transfer from the surface waves of the core to surface waves in the background structure. It is observed experimentally that the excited surface waves of the background structure guide energy away from the axis of the waveguide core [3.10], hence the name of mode leakage.

This phenomenon manifests itself in our mathematical formulation through the presence of simple pole singularities in the reflection and coupling coefficients in the transformed reflected Green's dyad for complex ξ . These singularities will be shown to occur at such that will cause the factor λ , with

$$\lambda^2 = \xi^2 + \zeta^2 \tag{50}$$

which occurs in the definition (14) of p_{ℓ} , to be an eigenvalue of the TE or TM characteristic equation of the background asymmetric slab waveguide. An alternative representation for the components of the reflected Green's dyad is provided by use of the residue theorem, by which the real line integral on ξ in equation (13) can be replaced by a sum of residues of the integrand at any poles enclosed by a deformed integration contour plus integrals around any necessary branch cuts. This situation is illustrated in Figure 3.4. Thus we see explicitly the influence on the reflected Green's dyad of the surface wave spectrum of the asymmetric slab waveguide which forms the background medium for the integrated dielectric waveguide.

We now turn to finding the location of the singularities of the reflected Green's dyad. First we note from Appendix A that the denominator of both the transverse reflection coefficient, $R_{\rm t}(\xi)$, and

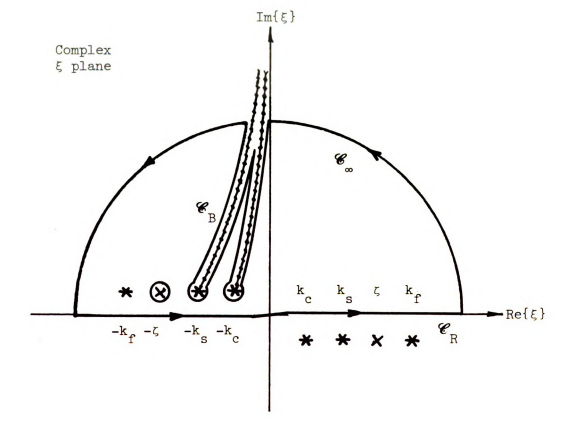


Figure 3.4: Deformed spectral integration contour in the complex ξ plane for components of transformed Hertzian potential Green's dyad.

the coupling coefficient, $C(\xi)$, contain the factor

$$D_{\mathbf{t}}(\xi) = 1 - R_{\mathbf{cr}} R_{\mathbf{sr}} e$$
 (51)

These coefficients are singular when this factor is zero. Substitution of the definitions of R_{cf}^t and R_{sf}^t from Appendix A into equation (51) and equating the result to zero gives

$$(p_f^2 + p_c p_s) \tanh p_f t + p_f (p_c + p_s) = 0$$
 (52)

For surface wave modes of an asymmetric slab waveguide with $k_c \le k_s < k_f$, it is known [3.11] that ζ must lie between k_f and k_s . Thus we define

$$p_{\mathbf{c}} = \sqrt{\lambda^2 - k_{\mathbf{c}}^2} = \delta > 0$$

$$p_{\mathbf{s}} = \sqrt{\lambda^2 - k_{\mathbf{s}}^2} = \gamma > 0$$

$$p_{\mathbf{f}} = \mathbf{j} \sqrt{k_{\mathbf{f}}^2 - \lambda^2} = \mathbf{j} \kappa, \kappa > 0$$
(53)

where λ is as in equation (50) (compare with equation (14)). Substitution of these factors into equation (52) results in

$$\tan \kappa t = \frac{\kappa(\gamma + \delta)}{\kappa^2 - \gamma \delta}$$
 (54)

which we recognize as the TE surface wave characteristic equation of the asymmetric slab waveguide which forms the background structure of our waveguide system [3.12].

The denominators of the reflection and coupling coefficients $R_n(\xi) \text{ and } C(\xi) \text{ given in Appendix A contain the factor}$

$$D_{\mathbf{n}}(\xi) = 1 + R_{\mathbf{re}}^{n} R_{\mathbf{sr}}^{n} e$$
 (55)

Setting this factor equal to zero leads in a similar manner to the equation

$$\tan \kappa t = \frac{n_f^2 \kappa (n_c^2 \gamma + n_s^2 \delta)}{n_s^2 n_c^2 \kappa^2 - n_f^4 \gamma \delta}$$
(56)

which is the characteristic equation of TM surface waves of the asymmetric slab waveguide [3.12].

We have shown that the coerricients R_t , R_n , and C associated with the reflected Green's dyad have pole singularities at the surface wave eigenvalues of the asymmetric slab waveguide. R_t is singular at TE surface wave poles, R_n is singular at TM surface wave poles, and C is singular at both TE and TM surface wave poles. These poles lead to residue contributions to the transformed reflected Green's dyad which correspond to the surface waves of the tri-layered background structure.

Now let λ_p denote a surface wave pole of the background asymmetric slab structure. We know that λ_p must lie in the fourth quadrant of the complex ζ plane so that $\exp(-j\lambda_p r)$ represents a decaying, outward propagating wave. Now the spatial frequency corresponding to this surface wave pole satisfies

$$\xi_{\rm p}^2 = \lambda_{\rm p}^2 - \zeta^2 \tag{57}$$

The factor $\exp(j_{\xi}|x-x'|)$ occurring in \widehat{g}^r tells us we must have $\text{Im}\{\xi_p\} > 0$, so that we can write

$$\xi_{\mathbf{p}} = \mathbf{j}\sqrt{\delta - \lambda_{\mathbf{p}}} \sqrt{\delta + \lambda_{\mathbf{p}}} \tag{58}$$

From the construction in Figure 3.5 we see that in the low loss limit

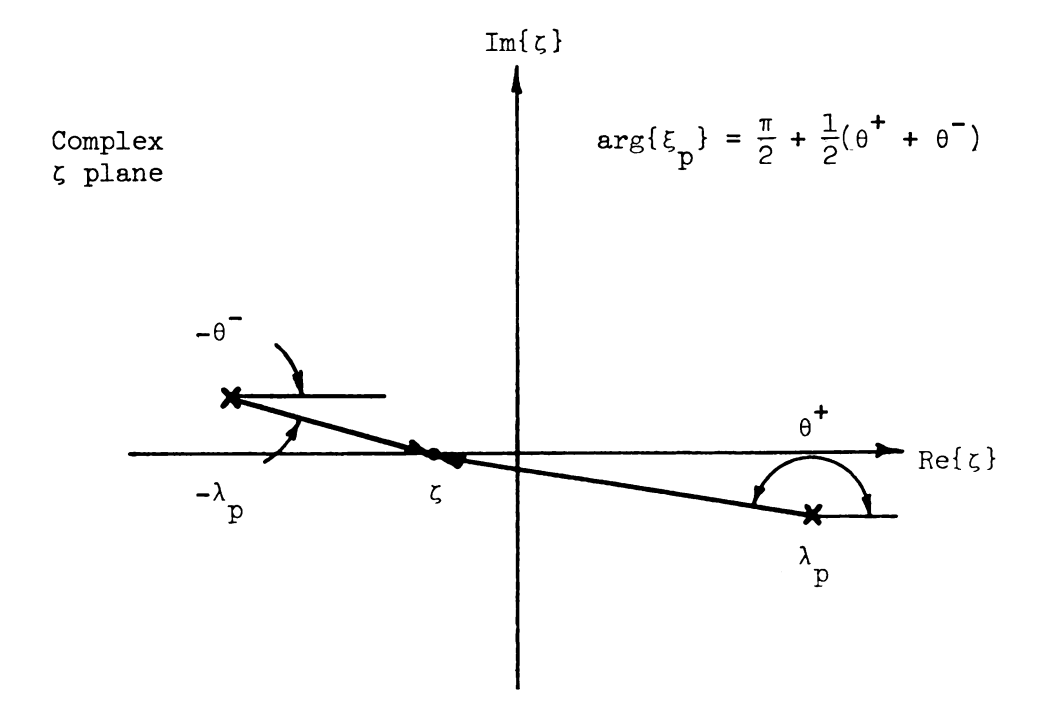


Figure 3.5: Complex ς plane construction defining $arg\{\xi_p\}$.

we have two cases:

$$\max(k_{c},k_{f}) < Re\{\zeta\} < \lambda_{p} ; Arg\{\xi_{p}\} = \pi$$

$$\lambda_{p} < Re\{\zeta\} < k_{f} ; Arg\{\xi_{p}\} = \pi/2$$
(59)

The residue contribution to g^p at ξ_p contains the ractor $\exp(j\;\xi_p\;|x-x|^p)$ which then becomes

$$e^{j \xi_{p} | \mathbf{x} - \mathbf{x}^{\dagger}|} = \begin{cases} -j | \xi_{p} | | \mathbf{x} - \mathbf{x}^{\dagger}| \\ e | \xi_{p} | | \mathbf{x} - \mathbf{x}^{\dagger}| \end{cases}$$

$$(60)$$

for the two cases cited above. We see that this factor represents a traveling wave in the x direction in the first case and an exponential decay in the x direction in the second case. The first case is one in which the surface wave mode of the core leaks, or couples into the surface waves of the background asymmetric slab structure, whereas in the second case no coupling occurs and the mode is guided along the waveguide axis only. This situation is illustrated in Figure 3.6, where we identify the angle at which the surface wave leaks with respect to the guiding axis as

$$\tan \theta = \frac{|\xi|}{\text{Re}\{\zeta\}}$$
 (61)

(compare with equation (4) or [3.14]).

3.3.6 TE Excitation of the Asymmetric Slab

We now turn to an example to illustrate the excitation theory presented above. We will use the transformed integral equation (5) to solve for the guided modes excited in the asymmetric slab waveguide by

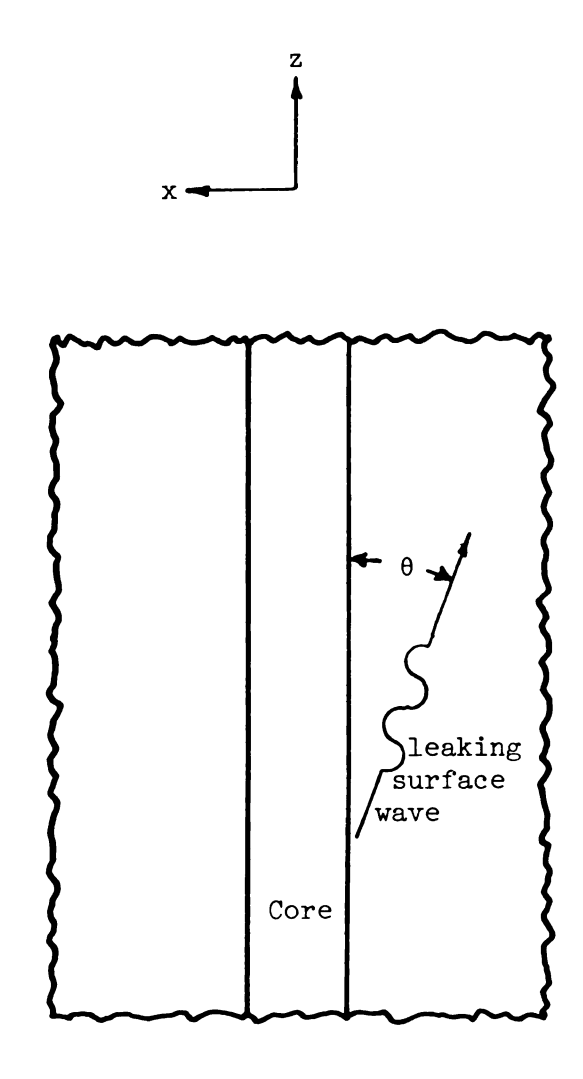


Figure 3.6: Construction defining leakage angle for leaking waves of an integrated waveguide.

an x directed uniform line polarization source. This problem is particularly easy to solve, since the infinite symmetry of the asymmetric slab in the x direction permits closed form evaluation of the spectral integrals in the transformed dyadic Green's function. We will show that the line source excites TE surface waves and TE radiation field spectral components in the asymmetric slab. The modal and spectral excitation amplitudes are shown to be identical with those predicted by conventional excitation theory.

Consider an asymmetric slab waveguide excited by an x directed line current at location (y_0,z_0) , as shown in Figure 3.7. The slab is or infinite extent in the x and z directions, and is of thickness t. The slab has a uniform refractive index n, and is surrounded above and below by infinite uniform dielectric regions with refractive indices n_c and n_s , respectively. The wave guiding axis is taken as the z axis.

The field of any longitudinally invariant dielectric waveguide such as the asymmetric slab satisfies the transformed integral equation (5). The transformed incident field is related to a transformed impressed polarization $\overrightarrow{p}^e(\overrightarrow{\rho},\zeta)$ at location y>0 by the equation

$$\vec{e}^{i}(\vec{\rho},\zeta) = (k_{C}^{2} + \tilde{\nabla}\tilde{\nabla} \cdot) \int_{CS} \vec{g}_{\zeta}(\vec{\rho}|\vec{\rho}') \cdot \frac{\vec{p}^{e}(\vec{\rho}',\zeta)}{\varepsilon_{C}} dS'$$
 (62)

where the Hertzian potential Green's dyad is given in section 3.2 and CS_{∞} denotes the infinite transverse cross-section $|\stackrel{\rightarrow}{\rho}|<\infty$. The refractive index contrast factor of equation (2.2) is in this case

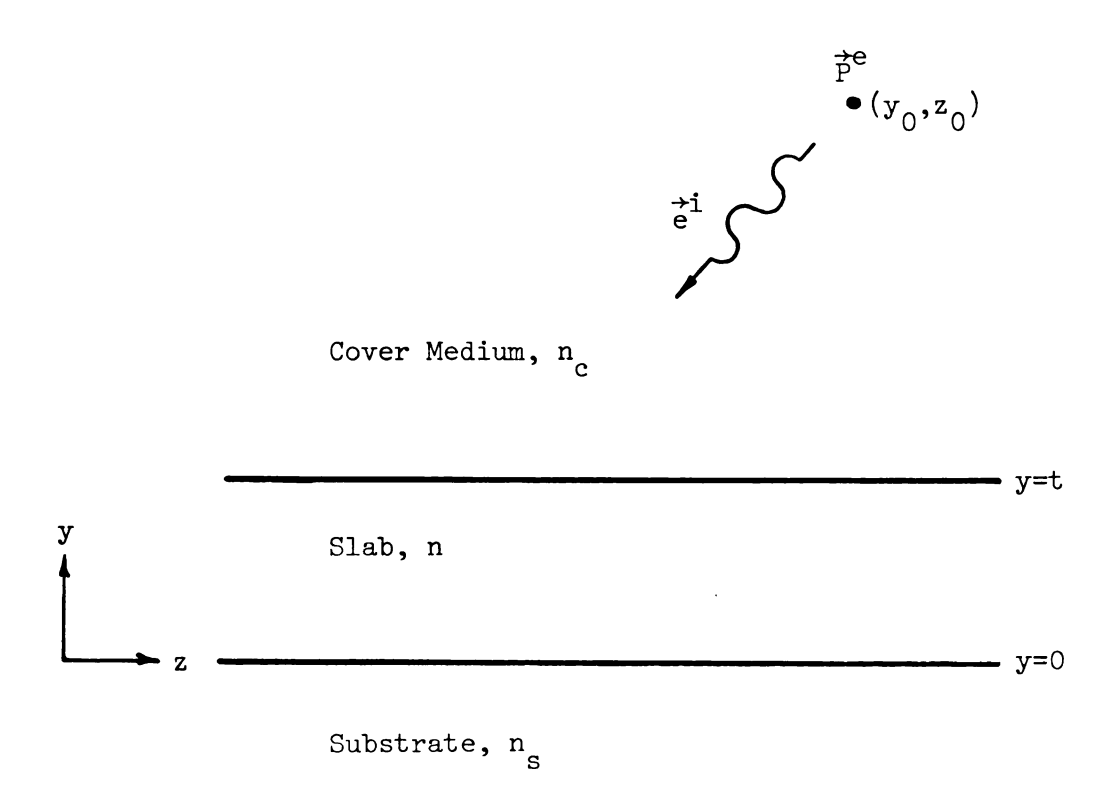


Figure 3.7: An asymmetric slab waveguide excited by a line polarization source. The structure is uniform in the x direction.

$$\delta_{\mathbf{n}}^{2}(\stackrel{\rightarrow}{\rho}) = \begin{cases} \Delta n^{2} = n^{2} - n_{0}^{2}, & 0 < y < t \\ 0, & \text{elsewhere} \end{cases}$$
 (63)

If we assume that the excitation is x invariant, then the Hertzian potential Green's dyad can be simplified by evaluation of the ξ integrals in equations (13) and (15). This is done by first performing the x' integrals in the integral equation (5) and the excitation equation (62) as follows:

$$\int_{-\infty}^{\infty} F(\xi) \frac{e^{j\xi(x-x')}e^{-p_{c}r(y)}}{4\pi p_{c}} d\xi dx' = \int_{-\infty}^{\infty} F(\xi) \frac{\delta(\xi)e^{-p_{c}r(y)}}{2p_{c}}$$

$$= F(0) \frac{e^{-\gamma_{c}r(y)}}{2\gamma_{c}} \tag{64}$$

where we have defined the reduced transverse wavenumber parameters $\gamma_{_{0}}$ related to the p $_{_{0}}$ by

$$\gamma_{\ell}(\zeta) = p_{\ell}(\xi = 0) = \sqrt{\zeta^2 - k_{\ell}^2}$$
(65)

with $\ell = c$ or s for the cover and substrate regions or Figure 3.7. Using these results we can state our problem as rinding the solution to integral equation

$$\vec{e}(y,\zeta) - (k_c^2 + \tilde{\nabla}\tilde{\nabla} \cdot) \int_0^t \frac{\Delta n^2}{n_c^2} \vec{g}_{\zeta}(y|y') \cdot \vec{e}(y',\zeta) dy'$$

$$= (k_c^2 + \tilde{\nabla}\tilde{\nabla} \cdot) \int_0^t \vec{g}_{\zeta}(y|y') \cdot \frac{\vec{p}^e(y',\zeta)}{\epsilon_c} dy'$$
(66)

where we have defined $\tilde{\nabla} = \hat{y} \frac{\partial}{\partial y} + \hat{z}j\zeta$ since $\frac{\partial}{\partial x} = 0$ here. We make use of equation (64) to write the Hertzian potential Green's dyad in closed form:

$$\vec{g}_{\zeta} = \vec{g}_{\zeta}^{p} + \vec{g}_{\zeta}^{r}, \quad \vec{g}_{\zeta}^{p} = \vec{T} \frac{e^{-\gamma} e^{|y-y'|}}{2\gamma_{c}}$$

$$\vec{g}_{\zeta}^{r} = \hat{x} \vec{g}_{\zeta}^{r} \hat{x} + \hat{y} (\vec{g}_{\eta}^{r} \hat{y} + j\zeta g_{\zeta} e^{\hat{z}}) + \hat{z} g_{\zeta}^{r} \hat{z}$$

$$\begin{cases}
g_{\zeta t}^{r} \\ g_{\zeta n}^{r} \\ g_{\zeta c}
\end{cases} = \begin{cases}
R_{t} \\ R_{n} \\ c
\end{cases}$$

$$\frac{e^{-\gamma} e^{(y+y')}}{2\gamma_{c}}$$

$$R_{t} = \frac{\gamma_{c} - \gamma_{s}}{\gamma_{c} + \gamma_{s}}$$

$$R_{n} = \frac{N^{2} \gamma_{c} - \gamma_{s}}{N^{2} \gamma_{c} + \gamma_{s}}$$

$$C = \frac{2\gamma_{c} (N^{2} - 1)}{(N^{2} \gamma_{c} + \gamma_{s}) (\gamma_{c} + \gamma_{s})}$$

$$N^{2} = \frac{n_{s}^{2}}{n_{c}^{2}}$$
(67)

where the reflection and coupling coefficient R_t , R_n , and C are defined in Appendix A. If the impressed polarization in equation (62) is x directed it is evident from equation (66) and (67) that the resultant electric fields will be x directed as well. Thus, this line polarization source will excite only TE modes of the asymmetric slab. This observation allows us to write equation (66) in scalar form.

We will solve our excitation problem for an x directed uniform line polarization source at location (y_0, z_0) , with $y_0 > 0$ as shown in Figure 3.7. Any arbitrary extended x invariant, x directed source can be accompdated by superposing solutions for such line sources. Thus we let

$$\hat{p}^{e}(y,\zeta) = \hat{x}p^{e}e^{-j\zeta}zO\delta(y-y_{O})$$
(68)

where p^e is the constant strength of the line polarization source. Then the integral equation (66) can be written

$$e(y,\zeta) - k_0^2 \Delta n^2 \int_0^t g_{\zeta}(y|y') e(y',\zeta) dy'$$

$$= \frac{k_0^2 p^e}{\epsilon_0} e^{-j\zeta Z_0} g_{\zeta}(y|y_0)$$
(69)

with the scalar Green's function given by

$$g_{\zeta} = g_{\zeta}^{p} + g_{\zeta}^{r} = \frac{1}{2\gamma_{c}} \left[e^{-\gamma_{c} |y-y'|} + R_{t} e^{-\gamma_{c} (y+y')} \right]$$
 (70)

The system or equation (69) and (70) can be solved in closed form. One method of solution utilizing Fourier transforms is detailed in Appendix B. The result is the transformed total field in the slab core:

$$e(y,\zeta) = \frac{k_0^2 p^e}{\varepsilon_0} - \left[\gamma_c(y_0 - t) + j\zeta z_0\right] \frac{\sigma \cos \sigma y + \gamma_s \sin \sigma y}{D(\zeta)}$$
(71)

valid for 0 < y < t, where $\rm Y_{c}$ and $\rm Y_{s}$ are given in equation (65) and

$$\sigma^2 = k^2 - \zeta^2 \tag{72}$$

The denominator factor $D(\zeta)$ is

$$D(\zeta) = (\sigma^2 - \gamma_c \gamma_s) \sin \sigma t - \sigma(\gamma_c + \gamma_s) \cos \sigma t$$
 (73)

We now turn to the task of inverting the transformed total electric field of equation (71) with the aid of the residue theorem. First note that the expression for $e(y, \zeta)$ has simple poles where D = 0. Setting equation (73) equal to zero results in

$$\tan \sigma t = \frac{\sigma(\gamma_c + \gamma_s)}{\sigma^2 - \gamma_c \gamma_s}$$
 (74)

which is the ramiliar TE surface wave characteristic equation of the asymmetric slab waveguide [3.12]. This equation is satisfied when takes on values ζ_n which are the eigenvalues for TE surface waves of the asymmetric slab waveguide. Calculation of the residues of the integrand of the Fourier inversion integral (20) at these poles is straight-forward but messy. We will assume that the waveguide is slightly lossy so that $\mathrm{Im}\{\zeta_n\}<0$. If we write

$$e(y,\zeta)e^{j\zeta Z} = \frac{N(\zeta)}{D(\zeta)}$$
 (75)

then the residue at a pole $-\zeta_{\tilde{m}}$ in the enclosed upper half plane is given by

$$\operatorname{Res}_{-\zeta_{\mathbf{m}}} \{ e(\mathbf{y}, \zeta) e^{\mathbf{j} \zeta \mathbf{z}} \} = \frac{N(\zeta)}{D'(\zeta)} \Big|_{-\zeta_{\mathbf{m}}}$$
(76)

Carrying out the indicated operations yields

Res{e(y,
$$\zeta$$
)e^{j ζz} } = - $\frac{k_O^2 p^e}{\epsilon_O}$ = -[$\gamma_C(y_O - t) + j \zeta_m(z - z_O)$ } x

where $_{\sigma}\text{, }\gamma_{c}\text{, and }\gamma_{s}$ are evaluated at $^{-\zeta}_{m}$ and

$$\Delta_{\ell}^2 = \sigma^2 + \gamma_{\ell}^2 \quad , \quad \ell = c,s \tag{78}$$

Now we claim that this residue is proportional the the $m^{\mbox{th}}$ TE surface wave modal field of the asymmetric slab, or

Here e_{m} is the m^{th} TE surface wave modal rield of the asymmetric slab, and we further claim that $\mathbf{a}_{\mathbf{m}}$ is the modal excitation coefficient [3.15]

$$a_{m} = -\frac{\int_{CS_{\infty}} J^{e}(y,z) E_{m}(y,z) dS}{\frac{2}{Z_{TEM}} \int_{-\infty}^{\infty} e_{m}^{2}(y) dy}$$
(80)

with $Z_{TE\,\mbox{\scriptsize M}}$ = $\omega\mu_0/\zeta_{\mbox{\scriptsize m}^{\bullet}}$. Note that the ractors of 2π in the numerator and denominator of the residue term in equation (22) cancel, leading to the claim in equation (79).

Here we let the current in equation (80) be given by $\overrightarrow{J}^e = \overrightarrow{J}^{e}$ with \overrightarrow{P}^e as in equation (68). We will use Marcuse's [3.16] expression for the mth TE surface wave of the asymmetric slab.

$$e_{m}(y) = A[\cos\sigma(y-t) - \frac{\gamma_{c}}{\sigma} \sin\sigma(y-t)]$$
 (81)

Substitution or (81) and (60) into (80) results in

$$a_{m}e_{m}(y)e^{-j\zeta_{m}z} = -\frac{j\kappa_{O}^{2}p^{e}}{\frac{\varepsilon}{O}} e^{-[\gamma_{C}(y_{O}-t)+j\zeta_{m}(z-z_{O})]} x$$

$$x = \frac{\cos \sigma y + \gamma_{s} \sin \sigma y}{\frac{\zeta \Delta_{c} \Delta_{s}}{\sigma} \left[t + \frac{1}{\gamma_{c}} + \frac{1}{\gamma_{s}} \right]}$$
(82)

which is precisely j times equation (77) as claimed.

The transformed field solution of equation (71) also has branch points in the upper half plane associated with the multi-valued reduced transverse wavenumber parameters σ_{r} γ_{c} , and $\gamma_{\text{s}}.$ Fourier

inversion or the transformed rield is accomplished by deforming the inversion contour to enclose the upper half of the complex ζ plane and utilizing the residue theorem, as discussed in section 3.3. Closure in the upper half complex ζ plane is dictated by the presence of the ractor $\exp(j\,\zeta z)$ in the inversion integral or equation (20) when $z>z_0$ in order to obtain convergence of the integrand on the infinite semi-circular contour C_∞ or Figure 3.3. Since the branch points of σ , γ_C , and γ_S are enclosed by the contour we must choose branch cuts for these factors and ensure that our closed inversion contour detours around these branch cuts.

The branches chosen for the transverse wavenumber parameters are

$$Re \left\{ \begin{array}{c} \mathbf{j}\sigma \\ \mathbf{\gamma_c} \\ \mathbf{\gamma_s} \end{array} \right\} > 0 \quad , \quad I_m \quad \left\{ \begin{array}{c} \mathbf{j}\sigma \\ \mathbf{\gamma_c} \\ \mathbf{\gamma_s} \end{array} \right\} > 0 \tag{83}$$

so that the ractors $\exp(-\gamma_{\rm C} y)$, $\exp(\gamma_{\rm S} y)$ appearing in the expressions $\operatorname{rorg}_{\zeta}$ in equation (70) represent waves traveling and decaying in the $\pm y$ directions, respectively. The choice for the wavenumber parameter is arbitrary, and will be shown to be immaterial in the subsequent expression for the total electric field. If the dielectric media of the cladding and substrate regions are slightly lossy, with

$$k_{\ell} = k_{\ell}^{\bullet} - jk_{\ell}^{\bullet} ; \quad k_{\ell}^{\bullet}, \quad k_{\ell}^{\bullet} > 0$$
 (84)

then the requirements of equation (83) lead to the equations

$$Re\{\zeta\} = -\frac{k_{\ell}^{\dagger}k_{\ell}^{\dagger}}{I_{m}\{\zeta\}}$$
 (85)

describing the standard hyperbolic branch cuts shown in Figure 3.8 (see, for example Collin [3.17]).

The reason that the branch cut corresponding to the transverse wavenumber parameter σ is immaterial as mentioned above is that an examination of the form of the transformed electric field as given in equations (71) and (73) reveals that this expression is even in σ . Hence the path integrals up and down the branch cut associated with shown in Figure 3.8 will cancel, yielding no contribution to the inversion integral by this portion of the branch cut integration.

We will now consider the low loss limiting case for the cover and substrate media. This specialization is accomplished by letting k" approach zero from the left in equation (85) for the branch cuts. In the low loss limit the branch cuts of Figure 3.8 coelesce to form the single branch cut shown in Figure 3.9. Note that the integration up the left side of the branch cut associated with γ_c has cancelled part of the integration down the adjacent right side of the branch cut associated with γ_s . We have also removed the branch cut associated with γ_s from Figure 3.9 for the reasons cited above.

We note in Figure 3.9 that the branch integral contribution to the total radiation spectrum of the rield decomposes naturally into three cases: $-k_S < Re\{\zeta\} < -k_C; -k_C < Re\{\zeta\} < 0;$ and $0 < Im\{\zeta\} < \infty$. The physical significance of these three cases will be detailed presently.

In the following material we will make use of the following notation:

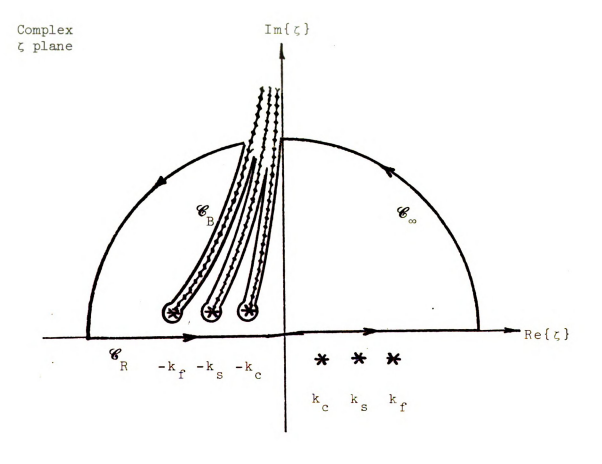


Figure 3.8: Deformed Fourier inversion contour in complex ζ plane for total core field in the asymmetric slab.

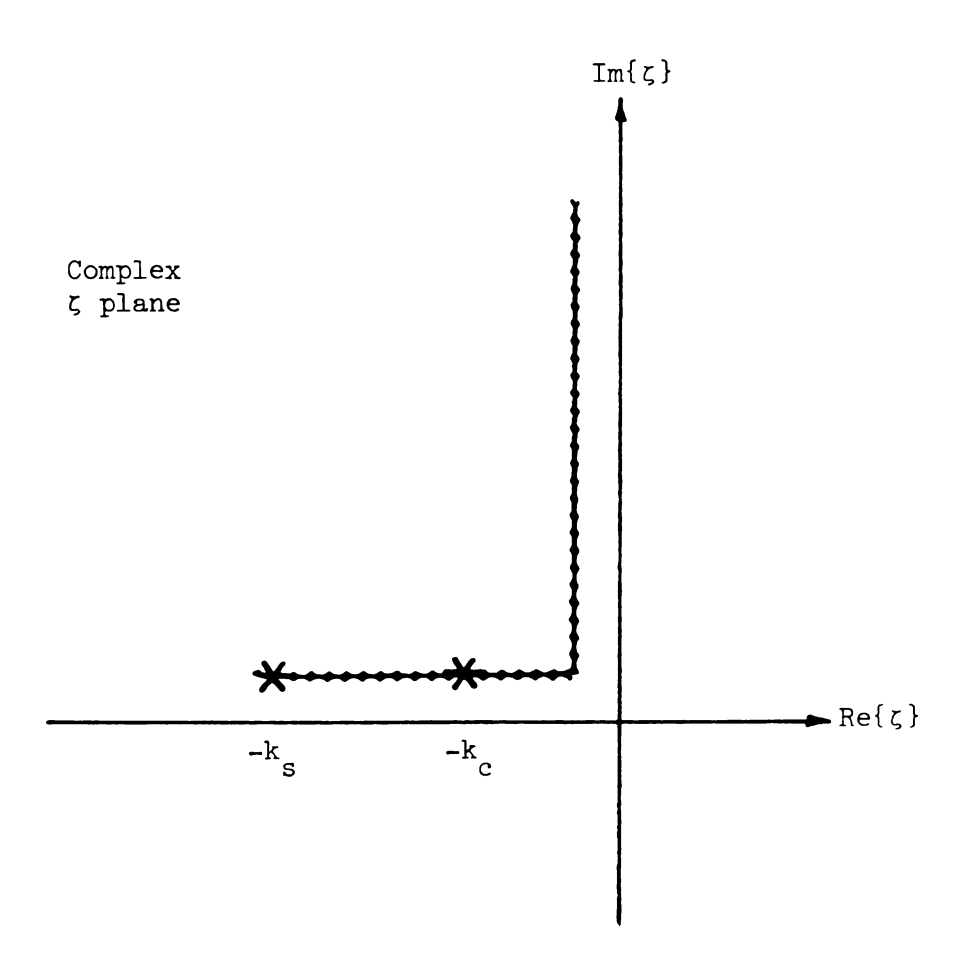


Figure 3.9: Detail of branch cuts in the comple ζ plane for transformed field in the asymmetric slab waveguide in the low loss limit.

$$\gamma_{\ell} = \sqrt{\zeta^{-}k_{\ell}} \quad \sqrt{\zeta^{+}k_{\ell}}$$

$$\theta_{\ell} = \operatorname{Arg}\{\gamma_{\ell}\}, \quad \theta_{\ell}^{\pm} = \operatorname{Arg}\{\zeta^{+}k_{\ell}\}$$

$$\theta_{\ell} = \frac{1}{2}(\theta_{\ell}^{+} + \theta_{\ell}^{-})$$
(86)

These definitions are illustrated in Figure 3.10.

First consider the portion of the branch cut integration in Figure 3.8 where $-k_S < Re\{\zeta\} < -k_C$, $Im\{\zeta\} = 0$. Along the lower portion of the branch cut we have

$$\theta_{\mathbf{S}} = \frac{\pi}{2} \quad , \quad \theta_{\mathbf{C}} = 0 \tag{87}$$

and along the upper portion of the branch cut,

$$\theta_{\mathbf{S}} = -\frac{\pi}{2} \quad , \quad \theta_{\mathbf{C}} = 0 \tag{88}$$

so that the transverse wavenumber parameters are

$$\gamma_{\rm S} = \frac{+}{2} j \nu$$
 , { lower upper } side of branch cut $\gamma_{\rm C} > 0$ (89)

where $v = \sqrt{k_s^2 - \zeta^2} > 0$. We can combine the integrals along the two sides of this portion of the branch cut so that only a single integral along $-k_s < \text{Re}\{\zeta\} < -k_c$ is necessary. To this end, define

$$\hat{e}(y,\zeta) = e(y,\zeta)$$
 | $-e(y,\zeta)$ | lower part or branch cut or branch cut (90)

Using the above results in the transformed field of equation (71) yields an expression for the transformed mode spectral component along

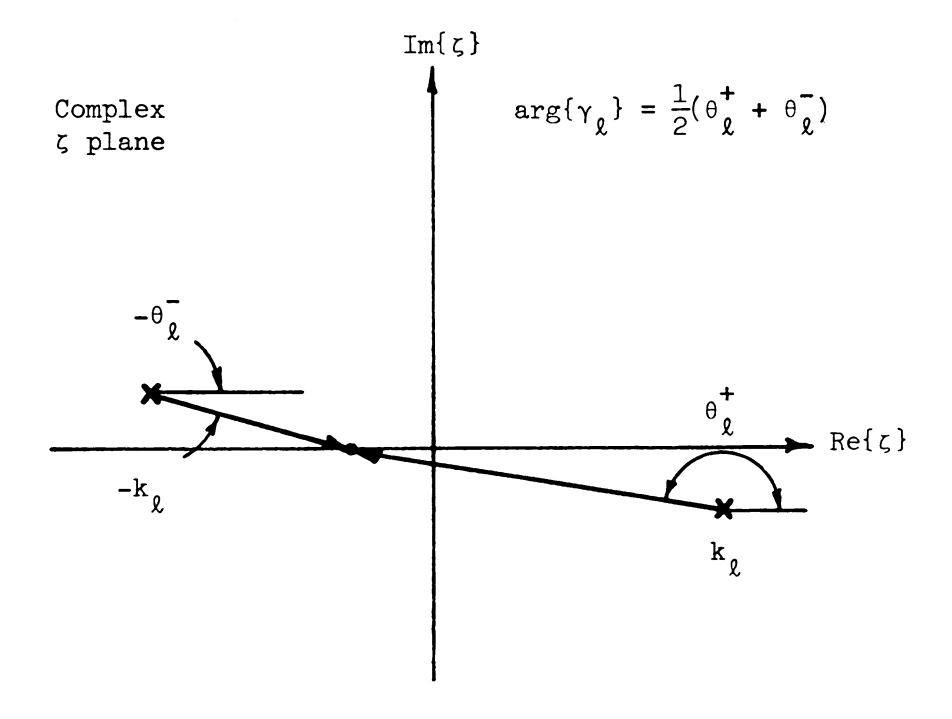


Figure 3.10: Complex ζ plane construction defining branch choice for reduced transverse wavenumber parameters, $\gamma_{\ell}.$

this portion or the branch integration:

$$\hat{e}_{1}(y,\zeta) = \frac{N_{1}}{D_{1}^{2}} \left[\gamma_{c} \sin \sigma (y-t) - \sigma \cos \sigma (y-t) \right], \quad 0 < y < t$$

$$- k_{s} < \text{Re}\{\zeta\} < -k_{c}, \quad \text{Im}\{\zeta\} = 0$$
(91)

where

$$N_{1} = 2j\sigma v \frac{k_{0}^{2}p^{e} - [\gamma_{c}(y_{0}-t)+j\zeta z_{0}]}{\varepsilon_{0}}$$

$$D_{1}^{2} = \sigma^{2}(\sigma \sin \sigma t - \gamma_{c}\cos \sigma t)^{2} + v^{2}(\gamma_{c}\sin \sigma t + \sigma \cos \sigma t)^{2}$$
(92)

Then the part of the total radiation field of the asymmetric slab contributed to by integration along this portion of the branch cut is

$$E_{RAD}(\mathbf{y}, \mathbf{z}) = -\frac{1}{2\pi} \int_{-\mathbf{k}_{\mathbf{S}}}^{-\mathbf{k}_{\mathbf{C}}} \hat{\mathbf{e}}_{1}(\mathbf{y}, \zeta) e^{\mathbf{j}\zeta \mathbf{z}} d\zeta$$
 (93)

The integrand in this portion of the radiation spectrum is called a partial radiation field spectral component [3.18]. The reason for this name is that the field is oscillatory in the spatial variable y in the substrate of the slab, but exponentially decaying in y away from the slab in the cover region of the waveguide. This is evident by the factors $\exp(\pm \gamma_{\ell} y)$ in the transformed Green's function of equation (70) and the observations made in equation (89).

The next portion of the branch cut integration of Figure 3.9 is that portion where $-k_c < \text{Re}\{\zeta\} < 0$ and $\text{Im}\{\zeta\} = 0$. Along the lower side of this portion of the branch cut,

$$\theta_{S} = \frac{\pi}{2}, \qquad \theta_{C} = \frac{\pi}{2} \tag{94}$$

and along the upper side of the branch cut

$$\theta_{S} = -\frac{\pi}{2} \quad , \quad \theta_{C} = -\frac{\pi}{2} \tag{95}$$

so that the transverse wavenumber parameters can be written as

$$\gamma_s = \pm j \nu$$
, $\gamma_c = \pm j \delta$, { lower upper } side of branch cut (96)

with $v=k_s^2-\zeta^2>0$, $\delta=k_c^2-\zeta^2>0$ here. We once again combine the integrals along the two sides of the branch cut as in equation (90) to obtain

$$\hat{e}_{2}(y,\zeta) - \frac{N_{2}}{D_{2}} \{ \sigma \cos \sigma y \cos [\delta(y_{0}-t)+\psi] + \nu \sin \sigma y \sin [\delta(y_{0}-t)+\psi] \}$$

$$- k_{c} < \text{Re}\{\zeta\} < 0, \quad I_{m}\{\zeta\} = 0 \qquad 0 < y < t \qquad (97)$$

where

$$N_{2} = -2j \frac{k_{0}^{2}p^{e}}{\varepsilon_{0}} - j\zeta_{0}z$$

$$D_{2}^{2} = [(\sigma^{2} + \delta v)\sin \sigma t]^{2} + [\sigma(\delta + v)\cos \sigma t]^{2}$$

$$\tan \psi = \frac{\sigma^{2} + \delta v}{\sigma(\delta + v)} \tan \sigma t$$
(98)

The part of the total radiation spectrum contributed to by integration along this portion of the branch cut is given by

$$E_{RAD_2}(y,z) = \frac{-1}{2\pi} \int_{-k_c}^{0} \hat{e}_2(y,\zeta) e^{j\zeta z} d\zeta$$
 (99)

The integrand in this portion of the radiation field is called a full radiation mode spectral component [3.18] of the asymmetric slab. The reason for this name is that the field is oscillatory in the

spatial variable y away from the slab in both the cover and substrate regions of the waveguide. This is evident from the factors $\exp(\pm \gamma_{\ell} y)$ in the transformed Green's function of equation (70) and the nature of as given in equation (96).

The last contribution to the total radiation rield is integration along that portion of the branch cut of Figure 3.9 where $\text{Re}\{\zeta\}=0$ and $0<\text{Im}\{\zeta\}<\infty$. Along the right side of this branch cut the arguments of γ_{ℓ} are as given in equation (96) and along the left side they are as in equation (97). Thus we have $\hat{e_3}(y,\zeta)$ identical in form to equation (97), where we now have ζ positive imaginary. The part of the total radiation field due to integration along this part of the branch cut is

$$E_{RAD_3}(y,z) = \frac{-1}{2\pi} \int_0^{\infty} \hat{e}_3(y,\zeta) e^{j\zeta} z_{d\zeta}$$
 (100)

The integrand in this portion or the radiation spectrum is called a full radiation rield spectral component for the reasons cited for equation (99). Note, however, that in this case the radiation rield spectral components are exponentially decaying in the waveguiding direction since ζ is imaginary on this part of the spectral integration path.

What we have accomplished in this section is to use the excitation theory developed in this chapter to recover several well known results of conventional excitation theory. This fact gives us confidence in our formulation, which can now be used to analyze problems which were formerly intractable when dealt with by conventional means.

3.4 Rectangular Strip Waveguide

The goal of this part of the chapter is to use the axially transformed equivalent polarization integral equation developed in this chapter to obtain an approximate, closed form solution for the transformed total electric field distribution in the core of a uniform rectangular strip waveguide. The uniform rectangular strip waveguide consists of an axially infinite uniform rectangular dielectric core of width 2a and height d integrated over the film layer of the trilayered infinite background structure introduced earlier. This waveguide configuration is shown in Figure 3.11. It is a structure of great interest to workers in the area of integrated optics due to its practicality and ease of fabrication, and has been widely studied (see, for example, [3.19], [3.20]).

We will proceed with our approximate closed form solution by postulating the functional forms of the transformed longitudinal electric and magnetic fields in the core. Our representations for the transformed longitudinal fields are each in terms of two unknown amplitude constants and two unknown transverse spatial frequency constants. The propagation constant ζ is also unknown in the expressions for the longitudinal fields. The Fourier transformed version of Maxwell's equations allow us to find expressions for the transformed transverse electric field components in terms of these longitudinal field components.

The resulting expression for the unknown transformed total electric field in the core of the strip waveguide is then substituted into the transformed equivalent polarization integral equation of

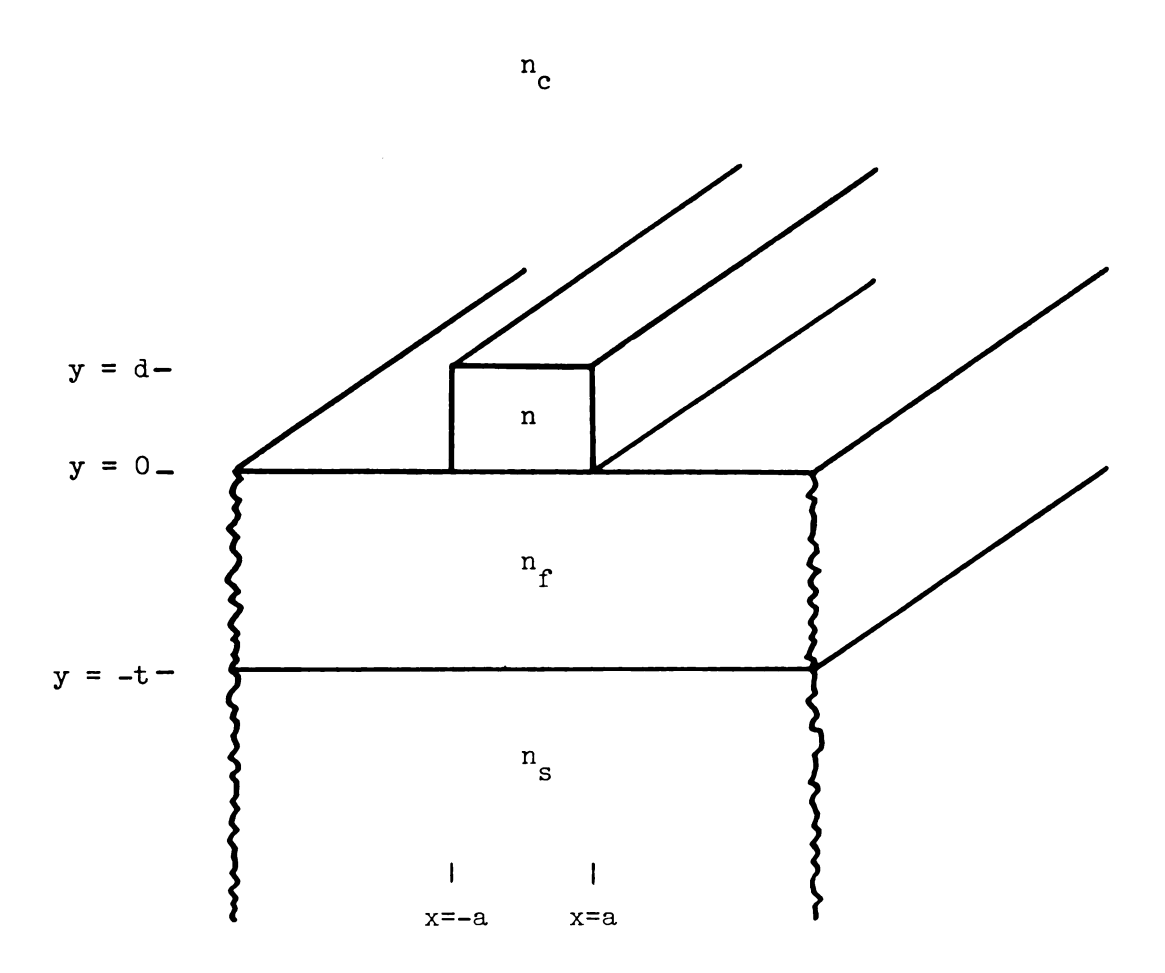


Figure 3.11: The uniform dielectric rectangular strip integrated over a tri-layered background structure.

section 3.1. The transformed integral equation is seperated into its three spatial components, yielding three scalar equations in the scalar components of the unknown total core rield. Each component equation is then enforced at four points inside the waveguide core, allowing elimination of the four unknown amplitude constants in the transformed field representations. What we are left with is three determinental equations in the unknown wavenumber parameters. These equations are solved simultaneously by numerical methods to find the unknown wavenumbers. Once the values of the unknown wavenumber parameters are determined, resubstitution into the matched component equations allows for evaluation of the four unknown amplitude constants. We thus obtain an approximate closed form expression for the unknown total transformed electric field in the waveguide core.

We first solve by this means the simpler problem of the rectangular strip waveguide in a uniform background region with $n_c = n_f = n_s$ to familiarize ourselves with the analytic technique described above. We then attack the full problem of the rectangular strip in the tri-layered background region of Figure 3.11. This is a more difficult problem since the phenomenon of guided mode leakage can occur here, as discussed in section 3.3. Numerical results are presented and compared with the results of other techniques.

3.4.1 Field Representation

In this section we postulate a general form for the longitudinal components of the transformed total electric field and magnetic field in the core of the strip waveguide. Parity arguments based on the

Fourier transformed version of Maxwell's equations allow identification of two classes of modes when the refractive index of the core is even in the transverse position variable, x. We restrict ourselves to the case of longitudinal electric fields odd in x and longitudinal magnetic rields even in x; the other rield parity can be handled in a similar manner.

The functional forms chosen for the axially transformed longitudinal fields satisfy the transformed version of Maxwell's equations and fit experimentally observed waveguide core field distributions. There is one difference, however, between the forms chosen here and those chosen by other workers [3.21]: we do not assume that the transverse wavenumbers associated with the transformed longitudinal electric field and magnetic field are identical. Given these transformed longitudinal field components, the transformed version of Maxwell's equations allow us to find all other transformed field components in terms of them.

If the refractive index of the core of the rectangular strip waveguide is assumed to be even in the transverse position variable x, so that n(x,y) = n(-x,y), then the components of the transformed total field, $\hat{e}(\hat{\rho},\zeta)$, must each posess either even or odd symmetry in x. The relationships of the symmetries of the various transformed field components can be found by considering the longitudinal parts of the transformed Maxwell's equations

$$(\nabla_{t} + j\zeta\hat{z}) \times (\stackrel{\rightarrow}{e_{t}} + \hat{z}e_{z}) = -j\omega\mu_{o}\stackrel{\rightarrow}{h}$$

$$(\nabla_{t} + j\zeta\hat{z}) \times (\stackrel{\rightarrow}{h_{t}} + \hat{z}h_{z}) = j\omega\stackrel{\rightarrow}{e}e$$
(101)

where we have decomposed the transformed fields into their transverse

and longitudinal parts. The longitudinal parts of equations (101) are

$$\frac{\partial e_{y}}{\partial x} - \frac{\partial e_{x}}{\partial y} = -j_{\omega\mu} _{O} h_{z}$$

$$\frac{\partial h_{y}}{\partial x} - \frac{\partial h_{x}}{\partial y} = +j_{\omega\epsilon} e_{z}$$
(102)

We see that if h_z has a given parity in x, then e_x has the same parity and e_y is of opposite parity. Similarly, h_x and h_y have the same and opposite parity, respectively as e_z . The transverse components of the transformed Maxwell's equations (101) can be solved to give expressions for the transverse field components in terms of the longitudinal components. We obtain

$$\vec{\mathbf{e}}_{t} = \frac{1}{\omega^{2} \mu_{o} \varepsilon^{-\zeta^{2}}} \left[\mathbf{j} \zeta \nabla_{t} \mathbf{e}_{z} + \mathbf{j} \omega \mu_{o} \hat{\mathbf{z}} + \nabla_{t} \mathbf{h}_{z} \right]$$
 (103)

Equation (103) gives us the following parity rules for the transverse components of the transformed electric field in the core of the rectangular strip waveguide:

since ε in equation (103) is even in x.

In the remainder of this section we will assume functional forms for the longitudinal components of the transformed total core fields that will make $\mathbf{e}_{\mathbf{x}}$ even in \mathbf{x} and $\mathbf{e}_{\mathbf{y}}$ odd in \mathbf{x} . The case of core fields

of opposite parity can be handled in a manner identical to that outlined below.

The general form we will assume for the longitudinal components of the transformed total waveguide core fields is

$$e_z = \sin \kappa_x \times [A'\cos \kappa_y y + B'\sin \kappa_y y]$$

 $h_z = \cos \sigma_x \times [C'\cos \sigma_y y + D'\sin \sigma_y y]$
(105)

These transformed longitudinal rields match experimentally determined field distributions and satisfy the transformed Maxwell's equations (101) if the transverse wavenumber parameters obey the relations

$$\kappa_{\mathbf{x}}^{2} + \kappa_{\mathbf{y}}^{2} = \sigma_{\mathbf{x}}^{2} + \sigma_{\mathbf{y}}^{2} = k^{2} - \zeta^{2}$$
 (106)

Other workers have assumed $\kappa_{\mathbf{X}} = \sigma_{\mathbf{X}}$ and $\kappa_{\mathbf{y}} = \sigma_{\mathbf{y}}$ [3.21], whereas we can find no a-priori reason for making such an assumption. We can later use the results of our analysis as a check on the validity of this choice.

Substitution or the transformed longitudinal rields of equation (105) into equation (103) allows us to find expressions for the transverse components of the transformed total core electric field.

We get

$$\begin{array}{l} \mathbf{e_x} = \kappa_x \cos \kappa_x \ \mathbf{x} \ [\mathsf{Acos} \ \kappa_y \ \mathbf{y} + \mathsf{Bsin} \ \kappa_y \ \mathbf{y}] + \sigma_y \mathbf{z} \ \cos \ \sigma_x \ \mathbf{x} \ [\mathsf{Csin} \ \sigma_y \ \mathbf{y} \\ - \ \mathsf{Dcos} \ \sigma_y \ \mathbf{y}] \end{array} \tag{107}$$

$$\mathbf{e_y} = \kappa_y \mathbf{sin} \ \kappa_x \ \mathbf{x} \ [\mathsf{-Asin} \ \kappa_y \ \mathbf{y} + \mathsf{Bcos} \ \kappa_y \ \mathbf{y}] - \sigma_x \mathbf{zsin} \ \sigma_x \ \mathbf{x} \ [\mathsf{Ccos} \ \sigma_y \ \mathbf{y} \\ + \ \mathsf{Dsin} \ \sigma_y \ \mathbf{y}] \end{array}$$

where we have derined

$$z = \frac{\omega \mu_0}{\zeta} , \begin{cases} A \\ B \\ C \\ D \end{cases} = \frac{j_{\zeta}}{\kappa^2 - \zeta^2} \begin{cases} A' \\ B' \\ C' \\ D' \end{cases}$$
(108)

We now have general expressions for the total transformed electric field in the core of the rectangular strip waveguide. There are seven unknowns involved: the amplitude constants A, B, C, and D; and three of the wavenumber parameters, which we take as $\kappa_{\mathbf{x}}$, $\sigma_{\mathbf{x}}$ and ζ . Note that the other two transverse wavenumber parameters, $\kappa_{\mathbf{y}}$ and $\sigma_{\mathbf{y}}$, can be found from these by application of the realations in equation (106). We will use these forms of the transformed unknown total core electric field in the transformed equivalent polarization integral equation of section 3.1. Demanding the integral equation be satisfied will allow us to determine the propagation characteristics and field distributions in the rectangular strip waveguide.

3.4.2 Principle Terms

Before we substitute our expressions of part 3.4.1 for the transformed total core electric field into the transformed equivalent polarization integral equation or section 3.1 we will rewrite the integral equation in a slightly different form. Since the dyadic Green's function in the integral of our integral equation (5) has two parts as shown in equation (9), we can split the integral into two terms, a principle and a reflected term:

$$\stackrel{?}{e}(\stackrel{?}{\rho}) - N^{2} (k_{o}^{2} + \stackrel{\tilde{\nabla}\tilde{\nabla}}{\nabla}) \int_{CS} \stackrel{?}{g^{p}}(\stackrel{?}{\rho}|\stackrel{?}{\rho}) \stackrel{?}{e}(\stackrel{?}{\rho}) dS'$$

$$- N^{2} (k_{o}^{2} + \stackrel{\tilde{\nabla}\tilde{\nabla}}{\nabla}) \int_{CS} \stackrel{?}{g^{r}}(\stackrel{?}{\rho}|\stackrel{?}{\rho}) \stackrel{?}{e}(\stackrel{?}{\rho}) dS' = 0$$
(109)

where we have specialized to surface waves of the rectangular strip waveguide by setting the incident field equation to zero in equation (5). Here CS denotes the rectangular cross section of the waveguide core, $-a < x^* < a$, $0 < y^* < d$, and N^2 is the constant refractive index contrast of the uniform dielectric core, $N^2 = n^{-2}_{C}(n^2 - n_{C}^2)$. The transformed principle and reflected Hertzian potential Green's functions have the forms given in section 3.2 and the ζ dependence of all terms in equation (109) has been suppressed for clarity.

In this section we will deal with the terms in equation (109) corresponding to the principle Green's dyad. In the next section the reflected terms in equation (109) are dealt with in a different manner. The results of the analysis in this section can be considered the solution of the problem of an isolated rectangular strip waveguide. In this case the tri-layered background region is absent and thus reflected part of the transformed Green's dyad is zero. If the integral equation (109) is written as

$$\overrightarrow{e}(\overrightarrow{\rho}) - \overrightarrow{P}(\overrightarrow{\rho}) - \overrightarrow{R}(\overrightarrow{\rho}) = 0$$
 (110)

we are here concerned with the term $\overrightarrow{P}(\overrightarrow{\rho})$,

$$\vec{P}(\vec{\rho}) = N^{2}(k_{c}^{2} - \vec{\nabla}\vec{\nabla} \cdot) \int_{CS} g^{p}(\vec{\rho} | \vec{\rho} ') \vec{e}(\vec{\rho} ') dS'$$
(111)

If the Sommerfeld integral representation in equation (15) is used for the transformed principle Green's function, then we obtain for the α th component of \overrightarrow{P} the formula

$$P_{\alpha}(\vec{p}) = N^{2} \int_{-\infty}^{\infty} \frac{e^{j \xi x}}{4 \pi p_{c}} \left[k_{c} Q_{\alpha}(y) + \hat{x}_{\alpha} \cdot \vec{\nabla} (\vec{\nabla} \cdot \vec{Q}(y)) \right] d\xi$$
 (112)

where $\alpha = x$, y, or z. Here $\tilde{\nabla} = j\xi\hat{x} + \frac{\partial}{\partial y} \hat{y} + j\zeta\hat{z}$ since the x variation in the integral terms in equation (109) is or the form $\exp(j\xi x)$. We have derined $\vec{Q}(y)$ as the spatial integral

$$\vec{Q}(y) = \int_{CS} e^{-j \xi x'} e^{-p_C |y-y'|} |\vec{e}(\vec{\rho}') dS'$$
(113)

Substitution or the general transformed field expressions of equations (96) and (98) into equation (103) gives

$$Q_{x} = \kappa_{x} X_{c_{\kappa}} [AY_{c_{\kappa}} + BY_{s_{\kappa}}] + \sigma_{y} ZX_{c_{\sigma}} [CY_{s_{\sigma}} - DY_{c_{\sigma}}]$$

$$Q_{y} = \kappa_{y} X_{s_{\kappa}} [-AY_{s_{\kappa}} + BY_{c_{\kappa}}] - \sigma_{x} ZX_{s_{\sigma}} [CY_{c_{\sigma}} + DY_{s_{\sigma}}]$$

$$Q_{z} = \frac{k^{2} - \zeta^{2}}{J_{\zeta}} X_{s_{\kappa}} [AY_{c_{\kappa}} + BY_{s_{\kappa}}]$$
(114)

where the results or the spatial integrals in (113) give rise to the terms

$$X_{\{c\}} \gamma = \begin{cases} 1 \\ -j \end{cases} \left[\frac{\sin a(\xi - \gamma)}{\xi - \gamma} + \frac{\sin a(\xi + \gamma)}{\xi + \gamma} \right]$$

$$Y_{\{c\}} \delta (y) = \frac{1}{p_c^2 + \delta^2} \left[2p_c \begin{cases} \cos \delta y \\ \sin \delta y \end{cases} + \begin{cases} -p_c \\ \delta \end{cases} e^{-p_c y}$$

$$-e^{p_c (y - d)} \left(\begin{cases} p_c \cos \delta d - \delta \sin \delta d \\ p_c \sin \delta d + \delta \cos \delta d \end{cases} \right) \right]$$
(115)

Next we examine the term $\nabla (\nabla \cdot \mathbf{Q}(\mathbf{y}))$ of equation (112). It is

$$\hat{\mathbf{x}} \cdot \hat{\nabla} \hat{\nabla} \cdot \hat{\mathbf{Q}} = - \xi^{2} [\kappa_{\mathbf{X}} \mathbf{X}_{c_{\mathbf{K}}} (\mathbf{A} \mathbf{Y}_{c_{\mathbf{K}}} + \mathbf{B} \mathbf{Y}_{s_{\mathbf{K}}}) + \sigma_{\mathbf{y}} \mathbf{Z} \mathbf{X}_{c_{\mathbf{Q}}} (\mathbf{C} \mathbf{Y}_{s_{\mathbf{Q}}} - \mathbf{D} \mathbf{Y}_{c_{\mathbf{Q}}})]$$

$$+ \mathbf{j} \xi \mathbf{p}_{c} [\kappa_{\mathbf{y}} \mathbf{X}_{s_{\mathbf{K}}} (-\mathbf{A} \mathbf{Y}_{s_{\mathbf{K}}}^{*} + \mathbf{B} \mathbf{Y}_{c_{\mathbf{K}}}^{*}) - \sigma_{\mathbf{x}} \mathbf{Z} \mathbf{X}_{s_{\mathbf{Q}}} (\mathbf{C} \mathbf{Y}_{c_{\mathbf{Q}}}^{*} - \mathbf{D} \mathbf{Y}_{s_{\mathbf{Q}}}^{*})]$$

$$+ \mathbf{j} (\mathbf{k}^{2} - \zeta^{2}) \mathbf{X}_{s_{\mathbf{K}}} (\mathbf{A} \mathbf{Y}_{c_{\mathbf{K}}} + \mathbf{B} \mathbf{Y}_{s_{\mathbf{K}}})$$

$$\hat{\mathbf{y}} \cdot \hat{\nabla} \hat{\nabla} \cdot \hat{\mathbf{Q}} = \mathbf{j} \xi \mathbf{p}_{c} [\kappa_{\mathbf{X}} \mathbf{X}_{c_{\mathbf{K}}} (\mathbf{A} \mathbf{Y}_{c_{\mathbf{K}}}^{*} + \mathbf{B} \mathbf{Y}_{s_{\mathbf{K}}}^{*}) + \sigma_{\mathbf{y}} \mathbf{Z} \mathbf{X}_{c_{\mathbf{Q}}} (\mathbf{C} \mathbf{Y}_{s_{\mathbf{Q}}}^{*} - \mathbf{D} \mathbf{Y}_{c_{\mathbf{Q}}}^{*})]$$

$$+ p_{c}[\kappa_{y}X_{s\kappa}(-AY_{s\kappa}^{"} + BY_{c\kappa}^{"}) - \sigma_{x}ZX_{s\sigma}(CY_{s\sigma}^{"} + DY_{s\sigma}^{"})]$$

$$+ p_{c}(k^{2} - \zeta^{2})X_{s\kappa}(AY_{c\kappa}^{!} + BY_{s\kappa}^{!})$$

$$\hat{z} \cdot \tilde{\nabla} \tilde{\nabla} \cdot \tilde{Q} = \xi \zeta[\kappa_{x}X_{c\kappa} + BY_{s\kappa}) + \sigma_{y}ZX_{c\sigma}(CY_{s\sigma} - DY_{c\sigma})]$$

$$+ j\zeta p_{c}[\kappa_{y}X_{s\kappa}(-AY_{s\kappa}^{!} + BY_{c\kappa}^{!}) - \sigma_{x}ZX_{s\sigma}(CY_{c\sigma}^{!} + DY_{s\sigma}^{!})]$$

$$+ j\zeta(\kappa^{2} - \zeta^{2})X_{s\kappa}(AY_{c\kappa} + BY_{s\kappa})$$

$$(116)$$

where we have defined

$$Y_{\begin{Bmatrix} s \\ c \end{Bmatrix}} \delta = \frac{1}{p_c} \frac{\partial}{\partial y} Y_{\begin{Bmatrix} s \\ c \end{Bmatrix}} \delta, \quad Y_{\begin{Bmatrix} c \\ s \end{Bmatrix}} \delta = \frac{\partial}{\partial y} Y_{\begin{Bmatrix} c \\ s \end{Bmatrix}} \delta$$
 (117)

with \mathbf{Y}_{δ} as given in equation (115).

We can now substitute the results in equations (114) and (117) into the expression in equation (112) for \vec{P} . The result is presented most compactly by collecting multiples or the four unknown amplitude constants, A, B, C, and D. Each component of \vec{P} then has the form

$$P_{\alpha}(\stackrel{\rightarrow}{\rho}) = AF_{1}^{\alpha}(\stackrel{\rightarrow}{\rho}) + BF_{2}^{\alpha}(\stackrel{\rightarrow}{\rho}) + CF_{3}^{\alpha}(\stackrel{\rightarrow}{\rho}) + DF_{4}^{\alpha}(\stackrel{\rightarrow}{\rho})$$
 (118)

for α = x, y, or z. The terms F^{α} in equation (118) are complicated functions involving integration on the spectral variable, ξ . They are detailed in Appendix C. It is important to note that the functions F^{α} depend on the transverse position variables and the unknown wavenumbers κ_{χ} , σ_{χ} , and ζ (we view κ_{γ} and σ_{γ} as dependent on these wavenumbers, as discussed above).

3.4.3 Reflected Terms

In this section we will find a closed form approximation for the reflected Green's function integral $\vec{R}(\vec{\rho})$ of equation (110). This

approximation is based on the fact that the transformed reflection and coupling coefficients appearing in the integral expressions for the components of the transformed reflected Green's dyad have simple poles in the complex ξ plane. We will use the residue theorem to approximate the components of the transformed reflected Green's dyad by its residues at these poles and neglect the branch integral contributions.

This approximation corresponds to decomposing the transformed reflected Green's dyad into a portion given corresponding to surface waves of the tri-layered background structure and a portion corresponding to the radiation field of the background, and then neglecting the radiation field contribution to the reflected Green's dyad. The validity of this approximation can be guaged by the accuracy of the results it produces.

In section 3.3.5 we round the locations in the complex ξ plane or the poles of the transformed reflection coefficients $R_t(\xi)$ and $R_n(\xi)$ and the coupling coefficient $C(\xi)$ occurring in the integral expressions for the components of the transformed reflected Green's dyad. Since the parameters κ , γ , and δ in equation (53) depend on ξ^2 , then if ξ_p is a pole of one of these coefficients, then so is $-\xi_p$. This fact that the poles of the reflection and coupling coefficients are symmetrically located in the ξ plane with respect to the origin is illustrated in Figure 3.4. As shown there, in using the residue theorem to evaluate the real line ξ integral we must choose a deformation of the integration contour into either the upper half or lower half complex ξ plane. This choice is made based on the convergence properties of the integrand. We want the integrand of the

reflected Green's dyad components to decay on the infinite semi-circular contour, \mathscr{C}_{∞} . As evidenced by equation (13), the decay of the integrands is governed by the presence of the factor $\exp(j\xi(x-x'))$. Thus if x is greater than x' the closure must be made in the upper half complex ξ plane, and otherwise in the lower half plane.

Both cases x > x' and x < x' can be accommodated at once. Consider the contribution to an integral $\int_{-\infty}^{\infty} r(\xi)e^{j\xi(x-x')}d\xi$ due to a pair of poles of $f(\xi)$ at $\pm \xi_{D}$. Here $f(\xi)$ represents the remainder of the integrand or a component of the reflected Green's dyad. We assume slightly lossy media so that $\text{Im}\{\xi_D\}$ < 0. If x>x' we must choose upper half plane closure to insure convergence along $\mathscr{C}_{\underline{\ }}$ (see Figure 3.4). The residue at enclosed pole at $-\xi_p$ is $2\pi j \text{Res}\{f(\xi)\}e^{-j\xi_p(x-x^*)}$. On the other hand, if x < x' we must choose lower half plane closure to ensure convergence along $\mathscr{C}_{\mathbb{R}}$. The residue at the enclosed pole at ξ_p is $-2\pi j Res\{f(\xi)\}e^{j\xi}p^{(x-x')}$. The reason for the change in sign of the residue contribution is that the orientation of the closed integration contour has changed (see [3,22]). The contour had a counter clockwise orientation for the case x > x', but now has a clockwise orientation when x < x'. Now if the residue of $f(\xi)$ is odd in & we can write the residue contribution in the latter case as $2jRes\{r(\xi)\}e^{j\xi}p^{(x-x')}$. Comparing this with the residue term for the case x > x' we see that both cases are accommodated at once if we replace the exponential term with $\exp(j\xi|x-x'|)$. It will be shown below that the residues of the transformed reflected Green's function component integrands are indeed odd in &, and we will always assume upper half plane closure for the deformed integration path with the modified exponential term above.

We now turn to the evaluation or the residues of the transformed reflection and coupling coefficients in the reflected Green's dyad.

In Appendix A it is shown that the tangential reflection coefficient has the form

$$R_{t}(\xi) = N_{t}(\xi)$$

$$D_{t}(\xi)$$
(119)

where $D_{\mathbf{t}}(\xi)$ is as given in equation (44). The residue of $R_{\mathbf{t}}$ at a zero of $D_{\mathbf{t}}$ is given by the usual formula: If is a simple pole of $R_{\mathbf{t}}$ then

$$\operatorname{Res}_{\xi_{n}} \{R_{t}(\xi)\} = \frac{N_{t}(\xi)}{\partial \xi} D_{t}(\xi) \Big|_{\xi_{n}}$$
(120)

Dirrerentiation or equation (44) for D_t is done with the aid of the chain rule and the expressions in Appendix A. The result is

$$\operatorname{Res}\{R_{t}(\xi)\} = \frac{P_{rn}N_{t}(\xi_{n})}{2\xi_{n}\left[t + \frac{1}{p_{cn}} + \frac{1}{p_{rn}}\right]}$$
(121)

where $p_{\ell n} = p_{\ell}(\xi = \xi_n)$. Note that this residue is odd in ξ as mentioned above. The residues of the coefficients R_n and C are found in an identical manner. The result is

$$\frac{p_{sn}N_{n}(\xi_{n})}{\xi} = \frac{p_{sn}N_{n}(\xi_{n})}{2\xi_{n}\left[t + \frac{1}{p_{sn}}\left(\frac{p_{rn}^{2} - p_{sn}^{2}}{N_{sr}^{2}p_{rn}^{2} - N_{rs}^{2}p_{sn}^{2}}\right) + \frac{1}{p_{cn}}\left(\frac{p_{cn}^{2} - p_{rn}^{2}}{N_{rc}^{2}p_{cn}^{2} + N_{cr}^{2}p_{rn}^{2}}\right)\right]}$$

$$\text{Res}\{C(\xi)\} = \begin{cases} \frac{N_{c}(\xi_{n})}{N_{t}(\xi_{n})D_{n}(\xi_{n})} & \text{Res}\{R_{t}(\xi)\} \\ N_{t}(\xi_{n})D_{n}(\xi_{n}) & \xi_{n} \end{cases} , \quad \xi_{n} \text{ a zero of } D_{t}$$
 (122)
$$\frac{N_{c}(\xi_{n})}{N_{n}(\xi_{n})D_{t}(\xi_{n})} & \text{Res}\{R_{n}(\xi)\} , \quad \xi_{n} \text{ a zero of } D_{n}$$

where the factors in equation (122) are given in Appendix A. Note that these residues are also odd in ξ .

We now turn to the approximation or the reflected term $R(\)$ in equation (110). It is given by

$$\vec{R}(\vec{\rho}) = N^2(k_c^2 + \nabla \nabla \cdot) \int_{CS} \vec{g}^r(\vec{\rho} \mid \vec{\rho}') \cdot \vec{e}(\vec{\rho}') dS'$$
 (123)

Now by equation (12) we have

$$\hat{\mathbf{g}}^{\mathbf{r}} \cdot \hat{\mathbf{e}} = \hat{\mathbf{x}} \mathbf{g}_{\mathbf{t}}^{\mathbf{r}} \mathbf{e}_{\mathbf{x}} + \hat{\mathbf{y}} \left(\frac{\partial}{\partial} \mathbf{g}_{\mathbf{c}}^{\mathbf{r}} \mathbf{e}_{\mathbf{x}} + \mathbf{g}_{\mathbf{n}}^{\mathbf{r}} \mathbf{e}_{\mathbf{y}} + \mathbf{j} \xi \mathbf{g}_{\mathbf{c}}^{\mathbf{r}} \mathbf{e}_{\mathbf{z}} \right) + \hat{\mathbf{z}} \mathbf{g}_{\mathbf{t}}^{\mathbf{r}} \mathbf{e}_{\mathbf{z}} \tag{124}$$

We use the above results to write a residue contribution approximation to the components of the reflected Green's dyad

where the sum is over all TE and TM surface wave poles of the trilayered background structure located in the upper half complex ξ plane. We have derined

The spatial integration in equation (123) can be done with the help of equations (124) and (125). It gives a result of the form

$$\int_{CS} \overrightarrow{g}^{r} \cdot \overrightarrow{e} dS' = \hat{x}I_{tx} + \hat{y}(\frac{\partial}{\partial x} I_{ex} + I_{ny} + j\xi I_{ez}) + \hat{z}I_{tz}$$
 (127)

Here we have defined

$$I \begin{Bmatrix} t \\ n \\ c \end{Bmatrix} \alpha = \sum_{n} \begin{Bmatrix} R_{tn} \\ R_{nn} \\ C_{n} \end{Bmatrix} \xrightarrow{e} \frac{-p_{cn}y}{\xi_{n}} \mathscr{I}_{\alpha}(x)$$

$$\alpha = x,y,z \qquad (128)$$

$$\mathscr{I}_{\alpha}(x) = \int_{CS} e^{j\xi_{n}|x-x'|} e^{-p_{cn}y'} e^{-(p')dS'}$$

where e_{α} is the α^{th} component or $\stackrel{\rightarrow}{e}$ as given in equations (105) and (107).

We can now dirrerentiate equation (127). The result is

$$\widetilde{\nabla}\widetilde{\nabla} \cdot \int_{CS} \overset{\text{dr}}{\text{gr}} \cdot \overset{\text{deds'}}{\text{eds'}} = \hat{\mathbf{x}}[\mathbf{I}_{t_{\mathbf{x}}}^{"} - \mathbf{p}_{en}\mathbf{I}_{e_{\mathbf{x}}}^{"} - \mathbf{p}_{en}\mathbf{I}_{n_{\mathbf{y}}}^{"} - \mathbf{j}\zeta\mathbf{p}_{en}\mathbf{I}_{e_{\mathbf{z}}}^{"} + \mathbf{j}\zeta\mathbf{I}_{t_{\mathbf{z}}}^{"}]$$

$$+ \hat{\mathbf{y}}[-\mathbf{p}_{en}\mathbf{I}_{t_{\mathbf{x}}}^{"} + \mathbf{p}_{en}^{2}(\mathbf{I}_{e_{\mathbf{x}}}^{"} + \mathbf{I}_{n_{\mathbf{y}}}^{"} + \mathbf{j}\zeta\mathbf{I}_{e_{\mathbf{z}}}^{"}) - \mathbf{j}\zeta\mathbf{p}_{en}\mathbf{I}_{t_{\mathbf{z}}}^{"}]$$

$$+ \hat{\mathbf{z}}[\mathbf{j}\zeta\mathbf{I}_{t_{\mathbf{x}}}^{"} - \mathbf{j}\zeta\mathbf{p}_{en}(\mathbf{I}_{e_{\mathbf{x}}}^{"} + \mathbf{I}_{n_{\mathbf{y}}}^{"} + \mathbf{j}\zeta\mathbf{I}_{e_{\mathbf{z}}}^{"}) - \zeta^{2}\mathbf{I}_{t_{\mathbf{z}}}^{"}]$$
(129)

with $I_{\alpha}^{p} = \frac{\partial^{p}}{\partial x^{p}}$ I_{α} . The result of the spatial integration in equation (128) is

We are now in a position to evaluate $\overrightarrow{R}(\overrightarrow{\rho})$ as in equation (123) by substitution or equations (127) and (129). The results is expressed most compactly by collecting multiples of the unknown amplitude constants, A, B, C, and D. Each component of \overrightarrow{R} then has the form

$$R_{\alpha}(\vec{\rho}) = AG_{1}^{\alpha}(\vec{\rho}) + BG_{2}^{\alpha}(\vec{\rho}) + CG_{3}^{\alpha}(\vec{\rho}) + DG_{4}^{\alpha}(\vec{\rho})$$
 (131)

for α = x, y, or z. The terms G^{α} in equation (131) are complicated functions involving factors such as those in equation (130). These terms are detailed in Appendix C. It is important to note that the functions G^{α} depend on transverse position variables and the unknown wavenumbers κ_{x} , σ_{x} , and ζ (we again view κ_{y} and σ_{y} as dependent on these).

3.4.4 Computational Considerations

We can now write out each component of the transformed integral equation for the rectangular strip waveguide. By equation (110) we

have the three component equations

$$e_{\alpha}(\vec{\rho}) - P_{\alpha}(\vec{\rho}) - R_{\alpha}(\vec{\rho}) = 0$$
 (132)

where α = x, y, or z. Each term in equation (132) contains the four unknown amplitude coerricients, A, B, C, and D. The runctions multiplying the amplitude constants are themselves dependent on the three unknown wavenumbers $\kappa_{\rm X}$, $\sigma_{\rm X}$, and ζ . We need to solve for all seven unknowns to determine our approximate close form solution for the total transformed electric field in the waveguide core.

We can eliminate the amplitude constants by evaluating equation (132) at rour points, (x_i, y_i) , with i = 1,...,4, inside the waveguide core. This results in rour equations of the type

$$\begin{bmatrix} H_{ij}^{\alpha}(\kappa_{\mathbf{x}}, \sigma_{\mathbf{x}}, \zeta) \end{bmatrix} \begin{bmatrix} A \\ B \\ C \\ D \end{bmatrix} = 0$$
 (133)

where, for $\alpha = x$, y, or z, we define

$$H_{ij}^{\alpha} = \begin{cases} \text{multiple or } i^{\text{th}} \\ \text{amplitude const.} \\ \text{in } e_{\alpha} \text{ evaluated} \\ \text{at } (x_{j}, y_{j}) \end{cases} + F_{i}^{\alpha}(x_{j}, y_{j}) + G_{i}^{\alpha}(x_{j}, y_{j})$$

$$(134)$$

and F $^{\alpha}$, G $^{\alpha}$ are as given in equations (118) and (131). A non-trivial solution for the transformed core field requires

$$Det\{H_{ij}^{\alpha}(\kappa_{x},\sigma_{x},\zeta)\} = 0$$
 (135)

for all three component equations. Since the matrix elements H_{ij}^{α} depend on the unknown wavenumbers κ_{x} , σ_{x} , and ζ , what we have round are three determinental equations in these three unknowns.

We will solve these equations numerically by Newton's iterative method. First write

$$\overrightarrow{w} = \begin{bmatrix} \kappa \\ \sigma \\ \chi \\ \zeta \end{bmatrix}, \overrightarrow{D}(\overrightarrow{w}) = \begin{bmatrix} \text{Det}\{H^{X}(\overrightarrow{w})\} \\ \text{Det}\{H^{Y}(\overrightarrow{w})\} \\ \text{Det}\{H^{Z}(\overrightarrow{w})\} \end{bmatrix}$$
(136)

We want to rind \vec{w}_r with $\vec{D}(\vec{w}_r) = 0$. If we are given an initial guess, \vec{w}_0 , at this root, Newton's iterative method tells us to calculate [3.23]

$$\overrightarrow{\mathbf{w}}_{i+1} = \overrightarrow{\mathbf{w}}_{i} = [\partial D^{T}(\overrightarrow{\mathbf{w}}_{i})]^{-1} \overrightarrow{\mathbf{D}}(\overrightarrow{\mathbf{w}}_{i})$$
(137)

where ∂D^T is the transpose of the Jacobian matrix,

$$\partial D_{ij} = \frac{\partial D_{i}}{\partial w_{i}}$$

Given a sufficiently good initial guess, equation (137) will converge to the root \overrightarrow{w}_r .

Once we have found a root of \vec{D} we can find the core field distribution by evaluating the amplitude constants A, B, C, and D. To do this we choose one component matrix equation (133). Since this matrix is singular, we set one of the amplitude constants equal to one, eliminate one row of the matrix, and solve the resultant inhomogeneous matrix equation for the other three amplitude coefficients.

3.4.5 Numerical Results

A computer program was written to implement this method of solution for the transformed core electric field in an integrated rectangular dielectric strip waveguide. In this section we present numerical results of the execution of this program for several different rectangular strip waveguide configurations.

The first waveguide configuration we consider here is the isolated rectangular strip in a uniform dielectric surround. This is a particularly simple case to analyze since the reflected part of the transformed Hertzian potential Green's dyad is zero in the absence of the tri-layered background structure of Figure 3.11. This is clear physically because there are no background structure interfaces to reflect the primary Hertzian potential. This face is seen mathematically by setting $n_{\rm S} = n_{\rm f} = n_{\rm c}$. Then the reflection and coupling coefficients $R_{\rm t}$, $R_{\rm n}$, and C occurring in the Sommerreld integral representations of the components of the reflected Green's dyad are zero, thus giving a zero result for the reflected Green's dyad in this case (set $p_{\rm C} = p_{\rm f} = p_{\rm s}$ in the expressions for $R_{\rm t}$, $R_{\rm n}$, and C in appendix A).

The isolated rectangular strip waveguide examined here consists or a uniform rectangular dielectric core of refractive index n = 1.5 surrounded by a uniform medium of refractive index n_c = 1.0. The rectangular core is of width 2a and height d = a. The program was executed for several electric core sizes by letting the ratio a/λ_0 vary with λ_0 = $2\pi c/\omega$ as usual.

The program requires an initial guess at the unknown wavenumbers $\kappa_{\mathbf{x}}$, $\sigma_{\mathbf{x}}$, and ζ to begin iteration of the Newton's method root finder (see equation (137)). We always assume that $\kappa_x = \sigma_x$ and $\kappa_y = \sigma_y$ for the initial guess. We input κ_{χ} and κ_{ψ} and find ζ from equation (106). The initial guesses for κ_{χ} and $~\kappa_{\psi}~$ were obtained by a method essentially identical to that used by Marcatilli [3.24] to approximate the eigenvalues or isolated rectangular strip waveguide. The approximation of $\kappa_{\boldsymbol{x}}$ is accomplished by ignoring the \boldsymbol{y} variation of the core rields. This corresponds physically to allowing the rectangular core height tend to infinity, giving rise to a structure uniform in the y direction. Then the structure being considered is a symmetric slab waveguide or width 2a as shown in Figure 3.12. The characteristic equation of the symmetric slab is solved, yielding which we use as our guess at $\kappa_{\chi^{\bullet}}$. The approximation of κ_{χ} is accomplished in a similar manner by ignoring the x variation of the core fields. The rectangular core width is allowed to tend to infinity, giving rise to a symmetric slab waveguide of width d = a as shown in Figure 3.12. The solution κ for this symmetric slab is used as the initial guess for κ_{v} .

In table 3.1 we present the numerical results of the program for the isolated rectangular strip waveguide. The agreement between the Marcatilli approximation of $\kappa_{\mathbf{X}}$, $\kappa_{\mathbf{y}}$ and ζ and the program results for these wavenumbers is seen to be quite good for electrically large waveguides, with decreasing agreement as a/λ_0 approaches zero. We also note that the assumption $\kappa_{\mathbf{X}} = \sigma_{\mathbf{X}}$ and $\kappa_{\mathbf{y}} = \sigma_{\mathbf{y}}$ made by other workers seems to be valid for large waveguides, but not for electrically small guides. The program results for the transverse

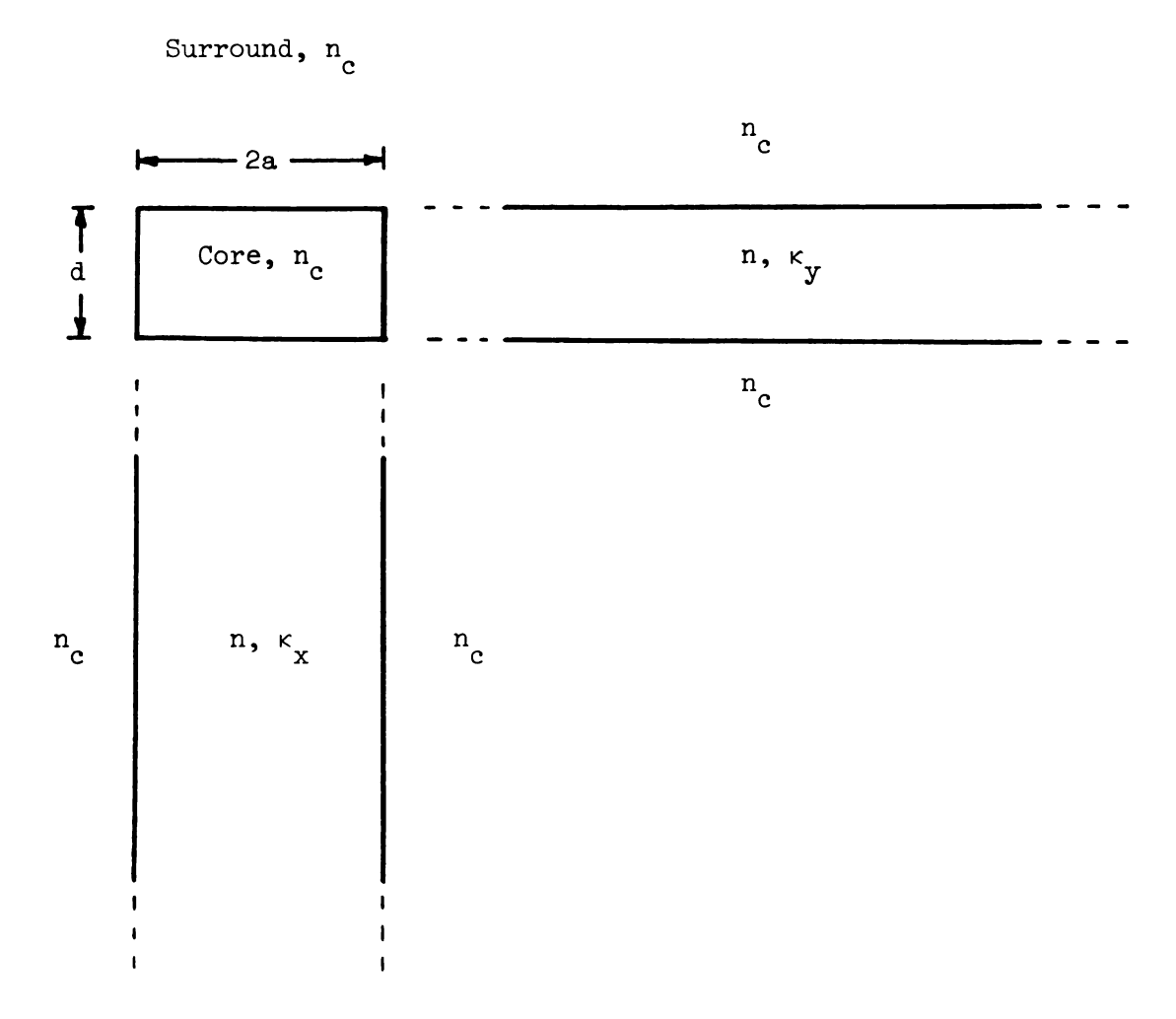


Figure 3.12: Diagram illustrating Marcatili's approximation of the eigenvalues of the isolated uniform rectangular strip waveguide.

Normalized eigenvalues of the isolated uniform rectangular strip waveguide for Table 3.1:

Table 3.1:	 	Normal1 several approx	Normalized eigenvalues c several normalized guide approximate technique.	ized gu: echniqu	s or thide wide. e. Her	the isola widths com Here n = 1	olated uni compared to = 1.5, n _c ^a	form rectal to the resu = 1.0, d/a	Normalized eigenvalues of the isolated uniform rectangular strip waveguide several normalized guide widths compared to the results of Marcatili's approximate technique. Here $n=1.5,n_{\rm C}=1.0,d/a=1.0.$	strip w Marcati	aveguide 11's
a/ y0		× ×			куа		g × a	oya		ζa	
	Marc.	s. Iter.	8€	Marc.	Iter.	8€	Iter.	Iter.	Marc.	Iter.	8 ∨
0.22	1	1.22	;	1	0.88	•	1.09	1.04		1.48	;
0.27	1.21	1.23		1.43	1.26	-11.6	1.06	1.41	1.70	1.82	8 ° 9
0.36	1.31	1.34	2.7	1.68	1.61	-4.2	1.19	1.72	2.62	2.64	1.0
0.45	1.36	1.38	1.8	1.87	1.88	0.5	1.27	1.96	3.53	3.51	ħ.0-
0.54	1.37	1.40	η•0	2.01	2.15	6.9	1.32	2.21	£4° tr	4.36	1 .5
0.72	1.44	1.43	-0.7	2.23	2.32	ก . ก	1.40	2.34	6.20	6.17	-0.5
0.89	1.47	1.45	±.1-	2.37	2.51	5.8	1.43	2.52	7.96	7.92	-0.5
1.07	1.48	1.48	-0.5	2.47	2.48	0.3	1.48	2.48	9.70	9.70	0.0
1.25	1.49	1.49	-0.2	2.55	2.49	-2.6	1.51	2.48	11.43	11.44	0.1

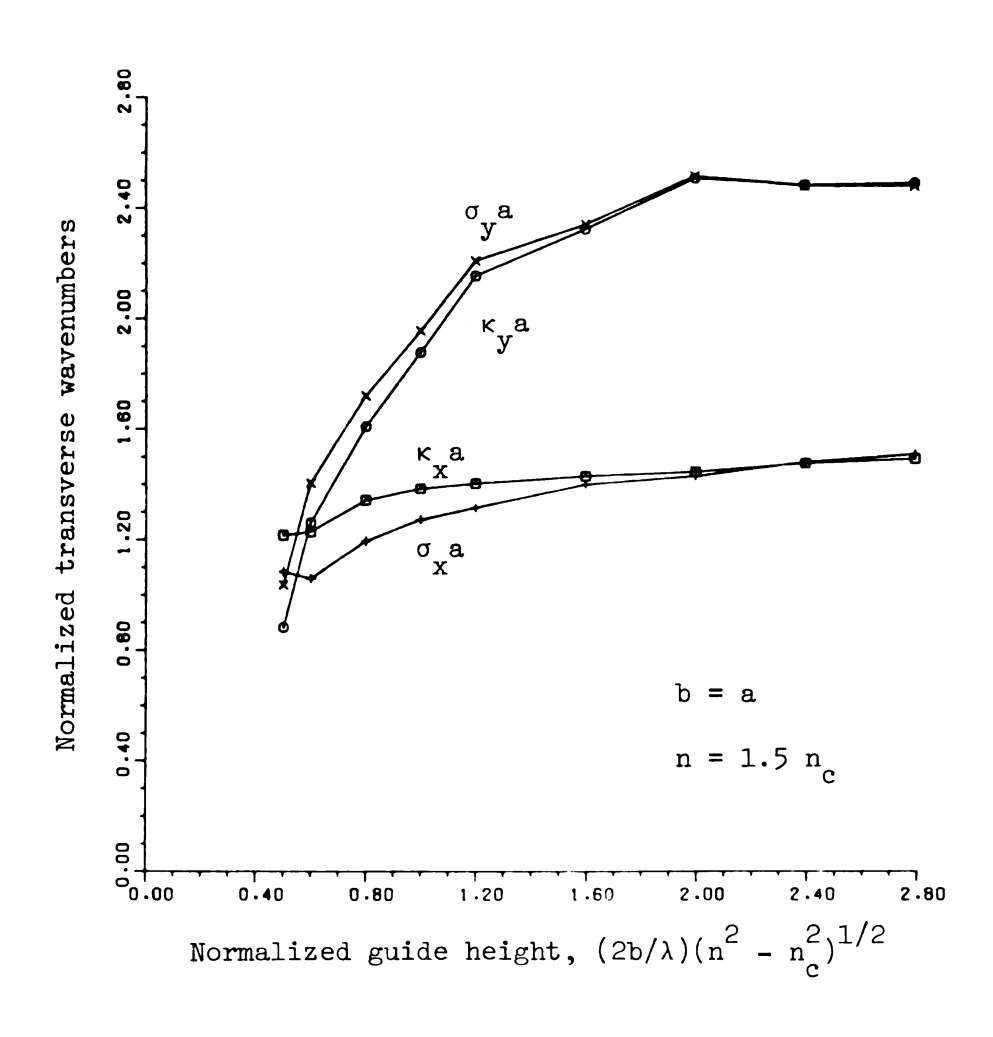


Figure 3.13: Normalized transverse wavenumbers of the isolated uniform rectangular strip waveguide versus normalized waveguide height.

wavenumbers are plotted versus normalized core size in Figure 3.14. The propagation constant is normalized and compared with the numerical results obtained by Goell [3.25] in a different manner in Figure 3.14. Good agreement is observed even for small waveguide core sizes. In Figure 3.15 and 3.16 we plot the normalized dominant field component in the waveguide core versus normalized position x/a and y/a, respectively, for several core sizes. These plots reveal that we are dealing here with the principle waveguide mode.

The next waveguide configuration considered here is a uniform integrated rectangular dielectric rib waveguide. In this case the refractive index of the rectangular core and the film layer refractive index are identical, n = n_f. The presence of the tri-layered background structure gives rise to a non-zero contribution from the reflected terms in the Green's dyad. The core and film refractive indices are both 1.5, the substrate has refractive index n_s = 1.1 and the cover medium has refractive index n_c = 1.0. The dielectric rib has width 2a and height a, and the film thickness is t = a. The program was executed for several sizes or waveguide by letting a/λ_0 vary.

In this case the initial guesses for the waveguide eigenvalues were obtained by the effective dielectric constant (EDC) method (see Oliner [3.10]). This method consists of finding effective dielectric constants, $n_{eff} = \zeta/k_0$, for the asymmetric slab waveguides made by letting the rib width go to zero and infinity, as shown in Figure 3.17. The latter case gives a good approximation for the eigenvalue κ_y of the rib waveguide since we are essentially using the Marcatilli method described above. An approximation for κ_x is then obtained by

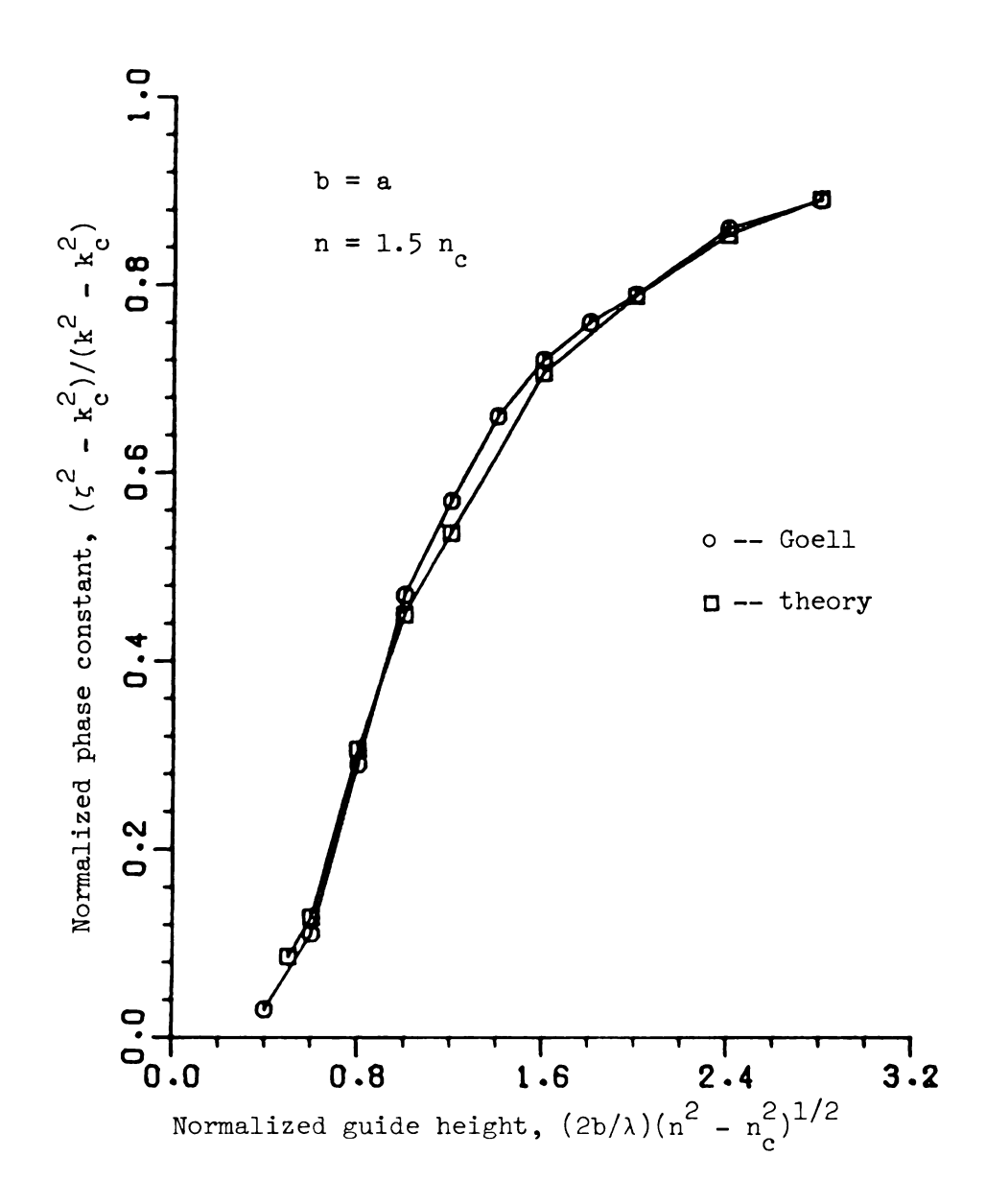


Figure 3.14: Normalized propagation constant for the isolated uniform rectangular strip waveguide versus normalized waveguide size compared to Goell's circular harmonic analysis results.

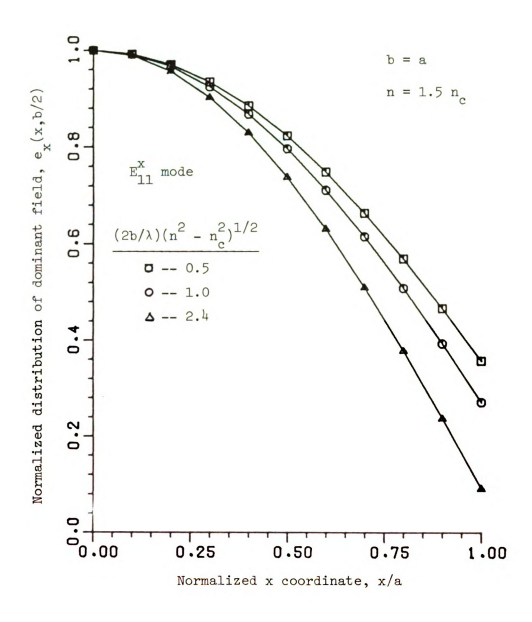


Figure 3.15: Normalized distribution of dominant field component in isolated uniform rectangular strip waveguide versus normalized x coordinate for several normalized waveguide heights.

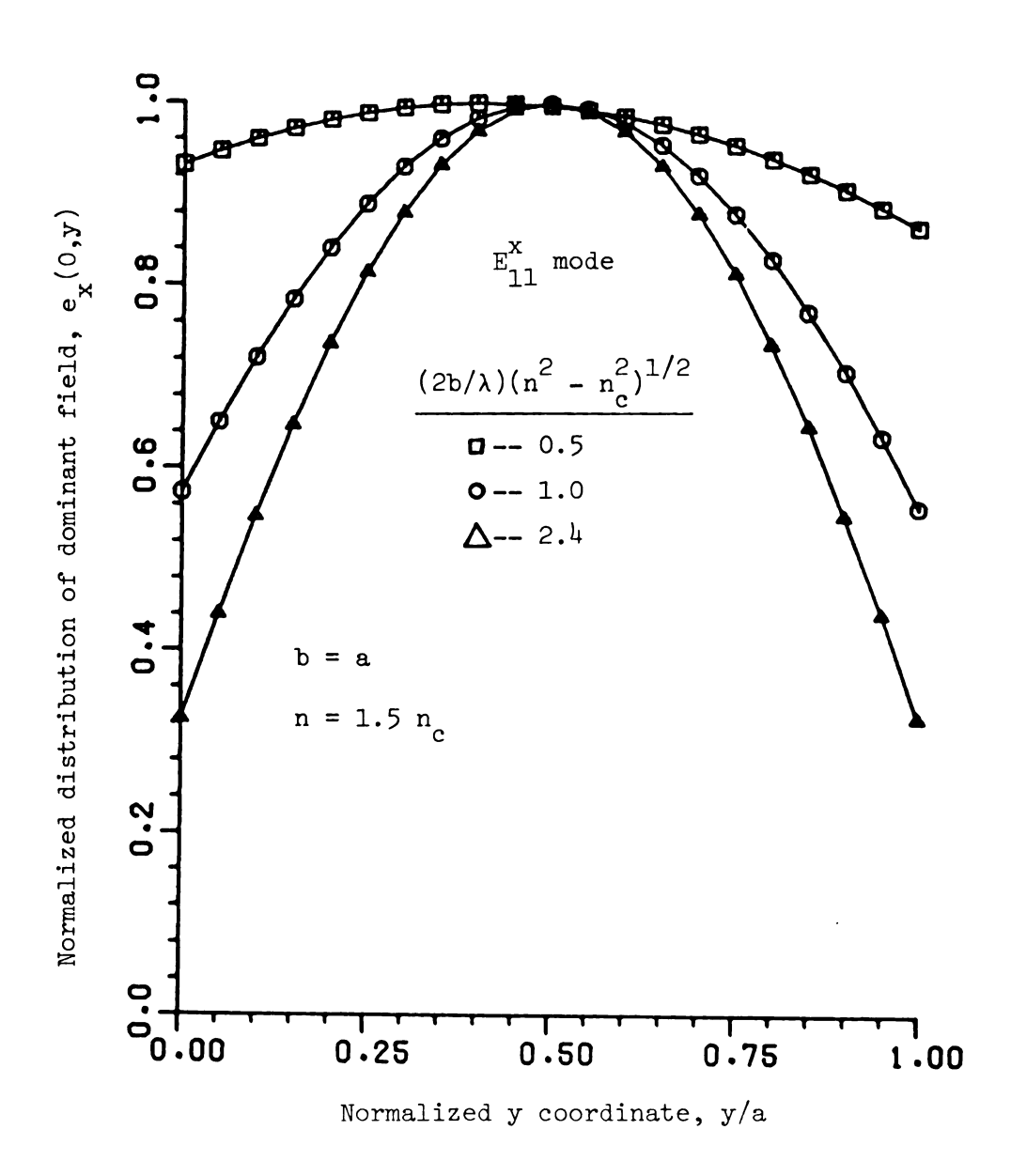


Figure 3.16: Normalized distribution of dominant field component in isolated uniform rectangular strip waveguide versus normalized y coordinate for several normalized waveguide heights.

solving the characteristic equation for the symmetric slab waveguide with the effective dielectric constants found above. This is depicted schematically in Figure 3.17.

The EDC and program results are summarized in Table 3.2. Here $\lambda_{\rm TE}$ and $\lambda_{\rm TM}$ are the TE and TM surface wave eigenvalues of the background asymmetric slab used to approximate the reflected Green's dyad as described in section 3.4.3. The propagation constants predicted by the EDC method are compared with the program results for several rib waveguide sizes in Figure 3.18.

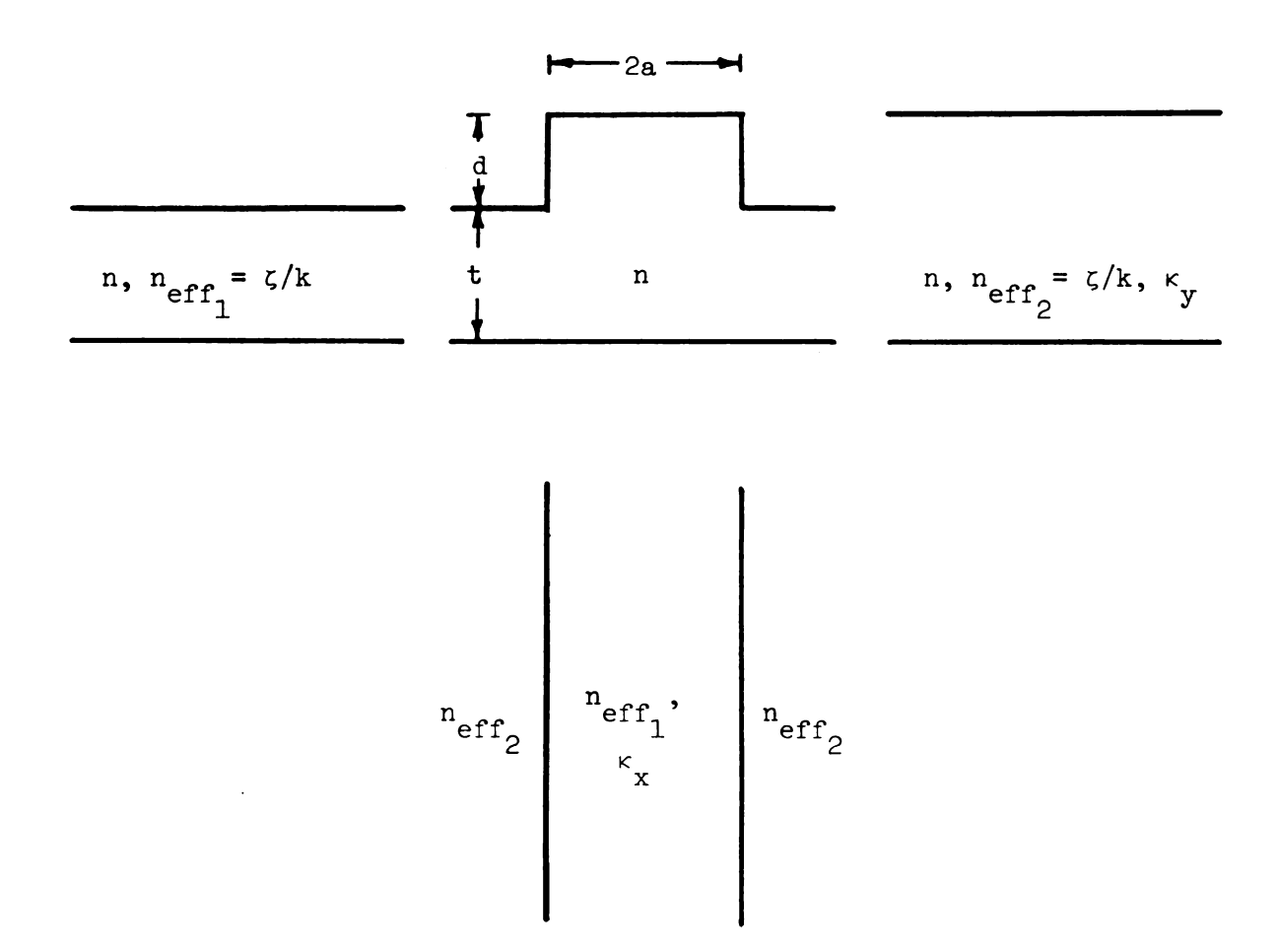


Figure 3.17: Diagram illustrating the application of the effective dielectric constant (EDC) method to a uniform rectangular dielectric rib waveguide.

Normalized eigenvalues of the uniform rectangular dielectric rib waveguide ror several normalized guide sizes compared to the results of the EDC method. Here d = t = a, n = n_f = 1.5, n_s = 1.1, n_c = 1.0. Table 3.2:

	5 € Z	O. 43	-3.09	5.23	3.93	2.62	1.20	0.91
	איטי	0.71 -jo.01	1.51 +jo.02	2.64 -jo.03	3.62+10.02	4.58 +jo.00	5.49 -j0:05	6.45
ults	σy	0.69	1.04 -jo.08	0.57	0.27	0.49	0.08	0.73
program results	ď	0.53	0.48	0.89 -jo.07	1.11	1.14	1.37	1.18
	κ	0.62	1.07 -jo:02	0.33	0.05	0.35	0.56	0.20
	×	0.01 +50.00	0.38	0.99	1.08 -J0.07	1.08	1.24 +j0.12	1.37
ts	۲,	0.70	1.55	2.51	3.48	94.4	5,43	6.39
EDC results	γ	95.0	0.87	1.032	1.13	1.20	1.25	1.28
<u> </u>	×	0.27	0.62	0.80	0.89	ħ6°0	26.0	1.00
background slab poles	УΤМ	;	1.41	2.34	3.16	4.13	5.11	4.94
	$^{\lambda}{ m TE}$	0.70	1.51	2.41	3.35	η·30	4.21	5.15
	t/ 30	0.1	0.2	0.3	ħ.0	0.5	9.0	0.7

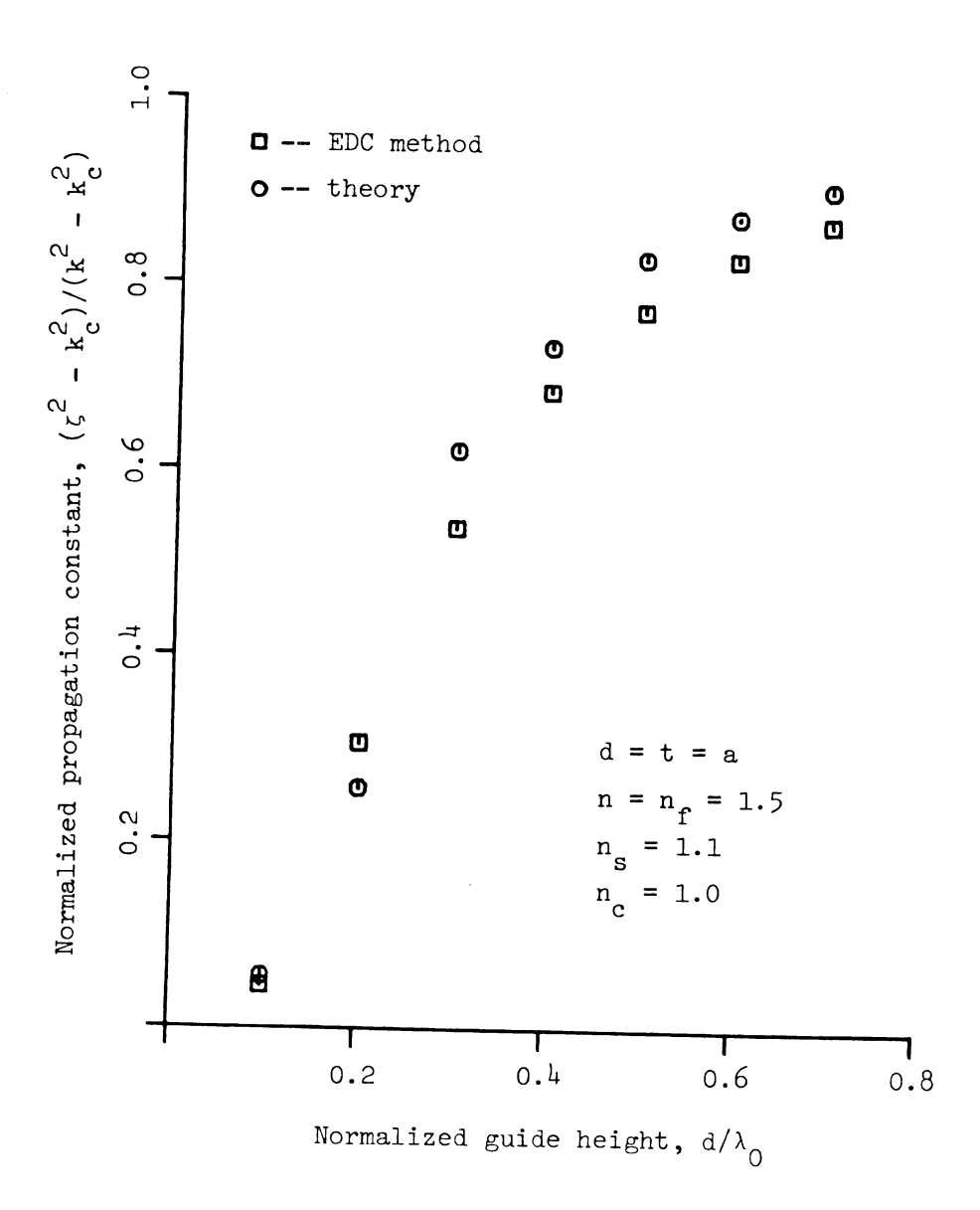


Figure 3.18: Normalized propagation constant for uniform rectangular dielectric rib waveguide versus normalized waveguide height compared to results of the EDC method.

;		
i •		

4. PLANE TRUNCATED WAVEGUIDES

In this chapter we apply the equivalent polarization integral equation to the problem of coupling energy into and out of plane truncated waveguides. Truncated integrated waveguide structures such as that depicted in Figure 4.1 are of considerable interest to workers in the area of integrated optics, where they are widely used as integrated laser cavities [4.1]. This type of structure is also used to model junctions between separate integrated optical components.

We will restrict ourselves to consideration of truncated integrated waveguides that have generally transversely graded cores of arbitrary but constant transverse cross sectional shape. The only allowed variation of the refractive index contrast factor of the waveguide core in the longitudinal direction is of the form $u(z_0-z)$. This factor describes a waveguide core that is truncated at the plane $z = z_0$ and vanishes for all z greater than z_0 .

In the first part of this chapter we review some results on the complete modal spectrum of a waveguide and develop notation to be utilized in the remainder of the chapter. We also introduce the concept of partial fields in a truncated waveguide. The two partial fields, \vec{E}^L and \vec{E}^R , are the total electric field in the system for points z behind and in front of the plane of truncation at $z=z_0$, respectively, and are zero elsewhere. The total electric field in the waveguiding system can be expressed in terms of these partial fields

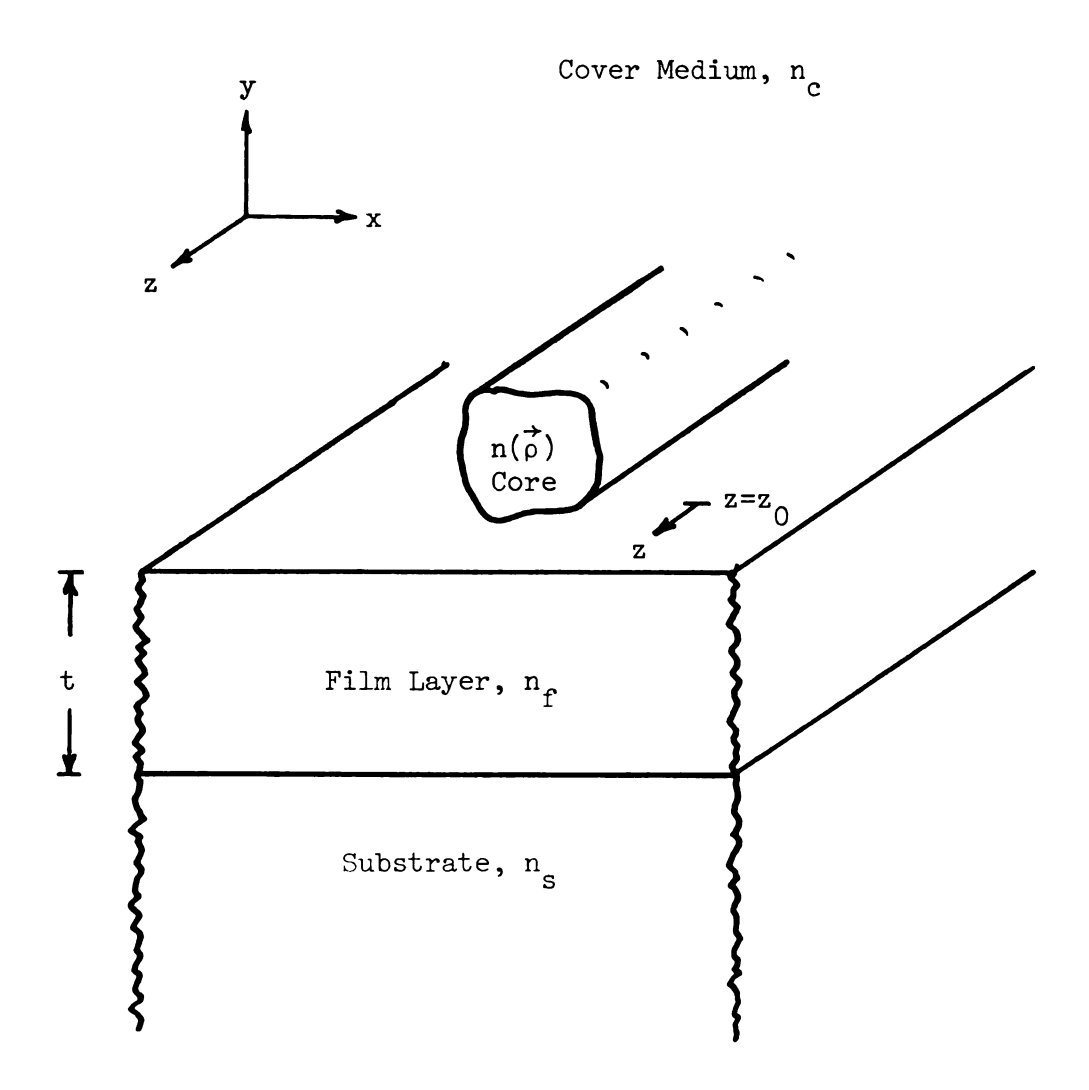


Figure 4.1: A generalized plane truncated axially uniform integrated dielectric waveguide.

as $\vec{E} = \vec{E}^L + \vec{E}^R$. The partial fields play a central role in the analysis to follow.

In the second part of this chapter we analyze the problem of the reflection and radiation of a single surface wave mode of arbitrary amplitude that is incident on the truncation from within the waveguide. The partial field within the waveguide, \vec{E}^L , is written as a modal sum with unknown amplitude coefficients, and is substituted into the alternative form of the equivalent polarization integral equation. A linear integral operator, \mathscr{L}_m , is applied to the resultant expressions. This leads to an iterative equation which can be used to find the unknown reflected surface wave amplitudes in the modal expansion of \vec{E}^L . Once these reflected wave amplitudes are determined, the expressions also allow for evaluation of the electric field radiated out of the truncated waveguide, which is the partial field, \vec{E}^R .

In the third part of the chapter we examine the converse problem, that of excitation of surface waves in the truncated waveguide. Here we assume that an impressed electric field is incident on the truncation from outside of the waveguide. A technique similar to that described above is applied to the alternative equivalent polarization integral equation, resulting in an iterative formula for the unknown amplitudes of the surface wave modes excited in the waveguide.

We conclude the chapter in part four by applying the techniques developed here to the problem of coupling energy into and out of a truncated asymmetric slab waveguide. Numerical results are presented and discussed.

4.1 Preliminaries

In this part we review some background material that will be used in this chapter. We first review some results from chapter three on the complete modal spectrum of an axially uniform integrated dielectric waveguide. We establish notation for surface waves and the radiation field and review the equivalent polarization integral equation satisfied by surface waves.

We next introduce the notion of partial rields in a truncated waveguide. The unknown total electric field in the alternative equivalent polarization integral equation of chapter two is expressed in terms of these partial fields. The resultant integral equation forms the basis for the analysis in the remainder of the chapter.

4.1.1 Modal Expansion

Referring to the results of section 3.3.2 we find that the total field in an integrated dielectric waveguide can be written as a modal expansion:

$$\vec{E}(\vec{r}) = \sum_{n} a_{n}^{+} \vec{E}_{n}^{+}(\vec{r}) + \vec{E}_{RAD}^{+}(\vec{r})$$
 (1)

at points to the right or left of all sources, respectively. The surface wave modes have the form

$$\vec{E}_{n}^{\dagger}(\vec{r}) = \vec{e}_{n}^{\dagger}(\vec{\rho})e^{\mp j\zeta_{n}z}$$
(2)

and they satisfy the following homogeneous form of the alternative equivalent polarization integral equation:

$$\vec{E}_{n}^{+}(\vec{r}) - \int_{V} \frac{\delta n^{2}(\vec{\rho}^{\dagger})}{n_{c}^{2}} \overleftrightarrow{G}_{e}(\vec{r}|\vec{r}^{\dagger}) \cdot \vec{E}_{n}^{+}(\vec{r}^{\dagger}) dV = 0$$
(3)

These results will be used in the rollowing analysis.

4.1.2 Partial Fields

If the integrated waveguide under consideration is truncated in the plane $z = z_0$ as shown in Figure 4.1. Then the refractive contrast factor of equation (2.2) has the form

$$\delta n^2(\vec{r}) = \delta n^2(\vec{\rho}) u(z_0 - z) \tag{4}$$

where u(z) is the unit-step function, u(z) = 1 for z > 0 and u(z) = 0 otherwise. In this case the alternative form of the equivalent polarization integral equation in equation (2.13) can be written

$$\vec{E}(\vec{r}) - \int_{V} \frac{\delta n^{2}(\vec{\rho'})}{n_{c}^{2}} u(z_{o} - z') \vec{G}_{e}(\vec{r}|\vec{r'}) \cdot \vec{E}(\vec{r'}) dV' = \vec{E}^{i}(\vec{r})$$
 (5)

The presence of the factor $\vec{E}(\vec{r}')u(z_0-z')$ in the integral prompts us to define the two partial fields, \vec{E}^L and \vec{E}^R , as

$$\vec{E}^{L}(\vec{r}) = \vec{E}(\vec{r})u(z_{o} - z)$$

$$\vec{E}^{R}(\vec{r}) = \vec{E}(\vec{r})u(z - z_{o})$$
(6)

Then we can write the unknown total electric field in terms of these partial fields, $\vec{E} = \vec{E}^L + \vec{E}^R$. Using these definitions in the integral equation (5) results in

$$\vec{E}^{L}(\vec{r}) + \vec{E}^{R}(\vec{r}) - \int_{V} \frac{\delta n^{2}(\vec{\rho'}) \overleftrightarrow{G}_{e}(\vec{r}|\vec{r'})}{n_{c}^{2}} \vec{G}_{e}(\vec{r}|\vec{r'}) \cdot \vec{E}^{L}(\vec{r'}) dV'$$

$$= \vec{E}^{I}(\vec{r})$$
(7)

This is the form of the alternative equivalent polarization integral equation that will be used in the remainder of this chapter.

An important result can be obtained immediately from equation (7). If we multiply equation (7) by $u(z-z_0)$ then the partial field \vec{E}^L is annhilated and the partial field \vec{E}^R is unchanged. The result can be written

$$\vec{E}^{R}(\vec{r}) = u(z - z_{o}) \int_{V} \frac{\delta n^{2}(\vec{\rho}') \leftrightarrow \vec{r}}{n_{c}^{2}} \vec{G}_{e}(\vec{r}|\vec{r}') \cdot \vec{E}^{L}(\vec{r}') dV'$$

$$+ u(z - z_{o}) \vec{E}^{1}(r)$$
(8)

The significance of this result is that it gives us an expression for the partial field \vec{E}^R in terms of the other partial field \vec{E}^L and the incident electric field \vec{E}^i .

4.2 Surface Wave Reflection and Radiation

In this part of the chapter we analyze the reflection and radiation of a single surface wave mode traveling down the waveguide and incident on the truncation at $z=z_0$. This surface wave will be partially reflected back up the waveguide and partially radiated out of the waveguide through the truncation. This situation is depicted in Figure 4.2. Note that mode conversion can occur at the truncation,

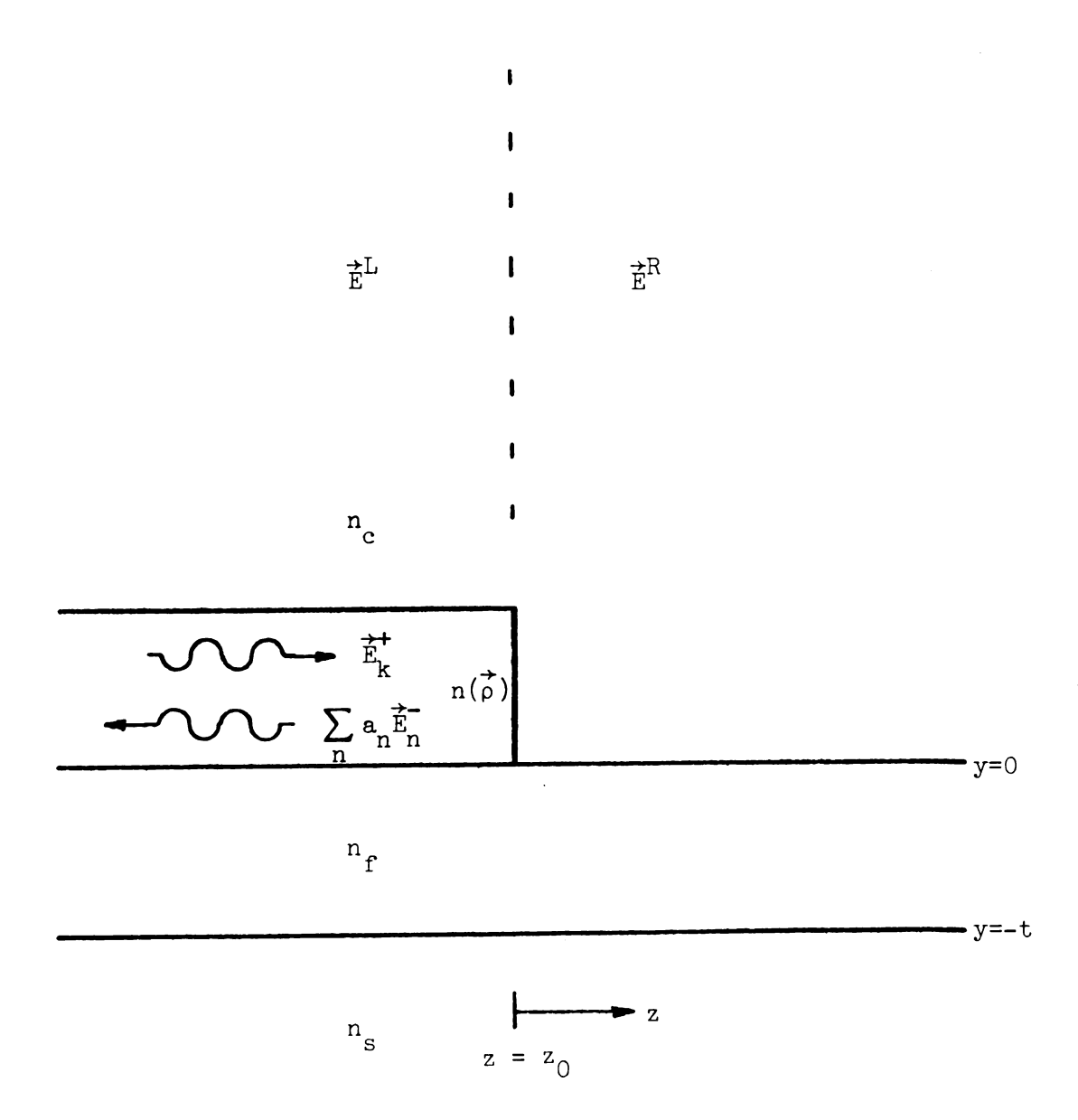


Figure 4.2: Surface wave reflection and radiation in a plane truncated dielectric waveguide when a single surface wave is incident on the truncation.

so that other surface wave modes and the radiation rield may be excited in the waveguide.

We will make use of the specialized integral equation (7) with a zero incident field. The surface wave which is incident on the truncation is included in a modal expansion for the total field in the waveguide. This total field in the waveguide also comprises the reflected surface wave modes with unknown amplitude coefficients and the reflected radiation field. Substitution of this modal expansion for the partial field \vec{E}^L into the integral equation and subsequent operation by a linear integral operator \mathscr{L}_m results in an iterative formula for the unknown modal amplitude coefficients for the reflected surface waves. Then equation (8) will allow us to use the resultant known surface wave modal expansion for \vec{E}^L to find the partial field radiated out of the truncation.

4.2.1 Modal Expansion of E^L

If a single surface wave of the k^{th} mode type is incident on the truncation from inside the waveguide we set \vec{E}^i in the integral equation (7) equal to zero and incorporate this surface wave in the modal expansion for the field in the waveguide core. Then partial field \vec{E}^L can be written in accordance with the notation in section 4.1.1 as

$$\vec{E}^{L}(\vec{r}) = u(z_{o} - z)[\vec{A}\vec{E}_{k}(\vec{r}) + \sum_{n} \vec{a_{n}}\vec{E_{n}}(\vec{r}) + \vec{E}_{RAD}(\vec{r})]$$
(9)

Here the constant A is the amplitude of the $k^{\mbox{th}}$ surface wave mode incident on the truncation, assumed to be known. The coefficients a_n

are the unknown amplitudes of the surface waves reflected by the truncation.

Equation (9) is now substituted into the homogeneous form of the integral equation (7). The result can be written as

$$-\vec{E}^{R}(\vec{r}) = u(z_{o} - z)[\vec{A}\vec{E}_{k}^{\dagger}(\vec{r}) + \sum_{n} a_{n}\vec{E}_{n}^{-}(\vec{r}) + \vec{E}_{RAD}(\vec{r})]$$

$$-\int_{V} \frac{\delta n^{2}(\vec{\rho}')}{n_{c}^{2}} \vec{G}_{e}(\vec{r}|\vec{r}') \cdot u(z_{o} - z')[\vec{A}\vec{E}_{k}^{\dagger}(\vec{r}')]$$

$$+ \sum_{n} a_{n}\vec{E}_{n}^{-}(\vec{r}') + \vec{E}_{RAD}^{-}(\vec{r}')]dV'$$
(10)

Our goal now is to rind the unknown reflected surface wave amplitude coefficients a_n in equation (10).

4.2.2 Integral Operator

We now derine a linear integral operator, $\mathscr{L}_{\rm m}$, and apply it to equation (10) term by term. $\mathscr{L}_{\rm m}$ is derined as

$$\mathcal{L}_{\mathbf{m}}\{\cdot\} = \lim_{\zeta \to \zeta_{\mathbf{m}}} \int_{V} \frac{\delta n^{2}(\overset{\rightarrow}{\rho})}{n_{\mathbf{c}}^{2}} \overset{\rightarrow}{\mathbf{e}_{\mathbf{m}}^{+}}(\overset{\rightarrow}{\rho}) e^{-j\zeta z} \cdot \{\cdot\} dV$$
 (11)

with \vec{e}_m^+ as defined by equations (2) and (3.26). In the limit where ζ = ζ_m this operation becomes the dot product with $\frac{\delta n^2}{n_c^2}$ $\vec{E}_m^+(\vec{r})$ and integration over the volume of the un-truncated waveguide core. The reason for the limiting process in the definition will become apparent shortly.

Application or this operator to the left hand side of equation (10) results in the term

$$L = \mathcal{L}_{\mathbf{m}} \{ -\overrightarrow{E}^{R}(\overrightarrow{r}) \} = - \lim_{\zeta \to \zeta_{\mathbf{m}}} \int_{V} \frac{\delta n^{2}(\overrightarrow{\rho})}{n_{\mathbf{c}}^{2}} \overrightarrow{e}_{\mathbf{m}}^{+}(\overrightarrow{\rho}) e^{-j\zeta Z}$$

$$\bullet \stackrel{\rightarrow}{E}^{R}(\overrightarrow{r}) dV$$
(12)

where the limit $\zeta \rightarrow \zeta_m$ will be taken later.

Upon application of \mathscr{L}_m to the right hand side of equation (10) we obtain six terms, denoted $R = \sum_{i=1}^{n} R_i$. The first three are

$$R_{1} = \mathcal{L}_{m} \{ A \vec{E}_{k}^{+}(\vec{r}) u(z_{o} - z) \}$$

$$= A \int_{V} \frac{\delta n^{2}(\vec{\rho}) \vec{E}_{m}^{+}(\vec{r}) \cdot \vec{E}_{k}^{+}(\vec{r}) u(z_{o} - z) dV$$

$$R_{2} = \mathcal{L}_{m} \left\{ \sum_{n} a_{n} \overrightarrow{E}_{n}(\overrightarrow{r}) u(z_{o} - z) \right\}$$

$$= \sum_{n} a_{n} \int_{V} \frac{\delta n^{2}(\overrightarrow{\rho})}{n^{2}} \overrightarrow{E}_{m}(\overrightarrow{r}) \cdot \overrightarrow{E}_{n}(\overrightarrow{r}) u(z_{o} - z) dV \qquad (13)$$

$$R_{3} = \mathcal{L}_{m}\{\overrightarrow{E}_{RAD}(\overrightarrow{r})u(z_{o} - z)\}$$

$$= \int_{V} \frac{\delta n^{2}(\overrightarrow{\rho})}{n_{c}^{2}} \overrightarrow{E}_{m}(\overrightarrow{r}) \cdot \overrightarrow{E}_{RAD}(\overrightarrow{r})u(z_{o} - z)dV$$

Where the limit $\zeta \to \zeta_m$ has been taken. The last three terms on the right hand side are more complicated. The rirst of these is

$$R_{\mu} = \mathcal{L}_{m} \left\{ -A \int_{V} \frac{\delta n^{2}(\vec{\rho}')}{n_{c}^{2}} \stackrel{\leftrightarrow}{G}_{e}(\vec{r}|\vec{r}') \cdot \stackrel{\rightarrow}{E}_{k}^{+}(\vec{r}') u(z_{o} - z') dV' \right\}$$
(14)

$$= -A \int_{V} \int_{V} \frac{\delta n^{2}(\vec{\rho}) \vec{E}_{m}^{+}(\vec{r})}{n_{c}^{2}} \cdot \frac{\delta n^{2}(\vec{\rho}') \vec{E}_{m}^{+}(\vec{r})}{n_{c}^{2}} \cdot \frac{\delta n^{2}(\vec{\rho}') \vec{E}_{m}^{+}(\vec{r}') \vec{E}_{k}^{+}(\vec{r}') u(z_{o} - z') dV' dV}{n_{c}^{2}}$$

Where we have again taken the limit $\zeta \to \zeta_{m}$. The integral on unprimed variables in equation (914) can be carried out with the help of the reciprocity property of the electric dyadic Green's function given in equation (2.23) and the natural mode integral equation (3). The result is

$$R_{\mu} = -A \int_{V} \frac{\delta n^{2}(\vec{\rho}^{\dagger})}{n_{c}^{2}} \vec{E}_{m}^{\dagger}(\vec{r}^{\dagger}) \cdot \vec{E}_{k}^{\dagger}(\vec{r}^{\dagger}) u(z_{o} - z^{\dagger}) dV^{\dagger}$$
(15)

The firth and sixth term on the right hand side are handled in an identical manner upon application of \mathscr{L}_{m} , resulting in

$$R_{5} = -\sum_{n} a_{n} \int_{V} \frac{\delta n^{2}(\vec{\rho'})}{n_{c}^{2}} \vec{E}_{m}^{\dagger}(\vec{r'}) \cdot \vec{E}_{n}(\vec{r'}) u(z_{o} - z') dV'$$

$$R_{6} = -\int_{V} \frac{\delta n^{2}(\vec{\rho'})}{n_{c}^{2}} \vec{E}_{m}^{\dagger}(\vec{r'}) \cdot \vec{E}_{RAD}(\vec{r'}) u(z_{o} - z') dV'$$
(16)

Note that by the above equations we have $R_4 = -R_1$, $R_5 = -R_2$, and $R_6 = -R_3$. By this analysis we may feel compelled to conclude that the left 6 hand side, L in equation (12), is zero, since $R = \sum_{i=1}^{\infty} R_i = 0$. This is not, however, the case, since we will show that the two terms R_2 and R_5 on the right hand side are singular when the modal summation index n is equal to the linear integral operator index m. In this case the two terms R_2 and R_5 do not add to zero, but rather assume an indeterminate form. The other terms in the modal summation in equations (13) and (16) with $n \neq m$ do indeed cancel between R_2 and R_5 , but when n = m we must proceed with caution. This is the reason mentioned above for the presence of the limit as ζ approaches ζ_m in the definition in equation (11) of the linear integral operator \mathscr{L}_m .

The singular nature of the terms R_2 and R_5 is due to the result of the z integration. The modal fields \vec{E}_m^+ and \vec{E}_m^- in the integrals of equations (13) and (16) have z dependences of $\exp(-j\zeta_m z)$ and $\exp(j\zeta_m z)$, respectively. Then if we perform the z integrals, we see that R_2 and R_5 contain the factor

$$\int_{-\infty}^{\infty} e^{-j(\zeta_{m} - \zeta_{n})z} u(z_{0} - z)dz = -\frac{e^{-j(\zeta_{m} - \zeta_{n})z_{0}}}{j(\zeta_{m} - \zeta_{n})}$$
(17)

where we have assumed that $\zeta_m - \zeta_n$ has a slightly positive imaginary part so that the integral converges. Note that when n = m the integral is divergent, giving rise to a singularity in R_2 and R_5 as $\zeta + \zeta_m$ as claimed above. It is important to note that the other terms R_1 , R_3 , R_4 and R_6 or the right hand side are not singular. In the cases of R_1 and R_4 this is due to the fact that the exponential in the z integration is $\exp(j(\zeta_m + \zeta_k))$ which is always oscillatory, giving convergence when integrated as in equation (17). In the cases of R_3 and R_6 we know that ζ of a radiation field component is always less then the ζ of any surface wave mode, and this fact again renders the z integral convergent. In summary, the terms R_1 and R_4 on the right hand side are not indeterminate and thus cancel, as do the terms R_3 and R_6 . The remaining terms R_2 and R_5 cancel for all values of the summation index n except when n = m, in which case both terms are singular. Thus the right hand side becomes

$$R = R_2 \Big|_{n=m} + R_5 \Big|_{n=m}$$
 (18)

We now use equations (13) and (16) in equation (18) and take the limit as ζ approaches $\zeta_{\rm m}$ more carefully. We get

$$R = \lim_{\zeta \to \zeta_{m}} a_{m} \int_{V} \frac{\delta n^{2}(\overset{\rightarrow}{\rho}) \overset{\rightarrow}{\rightarrow} + (\overset{\rightarrow}{\rho})}{e_{m}^{2}} e_{m}^{+}(\overset{\rightarrow}{\rho}) e^{-j\zeta z} \cdot \overset{\rightarrow}{e_{m}} (\overset{\rightarrow}{\rho}) e^{-j\zeta m^{z}} u(z_{0} - z) dV$$

$$- \lim_{\zeta \to \zeta_{m}} a_{m} \int_{V} \int_{V} \frac{\delta n^{2}(\overset{\rightarrow}{\rho}) \overset{\rightarrow}{\rightarrow} + (\overset{\rightarrow}{\rho})}{n_{c}^{2}} e_{m}^{+}(\overset{\rightarrow}{\rho}) e^{-j\zeta z} \cdot \frac{\delta n^{2}(\overset{\rightarrow}{\rho}') \overset{\rightarrow}{\rightarrow} (\overset{\rightarrow}{\rho}') \overset{\rightarrow}{\rightarrow} (\overset{\rightarrow}{\rho}') \overset{\rightarrow}{\rightarrow} (\overset{\rightarrow}{\rho}') e^{-j\zeta m^{z}} u(z_{0} - z) dV$$

$$\cdot \overset{\rightarrow}{e_{m}} (\overset{\rightarrow}{\rho}') e^{-j\zeta m^{z}} u(z_{0} - z') dV' dV$$

$$(19)$$

We first perform the z integrals in equation (19) with the result

$$R = a_{m} \lim_{\zeta \to \zeta_{m}} \left\{ \frac{-j(\zeta - \zeta_{m})z_{o}}{-e} \right\} \left\{ \int_{CS} \frac{\delta n^{2}(\overset{\rightarrow}{\rho}) \to_{+}(\overset{\rightarrow}{\rho})}{n_{c}^{2}} e_{m}^{+}(\overset{\rightarrow}{\rho}) \cdot \overset{\rightarrow}{e_{m}}(\overset{\rightarrow}{\rho}) dS \right\}$$

$$- a_{m} \lim_{\zeta \to \zeta_{m}} \int_{CS} \int_{V} \frac{\delta n^{2}(\overset{\rightarrow}{\rho}) \to_{+}(\overset{\rightarrow}{\rho}) e^{-j\zeta z'}}{n_{c}^{2}} \cdot \frac{\delta n^{2}(\overset{\rightarrow}{\rho}') \leftrightarrow_{m}(\overset{\rightarrow}{\rho}) dS}{n_{c}^{2}} e_{m}^{+}(\overset{\rightarrow}{\rho}) e^{-j\zeta z'} \cdot \frac{\delta n^{2}(\overset{\rightarrow}{\rho}')}{n_{c}^{2}} e_{m}^{+}(\overset{\rightarrow}{\rho}) dS$$

$$\cdot \overset{\rightarrow}{e_{m}}(\overset{\rightarrow}{\rho}') e^{-j\zeta_{m}z'} u(z_{o} - z') dV' dS$$
(20)

where we have used the definition of the transformed electric Green's dyad given in equation (3.8) and CS denotes the transverse cross sectional area of the waveguide core. We now evaluate the z' integral in equation (20) and combine terms. This gives

$$R = -a_{m} \lim_{\zeta \to \zeta_{m}} \left\{ \frac{-j(\zeta - \zeta_{m})z_{o}}{e} \right\} \left\{ \int_{CS} \frac{\delta n^{2}(\hat{\rho})}{n_{c}^{2}} \stackrel{+}{e}_{m}^{+}(\hat{\rho}) \right\}$$

$$\cdot \left[\stackrel{-}{e}_{m}^{-}(\hat{\rho}) - \int_{CS} \frac{\delta n^{2}(\hat{\rho}')}{n_{c}^{2}} \stackrel{+}{g}_{e\zeta}^{-}(\hat{\rho}|\hat{\rho}') \cdot \stackrel{+}{e}_{m}^{-}(\hat{\rho}') ds' \right] ds$$

$$(21)$$

We can now see the indeterminate form of the right hand side as ζ approaches ζ_{m} . The first term in brackets is obviously singular, and the second term is seen to approach zero in the limit with the aid of

equation (3.26). Thus R has the form

$$R = -a_{m} \lim_{\zeta \to \zeta_{m}} \frac{x(\zeta)}{y(\zeta)}$$
 (22)

with $\mathbf{x}(\zeta)$, $\mathbf{y}(\zeta) \to 0$ as $\zeta \to \zeta_{\mathbf{m}^*}$ We use L'Hopital's rule to evaluate the indeterminate form. The result is

$$R = -j a_{m} \int_{CS} \frac{\delta n^{2}(\overrightarrow{\rho})}{n_{c}^{2}} \overrightarrow{e_{m}}(\overrightarrow{\rho}) \cdot \int_{CS} \frac{\delta n^{2}(\overrightarrow{\rho'})}{n_{c}^{2}} \frac{\partial}{\partial \delta} \overrightarrow{g_{e}} (\overrightarrow{\rho}|\overrightarrow{\rho'}) | \cdot \overrightarrow{e_{m}}(\overrightarrow{\rho'}) dS' dS$$
(23)

We now set the left hand side as given in equation (12) equal to this right hand side. The result can be solved for the unknown amplitude of the m^{th} reflected surface wave mode in the truncated waveguide, a_m :

$$a_{m} = \frac{1}{c_{m}} \lim_{\zeta \to \zeta} \int_{m} \frac{\delta n^{2}(\vec{\rho})}{n_{c}^{2}} e_{m}^{+}(\vec{\rho}) e^{-j\zeta z} \cdot \vec{E}^{R}(\vec{r}) dV$$

$$c_{m} = j \int_{CS} \frac{\delta n^{2}(\vec{\rho})}{n_{c}^{2}} e_{m}^{+}(\vec{\rho}) \cdot \int_{CS} \frac{\delta n^{2}(\vec{\rho}')}{n_{c}^{2}} x$$

$$x \frac{\partial}{\partial \delta} \overrightarrow{g}_{e\zeta}(\vec{\rho}|\vec{\rho}') \cdot \int_{\zeta_{m}} \cdot \vec{e}_{m}^{-}(\vec{\rho}') dS' dS$$
(24)

It is instructive to compare the normalization constant of equation (24) with that in equation (3.31) which was derived for our excitation theory. The two terms are seen to differ only by a factor of j.

4.2.3 Iterative Equation

We now use the results of the previous section to develop an approximate, iterative scheme for evaluating the unknown amplitude

coerricients or the rerlected surrace waves in the modal expansion for the field in the truncated waveguide.

The iterative equation is obtained by substituting equation (8) for \vec{E}^R in terms of \vec{E}^L into equation (24) for a_m . Note that we again let $\vec{E}^i = 0$ in equation (8). The result is

$$a_{m} = \frac{1}{c_{m}} \lim_{\zeta \to \zeta} \int_{m} \frac{\delta n^{2}(\vec{\rho})}{v^{2}} e_{m}^{+}(\vec{\rho}) e^{-j\zeta z} \cdot u(z - z_{0}) x$$

$$x \int_{V} \frac{\delta n^{2}(\vec{\rho}')}{nz} \frac{dz}{dz} e_{m}^{+}(\vec{\rho}) e^{-j\zeta z} \cdot u(z - z_{0}) x$$

This result gives us an equation for the amplitude or the m^{th} reflected surface wave in the waveguide in terms of the total field in the waveguide. We can use equation (25) to implement an iterative scheme for approximating a_m . First make a guess at the unknown modal expansion inside the waveguide. Such a guess will be of the form

$$\vec{E}^{L}(\vec{r}) \simeq u(z_{o} - z)[A\vec{E}_{k}^{+}(\vec{r}) + \sum_{n} a_{n}\vec{E}_{n}^{-}(\vec{r})]$$
(26)

if we neglect the radiation field. Here the coefficients a_m are our educated guesses at the reflected surface wave modal amplitudes. Now substitute the expression of equation (26) for \overrightarrow{E}^L into equation (25). The resultant equation can be evaluated for all modal indices m to find more refined values for the unknown reflected modal amplitude coefficients. This process can be repeated to find better and better values for the modal expansion coefficients if desired.

4.2.4 Radiated Field

Once the reflected modal expansion coefficients are obtained with desired accuracy by the iterative technique described above we can use the resultant expression for the partial field \vec{E}^L to find the field radiated out of the waveguide truncation. This field, \vec{E}^R , is obtained by using the expansion for \vec{E}^L in equation (8) after setting $\vec{E}^i = 0$.

4.3 Excitation of Truncated Waveguides

In this part of the chapter we examine the problem of excitation of plane truncated integrated dielectric waveguides. Here we assume that a source to the right or the truncation at $z=z_0$ produces an impressed field, \vec{E}^i , which interacts with the truncated dielectric waveguide. This situation is depicted in Figure 4.3. This incident rield will excite both surface waves and the radiation rield of the waveguide. Our aim is to find the amplitudes or the various surface waves excited in the waveguide.

Our analysis proceeds in a very similar manner to that in the previous part. The unknown partial rield \vec{E}^L is expressed as a modal expansion and substituted into the modified alternative equivalent polarization integral equation (7). Application of the linear integral operator \mathscr{L}_m defined in equation (11) allows us to find an iterative formula for approximating the unknown amplitude coefficients of the surface waves in the modal expansion of the electric field excited in the waveguide.

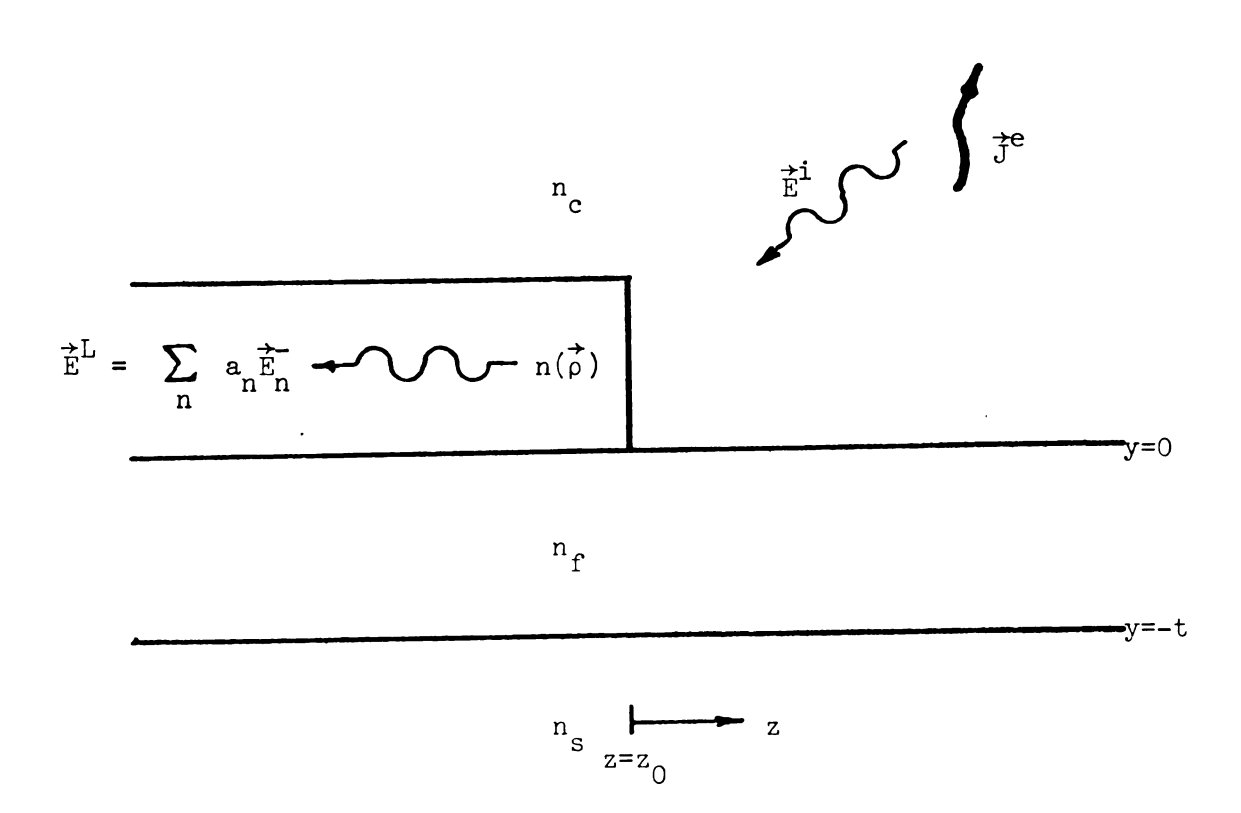


Figure 4.3: Excitation of surface waves in a plane truncated dielectric waveguide by a source outside of the truncation.

4.3.1 Modal Expansion or $\stackrel{\rightarrow}{E}^L$

An electric field incident on the truncation from outside of the waveguide will excite both surface waves and the radiation field of the waveguide. These waves will then propagate up the waveguide in the negative z direction. This situation is illustrated in Figure 4.3. In this case the partial field \overrightarrow{E}^L can be written in a modal expansion as

$$\vec{E}^{L}(\vec{r}) = u(z_0 - z) \begin{bmatrix} \Sigma & a_n \vec{E}_n(\vec{r}) + \vec{E}_{RAD}(\vec{r}) \end{bmatrix}$$
(27)

Ir this representation is substituted into the modified alternative integral equation (7) we obtain the result

$$\vec{E}^{1}(\vec{r}) - \vec{E}^{R}(\vec{r}) = u(z_{o} - z)[\sum_{n} a_{n}\vec{E}_{n}(\vec{r}) + \vec{E}_{RAD}(\vec{r})]$$

$$- \int_{V} \frac{\delta n^{2}(\vec{\rho}')}{n_{c}^{2}} \vec{G}_{e}(\vec{r}|\vec{r}') \cdot u(z_{o} - z')[\sum_{n} a_{n}\vec{E}_{n}(\vec{r}')$$

$$+ \vec{E}_{RAD}(\vec{r}')]dV'$$
(28)

4.3.2 Integral Operator

We once again operate term by term on equation (28) by the linear integral operator \mathcal{L}_m , as defined in equation (11). The left hand side, L, or the result now consists of

$$L = \mathcal{Q}_{m}\{\vec{E}^{i}(\vec{r}) - \vec{E}^{R}(\vec{r})\}$$

$$= \lim_{\zeta \to \zeta_{m}} \int_{V} \frac{\delta n^{2}(\vec{\rho}) \to +}{n_{c}^{2}} (\vec{\rho}) e^{-j\zeta z} \cdot [\vec{E}^{i}(\vec{r}) - \vec{E}^{R}(\vec{r})] dV$$

$$(29)$$

The right hand side or equation (28) yields rour terms upon operation by \mathscr{L}_{m^*} . These rour terms are precisely the terms R_2 , R_3 , R_5 , and R_6 or section 4.2.2. An analysis identical to that in the previous part allows us to conclude that the terms R_3 and R_6 cancel, and all terms with the summation index $n \neq m$ in the modal expansions in terms R_2 and R_5 also cancel. The terms in R_2 and R_5 where the modal summation index n is equal to the integral operator index m are singular, producing an indeterminate form which can be evaluated using L'Hopital's rule. This analysis leads to the same right hand side as in equation (23), which is

$$R = -a_m c_m (30)$$

with the normalization constant c_m as given in equation (24). Equating the left hand side and the right hand side results in an expression for the unknown surface wave modal amplitude coefficient, a_m :

$$a_{m} = \frac{1}{c_{m}} \lim_{\zeta \to \zeta_{m}} \int_{V} \frac{\delta n^{2}(\overrightarrow{\rho}) + \overrightarrow{\rho}}{n_{c}^{2}} e_{m}^{+}(\overrightarrow{\rho}) e^{-j\zeta z} \cdot \left[\overrightarrow{E}^{R}(\overrightarrow{r}) - \overrightarrow{E}^{i}(\overrightarrow{r})\right] dV$$
(31)

4.3.3 Iterative Equation

Now equation (8) can be written as

$$\vec{E}^{R}(\vec{r}) - \vec{E}^{i}(\vec{r}) = u(z - z_{o}) \int_{V} \frac{\delta n^{2}(\vec{\rho}')}{n_{c}^{2}} \vec{G}_{e}(\vec{r}|\vec{r}')$$

$$\cdot \vec{E}^{L}(\vec{r}')dV' - u(z_{o} - z)\vec{E}^{i}(\vec{r})$$
(32)

by noting $u(z-z_0) = 1 - u(z_0-z)$. Substitution of equation (32) into

equation (31) gives the result

$$a_{m} = \frac{1}{c_{m}} \lim_{\zeta \to \zeta_{m}} \int_{V} \frac{\delta n^{2} (\stackrel{\rightarrow}{\rho}) \to +}{n_{c}^{2}} e_{m}^{+} (\stackrel{\rightarrow}{\rho}) e^{-j\zeta z} \cdot u(z - z_{0})$$

$$x \int_{V} \frac{\delta n^{2}(\vec{p}')}{n_{c}^{2}} \vec{G}_{e}(\vec{r}|\vec{r}') \cdot \vec{E}^{L}(\vec{r}') dV'dV$$
(33)

$$-\frac{1}{c_{m}}\lim_{\zeta \to \zeta_{m}}\int_{V}\frac{\delta n^{2}(\stackrel{\rightarrow}{\rho})}{n_{c}^{2}}e_{m}^{+}(\stackrel{\rightarrow}{\rho})e^{-j\zeta z} \cdot u(z_{o}-z)\stackrel{\rightarrow}{E}^{i}(\stackrel{\rightarrow}{r})dV$$

This result gives us a rormula for the amplitude of the mth surface wave excited in the truncated waveguide in terms of the incident electric field and the total field in the waveguide core. We can use equation (33) to implement an iterative scheme for finding the amplitude of the surface waves excited in the waveguide.

A zero-order approximation can be made by assuming that \vec{E}^L = 0 in equation (33) so that a_m can be round in terms of only the incident rield:

$$a_{m}^{O} = -\frac{1}{c_{m}} \int_{V}^{\delta} \frac{n^{2}(\vec{p})}{n_{c}^{2}} \vec{E}_{m}^{+}(\vec{r}) \cdot u(z_{O} - z) \vec{E}^{i}(\vec{r}) dV$$
 (34)

A more refined expression for the amplitude coefficients in the modal expansion can be found by using the zero-order coefficients to write

$$\vec{E}^{L}(\vec{r}) \simeq u(z_{0} - z) \sum_{n} a_{n}^{OE}(\vec{r})$$
(35)

and then substituting this expression for $\stackrel{\rightarrow}{E}^L$ into equation (33). This procedure can be repeated to obtain greater accuracy in the expression for the field in the waveguide core.

4.3.4 Radiation-Excitation Reciprocity

In this section we will demonstrate a reciprocal property of our iterative technique for the coupling of energy into and out of a truncated waveguide.

If the partial field inside the waveguide consists of a single surface wave of the mth mode incident on the truncation from within the waveguide then equation (8) tells us that the partial field radiated out of the truncation is proportional to

$$\vec{E}^{R}(\vec{r}) = \int_{V} \frac{\delta n^{2}(\vec{\rho'})}{n_{c}^{2}} \stackrel{\leftrightarrow}{G_{e}}(\vec{r}|\vec{r'}) \cdot u(z_{o} - z') \stackrel{\leftrightarrow}{E}_{m}^{+}(\vec{r'}) dV'$$
(36)

This expression corresponds to the radiated rield due to a zeroth order expression for the partial field \vec{E}^L - an expression where we neglect all mode reflection at the waveguide truncation.

Now consider the problem of finding the amplitude of excitation of the m^{th} surfaces wave mode due to a point current at location $\dot{\vec{r}}$ outside of the waveguide. Such a point current produces an incident field

$$\vec{E}^{i}(\vec{r}) = \frac{1}{j\omega\varepsilon} \overrightarrow{G}_{e}(\vec{r}|\vec{r}') \cdot \vec{J}^{e}(\vec{r}')$$
 (37)

It this expression for $\stackrel{\rightarrow}{E}^{i}$ is used in equation (34) for the zero order modal amplitude coefficient, the result is

$$a_{m}^{O} = \frac{-1}{j \omega \varepsilon} \overrightarrow{J}_{m}^{e}(\overrightarrow{r'}) \cdot \int_{V} \frac{\delta n^{2}(\overrightarrow{\rho}) \leftrightarrow G_{e}(\overrightarrow{r'}|\overrightarrow{r})}{n_{c}^{2}} \cdot u(z_{o} - z) \overrightarrow{E}_{m}^{+}(\overrightarrow{r}) dV$$
 (38)

where we have used the reciprocal property of the electric Green's dyad.

Note that the integrals in equations (36) and (38) are identical. This establishes a reciprocal property of the zero order coupling and decoupling problems for the truncated waveguide.

4.4 Truncated Asymmetric Slab

In this part of the chapter we will apply the iterative techniques developed above to the plane truncated asymmetric slab waveguide. The truncated asymmetric slab is shown in Figure 4.4.

In the first section we examine the phenomenon of surface wave reflection from the truncation. The general iterative formula of section 4.2.3 is specialized to this simple waveguide yielding results which can be programmed.

In the second section we find the field radiated out of the truncation of the asymmetric slab when a single surface wave is assumed to be incident on the truncation. Again the general formula of the previous part is specialized for this case.

In the third section we find the surface waves excited in the asymmetric slab by a uniform line polarization source outside of the waveguide truncation.

In section four we present numerical results of this analysis for the special case of the symmetric slab waveguide. These results are compared to results of other methods of analysis.

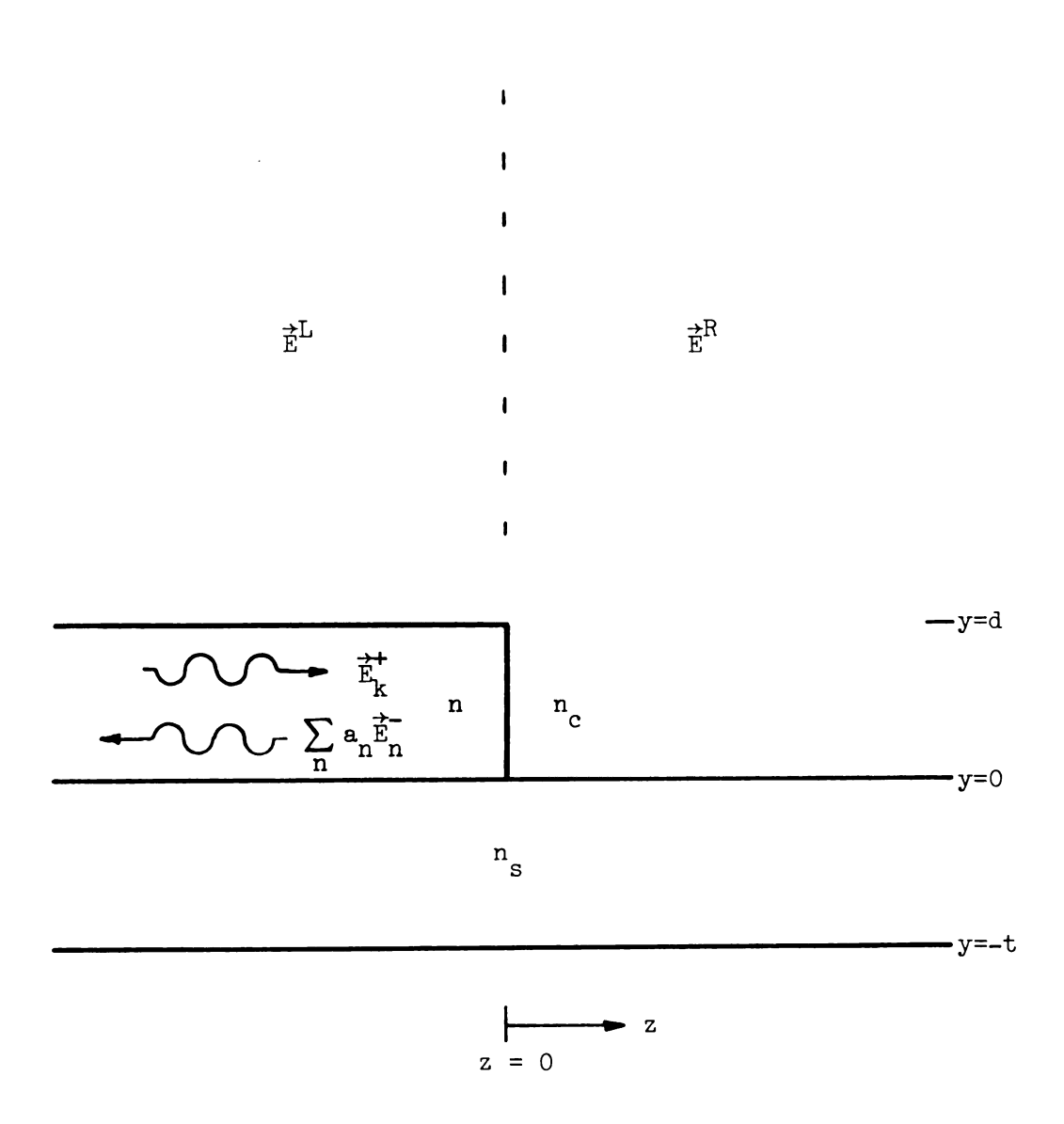


Figure 4.4: The plane truncated asymmetric slab waveguide with a surface wave incident on the truncation.

•	*		

4.4.1 Surface Wave Radiation

In this section we apply the iterative technique developed in part two of this chapter to the problem of surface wave reflection in a plane truncated asymmetric slab waveguide. We assume that a single TE surface wave mode is incident on the truncation plane at $z=z_0$ from within the asymmetric slab waveguide as depicted in Figure 4.4. The x invariance of this waveguiding structure allows us to conclude below that the surface waves reflected back up the waveguide are of the TE type. The x invariance of the waveguide will also allow a reduction in dimension of the spatial frequency integrals occurring in the Green's dyads used in the iterative formula. This reduction in dimension is accomplished in a manner similar to that used in section 3.3.6.

We now turn to specializing the iterative formula in equation (25) to the truncated asymmetric slab waveguide of Figure 4.4. We first note that the substrate and film refractive indices are identical in this case. This fact will have later implications for the reflection and coupling coefficients occurring in the spatial frequency integrals for the electric Green's dyad. Now the refractive index contrast factor is

$$\delta n^{2} \stackrel{\rightarrow}{(\rho)} = \begin{cases} \Delta n^{2} = n^{2} - n_{c}^{2} & , \quad 0 < y < t \\ 0 & , \quad \text{elsewhere} \end{cases}$$
 (39)

for the asymmetric slab. We will be working with TE surface waves of the asymmetric slab, which have the form

$$\overrightarrow{E_{m}}(\overrightarrow{r}) = \widehat{x} e_{m}(y)e^{\mp j\zeta_{m}Z}$$
(40)

where we have followed the notation established in section 4.1.1. If such a TE surface wave is incident on the truncation then the iterative formula (25) contains the factor $\hat{\mathbf{x}} \cdot \hat{\mathbf{G}}_{\mathbf{e}}$. The x invariance of the system implies that $\hat{\mathbf{x}} \cdot \nabla = \frac{\partial}{\partial \mathbf{x}} = 0$, so that the definition in equation (2.14) for the electric Green's dyad reduces to

$$\hat{\mathbf{x}} \cdot \hat{\mathbf{G}}_{e} = \mathbf{k}_{c}^{2} \hat{\mathbf{x}} \cdot \hat{\mathbf{G}}$$
 (41)

with \overrightarrow{G} the Hertzian potential Green's dyad or chapter two. Now by equations (2.17) and (2.19) we have

$$\hat{\mathbf{x}} \cdot \hat{\mathbf{G}}_{\mathbf{e}} = \mathbf{k}_{\mathbf{c}}^{2} \left[\mathbf{G}^{\mathbf{p}} + \mathbf{G}_{\mathbf{t}}^{\mathbf{r}} \right] \hat{\mathbf{x}}$$
 (42)

so that only TE modes will be reflected from the truncation is a TE mode is incident. Here the scalar Green's functions G^p and G^r_t are those given in equations (2.18) and (2.20).

We can use the x invariance of the waveguide to reduce the expressions for G^p and G^r_t to single spatial frequency integrals of the Sommerfeld type. This simplification rollows from the observation that the only x' dependence in the iteration formula of equation (25) is contained in the factor $\exp(j\xi_{\mathbf{X}}(\mathbf{x-x'}))$ or the Green's function in equation (42). Thus the x' integral in equation (25) can be evaluated immediately, giving (see Papoulis, [4.2])

$$\int_{-\infty}^{\infty} e^{j\xi_{\mathbf{X}}(\mathbf{x}-\mathbf{x}')} d\mathbf{x}' = 2 \pi \delta(\xi_{\mathbf{X}})$$
 (43)

This ractor now allow trivial evaluation of the spatial frequency integrals in the definitions of G^p and G^r_t . The result can be written

$$\mathbf{\mathscr{G}}(\mathbf{r}|\mathbf{r}') = \int_{\infty}^{\infty} k_{c}^{2}[G^{p} + G_{t}^{r}]dx'$$

$$= k_{c}^{2} \int_{-\infty}^{\infty} \frac{e^{j\xi(z-z')} - \gamma_{c}|y-y'|}{\mu_{\pi\gamma c}} [e^{-\gamma_{c}(y+y')}]d\xi$$

$$= k_{c}^{2} \int_{-\infty}^{\infty} \frac{e^{j\xi(z-z')}}{\mu_{\pi\gamma c}} [e^{-\gamma_{c}(y+y')}]d\xi$$

$$(44)$$

Here we have set $\xi_z = \xi$ and defined the reduced transverse wavenumber parameters

$$\gamma_{\ell}(\xi) = p_{\ell}(\xi_{\mathbf{X}} = 0, \xi_{\mathbf{Z}} = \xi) = \sqrt{\xi^2 - k_{\ell}^2}$$
 (45)

for ℓ = c, s. The transverse reflection coefficient $R_t(\xi)$ in equation (44) is obtained from the appropriate expressions in Appendix A by setting $n_f = n_s$ and $\xi_x = 0$. The result is

$$R_{t}(\xi) = \frac{\gamma_{c} + \gamma_{s}}{\gamma_{c} + \gamma_{s}} \tag{46}$$

The same simplifications made above can be applied to the expression for the normalization constant, $c_{\rm m}$, in equation (24). The x invariance of the system gives

$$\hat{\mathbf{x}} \cdot \stackrel{\leftrightarrow}{\mathbf{g}}_{e} = k_{c}^{2} [\mathbf{g}_{c}^{p} + \mathbf{g}_{c}^{r}] \mathbf{x}$$
 (47)

with g_{ζ}^{p} and g_{ζ}^{r} as in equations (3.11) and (3.14). Performing the x' integral in equation (24) results in

$$g_{\zeta} = \int_{-\infty}^{\infty} k_{c}^{2} [g_{\zeta}^{p} + g_{\zeta}^{r} t] dx'$$

$$= k_{c}^{2} \frac{1}{2\gamma_{c}} [e^{-\gamma_{c} |y-y'|} - \gamma_{c} (y+y')]$$
(48)

with γ_{C} and R_{t} as derined above.

We can combine these results to write the iterative equation (25) in the specialized scalar form

$$a_{m} = \frac{1}{c_{m}} \lim_{\zeta \to \zeta_{m}} \left(\frac{\Delta n^{2}}{n_{c}^{2}} \right)^{2} \int_{V} \int_{LCS} e_{m}(y) e^{-j\zeta} z_{u}(z - z_{o}) x$$

$$x \mathscr{G}(\overrightarrow{r}|\overrightarrow{r}') E^{L}(\overrightarrow{r}') dS' dV$$
(49)

where all fields are x directed. Here LCS denotes the longitudinal cross section $-\infty$ < z < ∞ , 0 < y < t. The normalization constant is now

$$c_{m} = j \left(\frac{\Delta n^{2}}{n_{c}^{2}}\right) \int_{CS} \int_{0}^{t} e_{m}(y) \frac{\partial}{\partial \delta} g_{\zeta}(y|y')| e_{m}(y') dy' dS$$
 (50)

where CS is the transverse waveguide core cross section — $\infty < x < \infty$, 0 < y < t.

We can now omit the integrals on x from $-\infty$ to ∞ that occur in the numerator and denominator of equation (49) (the denominator integral is in the normalization constant c_m of equation (50)) since the integrands are x invariant. The result is the final form of the surface wave reflection iterative equation specialized to TE modes of the asymmetric slab waveguide. It is

$$a_{m} = \frac{1}{c_{m}^{\prime}} \lim_{\zeta \to \zeta_{m}} \int_{LCS} \int_{LCS} e_{m}(y)e^{-j\zeta z}u(z - z_{o})$$

$$x \mathscr{S}(\vec{r}|\vec{r}^{\prime})E^{L}(\vec{r}^{\prime})dS'dS$$
(51)

with the modified normalization constant c_{m}^{\prime} given by

$$c_{m}^{\prime} = j \int_{0}^{t} \int_{0}^{t} e_{m}(y) \frac{\partial}{\partial \delta} g_{\zeta}(y|y') \Big|_{\zeta=m}^{t} e_{m}(y') dy' dy$$
 (52)

We now turn to the evaluation of the reflected surface wave amplitudes when the electric field in the core of the truncated asymmetric slab has the form

$$E^{L}(\vec{r}) = u(z_{o} - z) \left[AE_{k}^{+}(\vec{r}) + \sum_{n} a_{n}^{o} E_{n}^{-}(\vec{r})\right]$$
(53)

where $E_{\overline{m}}^+(r)$ are the TE surface wave modes of equation (40). This partial field is intended to represent either an initial guess at the core field to begin the iterative procedure with or an intermediate result of iteration with equation (51). When equation (53) is substituted into the specialized iterative equation (51) the result is or the form

$$a_{m} = \frac{1}{c_{m}^{*}} \left[A I_{mk}^{*} + \sum_{n} a_{n}^{(0)} I_{mn}^{-} \right]$$
 (54)

where the integrals I+ are derined as

$$I_{mn}^{+} = \lim_{\zeta \to \zeta_{n}} \int_{0}^{t} \int_{0}^{t} \mathcal{J}_{n}(y,y';\zeta) e_{m}(y) e_{n}(y') dy' dy$$

$$\mathcal{J}_{n}(y,y';\zeta) = \int_{-\infty}^{\infty} \int_{-\infty}^{\infty} \int_{-\infty}^{\infty} e^{-j\zeta z} u(z-z_{0}) \frac{e^{j\xi(z-z')}}{4\pi\gamma_{c}} \left[e^{-\gamma_{c}|y-y'|}\right]$$

$$+ R_{t}e^{-\gamma_{c}(y+y')} u(z_{0}-z') e^{+j\zeta_{n}z'} dz' dz d\xi$$
(55)

with $e_m(y)$ as given in equation (3.72). The longitudinal integrals in equation (55) can be evaluated by using the distributional relation (see Papoulis, [4.3])

$$\int_{-\infty}^{\infty} u(z)e^{-j\zeta z}dz = \frac{1}{i\zeta} + \pi\delta(\zeta)$$
 (56)

,
!
•

Equation (55) ror \mathcal{J} + becomes with the help or equation (56)

$$\mathcal{J} \frac{+}{n} (y, y'; \zeta) = \int_{\infty}^{\infty} \frac{1}{4\pi\gamma_{c}} \left[e^{-\gamma_{c} |y-y'|} + R_{t} e^{-\gamma_{c} (y+y')} - j(\zeta + \zeta_{n}) z_{o} \right] x$$

$$x \left\{ \frac{1}{j(\zeta - \xi)} + \pi \delta(\zeta - \xi) \right\} \left\{ \frac{-1}{j(\pm \zeta_{n} + \xi)} + \pi \delta(\pm \zeta_{n} + \xi) \right\} d\xi$$

$$= \int_{-\infty}^{\infty} r \frac{1}{n} (\zeta, \xi) d\xi + \frac{e^{-j(\zeta + \zeta_n) z_0}}{2j(\zeta + \zeta_n)} [g_{\zeta n} - g_{\zeta}]$$
(57)

where

$$f_{\overline{n}}^{+}(\zeta,\xi) = \frac{e^{-\gamma_{c}|y-y'|} - \gamma_{c}(y+y')}{e^{+R_{t}e}} e^{-j(\zeta+\zeta_{n})z_{o}}$$

$$= \frac{e^{+R_{t}e}}{4\pi\gamma_{c}(\zeta-\xi)(+\zeta_{n}+\xi)} e^{-(58)}$$

and \mathbf{g}_r is as in equation (48).

The integral of r^+ appearing in the equation (57) can be simplified by invoking the residue theorem (see section 3.3.1). We first modify the integration path to enclose the upper half complex plane in the usual manner, as shown in Figure 4.5. The illustrated branch cuts ensure that the factors γ_c and γ_s have positive real and imaginary parts (see the discussion in section 3.3.6 for the physical implications of this choice). The function r^+ has a pole at $-\zeta_n$ enclosed in the contour. The residue at this pole is

$$2\pi \mathbf{j} \operatorname{Res} \{ \mathbf{r}_{n}^{+}(\zeta, \xi) \} = - \frac{\mathbf{j}(\zeta + \zeta_{n}) \mathbf{z}_{0}}{\mathbf{j}(\zeta + \zeta_{n})} g_{\zeta n}(\mathbf{y} | \mathbf{y}^{*})$$

$$-\zeta_{n}$$

$$(59)$$

so that by equation (57) we have

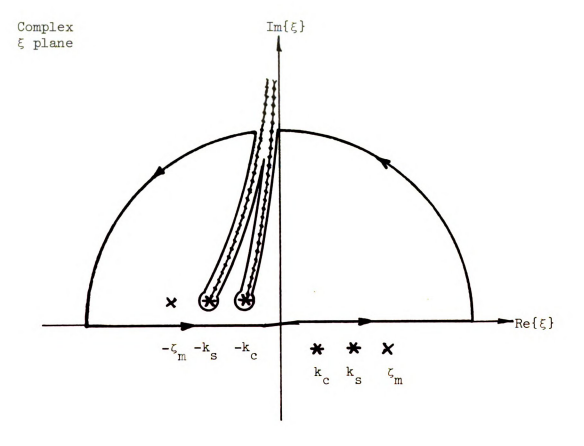


Figure 4.5: Integration contour in the complex ξ plane for the factor h^+_- .

$$\mathcal{J}_{n}^{+}(\mathbf{y},\mathbf{y'};\zeta) = -\int_{\mathcal{B}_{B}} r_{n}^{+}(\zeta,\xi)d\xi - \frac{e^{\mathbf{j}(\zeta+\zeta_{n})z_{0}}}{2\mathbf{j}(\zeta+\zeta_{n})}[g_{\zeta n} + g_{\zeta}]$$
 (60)

On the other hand, no pole of \vec{r} is enclosed, so that the result in this case is

$$\mathcal{J}_{n}^{-}(y,y';\zeta) = -\int_{\mathcal{C}B} r_{n}^{-}(\zeta,\xi)d\xi + \frac{-j(\zeta-\zeta_{n})z_{0}}{2j(\zeta-\zeta_{n})}[g_{\zeta n} - g_{\zeta}]$$
 (61)

We are now in a position to evaluate I^+ . We take the limit as $\zeta \to \zeta_m$ as indicated in equation (55) with no dirriculty. We obtain

$$I_{mn}^{+} = \frac{\int_{-e}^{j(\zeta_{m} + \zeta_{n})z_{o}}}{\int_{0}^{k_{o}^{2}/2}(\zeta_{m} + \zeta_{n})} \int_{0}^{t} e_{m}(y)e_{n}(y)dy - B_{mn}^{+}$$
 (62)

where we have used the one dimensional transformed asymmetric slab surface wave integral equation given by setting $e^{i} = 0$ in equation (3.69). Here we have derined

$$B_{mn}^{\frac{+}{m}} = \int_{\mathcal{C}} \left\{ \int_{0}^{t} \int_{0}^{t} r_{n}^{+}(\zeta_{n}, \xi) e_{m}(y) e_{n}(y') dy' dy \right\} d\xi$$
 (63)

This expression can be simplified by performing the spatial integrals and specializing the branch integration to the low loss limit. This procedure is carried out in Appendix D. For $n \neq m$ we obtain from equations (55) and (61) the result

$$I_{mn} = -B_{mn} \tag{64}$$

where the branch integral defined in equation (63) is simplified in Appendix D. If n = m we need to evaluate

$$I_{mm}^{-} = \lim_{\zeta \to \zeta} \frac{e^{-j(\zeta - \zeta_{m})z_{O}}}{2j(\zeta - \zeta_{m})} \int_{O}^{t} \int_{O}^{t} [g_{\zeta m}(y|y') - g_{\zeta}(y|y')] \times e_{m}(y)e_{m}(y')dy'dy - B_{mm}^{-}$$
(65)

This expression is indeterminate in the limit. We use L'Hopital's rule on equation (65) to obtain the result

$$I_{mm} = \frac{1}{2} c_{m}^{*} - B_{mm}^{-}$$
 (66)

Equations (62), (64) and (66) can be evaluated numerically and used in the iterative equation (54) to implement the iteration scheme for surface wave reflection in a truncated asymmetric waveguide.

4.4.2 Surface Wave Radiation

In this section we specialize equation (8) for the radiation or surface waves out of a truncated dielectric waveguide to the case of the truncated asymmetric slab. We then assume that a modal expansion is given for the slab core field in terms of TE surface waves and evaluate the resultant expression for the radiated field. $\overrightarrow{E}^R(r)$.

If the truncated slab core field \vec{E}^L consists of a TE surface wave modal expansion such as that given in equation (53) then the simplifications of the previous section apply here as well. Equation (8) becomes

$$E^{R}(\vec{r}) = u(z - z_{0})k_{0}^{2}\Delta n^{2}[AI_{k}^{+}(\vec{r}) + \sum_{n} a_{n}I_{n}^{-}(\vec{r})]$$
(67)

The modal expansion for $\stackrel{\rightarrow}{E}^L$ might be the result of the specialized iterative method of the previous section. The terms $\stackrel{+}{I}$ in equation (67) are defined as

$$I_{\overline{m}}^{+}(\overrightarrow{r}) = \int_{0}^{t} \int_{\infty}^{\infty} \int_{\infty}^{\infty} \frac{e^{j\xi(z-z')}e^{-\gamma_{c}|y-y'|} - \gamma_{c}(y+y')}{4\pi\gamma_{c}} + R_{t}e^{-\gamma_{c}(y+y')}$$

$$x u(z_{0} - z')e_{m}(y')e^{-j\zeta_{m}z'} d\xi dz'dy'$$
(68)

The longitudinal integral is again evaluated with the aid or equation (56). The result is

$$I_{\overline{m}}^{+}(\overrightarrow{r}) = \int_{0}^{t} \int_{\infty}^{\infty} \frac{1}{4\pi\gamma_{c}} \left[e^{-\gamma_{c}|y-y'|} + R_{t}e^{-\gamma_{c}(y+y')}\right] e_{m}(y')$$

$$x e^{j\xi(z-z_{o})} e^{-j\zeta_{m}z_{o}} \left\{ \frac{-1}{j(\xi+\zeta_{m})} + \pi\delta(\xi+\zeta_{m}) \right\} d\xi dy'$$
(69)

The second term in the integral is easily evaluated with the aid or the one dimensional transformed surface wave integral equation (3.69) with the result

$$I_{\overline{m}}^{+}(\overrightarrow{r}) = \frac{1}{2k_{O}^{2}\Delta n^{2}} E_{\overline{m}}^{+}(\overrightarrow{r}) - e^{+j\zeta_{\overline{m}}z_{O}} \int_{0}^{t} \int_{\infty}^{\infty} h_{\overline{m}}^{+}(\xi) e_{\overline{m}}(y') d\xi dy'$$
 (70)

where we have defined the integrand

$$h_{\overline{m}}^{+}(\xi) = \frac{-\gamma_{c}|y-y'| -\gamma_{c}(y-y')}{\frac{1}{4\pi j}\gamma_{c}(\xi+\zeta_{m})}$$

$$(71)$$

We will simplify the integral of h+by using the residue theorem. The term $z-z_0$ is greater than zero so that upper half ξ plane closure such as shown in Figure 4.5 is required. We see that the term h^+ has

a pole enclosed by the contour with residue

$$2\pi j \operatorname{Res}\{h_{m}^{+}(\xi)\} = g_{\zeta m}(y|y')e^{-\zeta_{m}}$$

$$(72)$$

whereas h has no pole inside or the contour. The result or this contour integration is

$$I_{\overline{m}}^{+}(\vec{r}) = + \frac{1}{2k_{0}^{2}\Delta n^{2}} E_{\overline{m}}^{+}(\vec{r}) + e^{-\frac{1}{2}\zeta_{m}z_{0}} C_{\overline{m}}^{+}(\vec{r})$$
 (73)

where $C\frac{+}{m}$ contains the branch cut integration term of the residue theorem. It is defined as

$$C_{\overline{m}}^{+}(\overrightarrow{r}) = \int_{\mathcal{C}} \left\{ \int_{0}^{t} h_{\overline{m}}^{+}(\xi) e_{\overline{m}}(y') dy' \right\} d\xi$$
 (74)

with h^+ as in equation (71). This term can be simplified by performing the spatial integration and specializing the branch cuts to the low loss limit. This procedure is carried out in Appendix D.

Equation (73) can be evaluated numerically and used in equation (67) to find the field radiated out of the truncated asymmetric slab waveguide.

4.4.3 Line Source Excitation

In this section we apply the theory developed in section 4.3.3 to the problem of excitation of surface waves in a truncated asymmetric slab waveguide by an x directed line polarization source.

We assume that the incident electric rield is supported by a uniform line polarization source of strength \overrightarrow{P}^e at location (y',z')

with $z' > z_0$, as shown in Figure 4.6. This impressed polarization is

$$\vec{P}^{e}(\vec{r}) = \hat{x} P^{e} \delta(y-y') \delta(z-z')$$
 (75)

It produces an x directed incident electric field in accordance with equation (2.25). The simplifications noted above due to the x invariance of the problem apply here as well. We obtain the incident field

$$\vec{E}^{\dot{1}}(\vec{r}) = \frac{P^{e}}{\varepsilon_{e}} \mathscr{G}(\vec{r}|\vec{r}^{\dagger}) \tag{76}$$

with $\vec{r}' = y \cdot \hat{y} + z \cdot \hat{z}$ and \mathscr{G} as given in equation (44).

The iterative equation (33) for the amplitude coefficients of the surface waves excited in a truncated waveguide has two terms. The first term is exactly the right hand side of the surface wave reflection iterative equation (25). This term was dealt with above in the case of the truncated asymmetric slab. We will here consider the second term in the iterative equation (33). It is identified in equation (34) as the zero order approximation for surface wave excitation when the waveguide field $\mathbf{E}^{\mathbf{L}}$ is equal to zero. The x invariance of the truncated asymmetric slab allows us to write equation (34) as

$$a_{m}^{(o)} = -\frac{1}{c_{m}^{\dagger}} \int_{LCS} e_{m}(y)e^{-j\zeta_{m}z} u(z_{o}-z) \frac{P^{e}}{\varepsilon_{c}} (\vec{r}|\vec{r}')dS$$
 (77)

with the normalization constant c_m^* as in equation (52). Substitution of equation (44) into this expression gives

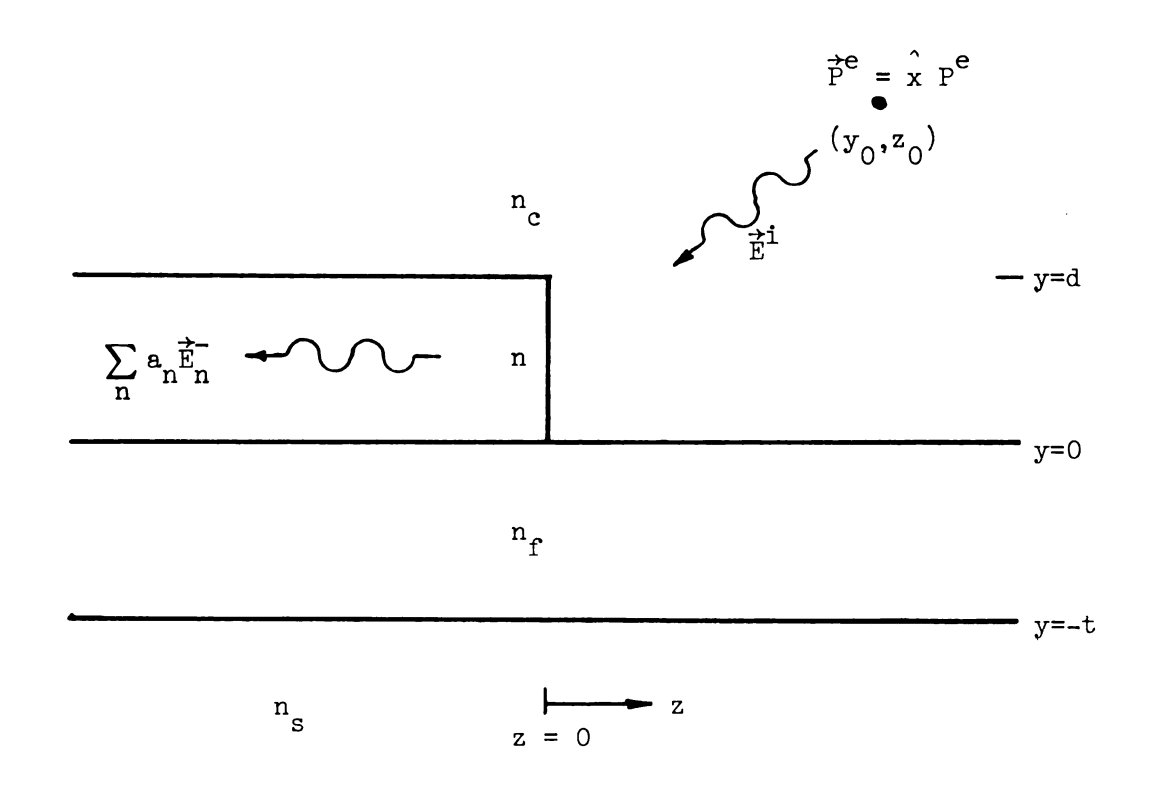


Figure 4.6: Uniform line polarization excitation of the truncated asymmetric slab waveguide.

$$a_{m}^{(o)} = -\frac{1}{c_{m}^{i}} \frac{k_{o}^{2} p^{e}}{\epsilon_{c}} \int_{o}^{t} \int_{\infty}^{\infty} \int_{\infty}^{\infty} \frac{e^{j \xi(z-z^{i})} - \gamma_{c} |y-y^{i}|}{4 \pi \gamma_{c}} + R_{t} e^{-\gamma_{c}(y+y^{i})}$$

$$x u(z_{o}-z)e_{m}(y)e^{-j\zeta_{m}z} d\xi dz dy$$

We see that this term has exactly the same form as that in equation (68) describing the radiation of surface waves from the truncated asymmetric slab waveguide. Thus we have

$$a_{m}^{(o)} = -\frac{1}{c_{m}^{*}} \frac{k_{o}^{2} p^{e}}{\varepsilon_{c}} I_{m}^{+}(\vec{r}^{*})$$
(78)

with I⁺ as given in equation (73). This ability to use the results of the radiation problem considered above is due to the radiation-excitation reciprocity discussed in section 4.3.4. The result in equation (78) can be numerically evaluated to rind the modal expansion or the rield excited in the truncated slab by a line polarization source.

4.4.4 Numerical Results

The above results were programmed for the truncated symmetric slab waveguide by setting $n_c = n_s$. The first results presented here are for the reflection of TE surface waves of the symmetric slab form a plane truncation at $z_0 = 0$. We assume that the incident surface wave consists of a unit amplitude TE_0 mode. We assume that the Fresnel reflection coefficient [4.4]

$$R_{r} = \frac{n - n_{c}}{n + n_{c}} \tag{79}$$

is a good approximation for the amplitude of the reflected TE_0 surface wave, and that no other reflected surface wave modes are excited. The results or both single and multiple iterations with equation (54) are graphed in Figure 4.7 versus normalized slab thickness. In Figure 4.8 we plot normalized radiated power as

$$E_{(0)}^{L}(\vec{r}) = u(z_0 - z)[E_0^{+}(\vec{r}) + R_r E_0^{-}(\vec{r})]$$
 (80)

versus normalized slab thickness. In Figure 4.9 we plot the results of equation (67) in the rar rield versus θ , where $\vec{r} = r\sin\theta \hat{y} + r\cos\theta \hat{z}$.

$$P_{RAD} = 1 - \sum_{n=0}^{\infty} |a_n|^2$$
 (81)

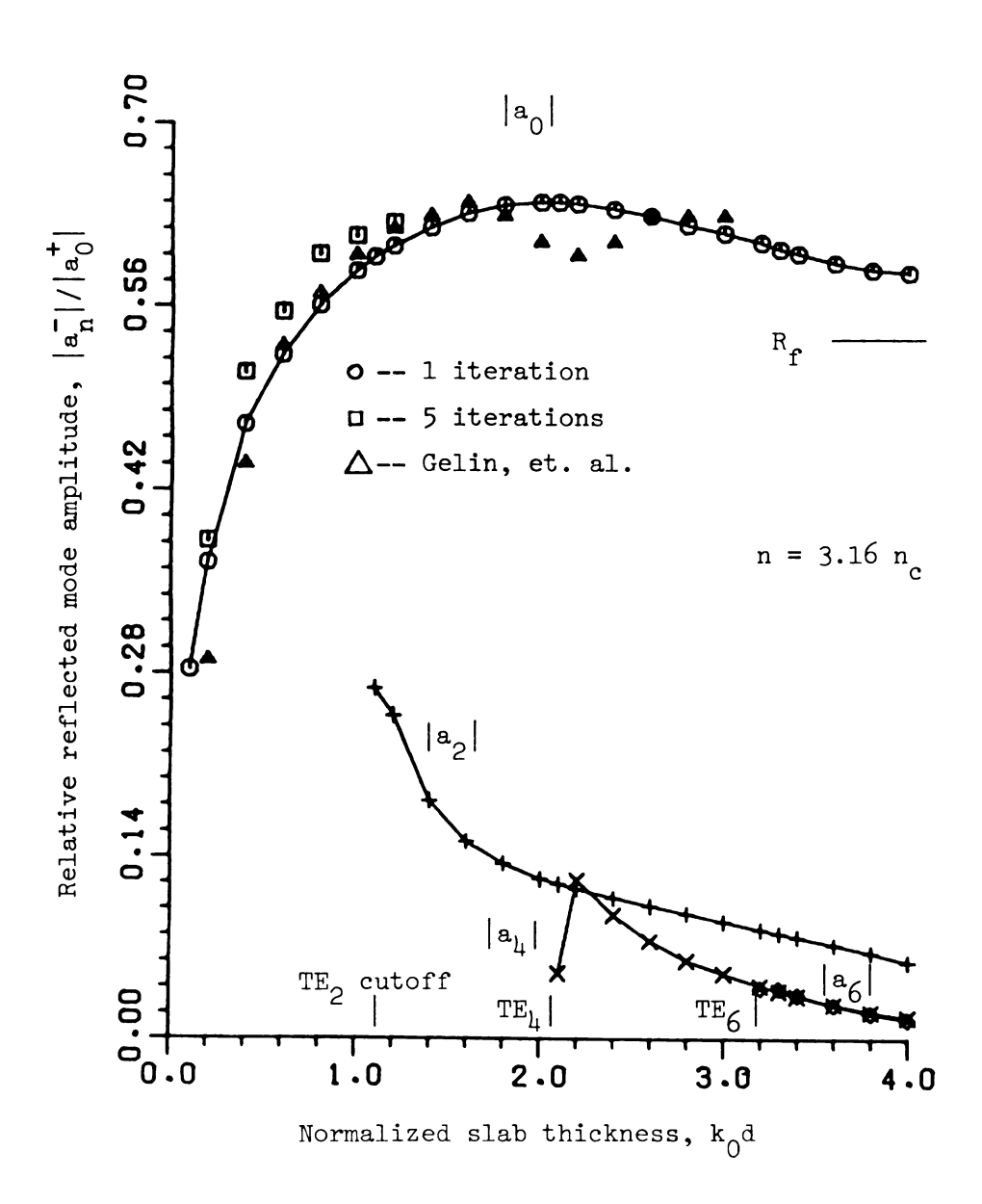


Figure 4.7: Normalized reflected mode amplitudes in truncated symmetric slab versus normalized slab thickness compared to the results of Gelin, et. al.

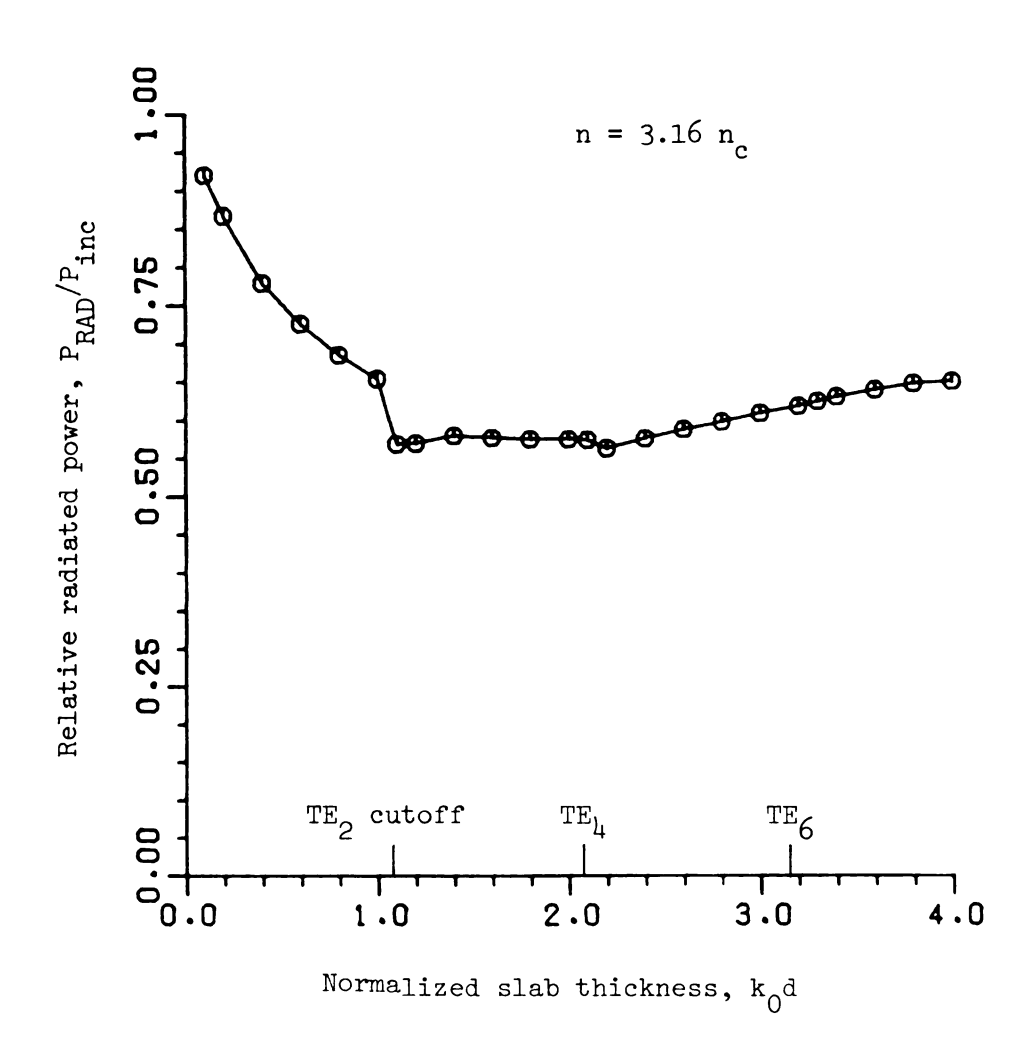


Figure 4.8: Relative radiated power from truncated symmetric slab waveguide versus normalized slab thickness.

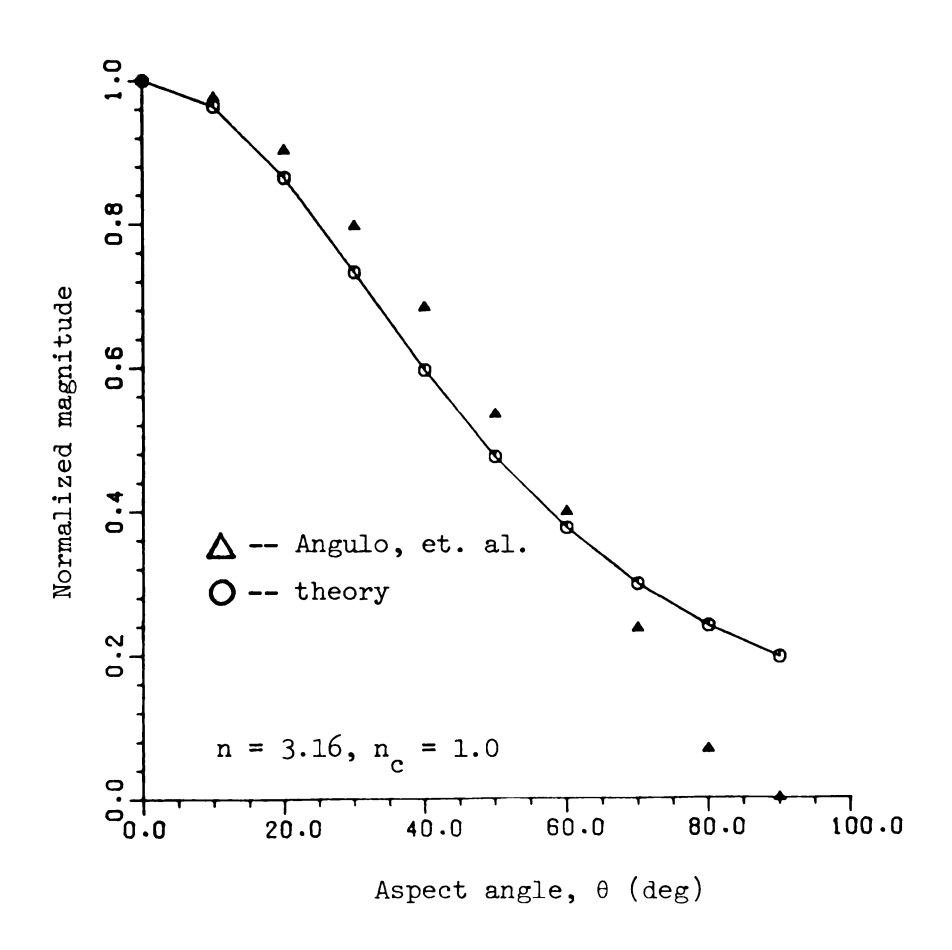


Figure 4.9: Normalized radiation and excitation patterns for the truncated symmetric slab versus aspect angle in degrees compared with the results of Angulo, et. al.

5. CONCLUSIONS

This dissertation investigated the application of an equivalent polarization integral equation to several problems involving integrated dielectric waveguides. Specifically, we applied this integral formulation to both longitudinally invariant waveguiding systems and to plane truncated dielectric waveguides.

Several important results were obtained for the case of axially uniform integrated dielectric waveguides. First we developed an excitation theory for a broad class of integrated waveguiding structures. This excitation theory allowed us to identify two major components of the total guided electromagnetic field - the surface waves of the system and the radiation field. The surface waves were shown to satisfy the expected homogeneous form of the equivalent polarization integral equation. On the other hand, the expressions found to be satisfied by the radiation field of the waveguiding system are to our knowledge new results. We were able to identify radiation field spectral components in a general manner and verify the conjecture that the full radiation field must in general be written as a two dimensional spectral superposition of such radiation field spectral components. We were also able through this analysis to generalize the recent theory by Oliner, et. al., regarding the leakage of surface waves from integrated dielectric waveguides. The leakage waves discovered by Oliner and Peng through geometrical and physical

arguments for uniform rectangular strip waveguides were shown to be a general phenomenon which occurs for a much broader class of integrated dielectric waveguiding structures. We were able to identify a new general criterion for determining if a given mode on an integrated dielectric waveguide will leak. We also applied this excitation theory to the special case of the asymmetric slab waveguide. We were able to recover several well known results of conventional excitation theory, thereby imparting confidence in our formulation. Finally, we established the reasability of using the equivalent polarization integral equation for generating numerical results for practical integrated dielectric waveguides. By postulating a general representation for the axial fields in a uniform rectangular strip waveguide we generated numerical results for the propagation characteristics of the rectangular strip which compared favorably to results of other analyses.

The results of our investigation of plane truncated integrated dielectric waveguides assumed the form of iterative equations.

Although a-priori knowledge of the surface wave field distributions is required, we are able to find the amplitudes of the surface waves generated in a truncated waveguide by an external impressed field, as well as the reflected and radiated fields when a surface wave is incident on the truncation from inside the waveguide. The numerical results of this iterative technique as applied to the truncated symmetric slab compare favorably to the results of other techniques.

Future studies utilizing the equivalent polarization integral equation could benefit by rapid numerical techniques of evaluating the Sommerfeld integrals involved in the dyadic Green's function

components. The use of standard trapazoidal integration routines proved to be slow and expensive in the work in chapter three. Several promising methods for increasing the efficiency and speed of such computations are proposed by Drachman and Nyquist in [5.1].

The method of moments could be used to generate numerical results similar to those of chapter three for more general transversely graded dielectric waveguides. This line of inquiry is being persued by Cloud [5.2], and would also benefit from the rapid numerical techniques discussed above.

The equivalent polarization integral equation used here can also be applied in a special simplified form to microstrip integrated circuits. This is another part of the proposal [5.1].

9	1			
	1 1			
	!			



APPENDIX A: HERTZIAN POTENTIAL GREEN'S DYAD

In this appendix we derive the dyadic Green's function for the electric Hertzian potential produced by an electric polarization source radiating in the top or middle layer of a tri-layered infinite uniform dielectric background structure. The dyadic Green's functions developed here are the kernels of the equivalent polarization integral equations of chapter two.

The dielectric medium that the Green's dyad describes is the trilayered background structure of the integrated dielectric waveguides of Figures 1.1 through 1.5. It consists of an infinite uniform dielectric slab of thickness t and generally complex refractive index $n_{\rm f}$. This slab is surrounded below and above by infinite uniform dielectric media of complex refractive indices $n_{\rm g}$ and $n_{\rm g}$, respectively.

Two different dyadic Green's functions are derived here. The first is valid when the polarization source and the location at which we want to find the Hertzian potential are both in the cover medium. This is the Green's dyad used in the strip-type dielectric waveguides of Figures 1.1, 1.2, 1.3, and 1.5. The second Green's dyad describes the situation where both the source point and field point are located in the film layer. This Green's dyad is the one applicable to channel waveguides such as the one depicted in Figure 1.4.

•	14	
:		
. '		
		•
		1
		1

The dyadic Green's functions are derived by direct solution of the inhomogeneous vector Helmholtz equation (2.7) satisfied by the electric Hertzian potential subject to the appropriate boundary conditions at the infinite planar interfaces at y = 0 and y = -t. This solution is obtained via the use of two dimensional Fourier transformation in the spatial variables tangential to the planar interfaces. In the inverse transform expressions for the Hertzian potential we are able to identify a dyadic Green's function for the problem in the form of a two-dimensional spectral superposition integrals of the Sommerfeld type.

Field Relations and Boundary Conditions

The electric Hertzian potential satisfies the inhomogeneous vector Helmholtz equation (2.7) in a uniform dielectric medium of permittivity ε . At a boundary between different dielectric media such as that in Figure A.1 the Hertzian potential components satisfy the following boundary conditions [A.1]

$$\pi_{1\alpha} = N_{21}^{2} \pi_{2\alpha} , \quad \alpha = x, y, z$$

$$\frac{\partial}{\partial y} \pi_{1\alpha} = N_{21}^{2} \frac{\partial}{\partial y} \pi_{2\alpha} , \quad \alpha = x, z$$

$$\frac{\partial}{\partial y} \pi_{2y} = \frac{\partial}{\partial y} \pi_{1y} = (N_{21}^{2} - 1)(\frac{\partial}{\partial x} \pi_{2x} - \frac{\partial}{\partial z} \pi_{2z})$$

$$N_{21} = \frac{n_{2}}{n_{1}}$$

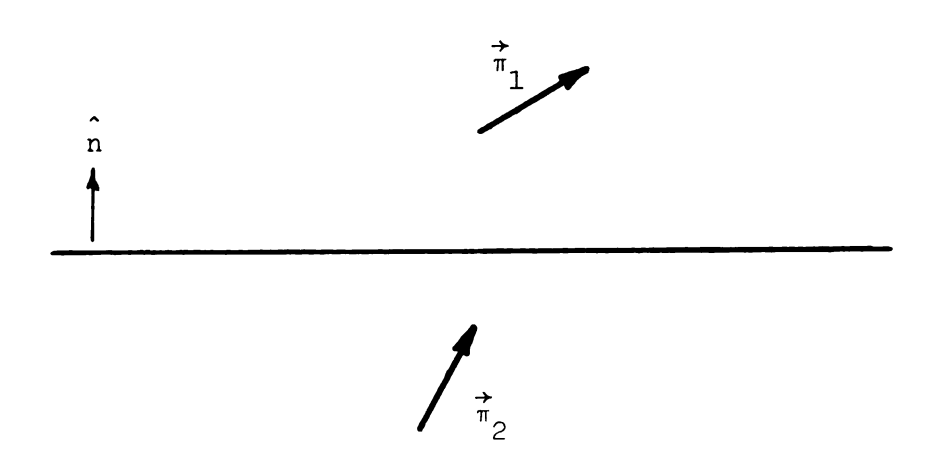
$$(1)$$

We will separate the total Hertzian potential in each uniform dielectric layer into two parts, a primary part and a scattered part.



Region 1

$$\varepsilon_1 = n_1^2 \varepsilon_0, \ \mu = \mu_0, \ \sigma = 0$$



Region 2

$$\varepsilon_2 = n_2^2 \varepsilon_0, \ \mu = \mu_0, \ \sigma = 0$$

Figure A.1: Hertzian potential boundary conditions at a dielectric interface.

The primary part is that part of the total Hertzian potential which propagates directly through the dielectric layer from a source in the layer to field point in the layer. The scattered part of the Hertzian potential is that part of the total Hertzian potential that arrives at field point after being scattered (reflected or transmitted) from interfaces between adjacent dielectric layers. By the above definitions, if we denote the principle and scattered parts of the Hertzian potential by $\vec{\pi}^p$ and $\vec{\pi}^s$, respectively, we have

$$\vec{\pi} = \vec{\pi}^{p} + \vec{\pi}^{g}$$

$$(\nabla^{2} + k^{2}) \begin{Bmatrix} \vec{\pi}^{p} \\ \vec{\pi}^{g} \end{Bmatrix} = \begin{Bmatrix} -\vec{p}/\epsilon \\ 0 \end{Bmatrix}$$
(2)

Note that by the above derinitions, the scattered Hertzian potential satisfies the homogeneous form of the vector Helmholtz equation (2.7). By the descriptions above we see that the Green's dyad for the primary part of the Hertzian potential is the one given in equations (2.17, 18) (see the discussion in section 2.2.1). Thus the primary Hertzian potential is given by

$$\pi_{\alpha}^{p} = \int_{V} G^{p}(r r') \frac{P_{\alpha}(\vec{r}')}{\varepsilon} dV' , \quad \alpha = x, y, z$$
 (3)

We will solve the Helmholtz equations (2) by use of two dimensional Fourier transformation on the tangential spatial variables x and z. To this end, we define the two dimensional transform pair

∯ 3.	ig (Mr.			
1				
	1			
	i - 1 - 1 - 1 - 1 - 1 - 1 - 1 - 1 - 1 -			

$$\tilde{f}_{\alpha}(\vec{\xi},y) = \iint_{\infty}^{\infty} r_{\alpha}(\vec{r}) e^{-j\vec{\xi}\cdot\vec{r}} dxdz$$

$$r_{\alpha}(\vec{r}) = \frac{1}{(2\pi)^{2}} \iint_{-\infty}^{\infty} \tilde{f}_{\alpha}(\xi,y) e^{j\vec{\xi}\cdot\vec{r}} d\xi xdz$$
(4)

where $\vec{\xi} = \vec{\xi}_X \hat{x} + \vec{\xi}_Z \hat{z}$ is a two dimensional spectral frequency. We will denote this relationship

$$\tilde{\mathbf{r}}_{\alpha}(\vec{\xi}, \mathbf{y}) = \mathscr{F}_{\mathbf{x}, \mathbf{z}} \{ \mathbf{r}_{\alpha}(\vec{\mathbf{r}}) \}
\mathbf{r}_{\alpha}(\vec{\mathbf{r}}) = \mathscr{F}_{\mathbf{x}, \mathbf{z}} \{ \tilde{\mathbf{r}}_{\alpha}(\vec{\xi}, \mathbf{y}) \}$$
(5)

The homogeneous Helmholtz equation (2) for the scattered potential transforms with the help of the Fourier differentiation theorem to

$$\left(\frac{\partial^2}{\partial \mathbf{y}^2} + \mathbf{p}^2\right) \tilde{\pi}_{\alpha}^{\mathbf{S}} = 0 \quad , \quad \mathbf{p}^2 = \xi_{\mathbf{x}}^2 + \xi_{\mathbf{z}}^2 - \mathbf{k}^2$$
 (6)

where p is one of the transverse wavenumbers as given in equation (2.22). The boundary conditions in equation (1) transform to

$$\vec{\pi}_{1\alpha} = N_{21}^{2} \vec{\pi}_{2\alpha} , \quad \alpha = \mathbf{x}, \mathbf{y}, \mathbf{z}$$

$$\frac{\partial}{\partial \mathbf{y}} \vec{\pi}_{1\alpha} = N_{21}^{2} \frac{\partial}{\partial \mathbf{y}} \vec{\pi}_{2\alpha} , \quad \alpha = \mathbf{x}, \mathbf{z}$$

$$\frac{\partial}{\partial \mathbf{y}} \vec{\pi}_{2y} - \frac{\partial}{\partial \mathbf{y}} \vec{\pi}_{1y} = (N_{21}^{2} - 1)[\mathbf{j} \xi_{\mathbf{x}} \vec{\pi}_{2x} + \mathbf{j} \xi_{\mathbf{z}} \vec{\pi}_{2z}]$$
(7)

The primary Green's function G^p or equation (2.18) transforms to

$$\mathcal{F}_{x,z}\{G^{p}(\vec{r}|\vec{r}')\} = G^{p}(\vec{\xi},y|y')e^{-j\vec{\xi}\cdot\vec{r}'}$$

$$G^{p}(\vec{\xi},y|y') = \frac{e^{-p|y-y'|}}{2p}$$
(8)

so that by the convolution theorem of Fourier theory we have the transformed primary Hertzian potential

$$\tilde{\pi}_{\alpha}^{p} = \int \frac{\tilde{P}_{\alpha}(\vec{\xi}, y')}{\tilde{G}} \tilde{G}^{p}(\vec{\xi}, y|y') e^{-j\vec{\xi}\cdot\vec{r}'} dy'$$
(9)

The homogeneous form of the transformed Helmholtz equation (6) has a simple solution

$$\pi_{\alpha}^{\mathbf{S}} = \mathbf{W}_{\alpha}(\xi) e^{\mathbf{T}p\mathbf{y}} \tag{10}$$

This will be the prototype solution for the transformed scattered potentials, whereas the prototype solution for the transformed primary potentials is given by equation (9).

Strip Guide Green's Dyad

In the case or both source and rield points in the cover medium, the total transformed potential in the cover consists of two parts as depicted in Figure A.2:

$$\pi_{e\alpha} = \pi_{e\alpha}^{p} + \pi_{e\alpha}^{r} \tag{11}$$

with $\tilde{\pi}^r_{c\alpha}$ the potential wave in the cover reflected off of the cover-film interface,

$$\tilde{\pi}_{C\alpha}^{r} = W_{C\alpha}^{r} e^{-p_{C}y}$$
(12)

and the transformed principle polarization as in equation (9). Note that the minus sign was chosen in equation (10) to represent an upward propagating wave of reflected potential.

The transformed total potential in the film layer consists of two transformed scattered potential waves, a potential wave transmitted through the cover-film interface and a potential wave reflected off of

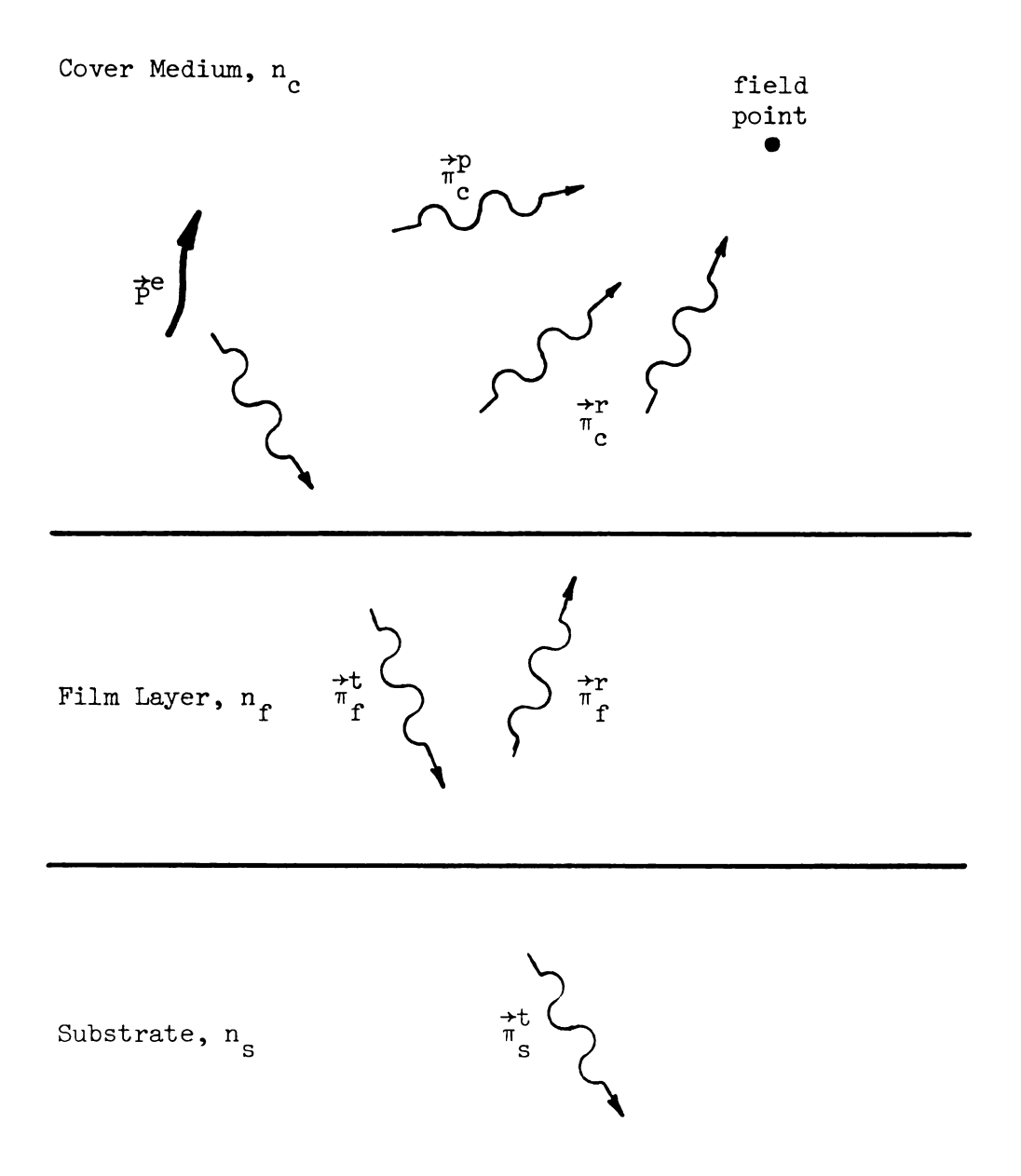


Figure A.2: Principle and scattered Hertzian potential components for a source in the cover medium.

•			

the rilm-substrate interrace. These scattered waves are illustrated in Figure A.2. They are written

$$\tilde{\pi}_{f\alpha} = \tilde{\pi}_{f\alpha}^{r} + \tilde{\pi}_{f\alpha}^{t}$$

$$\tilde{\pi}_{f\alpha}^{r} = W_{r\alpha}^{r} e^{-p_{f}y}$$

$$\tilde{\pi}_{f\alpha}^{t} = W_{f\alpha}^{t} e^{p_{f}y}$$
(13)

where the signs of the exponentials were chosen to give the proper direction of propagation for the scattered potential waves in the film layer.

The total potential in the substrate consists of only a potential wave transmitted through the film-substrate interface, as shown in Figure A.2. It is written

$$\tilde{\pi}_{S\alpha} = \tilde{\pi}_{S\alpha}^{t} = W_{S\alpha}^{t} e$$
 (14)

We now apply the transformed Hertzian potential boundary conditions in equation (7) to our prototype solutions to find the functions W_{α} . We begin with the tangential boundary conditions at the interface between cover and film at y=0. They become

$$-W_{c\alpha}^{r} + N_{rc}^{t}[W_{r\alpha}^{t} + W_{r\alpha}^{r}] = V_{\alpha}$$

$$, \alpha = x,z$$

$$W_{c\alpha}^{r} + \frac{N_{rc}^{2}}{p_{c}}[W_{r\alpha}^{t} - W_{r\alpha}^{r}] = V_{\alpha}$$

$$V_{\alpha} = \int \frac{\tilde{P}_{\alpha}(\tilde{\xi}, y')}{\varepsilon_{\alpha}} \frac{e^{-p_{c}y'}}{2p_{c}} e^{-j\tilde{\xi}\cdot\tilde{r}'}dy', \alpha = x,y,z$$
(15)

We can solve equations (15) for $W^r_{c_\alpha}$ and $W^t_{f_\alpha}$ in terms of $W^r_{f_\alpha}$ and V_α . The result is

$$W_{c\alpha}^{r} = R_{rc}^{t}V_{\alpha} + T_{rc}^{t}W_{r\alpha}^{r}$$

$$W_{r\alpha}^{r} = T_{cr}^{t}V_{\alpha} + R_{cr}^{t}W_{r\alpha}^{r}$$

$$(16)$$

where the tangential reflection and transmission coefficients associated with the cover-film interface are defined as

$$R_{rc}^{t} = \frac{p_{c}^{-p}r}{p_{c}^{+p}r} \qquad R_{cr}^{t} = -R_{rc}^{t}$$

$$T_{rc}^{t} = 2N_{rc}^{2} \frac{p_{r}}{p_{c}^{+p}r} \qquad T_{cr}^{t} = \frac{2}{N_{rc}^{2}} \frac{p_{c}}{p_{c}^{+p}r}$$
(17)

We now apply the tangential boundary equations at the film-substrate interface at y = -t. They give

$$W_{r\alpha}^{t} = {}^{p_{r}t} + W_{r\alpha}^{r} = {}^{p_{r}t} - N_{sr}^{2} W_{s\alpha}^{t} = 0$$

$$V_{r\alpha}^{t} = {}^{p_{r}t} - W_{r\alpha}^{r} = {}^{p_{r}t} - N_{sr}^{2} \frac{p_{s}}{p_{r}} W_{s\alpha}^{t} = 0$$

$$W_{r\alpha}^{t} = {}^{p_{r}t} - W_{r\alpha}^{r} = {}^{p_{r}t} - N_{sr}^{2} \frac{p_{s}}{p_{r}} W_{s\alpha}^{t} = 0$$

$$(18)$$

We can solve equations (18) for $W^r_{f^\alpha}$ and $W^t_{s^\alpha}$ in terms of $W^t_{f^\alpha}$. The result has the form

$$W_{r\alpha}^{r} = R_{sr}^{r} e \qquad W_{r\alpha}^{t}$$

$$W_{c\alpha}^{t} = T_{rs}^{t} e \qquad W_{r\alpha}^{t}$$

$$W_{r\alpha}^{t} = T_{rs}^{t} e \qquad W_{r\alpha}^{t}$$

$$(19)$$

where we have derined the tangential reflection and transmission coefficients associated with the film-substrate interface as

$$R_{sr}^{t} = \frac{p_{r}^{-p_{s}}}{p_{r}^{+p_{s}}}$$
 $T_{fs}^{t} = \frac{2}{N_{sr}^{2}} \frac{p_{r}}{p_{f}^{+p_{s}}}$ (20)

We now combine the results or equations (16) and (19). Substitution of equation (19) into equations (16) leads to results in terms of V only

$$W_{r_{\alpha}}^{t} = D_{t}^{-1} T_{cr}^{t} V_{\alpha}$$

$$W_{r_{\alpha}}^{r} = D_{t}^{-1} T_{cr}^{t} R_{sr}^{t} e^{-2p_{r}t} V_{\alpha}$$

$$W_{c_{\alpha}}^{t} = D_{t}^{-1} T_{cr}^{t} T_{rs}^{t} e^{-p_{r}t} V_{\alpha}$$

$$W_{c_{\alpha}}^{t} = D_{t}^{-1} (T_{rc}^{t} T_{rs}^{t} e^{-p_{r}t})^{t} V_{\alpha}$$

$$W_{c_{\alpha}}^{t} = D_{t}^{-1} (T_{rc}^{t} T_{rs}^{t} e^{-p_{r}t})^{t} + D_{t} R_{rc}^{t} V_{\alpha}$$

$$D^{t} = 1 - R_{cr}^{t} R_{sr}^{t} e^{-2p_{r}t}$$

$$D^{t} = 1 - R_{cr}^{t} R_{sr}^{t} e^{-2p_{r}t}$$

We now turn to application of the normal boundary conditions from equation (7). At the interface between cover and film layers at y = 0 they take the form

$$-w_{cy}^{r} + N_{rc}^{2} [w_{ry}^{t} + w_{ry}^{r}] = V_{y}$$

$$w_{cy}^{r} + \frac{p_{r}}{p_{c}} [w_{ry}^{t} - w_{ry}^{r}] = V_{y} + \frac{N_{rc}^{2-1}}{p_{c}} [j\xi_{x}(w_{rx}^{t} + w_{rx}^{r}) + j\xi_{z}(w_{rz}^{t} + w_{rz}^{r})]$$

$$(22)$$

Now, by equations (19) and (21),

$$W_{r'\alpha}^{t} + W_{r'\alpha}^{r} = \frac{p_{c}}{N_{rc}^{2-1}} FV_{\alpha} , \quad \alpha = x,z$$

$$F = \frac{N_{rc}^{2-1}}{p_{c}D_{t}} T_{cr}^{t} (1 + R_{sr}^{t} e^{-2p_{r}t})$$
(23)

so that equations (22) becomes

(F 1) !

$$-W_{cy}^{r} + N_{rc}^{2}[W_{ry}^{t} + W_{ry}^{r}] = V_{y}$$

$$W_{cy}^{r} + \frac{p_{r}}{p_{c}}[W_{ry}^{t} - W_{ry}^{r}] = V_{y} + F[j\xi_{x}V_{x} + j\xi_{z}V_{z}]$$
(24)

We combine equations (24) to solve for W^r_{cy} and W^t_{ry} in terms of W^r_{ry} and the V_α . The result is

$$W_{cy}^{r} = R_{rc}^{n}V_{y} + T_{rc}^{n}W_{ry}^{r} + C_{1}[j\xi_{x}V_{x} + j\xi_{z}V_{z}]$$

$$W_{ry}^{t} = T_{cr}^{n}V_{y} - R_{rc}^{n}W_{ry}^{r} + \frac{C_{1}}{N_{rc}^{2}}[j\xi_{x}V + j\xi_{z}V_{z}]$$
(25)

where the normal transmission and reflection coefficients associated with the cover-film interface are

$$R_{fc}^{n} = \frac{N_{fc}^{2} p_{c}^{-p} r}{N_{fc}^{2} p_{c}^{+p} r}$$
 (26)

$$T_{rc}^{n} = 2 \frac{p_{f}}{N_{cr}^{2}p_{c}^{+}p_{r}}$$
 $T_{cr}^{n} = 2 \frac{p_{c}}{N_{cr}^{2}p_{c}^{+}p_{r}}$

and the rirst coupling term is

$$C_{1} = \frac{N_{re}^{2}(N_{re}^{2}-1)}{N_{re}^{2}p_{e}+p_{r}} D_{t}^{-1} (1 + R_{sr}^{t}e^{-2p_{r}t})$$
 (27)

Now apply the normal boundary equations to the rilm-substrate interface at y = -t. We obtain in manner identical to that used above the results

$$W_{ry}^{r} = R_{sr}^{n} W_{ry}^{t} + C_{2} [j \xi_{x} V_{x} + j \xi_{z} V_{z}]$$

$$W_{sy}^{t} = -(p_{s} - p_{r})t = T_{rs}^{n} W_{ry}^{t} + \frac{C_{2}}{N_{sr}^{2}} [j \xi_{x} V_{x} + j \xi_{z} V_{z}]$$
(28)

where the normal transmission and reflection coefficients associated with the film-substrate interface and the second coupling term are

$$R_{sf}^{n} = \frac{N_{sr}^{2p}r^{-p}s}{N_{sr}^{2p}r^{+p}s} \qquad T_{rs}^{n} = 2 \frac{p_{r}}{N_{sr}^{2p}r^{+p}s}$$

$$C_{2} = \frac{N_{sr}^{2}(N_{sr}^{2-1})}{N_{sr}^{2p}r^{+p}s} \qquad D_{t}^{-1}T_{cr}^{t}T_{rs}^{t}$$
(29)

We can now use equations (25) and (28) to solve for all the W $_y$ in terms of the V $_\alpha$ only. The result takes the form

$$\begin{split} \mathbf{W}_{ry}^{r} &= D_{n}^{-1} \mathbf{T}_{cr}^{n} \mathbf{R}_{sf}^{n} e^{-2P_{r}t} \quad \mathbf{V}_{y} + D_{n}^{-1} (\mathbf{R}_{sf}^{n} \mathbf{N}_{rc}^{-2} \mathbf{C}_{1} + \mathbf{C}_{2}) \\ &= \mathbf{V}_{ry}^{-2p_{r}t} \quad [\mathbf{j}\xi_{x}\mathbf{V}_{x} + \mathbf{j}\xi_{z}\mathbf{V}_{z}] \\ \mathbf{W}_{ry}^{t} &= D_{n}^{-1} \mathbf{T}_{cr}^{n} \mathbf{V}_{y} + D_{n}^{-1} (\mathbf{N}_{rc}^{-2} \mathbf{C}_{1} - \mathbf{R}_{rc}^{n} \mathbf{C}_{2} e^{-2P_{r}t}) \\ &= \mathbf{X} \quad [\mathbf{j}\xi_{x}\mathbf{V}_{x} + \mathbf{j}\xi_{z}\mathbf{V}_{z}] \\ \mathbf{W}_{cy}^{r} &= D_{n}^{-1} (\mathbf{D}_{n}\mathbf{R}_{rc}^{n} + \mathbf{T}_{cr}^{n} \mathbf{R}_{sr}^{n} \mathbf{T}_{rc}^{n} e^{-2P_{r}t}) \mathbf{V}_{y} \\ &+ D_{n}^{-1} [\mathbf{D}_{n}\mathbf{C}_{1} + \mathbf{T}_{cr}^{n} (\mathbf{R}_{sr}^{n} \mathbf{N}_{rc}^{-2} \mathbf{C}_{1} + \mathbf{C}_{2}) e^{-2P_{r}t}] \\ &\times [\mathbf{j}\xi_{x}\mathbf{V}_{x} + \mathbf{j}\xi_{z}\mathbf{V}_{z}] \\ \mathbf{W}_{sy}^{t} &= D_{n}^{-1} \mathbf{T}_{cr}^{n} \mathbf{T}_{rs}^{n} \mathbf{V}_{y} + D_{n}^{-1} [\mathbf{D}_{n} \mathbf{N}_{sr}^{-2} \mathbf{C}_{2} + \mathbf{C}_{2}] \end{split}$$

4 4 - 4 - 4 ļ

+
$$T_{rc}^{n}(N_{fc}C_{1} - R_{rc}^{n}C_{2}e^{-2p_{r}t})] \times [j\xi_{x}V_{x}j\xi_{z}V_{z}]$$

 $D_{n} = 1 + R_{rc}^{n}R_{sf}^{n}e$

By equation (11) we need W_c^r to rind the total transformed potential in the cover region. We can use the above results to write

$$W_{c_{\alpha}}^{r} = R_{t}V_{\alpha} , \qquad \alpha = x,z$$

$$W_{cy}^{r} = R_{n}V_{y} + C[j\xi_{x}V_{x} + j\xi_{z}V_{z}]$$
(31)

where we have from equations (21) and (30)

$$R_{t} = D_{t}^{-1} [D_{t}R_{tc}^{t} + T_{cr}^{t}R_{sr}^{t}T_{rc}^{t}e^{-2p_{r}t}]$$

$$R_{n} = D_{n}^{-1} [D_{n}R_{rc}^{n} + T_{cr}^{n}R_{sr}^{n}T_{rc}^{n}e^{-2p_{r}t}]$$

$$C = D_{n}^{-1} [D_{n}C_{1} + T_{rc}^{n}(R_{sr}^{n}N_{rc}^{-2}C_{1} + C_{2})e^{-2p_{r}t}]$$
(32)

Now the total Hertzian potential in the cover region is

$$\pi_{e_{\alpha}} = \pi_{e_{\alpha}}^{p} + \pi_{e_{\alpha}}^{r} = \mathscr{F}_{x,z}^{-1} \left\{ \tilde{\pi}_{p_{\alpha}}^{e} \right\} + \mathscr{F}_{x,z}^{-1} \left\{ \tilde{\pi}_{r_{\alpha}}^{e} \right\}$$
(33)

The principle part of the potential is given by inverse transforming equation (9):

$$\pi_{C\alpha}^{p} = \mathscr{F}_{\mathbf{x},\mathbf{z}}^{-1} \left\{ \int \frac{\tilde{P}(\vec{\xi},\mathbf{y'}) e^{-p_{C}|\mathbf{y}-\mathbf{y'}|}}{\varepsilon_{C}} e^{-j\vec{\xi}\cdot\vec{r'}} d\mathbf{y'} \right\}$$

$$= \int_{V} \frac{P_{\alpha}(\vec{r'})}{\varepsilon_{C}} \int_{-\infty}^{\infty} \frac{e^{j\vec{\xi}\cdot(\vec{r}-\vec{r'})} e^{-p_{C}|\mathbf{y}-\mathbf{y'}|}}{2(2\pi)^{2}p_{C}} d^{2}\xi dV'$$
(34)

where we have made use of the Fourier convolution property. By

equations (12) and (31) we also have

$$\frac{1}{R_{c}} = \mathcal{F}_{x,z}^{-1} \left\{ e^{-p_{c}y} \left[\hat{x}R_{t}V_{x} + \hat{y}(cj_{\xi_{x}}V_{x} + R_{n}Vy + cj_{\xi_{z}}V_{z}) + \hat{z}R_{t}V_{z} \right] \right\}$$

$$= \hat{x} \int_{V} \frac{P_{x}(\vec{r}'\vec{r}'\vec{r})}{\varepsilon_{c}} \int_{-\infty}^{\infty} R_{t} \frac{e^{j\vec{\xi}\cdot(\vec{r}-\vec{r}')}e^{-p_{c}(y+y')}}{2(2\pi)^{2}p_{c}} d^{2}\xi dV$$

$$+ \hat{y} \int_{V} \left\{ \frac{(P_{x})(\vec{r}')}{\varepsilon_{c}} \frac{\partial}{\partial x} \int_{-\infty}^{\infty} c \frac{e^{j\vec{\xi}\cdot(\vec{r}-\vec{r}')}e^{-p_{c}(y+y')}}{2(2\pi)^{2}p_{c}} d^{2}\xi \right\}$$

$$+ \frac{P_{y}(\vec{r}'')}{\varepsilon_{c}} \int_{-\infty}^{\infty} R_{n} \frac{e^{j\vec{\xi}\cdot(\vec{r}-\vec{r}')}e^{-p_{c}(y+y')}}{2(2\pi)^{2}p_{c}} d^{2}\xi$$

$$+ \frac{P_{z}(\vec{r}'')}{\varepsilon_{c}} \frac{\partial}{\partial z} \int_{-\infty}^{\infty} c \frac{e^{j\vec{\xi}\cdot(\vec{r}-\vec{r}')}e^{-p_{c}(y+y')}}{2(2\pi)^{2}p_{c}} d^{2}\xi \right\} dV'$$

$$+ \hat{z} \int_{V} \frac{P_{z}(\vec{r}'')}{\varepsilon_{c}} \int_{-\infty}^{\infty} R_{t} \frac{e^{j\vec{\xi}\cdot(\vec{r}-\vec{r}')}e^{-p_{c}(y+y')}}{2(2\pi)^{2}p_{c}} d^{2}\xi dV'$$

where we have used the dirrerentiation theorem and the convolution property to obtain (35). The total Hertzian potential can be written more compactly as

$$\overrightarrow{\pi}_{c} = \overrightarrow{\pi}_{c}^{p} + \overrightarrow{\pi}_{c}^{r} = \int_{V} \overrightarrow{G}^{p}(\overrightarrow{r}|\overrightarrow{r}') \cdot \frac{\overrightarrow{P}(r')}{\varepsilon_{c}} dV'
+ \int_{V} \overrightarrow{G}^{r}(\overrightarrow{r}|\overrightarrow{r}') \cdot \frac{\overrightarrow{P}(\overrightarrow{r}')}{\varepsilon_{c}} dV'
= \int_{V} \overrightarrow{G}(\overrightarrow{r}|\overrightarrow{r}') \cdot \frac{\overrightarrow{P}(\overrightarrow{r}')}{\varepsilon_{c}} dV'$$
(36)

where by equations (34) and (35),

$$\overrightarrow{G}^{p} = \overrightarrow{I} G^{p} = \overrightarrow{I} \int_{-\infty}^{\infty} \frac{e^{j\overrightarrow{\xi} \cdot (\overrightarrow{r} - \overrightarrow{r}^{\dagger})} e^{-p_{c} |y-y^{\dagger}|}}{2(2\pi)^{2} p_{c}} d^{2}\xi$$

$$\overrightarrow{G}^{r} = \widehat{x} G_{t}^{r} \widehat{x} + \widehat{y} (\frac{\partial}{\partial x} G_{c}^{r} \widehat{x} + G_{n}^{r} \widehat{y} + \frac{\partial}{\partial z} G_{c}^{r}) + \widehat{z} G_{t}^{r} \widehat{z}$$
(37)

and

$$\begin{cases}
G_{\mathbf{t}}^{\mathbf{r}}(\vec{r}|\vec{r}') \\
G_{\mathbf{n}}^{\mathbf{r}}(\vec{r}|\vec{r}')
\end{cases} = \iint_{-\infty}^{\infty} \begin{cases}
R_{\mathbf{t}}(\xi) \\
R_{\mathbf{n}}(\xi) \\
C(\xi)
\end{cases} = \underbrace{\frac{e^{j\vec{\xi}\cdot(\vec{r}-\vec{r}')}e^{-p_{\mathbf{c}}(y+y')}}{2(2\pi)^{2}p_{\mathbf{c}}}} d^{2}\xi$$
(38)

Thus we have identified a dyadic Green's function for the total potential in the cover medium.

Channel Guide Green's Dyad

In this case we place both source and field points in the film region of the tri-layered background. The total potential in the film layer consists or a principle part and a scattered part satisfying the Helmholtz equations (2). The prototype transformed solutions for the two potential parts are given by equations (9) and (10). Referring to Figure A.3 we have

$$\tilde{\pi}_{r_{\alpha}} = \tilde{\pi}_{r_{\alpha}}^{p} + \tilde{\pi}_{r_{\alpha}}^{r} + \tilde{\pi}_{r_{\alpha}}^{r} + \tilde{\pi}_{r_{\alpha}}^{r} , \qquad \alpha = x,y,z$$
 (39)

We will write the total transformed potential in the cover medium as

$$\vec{\pi}_{C\alpha} = \vec{\pi}_{C\alpha}^{t} = W_{C\alpha}^{t} = W_{C\alpha}^{t} e \qquad , \quad \alpha = z, y, z$$
 (40)

in accordance with equation (10). In the film region we have

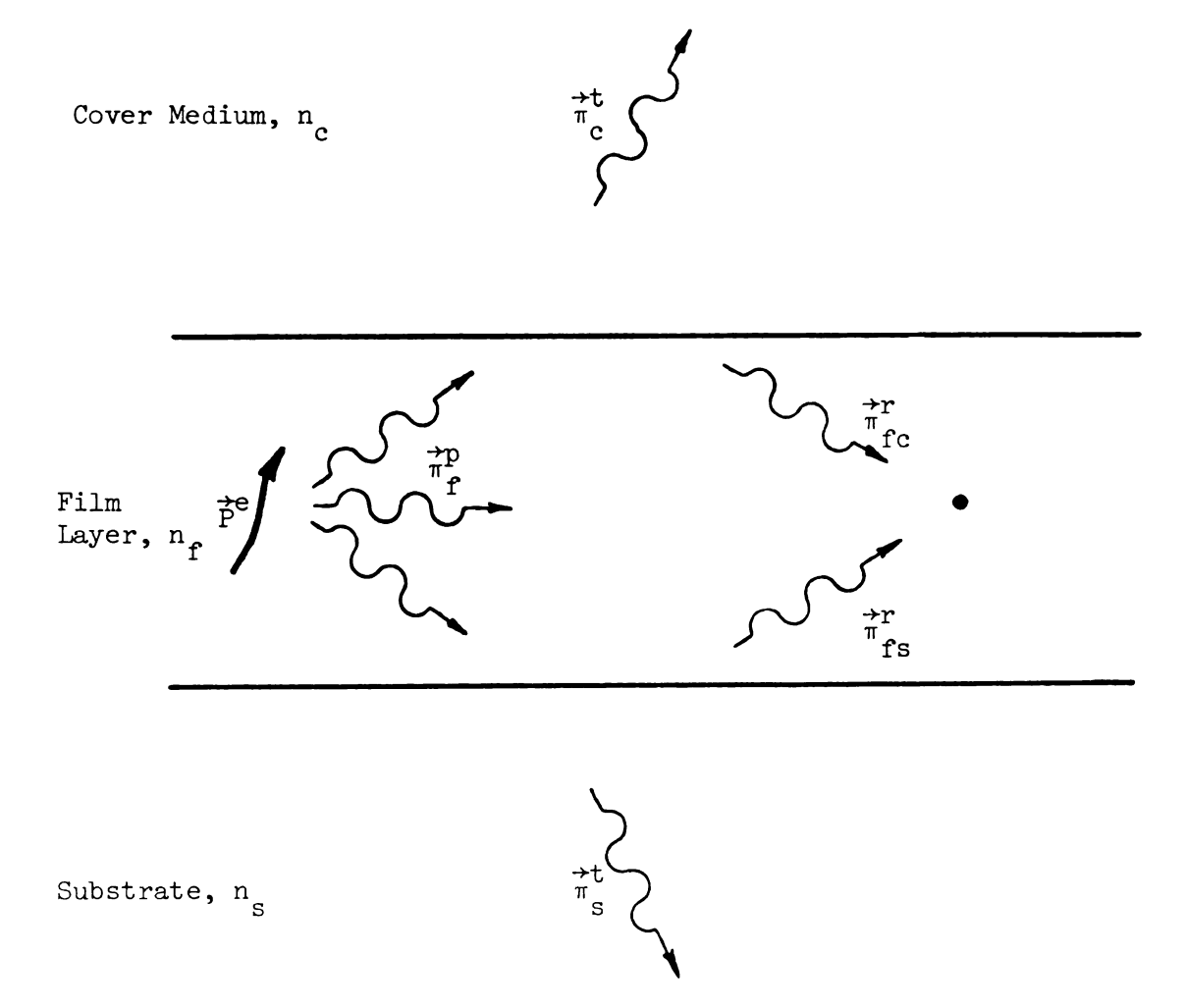


Figure A.3: Principle and scattered Hertzian potential components for a source in the film layer.

$$\tilde{\pi}_{r\alpha} = \int \frac{\tilde{P}_{\alpha}(\vec{\xi}, y')}{\varepsilon_{r}} \frac{e^{-p_{r}(y-y')}}{2p_{r}} e^{-j\frac{\vec{\xi}}{\varepsilon} \cdot \vec{r}'} dy'$$

$$+ W_{r\alpha}^{r} e^{p_{r}y} + W_{r\alpha}^{r} e^{-p_{r}y}, \quad \alpha = x,y,z$$
(41)

and in the substrate we write

$$\tilde{\pi}_{S\alpha} = \tilde{\pi}_{S\alpha}^{t} = W_{S\alpha}^{t} e^{p_{S}t}$$
(42)

We first apply the transformed tangential boundary conditions from equation (7) to our prototype solutions at the film-cover interface at y = 0. We obtain in a manner similar to that in the previous section

$$W_{re\alpha}^{r} = R_{ef}^{t} [W_{rs\alpha}^{r} + V_{e\alpha}]$$

$$\alpha = x,z$$

$$W_{e\alpha}^{t} = T_{re}^{t} [W_{rs\alpha}^{r} + V_{e\alpha}]$$
(43)

with

$$V_{r\alpha} = \int \frac{\tilde{P}(\vec{\xi}, y^{\dagger})}{\varepsilon_{r}} \frac{e^{-p_{r}y^{\dagger}}}{2p_{r}} e^{-j\vec{\xi}\cdot\vec{r}^{\dagger}} dy \qquad , \quad \alpha = x, y, z \quad (44)$$

and the tangential transmission and reflection coefficients for the film-cover interface as defined in the previous section. Application of the tangential boundary conditions at the film-substrate interface at y = -t gives results of the form

$$W_{rs\alpha}^{r} = R_{sr}^{t} \left[W_{rc\alpha}^{r} + V_{r\alpha} \right] e^{-2p_{r}t}$$

$$W_{s\alpha}^{t} = T_{rs}^{t} \left[W_{rc\alpha}^{r} + V_{r\alpha} \right] e^{-(p_{r}-p_{s})t}$$

$$W_{s\alpha}^{t} = T_{rs}^{t} \left[W_{rc\alpha}^{r} + V_{r\alpha} \right] e^{-(p_{r}-p_{s})t}$$

$$(45)$$

with

$$V_{f\alpha} = \int \frac{\tilde{P}_{\alpha}(\vec{\xi}, y')}{\varepsilon_{r}} \frac{e^{-p_{r}y'}}{2p_{r}} e^{-j\vec{\xi}\cdot\vec{r}'} dy' , \quad \alpha = x,y,z \quad (46)$$

We can combine equations (43) and (45) to get

$$W_{rs\alpha}^{r} = D_{t}^{-1} (R_{sr}^{r} R_{cr}^{t} V_{c\alpha} + R_{sr}^{t} V_{r\alpha}) e^{-2p_{r}t}$$

$$W_{rc\alpha}^{r} = D_{t}^{-1} (R_{cr}^{t} V_{c\alpha} + R_{sr}^{t} R_{cr}^{t} V_{r\alpha} e^{-2p_{r}t})$$

$$W_{c\alpha}^{t} = D_{t}^{-1} (T_{rc}^{t} V_{c\alpha} + R_{sr}^{t} T_{rc}^{t} V_{r\alpha} e^{-2p_{r}t})$$

$$W_{s\alpha}^{t} = D_{t}^{-1} (T_{rc}^{t} V_{c\alpha} + R_{sr}^{t} T_{rc}^{t} V_{r\alpha} e^{-(p_{r}^{-p_{s}})t})$$

$$W_{s\alpha}^{t} = D_{t}^{-1} (T_{rc}^{t} V_{c\alpha} + R_{sr}^{t} T_{rc}^{t} V_{r\alpha}) e^{-(p_{r}^{-p_{s}})t}$$

$$D_{t} = 1 - R_{cr}^{t} R_{sr}^{t} e^{-2p_{r}t}$$

Now implement the normal boundary conditions at the rilm-cover interface at y = 0. The result is

$$W_{rey}^{r} = R_{er}^{n} \left[W_{rsy}^{r} + V_{cy} \right] + \frac{(N_{re}^{2}-1)(1+R_{er}^{t})}{(N_{re}^{2}p_{e}+p_{r}^{t})D_{t}}$$

$$\times \left[j\xi_{x}V_{x} + j\xi_{z}V_{z} \right]$$

$$W_{cy}^{t} = T_{re}^{n} \left[W_{rsy}^{r} + V_{cy} \right] + \frac{N_{re}^{2}(N_{re}^{2}-1)(1+R_{er}^{t})}{(N_{re}^{2}p_{e}+p_{s}^{t})D_{t}}$$

$$\times \left[j\xi_{x}V_{x} + j\xi_{z}V_{z} \right]$$

$$V_{cy}^{r} = V_{cy}^{r} + R_{sr}^{t}V_{re}^{r} = \frac{-2p_{r}^{t}}{r^{2}}$$

Similarly, application of normal boundary conditions at the filmsubstrate interface at y = -t results in

$$W_{rsy}^{r} = R_{sr}^{n} \left[W_{rcy}^{r} + V_{ry} \right] + \frac{N_{sr}^{2} (N_{sr}^{2} - 1) T_{rs}^{t}}{(N_{sr}^{2} p_{r} + p_{s}) D_{t}}$$

$$\times \left[j \xi_{x} \overline{V}_{x}' + j \xi_{z} \overline{V}_{z}' \right]$$

$$W_{sy}^{t} = T_{rs}^{t} \left[W_{rc}^{r} + V_{ry} \right] + \frac{(N_{sr}^{2} - 1) T_{rs}^{t}}{(N_{sr}^{2} p_{r} + p_{s}) D_{t}}$$

$$\times \left[j \xi_{x} \overline{V}_{x}' + j \xi_{z} \overline{V}_{z}' \right]$$

$$\overline{V}_{\alpha} = R_{cr}^{t} V_{c\alpha} + V_{r\alpha} , \quad \alpha = x, y, z$$

$$(49)$$

We can now combine equations (48) and (49) and solve for the terms $W^{\mathbf{r}}_{\mathbf{f}\mathbf{s}\mathbf{y}}$ and $W^{\mathbf{r}}_{\mathbf{f}\mathbf{c}\mathbf{y}}$ in terms of the source terms \overline{V}_{α} and $\overline{V}_{\alpha}^{\mathbf{r}}$ only. This procedure gives

$$\begin{split} \mathbf{W}_{r}\mathbf{s}\mathbf{y} &= \mathbf{D}_{n}^{-1}(\mathbf{R}_{s}\mathbf{f}^{n}\mathbf{R}_{c}\mathbf{r}^{n}\mathbf{V}_{cy} + \mathbf{R}_{s}\mathbf{f}^{n}\mathbf{V}_{sy})e^{-2\mathbf{p}_{r}\mathbf{t}} \\ &+ \mathbf{C}_{1}\left[\mathbf{j}\boldsymbol{\xi}_{x}\mathbf{V}_{cx} + \mathbf{j}\boldsymbol{\xi}_{z}\mathbf{V}_{cz}\right] + \mathbf{C}_{2}\left[\mathbf{j}\boldsymbol{\xi}_{x}\mathbf{V}_{rx} + \mathbf{j}\boldsymbol{\xi}_{z}\mathbf{V}_{rz}\right] \\ \mathbf{W}_{r}\mathbf{c}\mathbf{y} &= \mathbf{D}_{n}^{-1}\left(\mathbf{R}_{c}\mathbf{r}^{n}\mathbf{V}_{cy} + \mathbf{R}_{c}\mathbf{r}^{n}\mathbf{R}_{s}\mathbf{r}^{n'}\mathbf{V}_{ry}\right) \\ &+ \mathbf{C}_{1}\mathbf{I}\left[\mathbf{j}\boldsymbol{\xi}_{x}\mathbf{V}_{cx} + \mathbf{j}\boldsymbol{\xi}_{z}\mathbf{V}_{cz}\right] + \mathbf{C}_{2}\mathbf{I}\left[\mathbf{j}\boldsymbol{\xi}_{x}\mathbf{V}_{rx} + \mathbf{j}\boldsymbol{\xi}_{z}\mathbf{V}_{rz}\right] \\ \mathbf{C}_{1} &= \mathbf{D}_{t}^{-1}\mathbf{D}_{n}^{-1}\left[\frac{\left(\mathbf{N}_{r}\mathbf{c}^{2}-1\right)\mathbf{T}_{c}\mathbf{R}^{n}\mathbf{R}_{s}\mathbf{r}^{n'}}{\mathbf{P}_{r}\mathbf{P}_{c}} + \frac{\left(\mathbf{N}_{s}\mathbf{c}^{2}-1\right)\mathbf{T}_{r}^{n'}\mathbf{R}_{c}\mathbf{t}}{\mathbf{P}_{r}\mathbf{P}_{s}}\right] \\ \mathbf{C}_{2} &= \mathbf{D}_{t}^{-1}\mathbf{D}_{n}^{-1}\left[\frac{\mathbf{N}_{c}\mathbf{c}^{2}(\mathbf{N}_{r}\mathbf{c}^{2}-1)\mathbf{T}_{r}\mathbf{R}_{s}\mathbf{r}^{n'}}{\mathbf{P}_{r}\mathbf{P}_{c}} + \frac{\left(\mathbf{N}_{s}\mathbf{c}^{2}-1\right)\mathbf{T}_{r}\mathbf{r}^{n'}}{\mathbf{P}_{r}\mathbf{P}_{s}}\right] \\ \mathbf{C}_{1}\mathbf{I} &= \mathbf{R}_{c}\mathbf{r}^{n}\mathbf{C}_{1} + \mathbf{D}_{t}^{-1}\left[\frac{\mathbf{N}_{c}\mathbf{c}^{2}(\mathbf{N}_{r}\mathbf{c}^{2}-1)\mathbf{T}_{r}\mathbf{c}}{\mathbf{P}_{r}\mathbf{P}_{c}}\right] \\ \mathbf{C}_{2}\mathbf{I} &= \mathbf{R}_{c}\mathbf{r}^{n}\mathbf{C}_{2} + \mathbf{D}_{t}^{-1}\left[\frac{\mathbf{N}_{c}\mathbf{c}^{2}(\mathbf{N}_{r}\mathbf{c}^{2}-1)\mathbf{T}_{r}\mathbf{c}}{\mathbf{P}_{r}\mathbf{P}_{c}}\right] \\ \mathbf{C}_{2}\mathbf{I} &= \mathbf{R}_{c}\mathbf{r}^{n}\mathbf{C}_{2} + \mathbf{D}_{t}^{-1}\left[\frac{\mathbf{N}_{c}\mathbf{c}^{2}(\mathbf{N}_{r}\mathbf{c}^{2}-1)\mathbf{T}_{r}\mathbf{c}}{\mathbf{P}_{r}\mathbf{P}_{c}}\right] \end{aligned}$$

Here the prime in R and T denotes multiplication of the factor by $\exp(-2p_Tt)$. We can write the results of equations (47) and (50) in the abbreviated form

$$W_{fc\alpha}^{r} = R_{t}^{11} V_{c\alpha} + R_{t}^{12} V_{f\alpha} , \quad \alpha = x,z$$

$$W_{fs\alpha}^{r} = R_{t}^{21} V_{c\alpha} + R_{t}^{22} V_{f\alpha}$$

$$W_{rcy}^{r} = R_{n}^{11} V_{cy} + R_{n}^{22} V_{ry} + C_{n}^{11} [j \xi_{x} V_{cx} + j \xi_{z} V_{cz}]$$

$$= C_{n}^{12} [j \xi_{x} V_{fx} + j \xi_{z} V_{fz}]$$
(51)

$$W_{rsy}^{r} = R_{n}^{21} V_{cy} + R_{n}^{22} V_{ry} + C^{21} [j \xi_{x} V_{cx} + j \xi_{z} V_{cz}] + C^{22} [j \xi_{x} V_{rx} + j \xi_{z} V_{rz}]$$

where we have defined

$$R_{t}^{11} = \overline{D}_{t}^{1} R_{cr}^{t} \qquad R_{n}^{11} = \overline{D}_{n}^{1} R_{cr}^{n} \qquad C_{11}^{11} = C_{1}^{1}$$

$$R_{t}^{12} = \overline{D}_{t}^{1} R_{cr}^{t} R_{sr}^{t} \qquad R_{n}^{12} = \overline{D}_{n} R_{cr}^{1} R_{sr}^{n} \qquad C_{12}^{12} = C_{2}^{1}$$

$$R_{t}^{21} = R_{t}^{12} \qquad R_{n}^{12} = R_{n}^{21} \qquad C_{21}^{21} = C_{1}$$

$$R_{t}^{22} = \overline{D}_{t}^{1} R_{sr}^{t} \qquad R_{n}^{22} = \overline{D}_{n} R_{sr}^{1n} \qquad C_{22}^{22} = C_{2}$$

$$(52)$$

Now the total potential in the film region is

$$\pi_{\Gamma_{\alpha}} = \pi_{\Gamma_{\alpha}}^{p} + \pi_{\Gamma_{\alpha}}^{r} + \pi_{\Gamma_{\alpha}}^{r}$$

$$= \mathcal{F}_{x,z} \left\{ \tilde{\pi}_{\Gamma_{\alpha}}^{p} \right\} + \mathcal{F}_{x,z} \left\{ \tilde{\pi}_{\Gamma_{\alpha}}^{r} \right\} + \mathcal{F}_{x,z} \left\{ \tilde{\pi}_{\Gamma_{\alpha}}^{r} \right\}$$

$$= \chi,z \left\{ \tilde{\pi}_{\Gamma_{\alpha}}^{p} \right\} + \mathcal{F}_{x,z} \left\{ \tilde{\pi}_{\Gamma_{\alpha}}^{r} \right\} + \mathcal{F}_{x,z} \left\{ \tilde{\pi}_{\Gamma_{\alpha}}^{r} \right\} + \mathcal{F}_{x,z} \left\{ \tilde{\pi}_{\Gamma_{\alpha}}^{r} \right\} \right\}$$

$$= \chi,z \left\{ \tilde{\pi}_{\Gamma_{\alpha}}^{p} \right\} + \mathcal{F}_{x,z} \left\{ \tilde{\pi}_{\Gamma_{\alpha}}^{r} \right\} + \mathcal{F}_{x$$

The principle part of the potential is obtained by inverse transforming the first term of equation (41):

$$\pi_{\mathbf{c}_{\alpha}}^{\mathbf{p}} = \mathscr{F}_{\mathbf{x},\mathbf{z}}^{-1} \left\{ \int \frac{\tilde{\mathbf{p}}_{\alpha}(\vec{\xi},\mathbf{y}') e^{-\mathbf{p}_{\Gamma}|\mathbf{y}-\mathbf{y}'|}}{\varepsilon_{\Gamma}} e^{-\mathbf{j}\vec{\xi}\cdot\vec{\mathbf{r}}'} d\mathbf{y}' \right\}$$

$$= \int_{\mathbf{V}} \frac{\mathbf{p}_{\alpha}(\vec{r}')}{\varepsilon_{\Gamma}} \iint_{-\infty}^{\infty} \frac{e^{\mathbf{j}\vec{\xi}\cdot(\vec{\mathbf{r}}-\vec{\mathbf{r}}')} e^{-\mathbf{p}_{\Gamma}|\mathbf{y}-\mathbf{y}'|}}{2(2\pi)^{2}\mathbf{p}_{\Gamma}} d^{2}\xi d\mathbf{V}'$$
(54)

where we have used the Fourier convolution theorem. By equation (41) we have

$$\begin{split} & \pi_{\mathbf{r}c\alpha}^{\mathbf{r}} = \mathscr{F}_{\mathbf{x},\mathbf{z}}^{-1} \left\{ e^{-\mathbf{p}_{\mathbf{r}}\mathbf{y}} [\mathbf{R}_{t}^{11} \ \mathbf{v}_{c\alpha} + \mathbf{R}_{t}^{12} \ \mathbf{v}_{r\alpha}] \right\} \\ & = \int_{V} \frac{\mathbf{p}_{\alpha}(\vec{r}^{\prime})}{\varepsilon_{r}} \int_{-\infty}^{\infty} \mathbf{R}_{t}^{\mathbf{c}} \frac{e^{\mathbf{j}\frac{\mathbf{f}}{\xi} \cdot (\vec{r}^{\prime} - \vec{r}^{\prime})} e^{\mathbf{p}_{r}\mathbf{y}}}{2(2\pi)^{2}\mathbf{p}_{r}} d^{2}\xi dV^{\prime} \\ & \pi_{\mathbf{r}s\alpha}^{\mathbf{r}} = \mathscr{F}_{\mathbf{x},\mathbf{z}}^{-1} \left\{ e^{-\mathbf{p}_{r}\mathbf{y}} [\mathbf{R}_{t}^{21} \ \mathbf{v}_{c\alpha} + \mathbf{R}_{t}^{22}\mathbf{v}_{r\alpha}] \right\} \\ & = \int_{V} \frac{\mathbf{p}_{\alpha}(\vec{r}^{\prime})}{\varepsilon_{r}} \int_{-\infty}^{\infty} \mathbf{R}_{t}^{\mathbf{r}} \frac{e^{\mathbf{j}\frac{\mathbf{f}}{\xi} \cdot (\vec{r} - \vec{r}^{\prime})} e^{-\mathbf{p}_{r}\mathbf{y}}}{2(2\pi)^{2}\mathbf{p}_{r}} d^{2}\xi dV^{\prime} \\ & \pi_{\mathbf{r}cy}^{\mathbf{r}} = \mathscr{F}_{\mathbf{x},\mathbf{z}}^{-1} \left\{ e^{-\mathbf{p}_{r}\mathbf{y}} [\mathbf{R}_{t}^{11} \ \mathbf{v}_{cy} + \mathbf{R}_{t}^{12} \ \mathbf{v}_{ry} + \mathbf{c}^{11} [\mathbf{j}\xi_{x}\mathbf{v}_{cx} + \mathbf{j}\xi_{z}\mathbf{v}_{cz}] \right. \\ & + \mathbf{c}^{12} [\mathbf{j}\xi_{x}\mathbf{v}_{rx} + \mathbf{j}\xi_{z}\mathbf{v}_{rz}] \right\} \\ & = \int_{V} \frac{\mathbf{p}_{x}(\vec{r}^{\prime})}{\varepsilon_{r}} \int_{-\infty}^{\infty} \mathbf{R}_{n}^{\mathbf{c}} \frac{e^{\mathbf{j}\frac{\mathbf{f}}{\xi} \cdot (\vec{r} - \vec{r}^{\prime})} e^{\mathbf{p}_{r}\mathbf{y}}}{2(2\pi)^{2}\mathbf{p}_{r}} d^{2}\xi dV^{\prime} \\ & + \int_{V} \frac{\mathbf{p}_{y}(\vec{r}^{\prime})}{\varepsilon_{r}} \frac{\partial}{\partial x} \int_{-\infty}^{\infty} \mathbf{c}^{\mathbf{c}} \frac{e^{\mathbf{j}\frac{\mathbf{f}}{\xi} \cdot (\vec{r} - \vec{r}^{\prime})} e^{\mathbf{p}_{r}\mathbf{y}}}{2(2\pi)^{2}\mathbf{p}_{r}} d^{2}\xi dV^{\prime} \\ & + \int_{V} \frac{\mathbf{p}_{z}(\vec{r}^{\prime})}{\varepsilon_{r}} \frac{\partial}{\partial z} \int_{-\infty}^{\infty} \mathbf{c}^{\mathbf{c}} \frac{e^{\mathbf{j}\frac{\mathbf{f}}{\xi} \cdot (\vec{r} - \vec{r}^{\prime})} e^{\mathbf{p}_{r}\mathbf{y}}}{2(2\pi)^{2}\mathbf{p}_{r}} d^{2}\xi dV^{\prime} \end{aligned}$$

$$\pi_{fsy} = \mathcal{F}_{x,z}^{-1} \left\{ e^{-p_{f}y} \left(R_{n}^{21} V_{cy} + R_{n}^{22} V_{fy} + C^{21} \left[j\xi_{x}V_{cx} + j\xi_{z}V_{z} \right] \right\}$$

$$+ C^{22} \left[j\xi_{x}V_{fx} + j\xi_{z}V_{fz} \right] \right\}$$

$$= \int_{V} \frac{P_{y}(\vec{r}')}{\varepsilon_{r}} \int_{-\infty}^{\infty} R_{n}^{s} \frac{e^{j\xi \cdot (\vec{r} - \vec{r}')} e^{-p_{f}y}}{2(2\pi)^{2}p_{f}} d^{2}\xi dV'$$

$$+ \int_{V} \frac{P_{x}(\vec{r}')}{\varepsilon_{r}} \frac{\partial}{\partial x} \int_{-\infty}^{\infty} C^{s} \frac{e^{j\xi \cdot (\vec{r} - \vec{r}')} e^{-p_{f}y}}{2(2\pi)^{2}p_{f}} d^{2}\xi dV'$$

$$+ \int_{V} \frac{P_{z}(\vec{r}')}{\varepsilon_{f}} \frac{\partial}{\partial z} \int_{-\infty}^{\infty} C^{s} \frac{e^{j\xi \cdot (\vec{r} - \vec{r}')} e^{-p_{f}y}}{2(2\pi)^{2}p_{f}} d^{2}\xi dV'$$

where we have derined

$$R_{t}^{c} = R_{t}^{11} e^{p_{r}y'} + R_{t}^{12} e^{-p_{r}y'}$$

$$R_{t}^{s} = R_{t}^{21} e^{p_{r}y'} + R_{t}^{22} e^{-p_{r}y'}$$

$$R_{t}^{c} = R_{t}^{11} e^{p_{r}y'} + R_{t}^{12} e^{-p_{r}y'}$$

$$R_{n}^{c} = R_{n}^{11} e^{p_{r}y'} + R_{n}^{12} e^{-p_{r}y'}$$

$$C^{c} = C^{11} e^{p_{r}y'} + C^{12} e^{-p_{r}y'}$$

$$C^{s} = C^{21} e^{p_{r}y'} + C^{22} e^{-p_{r}y'}$$

We can write equation (55) more compactly by defining

$$\tilde{\pi}_{r} = \int_{V} \stackrel{\leftrightarrow}{G}^{p}(\vec{r}|\vec{r'}) \cdot \frac{\vec{P}(\vec{r'})}{\varepsilon_{r}} dV' + \int_{V} \stackrel{\leftrightarrow}{G}^{rc}(\vec{r}|\vec{r'}) \cdot \frac{\vec{P}(\vec{r'})}{\varepsilon_{r}} dV' + \int_{V} \stackrel{\leftrightarrow}{G}^{rc}(\vec{r}|\vec{r'}) \cdot \frac{\vec{P}(\vec{r'})}{\varepsilon_{r}} dV' + \int_{V} \stackrel{\leftrightarrow}{G}^{rc}(\vec{r}|\vec{r'}) \cdot \frac{\vec{P}(\vec{r'})}{\varepsilon_{r}} dV'$$
(57)

with

$$\ddot{G}^{p} = \stackrel{\leftrightarrow}{I} \int_{-\infty}^{\infty} \frac{e^{j\vec{\xi} \cdot (\vec{r} - \vec{r}')} e^{-p_{r}|y - y'|}}{2(2\pi)^{2} p_{r}} d^{2}\xi$$

$$\ddot{G}^{r} \stackrel{\left\{c\right\}}{s} = \hat{x} G_{t}^{r} \stackrel{\left\{c\right\}}{s} \hat{x} + \hat{y} \left(\frac{\partial}{\partial x} G_{c}^{r} \left\{c\right\} \hat{x} + G_{n}^{r} \left\{c\right\} \hat{y} + \frac{\partial}{\partial z} G_{c}^{r} \left\{c\right\} \hat{z}\right)$$

$$+ \hat{z} G_{t}^{r} \stackrel{\left\{c\right\}}{s} \hat{z}$$
(58)

Here

$$\begin{cases}
G_{t}^{r} \begin{Bmatrix} c \\ s \end{Bmatrix} & (\overrightarrow{r} | \overrightarrow{r}^{\dagger}) \\
G_{n}^{r} \begin{Bmatrix} c \\ s \end{Bmatrix} & (\overrightarrow{r} | \overrightarrow{r}^{\dagger}) \end{Bmatrix} = \iint_{-\infty}^{\infty} \begin{Bmatrix} C \\ R_{t} \begin{Bmatrix} c \\ s \end{Bmatrix} (\xi) \\
R_{n} \begin{Bmatrix} c \\ s \end{Bmatrix} (\xi) \end{Bmatrix} \frac{e^{j \overrightarrow{\xi} \cdot (\overrightarrow{r} - \overrightarrow{r}^{\dagger})} e^{-p} r^{y}}{2(2\pi)^{2} p_{r}} d^{2} \xi}$$

$$C \begin{Bmatrix} c \\ s \end{Bmatrix} (\xi) \end{Bmatrix} (\xi)$$

APPENDIX B: TRANSFORMED FIELD IN THE ASYMMETRIC SLAB

In this appendix we solve the transformed equivalent polarization integral equation for the case of the asymmetric slab waveguide excited by an x invariant line polarization source at location (y_0,z_0) . The geometry of the problem is shown in Figure 3.6.

It is shown in section 3.3.6 of chapter three that the transformed equivalent polarization integral equation specializes in this case to

$$e(y,\zeta) - k_0^2 \Delta n^2 \int_{\mathbf{0}} g_{\zeta}(y|y') e(y',\zeta) dy'$$

$$= \frac{k_0^2 p^e}{\epsilon_0} e^{-\mathbf{j} \zeta z_0} g_{\zeta}(y|y_0)$$
(1)

with the scalar Green's runction given by

$$g_{\zeta}(y|y') = \frac{1}{2\gamma_{c}} e^{-\gamma_{c}|y-y'|} + R_{t}e^{-\gamma_{c}(y+y')}$$
 (2)

We will solve the specialized integral equation (1) by use of Fourier transformation on the spatial variable y. To this end, let $e(y,\zeta)$ be written as the inverse transform of the forward Fourier transform $\tilde{e}(\eta,\zeta)$:

$$e(y,\zeta) = \frac{1}{2\pi} \int_{-\infty}^{\infty} \hat{e}(\eta,\zeta)e^{j\eta y}d\eta$$
 (3)

Then substitution or equation (3) into the integral equation (1) and subsequent interchange or spatial and spatial frequency integrals gives

$$\int_{-\infty}^{\infty} \hat{e}(\eta,\zeta) \left\{ e^{j\eta y} - k_0^2 \Delta n^2 \int_{0}^{t} g_{\zeta}(y|y')e^{j\eta y'}dy' \right\} d\eta$$

$$= \frac{2\pi k_0^2 p^e}{\epsilon_0} e^{-j\zeta z_0} g_{\zeta}(y|y_0)$$
(4)

For 0 < y < t the y' integral in equation (4) is

$$2\gamma_{c} \int_{0}^{t} g_{\zeta}(y|y')e^{j\eta}y'dy' = \int_{0}^{t} \left[e^{-\gamma_{c}|y-y|} + R_{t}e^{-\gamma_{c}(y+y')}\right]e^{j\eta}y'$$

$$= e^{-\gamma_{c}y} \left\{ \frac{-1}{\gamma_{c}+j\eta} + R_{t} \frac{e^{(\gamma_{c}+j\eta)t}-1}{-\gamma_{c}+j\eta} \right\} + e^{\gamma_{c}y} \left\{ \frac{e^{(-\gamma_{c}+j\eta)t}}{-\gamma_{c}+j\eta} \right\}$$

$$+ e^{j\eta}y \left\{ \frac{2\gamma_{c}}{\gamma_{c}^{2+\eta}^{2}} \right\}$$
(5)

Substitution of equations (5) and (2) into the integral equation (4) gives

$$\int_{-\infty}^{\infty} \hat{\mathbf{e}}(\eta,\zeta) \left\{ e^{j\eta y} \left[1 - \frac{k_0^2 \Delta n^2}{\gamma_c^2 + \eta^2} \right] + \frac{e^{-\gamma} c^y}{2\gamma_c} k_0^2 n^2 \left[\frac{-1}{\gamma_c^{+j} \eta} + R_t \frac{e^{(-\gamma_c^{+j})t} - 1}{-\gamma_c^{+j} \eta} \right] \right.$$

$$\left. + \frac{e^{\gamma_c y}}{2\gamma_c} k_0^2 \Delta n^2 \frac{e^{(-\gamma_c^{+j} \eta)t}}{-\gamma_c^{+j} \eta} \right\} d\eta \qquad (6)$$

$$= \frac{2\pi k_0^2 p^e}{\epsilon_0} e^{-(\gamma_c y_0^{+j} \zeta z_0)} \left[\frac{e^{\gamma_c y}}{2\gamma_c} + R_t \frac{e^{-\gamma_c y}}{2\gamma_c} \right]$$

(6) gives the result

Now if we have $\gamma_c^2 + \eta^2 = 0$ in equation (6) then the three exponential terms in y occurring in the equation are linearly independent.

Matching the coerricients of the terms involving $\exp(j\eta y)$ in equation

$$\eta = \frac{+}{\sigma} \quad \sigma \quad , \quad \sigma = \sqrt{k^2 - \zeta^2}$$
 (7)

These are the only two values of the spatial frequency variable—can take on in order that equation (96) is satisfied. Then the only way to get a nontrivial transformed core field $e(y,\zeta)$ is if $e(\eta,\zeta)$ is of the form

$$\tilde{\mathbf{e}}(\eta,\zeta) = \mathbf{A}(\zeta)\delta(\eta - \sigma) + \mathbf{B}(\zeta)\delta(\eta + \sigma) \tag{8}$$

Substitution of this form for $e(\eta, \zeta)$ into the integral equation (96) gives the result

$$A(\zeta) \left\{ \frac{e^{-\gamma} c^{y}}{2\gamma_{c}} \left[\frac{-1}{\gamma_{c}^{+} j\sigma} + R_{t} \frac{e^{(-\gamma_{c}^{+} j\sigma)t} - 1}{-\gamma_{c}^{-} j\sigma} \right] + \frac{e^{\gamma} c^{y}}{2\gamma_{c}} \left[\frac{e^{(+\gamma_{c}^{+} j\sigma)t}}{-\gamma_{c}^{+} j\sigma} \right] \right\}$$

$$+ B(\zeta) \left\{ \frac{e^{-\gamma_{c} y}}{2\gamma_{c}} \left[\frac{-1}{\gamma_{c}^{-} j\sigma} + R_{t} \frac{e^{(-\gamma_{c}^{-} j\sigma)} - 1}{-\gamma_{c}^{-} j\sigma} \right] + \frac{e^{\gamma_{c} y}}{2\gamma_{c}} \left[\frac{e^{(-\gamma_{c}^{-} j\sigma)t}}{-\gamma_{c}^{-} j\sigma} \right] \right\}$$

$$= \frac{2\pi p^{e}}{\varepsilon_{o}^{\Delta} n^{2}} e^{-(\gamma_{c}^{y} y_{o}^{+} j\zeta z_{o})} \left[\frac{e^{\gamma_{c} y}}{2\gamma_{c}} + R_{t} \frac{e^{-\gamma_{c} y}}{2\gamma_{c}} \right]$$

$$(9)$$

We again utilize the linear independence of the y variation of $\exp(\frac{+}{2}\gamma_C y)$ in equation (9) to write this as two independent equations in the unknown functions $A(\zeta)$ and B(Q):

Α(ζ

A (3

Sc

ر...

×

€

T

$$A(\zeta) \frac{e^{j\sigma t}}{-\gamma_c + j\sigma} + B(\zeta) \frac{e^{-j\sigma t}}{-\gamma_c - j\sigma} = \frac{2^{\pi}p^e}{\epsilon_0 \Delta n^2} e^{-[\gamma_c(y_0 - t) + j\zeta z_0]}$$

$$A(\zeta) \left[\frac{-1}{\gamma_{c} + j\sigma} + R_{t} \frac{e^{(-\gamma_{c} + j\sigma)t} - 1}{-\gamma_{c} + j\sigma} \right] + B(\zeta) \left[\frac{-1}{\gamma_{c} - j\sigma} + R_{t} \frac{e^{(-\gamma_{c} - j\sigma)t} - 1}{-\gamma_{c} - j\sigma} \right]$$

$$= \frac{2\pi p^{e}}{\epsilon_{o} \Delta n^{2}} R_{t}^{e}$$
 (10)

Solution or the system in equation (10) yields

$$A(\zeta) = \frac{k_0^2 p^e - [\gamma_c(y_0 - t) + j\zeta z_0] \sigma - j\gamma_s}{\epsilon_0}$$

$$B(\zeta) = \frac{\pi k_0^2 p^e - [\gamma_c(y_0 - t) + j\zeta z_0] \sigma + j\gamma_s}{\epsilon_0}$$

$$(11)$$

where we have derined

$$D(\zeta) = (\sigma^2 - \gamma_c \gamma_s) \sin_\sigma t - (\gamma_c + \gamma_s) \cos_\sigma t$$
 (12)

We can now substitute equation (11) into the expression of equation (8) for the transform field $e(y,\zeta)$. Fourier inversion as in equation (3) is trivial. It results in the solution to the original integral equation (1). We obtain

$$e(y,\zeta) = \frac{k_0^2 p^e - [\gamma_c(y_0 - t) + j\zeta z_0] \cos_\sigma y + \gamma_s \sin_\sigma y}{\varepsilon_0}$$

$$(13)$$

This is the result quoted in section 3.3.6 or chapter three.

APPENDIX C: PRINCIPLE AND REFLECTED TERMS FOR THE RECTANGULAR STRIP

In this appendix we detail the functions F and G appearing in equations (3.118) and (3.131) or our analysis of the rectangular strip waveguide. These are the functions which multiply the unknown amplitude constants of the closed-form expression for the core field, once this expression is substituted into the transformed integral equation.

We can show

$$\begin{split} &F_{1}^{\mathbf{X}} = \kappa_{\mathbf{X}} \mathbf{I}_{\text{ccc}}^{\kappa_{0}}(\xi^{2} - \kappa_{c}^{2}) + \kappa_{\mathbf{y}} \mathbf{I}_{\text{css}}^{\kappa_{1}}(\xi p_{c}) - (\kappa^{2} - \zeta^{2}) \mathbf{I}_{\text{csc}}^{\kappa_{0}}(\xi) \\ &F_{2}^{\mathbf{X}} = \kappa_{\mathbf{X}} \mathbf{I}_{\text{ccs}}^{\kappa_{0}}(\xi^{2} - \kappa_{c}^{2}) - \kappa_{\mathbf{y}} \mathbf{I}_{\text{csc}}^{\kappa_{1}}(\xi p_{c}) - (\kappa^{2} - \zeta^{2}) \mathbf{I}_{\text{css}}^{\kappa_{0}}(\xi) \\ &F_{3}^{\mathbf{X}} = \mathbf{Z} \{ \sigma_{\mathbf{y}} \mathbf{I}_{\text{ccs}}^{\sigma_{0}}(\xi^{2} - \kappa_{c}^{2}) + \sigma_{\mathbf{X}} \mathbf{I}_{\text{csc}}^{\sigma_{1}}(\xi p_{c}) \} \\ &F_{4}^{\mathbf{X}} = \mathbf{Z} \{ -\sigma_{\mathbf{y}} \mathbf{I}_{\text{ccc}}^{\sigma_{0}}(\xi^{2} - \kappa_{c}^{2}) + \sigma_{\mathbf{X}} \mathbf{I}_{\text{css}}^{\sigma_{1}}(\xi p_{c}) \} \\ &F_{1}^{\mathbf{y}} = \kappa_{\mathbf{y}} \mathbf{I}_{\text{ssc}}^{\kappa_{0}}(\kappa_{c}^{2}) + \kappa_{\mathbf{x}} \mathbf{I}_{\text{scc}}^{\kappa_{1}}(\xi p_{c}) + \kappa_{\mathbf{y}} \mathbf{I}_{\text{sss}}^{\kappa_{2}}(p_{c}) - (\kappa^{2} - \zeta^{2}) \mathbf{I}_{\text{ssc}}^{\kappa_{1}}(p_{c}) \\ &F_{2}^{\mathbf{y}} = -\kappa_{\mathbf{y}} \mathbf{I}_{\text{ssc}}^{\kappa_{0}}(\kappa_{c}^{2}) + \kappa_{\mathbf{x}} \mathbf{I}_{\text{scs}}^{\kappa_{1}}(\xi p_{c}) - \kappa_{\mathbf{y}} \mathbf{I}_{\text{ssc}}^{\kappa_{2}}(p_{c}) - \kappa^{2} - \zeta^{2}) \mathbf{I}_{\text{sss}}^{\kappa_{1}}(p_{c}) \\ &F_{3}^{\mathbf{y}} = \mathbf{Z} \{ \sigma_{\mathbf{x}} \mathbf{I}_{\text{ssc}}^{\sigma_{0}}(\kappa_{c}^{2}) + \sigma_{\mathbf{y}} \mathbf{I}_{\text{scc}}^{\sigma_{1}}(\xi p_{c}) + \sigma_{\mathbf{x}} \mathbf{I}_{\text{ssc}}^{\sigma_{2}}(p_{c}) \} \\ &F_{4}^{\mathbf{y}} = \mathbf{Z} \{ \sigma_{\mathbf{x}} \mathbf{I}_{\text{sss}}^{\sigma_{0}}(\kappa_{c}^{2}) - \sigma_{\mathbf{y}} \mathbf{I}_{\text{scc}}^{\sigma_{1}}(\xi p_{c}) + \sigma_{\mathbf{x}} \mathbf{I}_{\text{sss}}^{\sigma_{2}}(p_{c}) \} \\ &F_{1}^{\mathbf{z}} = -(\kappa^{2} - \zeta^{2}) \mathbf{I}_{\text{ssc}}^{\kappa_{0}}(\kappa_{c}^{2} - \zeta^{2}) - \kappa_{\mathbf{y}}^{2} \mathbf{I}_{\text{scc}}^{\kappa_{0}}(\xi) - \kappa_{\mathbf{y}}^{2} \mathbf{I}_{\text{sss}}^{\kappa_{1}}(p_{c}) \end{split}$$

$$\begin{split} F_{2}^{z} &= -(\kappa^{2} - \varsigma^{2}) I_{sss}^{\kappa o} (\kappa_{c}^{2} - \varsigma^{2}) - \kappa_{x} \varsigma^{2} I_{scs}^{\kappa o} (\xi) + \kappa_{y} \varsigma^{2} I_{ssc}^{\kappa 1} (p_{c}) \\ F_{3}^{z} &= z \zeta^{2} \{ -\sigma_{y} I_{scs}^{\sigma o} (\xi) - \sigma_{x} I_{sss}^{\sigma 1} (p_{c}) \} \\ F_{4}^{z} &= z \zeta^{2} \{ \sigma_{y} I_{scc}^{\sigma o} (\xi) - \sigma_{x} I_{sss}^{\sigma 1} (p_{c}) \} \\ G_{1}^{x} &= \kappa_{x} [\kappa_{c}^{2} R_{tn} \overline{X}_{c\kappa} + \kappa_{n} \overline{X}_{c\kappa}^{"}] \overline{Y}_{c\kappa} + [\kappa_{y} p_{cn} R_{nn} \overline{Y}_{s\kappa} + (\kappa^{2} - \varsigma^{2}) \kappa_{n} \overline{Y}_{c\kappa}] \overline{X}_{s\kappa}^{'} \\ G_{2}^{x} &= \kappa_{x} [\kappa_{c}^{2} R_{tn} \overline{X}_{c\kappa} + \kappa_{n} \overline{X}_{c\kappa}^{"}] \overline{Y}_{s\kappa} + [-\kappa_{y} p_{cn} R_{nn} \overline{Y}_{c\kappa} + (\kappa^{2} - \varsigma^{2}) \kappa_{n} \overline{Y}_{s\kappa}] \overline{X}_{s\kappa}^{'} \\ G_{3}^{x} &= z \sigma_{y} \{ [\kappa_{c}^{2} R_{tn} \overline{X}_{c\sigma} + \kappa_{n} \overline{X}_{c\sigma}^{"}] \overline{Y}_{s\sigma} + p_{cn} R_{nn} \overline{X}_{s\sigma}^{'} \overline{Y}_{s\sigma} \} \\ G_{4}^{x} &= z \sigma_{y} \{ -[\kappa_{c}^{2} R_{tn} \overline{X}_{c\sigma} + \kappa_{n} \overline{X}_{c\sigma}^{"}] \overline{Y}_{c\kappa} + p_{cn} R_{nn} \overline{X}_{s\sigma}^{'} \overline{Y}_{s\sigma} \} \\ G_{4}^{y} &= z \sigma_{y} \{ -[\kappa_{c}^{2} R_{tn} \overline{X}_{c\sigma} + \kappa_{n} \overline{X}_{c\sigma}^{"}] \overline{Y}_{c\kappa} + p_{cn} R_{nn} \overline{X}_{s\sigma}^{'} \overline{Y}_{s\sigma} \} \\ G_{1}^{y} &= L_{n} [\kappa_{x} \overline{X}_{c}^{"} + (\kappa^{2} - \varsigma^{2}) \overline{X}_{s\kappa}] \overline{Y}_{c\kappa} + \kappa_{y} (\kappa_{c}^{2} + p_{cn}^{2}) R_{nn} \overline{X}_{s\kappa}^{'} \overline{Y}_{c\kappa} \\ G_{2}^{y} &= L_{n} [\kappa_{x} \overline{X}_{c\kappa}^{"} + (\kappa^{2} - \varsigma^{2}) \overline{X}_{s\kappa}] \overline{Y}_{s\kappa} + \kappa_{y} (\kappa_{c}^{2} + p_{cn}^{2}) R_{nn} \overline{X}_{s\kappa}^{'} \overline{Y}_{c\kappa} \\ G_{3}^{y} &= z \{ -\sigma_{y} L_{n} \overline{X}_{c\sigma}^{"} \overline{Y}_{s\sigma} - \sigma_{x} (\kappa_{c}^{2} + p_{cn}^{2}) R_{nn} \overline{X}_{s\sigma}^{"} \overline{Y}_{s\sigma} \} \\ G_{4}^{y} &= z \{ -\sigma_{y} L_{n} \overline{X}_{c\sigma}^{"} \overline{Y}_{c\kappa} + (\kappa^{2} - \varsigma^{2}) M_{n} \overline{X}_{s\kappa}] \overline{Y}_{c\kappa} - \kappa_{y} \varsigma^{2} p_{cn} R_{nn} \overline{X}_{s\kappa}^{"} \overline{Y}_{c\kappa} \\ G_{2}^{z} &= [-\kappa_{x} \varsigma^{2} k_{n} \overline{X}_{c\kappa}^{"} + (\kappa^{2} - \varsigma^{2}) M_{n} \overline{X}_{s\kappa}] \overline{Y}_{s\kappa} + \kappa_{y} \zeta^{2} p_{cn} R_{nn} \overline{X}_{s\kappa}^{"} \overline{Y}_{c\kappa} \\ G_{3}^{z} &= z \zeta^{2} \{ \sigma_{y} \kappa_{n} \overline{X}_{c\kappa}^{"} \overline{Y}_{c\sigma} - \sigma_{x} p_{cn} R_{nn} \overline{X}_{s\kappa}^{"} \overline{Y}_{c\sigma} \} \\ G_{4}^{u} &= z \zeta^{2} \{ \sigma_{y} \kappa_{n} \overline{X}_{c\kappa}^{"} \overline{Y}_{c\kappa} - \sigma_{x} p_{cn} R_{nn} \overline{X}_{s\kappa}^{"} \overline{Y}_{c\sigma} \} \\ G_{4}^{u} &= z \zeta^{2} \{ \sigma_{y} \kappa_{n} \overline{X}_{c\kappa}^{"} + (\kappa^{2} - \varsigma^{2}) M_{n} \overline{X}_{s\kappa}^{"} \overline{Y}_{s\kappa} \} \\ G$$

Here we have defined

$$I \begin{cases} \gamma_{p} \\ \{c \} \end{cases} \gamma_{\beta}(\Box) = N^{2} \int_{0}^{\infty} \begin{cases} \cos \xi x \\ \sin \xi x \end{cases} \frac{\Box}{2\pi p_{e}} \tilde{X}_{\alpha \gamma} Y_{\beta \gamma}^{p} d\xi$$

$$\tilde{X}$$
 $\{c \ \}$ γ = $\frac{\sin a(\xi - \gamma)}{\xi - \gamma} + \frac{\sin a(\xi + \gamma)}{\xi + \gamma}$

$$K_{n} = R_{tn} - p_{en}C_{n}$$

$$L_{n} = (k_{e}^{2} - p_{en}^{2})C_{n} - p_{en}R_{tn}$$

$$M_{n} = (k_{e}^{2} - \zeta^{2})R_{tn} - \zeta^{2}p_{en}C_{n}$$
(2)

and the other factors in equations (1) and (2) are round in sections 3.4.2 and 3.4.3.

APPENDIX D: BRANCH INTEGRALS FOR TRUNCATED ASYMMETRIC SLAB

In this appendix we specialize the branch integrals of sections 4.4.1 and 4.4.2 to the limiting case of a lossless asymmetric slab waveguide. This allows for considerable simplification of the branch integrals, which can then be easily programmed to obtain numerical results.

The branch integral terms B_{mn}^+ and C_m^+ are defined in equations (4.63) and (4.74), respectively. Both expressions involve integration around the branch contour \mathscr{C}_{B^*} . This contour is illustrated in Figure 4.5. Note that his contour is identical to the one or Figure 3.8. In the limit or zero loss this contour becomes one along the limiting branch cuts shown in Figure 3.9. As discussed in section 3.3.6, integration along this limiting contour decomposes into three cases. If we define $\xi = u + jv$, then these cases are: $-k_S < u < -k_C$, v = 0; $-k_C < u < 0$, v = 0; $0 < v < \infty$, u = 0. Defining our branch choices of as shown in Figure 3.10, we have

Case I: upper side -
$$\gamma_c$$
 = γ , γ_s = $-j\nu$, γ^2 = u^2 - k_c^2 lower side - γ_c = γ , γ_s = $j\nu$, ν^2 = k_s^2 - u^2 Case II: upper side - γ_c = γ - $j\delta$, γ_s = $-j\nu$, δ^2 = k_c^2 - u^2 lower side - γ_c = $j\delta$, γ_s = $j\nu$
Case III: upper side - γ_c = $-j\alpha$, γ_s = $-j\beta$, α^2 = ν^2 + k_c^2 lower side - γ_c = $j\alpha$, γ_s = $j\beta$, β^2 = ν^2 + k_s^2

Now for a function $q(\xi)$ we define

(3)

Then we can show

$$\tilde{f}_{n1}^{+} = \frac{e^{-j(\tau + \tau_n)z_0}}{4\pi(\tau - u)(+\tau_n + u)}\hat{g}_1$$

$$\tilde{h}_{m1}^{+} = \frac{e^{ju(z-z_1)}}{4\pi j(u+\tau_m)} \hat{g}_1$$

$$\tilde{\mathbf{f}}_{n2}^{\frac{+}{2}} = \frac{\mathrm{e}^{-\mathrm{j} \left(\tau + \tau_{n}\right) z_{0}}}{4\pi \left(\tau - u\right) \left(\pm \tau_{n} + u\right)} \hat{\mathbf{g}}_{2}$$

 $\tilde{n}_{m2}^{+} = \frac{e^{ju(z-z_0)}}{4\pi i(u+z_0)} \hat{g}_2$

$$\tilde{r}_{n3} = \frac{e^{-j(\tau + \tau_n)z_0}}{4\pi(\tau - jv)(+\tau_m + jv)} \hat{g}_3$$

$$\tilde{n}_{m3}^{+} = \frac{e^{-v(z-z_{0})}}{\mu_{\pi j(jv+\tau_{m})}} g_{3}$$

Here $r_{\overline{n}}^{+}$ and $h_{\overline{m}}^{+}$ are as derined in equations (4.58) and (4.71), respectively, and

$$\tilde{g}_{1} = \frac{4j\nu}{k_{s}^{2} - k_{c}^{2}} e^{-\gamma (y+y')}$$

$$\tilde{g}_{2} = \frac{2j}{\delta} [\cos\delta(y-y') + \tilde{R}_{t2}\cos\delta(y+y')]$$

$$\tilde{g}_{3} = \frac{2j}{\alpha} [\cos\alpha(y-y') + \tilde{R}_{t3}\cos\alpha(y+y')]$$

$$\tilde{R}_{t2} = \frac{\delta^{-\nu}}{\delta^{+\nu}} \qquad \tilde{R}_{t3} = \frac{\alpha^{-\beta}}{\alpha^{+\beta}}$$

$$\tilde{R}_{t3} = \frac{\alpha^{-\beta}}{\alpha^{+\beta}}$$
(4)

These expressions can be spatially integrated in closed form. If we define

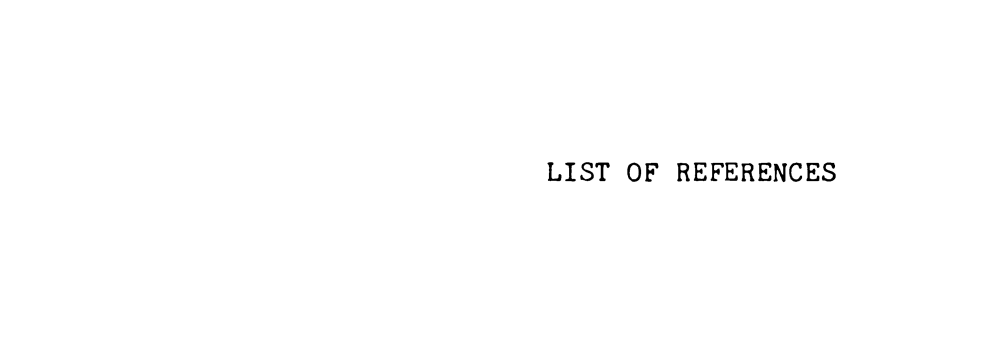
$$b_{mni}^{+} = \int_{0}^{t} \int_{0}^{t} \tilde{r}_{ni}^{+} e_{m}(y)e_{n}(y')dy'dy$$

$$c_{mni}^{+} = \int_{0}^{t} h_{mi}^{+} e_{m}(y')dy'$$
(5)

with $e_{m}(y)$ as given in equation (3.81), then we have the result

$$B_{\overline{m}n}^{+} = \int_{-k_{s}}^{-k_{c}} b_{mni} du + \int_{-k_{c}}^{0} b_{\overline{m}nz}^{+} du + j \int_{0}^{\infty} b_{\overline{m}n3}^{+} dv$$

$$C_{\overline{m}}^{+} = \int_{-k_{s}}^{-k_{c}} c_{\overline{m}1}^{+} du + \int_{-k_{c}}^{0} c_{\overline{m}2}^{+} du + j \int_{0}^{\infty} c_{\overline{m}3}^{+} dv$$
(6)



References

- [1.1] W.V. McLevige, T. Itoh, R. Mittra, "New Waveguide Structures for Millimeter and Optical Integrated Circuits," IEEE Trans. Microwave Theory Tech., vol. MTT-23, pp. 788-794, Oct. 1975.
- [1.2] H. Jacobs, M.M. Chrepta, "Semiconductor Dielectric Waveguides for Millimeter Wave Functional Circuits," in Dig. IEEE Int. Microwave Symp., pp. 28-29, 1973.
- [1.3] D. Hondros, P. Debye, "Elektromagnetische Wellen in Dielektrischen Drahten," Ann. Physik, vol. 32, pp. 456-476, 1910.
- [1.4] S-T. Peng, A.A. Oliner, "Guidance and Leakage Properties of a Class of Open Dielectric Waveguides: Part I Mathematical Formulations," IEEE Trans. Microwave Theory Tech., vol. MTT-29, no. 9, pp. 843-855, Sept. 1981.
- [1.5] A.A. Oliner, S-T. Peng, T-I. Hsu, A. Sanchez, "Guidance and Leakage Properties of a Class of Open Dielectric Waveguides: Part II New Physical Effects," IEEE Trans. Microwave Theory Tech., vol. MTT-29, no. 9, pp. 855-869, Sept. 1981.
- [1.6] D.P. Nyquist, D.R. Johnson, S.V. Hsu, "Orthogonality and Amplitude Spectrum or Radiation Modes Along Open Boundary Waveguides," JOSA, Vol. 71, pp. 49-54, Jan. 1981.
- [1.7] D. Marcuse, Theory of Dielectric Optical Waveguides, New York: Academic Press, Ch.I, 1974.
- [1.8] R.C. Pate, E.F. Kuester, "Fundamental Propagation Modes on a Dielectric Waveguide of Arbitrary Cross Section," Sci. Rpt. no. 45, U.S. Army Research Office, Contract no. DAA 29-78-C-0173, Electromagnetics Laboratory, University of Colorado, Boulder, Colorado, Feb. 1979.
- [1.9] N.S. Kapany, J.J. Burke, Optical Waveguides, New York: Academic Press, 1972.
- [1.10] E.A.J. Marcatili, "Dielectric Rectangular Waveguide and Directional Coupler for Integrated Optics," BSTJ, vol. 48, no. 9, pp. 2071-2102, Sept. 1969.

- [1.11] J.E. Goell, "A Circular-Harmonic Computer Analysis of Rectangular Dielectric Waveguides," BSTJ, vol. 48, no. 9, pp. 2133-2160, Sept. 1969.
- [1.12] B.Z. Katsenelenbaum, "On the Propagation of Electromagnetic Waves Along an Infinite Dielectric Cylinder at Low Frequencies," Dokl. Akad. Navk. SSSR, vol. 58, no. 7, 1947 (in Russian).
- [1.13] D.R. Johnson, D.P. Nyquist, "Integral-Operator Analysis for Dielectric Optical Waveguides Theory and Application," Digest of National Radio Science (URSI) Meeting, University of Colorado, Boulder Colorado, p. 104, Nov. 1978.
- [2.1] R.E. Collin, <u>Field Theory of Guided Waves</u>, New York: McGraw-Hill, 1960, p. 26.
- [2.2] R.E. Collin, op. cit., p. 59.
- [2.3] R.E. Collin, op. cit., p. 26.
- [2.4] R. Courant, D. Hilbert, Methods of Mathematical Physics, vol. I, New York: Interscience, 1962, p. 140.
- [2.4.5] R.V. Churchill, J.W. Brown, R.F. Verhey, <u>Complex Variables</u> and <u>Applications</u>, New York: McGraw-Hill, 1976, p. 182.
- [2.5] A.D. Yaghjian, "Electric Dyadic Green's Functions in the Source Region," Proc. IEEE, vol. 68, no. 2, Feb. 1980, pp. 248-263.
- [2.6] R.E. Collin, op. cit., p. 58.
- [2.7] R.E. Collin, op. cit., p. 63.
- [2.8] A. Banos, <u>Dipole Radiation in the Presence of a Conducting Half Space</u>, Oxrord: Pergamon Press, 1966, pp. 1-62.
- [2.9] J. VanBladel, "Some Remarks on Green's Dyadic for Infinite Space," IEEE Trans. Ant. Prop., vol. AP-9, no. 6, Nov. 1961, pp. 563-566.
- [2.10] A.D. Yaghjian, op. cit.
- [2.11] K-M. Chen, "A Simple Physical Picture of Tensor Green's Function in Source Region," Proc. IEEE, vol. 65, no. 8, Aug. 1977, pp. 1202-1204.
- [3.1] A. Papoulis, The Fourier Integral and Its Applications, New York: McGraw-Hill, 1962, p. 7.
- [3.2] A. Papoulis, op. cit., p. 16.
- [3.3] A. Papoulis, op. cit., p. 26.

- [3.4] I.S. Gradshteyn, I.M. Ryzhic, <u>Table of Integrals</u>, <u>Series and Products</u>, New York: Academic Press, 1965, p.
- [3.5] A.D. Yaghjian, op. cit.
- [3.6] R.V. Churchill, J.W. Brown, R.F. Verhey, op. cit., p. 172.
- [3.7] R.V. Churchill, J.W. Brown, R.F. Verhey, op. cit., p. 64.
- [3.8] R.E. Collin, op. cit., p. 289.
- [3.9] R. Courant, D. Hilbert, op. cit., p.
- [3.10] S-T. Peng, A.A. Oliner, op. cit.
- [3.11] D. Marcuse, op. cit., p. 6.
- [3.12] D. Marcuse, op. cit., p. 10.
- [3.13] D. Marcuse, op. cit., p. 15.
- [3.14] A.A. Oliner, S-T. Peng, T-I. Hsu, A. Sanchez, op. cit.
- [3.15] D. Marcuse, op. cit., p. 9.
- [3.16] D.P. Nyquist, D.R. Johnson, S.V. Hsu, op. cit.
- [3.17] R.E. Collin, op. cit., p. 492.
- [3.18] E.A.J. Marcatili, op.cit.
- [3.19] E.A.J. Marcatili, op. cit.
- [3.20] A.A. Oliner, S-T. Peng, T-I. Hsu, A. Sanchez, op. cit.
- [3.21] E.A.J. Marcatili, op. cit.
- [3.22] R.V. Churchill, J.W. Brown, R.F. Verhey, op. cit., p.
- [3.23] J. Stoer, R. Bulirsch, <u>Introduction to Numerical Analysis</u>, New York: Springer-Verlag, p. 244, 1980.
- [3.24] E.A.J. Marcatili, op. cit.
- [3.25] J.E. Goell, op. cit.
- [4.1] L. Lewin, "A Method for the Calculation of the Radiation Pattern and Mode-Conversion Properties of a Solid-State Heterojunction Laser," Trans. Microwave Theory Tech., vol. MTT-27, no. 4, pp. 310-315, April 1979.
- [4.2] A. Papoulis, op. cit., p. 37.

- [4.3] A. Papoulis, op. cit., p. 39.
- [4.4] R.E. Collin, op. cit., p. 77.
- [5.1] B.C. Drachman, D.P. Nyquist, "Computational Algorithms for Electromagnetic Interactions in High-Speed Integrated Electronic Circuits," Res. Proposal to AFOSR Fast Algorithms Initiative, Dept. of Eng. Res., Mich. St. Univ., E. Lansing, MI, July 1984.
- [5.2] M. Cloud, M.S. Thesis, Dept. of Elec. Eng., Mich. St. Univ., E. Lansing, MI, to be published, 1985.
- [A.1] A. Sommerfeld, Partial Dirrerential Equations in Physics, New York: Academic Press, pp. 236-265, 1964.